The role of the envelope cytoplasmic tail in Lentiviral replication

Tafhima Haider

Division of Infection and Immunity
University College London

A thesis submitted for the degree of
Doctor of Philosophy

March 2021

Declaration

I, Tafhima Haider, confirm that the work presented in this thesis is my own. Where information has been derived from other sources, I confirm that this has been indicated in the thesis.

The work from this thesis has since been published in the Proceedings of the National Academy of Sciences journal as a research article:
Haider, T., Snetkov, X., & Jolly, C. (2021). HIV envelope tail truncation confers resistance to SERINC5. *Proceedings of the National Academy of Sciences of the United States of America*, 118(21), e2101450118

.

Acknowledgements

This PhD has been an incredible experience of learning and self-exploration, which would not have been possible without the unwavering support of my parents, siblings, friends and colleagues. I dedicate this thesis to my parents who have always encouraged me to strive for excellence, but more importantly to be happy. Tasnim and Mushfiq, you are the most amazingly supportive siblings anyone could ever ask for. Thank you for all the random take-outs and mini celebrations about anything and everything. Farhana, I can't thank you enough for always being there for me, literally a phone call away every single time I needed you. Without these special people in my life, this PhD journey would not have been possible.

I would like to especially thank Clare for trusting me and believing in me at the very beginning when she offered me this opportunity to work with her. It was so unexpected, and I'm really grateful. You have been a great supervisor, providing infinite amounts of scientific knowledge and direction for my projects, as well as encouraging me continuously when imposter syndrome would get the best of me. A good supervisor is one who lets their students explore their own interests and that is exactly what Clare encouraged me to do, resulting in the exciting work in this thesis on HIV restriction factors. The entire Jolly lab team - AK, Dejan, Xenia and Maitreyi - have been great pillars of support, not just in the lab, but also emotionally. I love you all!

The Division of Infection and Immunity at UCL has been such an incredibly stimulating environment to be in. Thank you to everyone, especially the Towers and McCoy labs for all your helpful discussions. Greg, you've been a great mentor from the very beginning, when I started working with you during my MSc. The training I've received as a PhD student over the last 4 years is second to none and I hope my publications, career goals and future achievements in academia and beyond will be a testament to that.

4 years and 1 pandemic later, I am finally ready to finish this incredible journey. Thank you once again to everyone who believed in me, motivated me and inspired me.

Abstract

The envelope glycoprotein (Env) of lentiviruses plays an essential role in viral replication. Env is expressed on the plasma membrane of infected cells and is incorporated into budding virions, where it acts as the viral entry protein, binding to the CD4 receptor and coreceptors (CCR5 or CXCR4) on target cells to mediate attachment, fusion and entry of the viral capsid. Functional Env is a heterotrimeric structure composed of the receptor-binding surface subunit (gp120) and the transmembrane subunit (gp41) that contains the fusion peptide, a transmembrane domain and a cytoplasmic tail (CT). The HIV EnvCT is approximately 150 amino acids long, whereas the EnvCT of retroviruses are considerably shorter (approximately 50 amino acids). Conservation of the length of lentiviral EnvCTs suggests the presence of key determinants, many of which remain undefined, that are essential for efficient viral replication and spread. Previous studies have reported that HIV-2 and several SIVs truncate their EnvCT *in vitro* in order to gain a replicative advantage, although how this provides an advantage is currently unknown. To explore the biology of the EnvCT, HIV-1 and HIV-2 viruses with a truncated EnvCT were produced by site-directed mutagenesis and the requirement of the EnvCT has been explored in the context of viral replication, evasion of antiviral restriction factors and activation of signalling pathways. Data in this thesis show that HIV-1 and HIV-2 viruses have differential requirements for the long EnvCT, in a cell-type dependent manner. Whilst HIV-1 required a long EnvCT for efficient replication and spread in T cells, HIV-2 replication was not dependent on the EnvCT. This difference primarily mapped to differences in Env incorporation into virions, which is known to be a key determinant of infectivity. Notably, EnvCT truncation conferred resistance to two potent virus entry-targeting restriction factors, SERINC5 and IFITM. Further, results suggest that truncation of the EnvCT alters the susceptibility of virions to inhibition by neutralising antibodies. Together, this work provides new mechanistic insight into the role of the EnvCT in evasion of innate antiviral defences, revealing how viruses balance competing factors to adapt to their niche in the presence of differing selection pressures.

Impact statement

Lentiviruses encode a long, enigmatic EnvCT which is involved in various steps of the viral life cycle and modulates sensitivity to the adaptive immune system, through regulation of the global Env conformation. This thesis uncovers a role for this EnvCT in evading innate immune restriction. SERINCs and IFITMs are potent lentiviral restriction factors that inhibit infection by blocking viral entry into cells. Specifically, SERINCs inhibit viral fusion by targeting the Envelope glycoprotein by a mechanism that remains incompletely understood. Truncation of HIV-1 and HIV-2 EnvCT confers complete resistance to SERINC and IFITM restriction. However, while the EnvCT of HIV-1 is necessary for viral replication in T cells, HIV-2 does not require the EnvCT. These data suggest a new mechanism by which human lentiviruses can evade restriction that is mediated by the EnvCT, but highlight key differences in the likely fitness cost imposed by this on pandemic HIV-1 and non-pandemic HIV-2. This study highlights that lentiviruses continuously adapt to alterations in selection pressures, from the innate and adaptive immune system, when introduced into different niches, in order to successfully replicate and transmit. Currently, differences in HIV-1 and HIV-2 Env trafficking, Env incorporation and virion assembly are not well understood. The EnvCT truncated mutants used in this study could be used to aid our understanding of these differences, which might shed light on the role of Env in determining HIV pandemicity.

Table of Contents

List of figures

Abbreviations

Ab	Antibody
ADCC	Antibody-dependent cellular cytotoxicity
Ag	Antigen
agm	African green monkey
AIDS	Acquired immunodeficiency syndrome
ANOVA	Analysis of variance
AP-1	Adaptor protein 1; can also mean Activator protein 1
APC	Antigen presenting cell; can also mean Allophycocyanin
APOBEC	Apolipoprotein B mRNA editing enzyme catalytic polypeptide
ATCC	American type culture collection
BCL-10	B-cell lymphoma 10 protein
bnAb	Broadly neutralising antibody
CA	Capsid
Ca^{2+}	Calcium
CCR5	C-C chemokine receptor 5
CD	Cluster of differentiation
CDC42	Cell division control protein 42 homologue
cDNA	Complementary DNA
CFAR	Centre for AIDS reagents
cpz	Chimpanzee
CRAC	Calcium release-activated calcium channel
CT	Cytoplasmic tail
CTD	C-terminal domain
CTL	Cytotoxic T lymphocyte
CXCR4	C-X-C chemokine receptor 4
Cy3/5	Cyanine 3/5
DC	Dendritic cell
DMEM	Dulbecco's modified eagle medium
DMSO	Dimethyl sulphoxide
DNA	Deoxyribonucleic acid
dNTP	deoxynucleotide triphosphate
drl	Drill
ds	Double stranded
EDTA	Ethylene diaminetetracetic acid
eIF4	Eukaryotic translation initiation factor 4
ELISA	Enzyme linked immunoabsorbant assay

Env	Envelope
EnvCT	Envelope cytoplasmic tail
ER	Endoplasmic reticulum
ERK	Extracellular signal-regulated kinase
ESCRT	Endosomal sorting complex required for transport
F-actin	Actin filaments
FACS	Fluorescence activated cell sorting
FCS	Foetal calf serum
FDA	Food and drug administration
FSC-A/W/H	Forward scatter area/width/height
FWB	FACS wash buffer
Gag	Group-specific antigen
GALT	Gut associated lymphoid tissue
GBP	Guanylate-binding protein
GFP	Green fluorescent protein
gor	Gorilla
gp120	Envelope glycoprotein of 120 kDa
gp160	Envelope glycoprotein of 160 kDa
gp41	Envelope glycoprotein of 41 kDa
gsn	Greater spot-nosed monkey
h	Hour
HA	Hemagglutinin
HB	Helix bundle
HIV	Human immunodeficiency virus
HUSH	Human silencing complex
ICAM	Intercellular adhesion molecule
IF	Immunofluorescence
IFITM	Interferon inducible transmembrane protein
IFN	Interferon
Ig	Immunoglobulin
IL-2	Interleukin 2
IL-7	Interleukin 7
IN	Integrase
IP3	Inositol triphosphate
IRES	Internal ribosomal entry site
ITAM	immunoreceptor tyrosine-based activation motif
JNK	Jun N-terminal kinase
kb	Kilobase

KD	Knock-down
kDa	Kilo Dalton
KO	Knock-out
LAT	Linker for activation of T cells
LB	Luria Bertani
Lck	Lymphocyte-specific protein tyrosine kinase
LEDGF/p75	Lens epithelium-derived growth factor
LFA-1	Lymphocyte function-associated antigen 1
LTR	Long terminal repeat
MA	Matrix
mac	Rhesus macaque
MAPK	Mitogen activated protein kinase
MARCH	Membrane associated RING-CH domain protein
MEKK	MAP/ERK kinase kinase
MFI	Mean fluorescence intensity
MHC	Major histocompatibility complex
min	Minute
MKK	MAPK kinase
MLV	Murine leukaemia virus
mnd	Mandrill
MOI	Multiplicity of infection
mon	Mona monkey
MTOC	Microtubule organising centre
mTORC	Mammalian target of rapamycin complex
mus	Moustached money
MxB	Myxovirus resistance protein B
n/d	Not detectable
Nef	Negative regulatory factor
NF-kB	nuclear factor kappa-light-chain-enhancer of activated B cells
NFAT	Nuclear factor of activated T cells
NIBSC	National institute of biological standards and control
NIH	National institute for health
NMR	Nuclear magnetic resonance
NNRTI	Non-nucleoside reverse transcriptase inhibitor
NPC	Nuclear pore complex
NRTI	Nucleoside reverse transcription inhibitor
NTD	N-terminal domain
Nup	Nucleoporin

ORF	Open reading frame
P-TEFb	Positive transcription elongation factor b
p.i.	Post-infection
PBMC	Peripheral blood mononuclear cells
PBS	Phosphate buffered saline
pbs	Primer binding site
PCR	Polymerase chain reaction
PDK1	Phosphoinositide-dependent kinase 1
PE	Phycoerythrin
PFA	Paraformaldehyde
PHA	Phytohemagglutinin
PI	Protease inhibitor
PI3K	phosphoinositide 3-kinase
PIP2	Phosphatidylinositol 4,5-bisphosphate
PIP3	Phosphatidylinositol 3,4,5-risphosphate
PM	Plasma membrane
Pol	Polymerase
PPT	Polypurine tract
qPCR	Quantitative polymerase chain reaction
Ras	Rat sarcoma oncogene protein
rcm	Red-capped mangabey
Rev	Regulator of expression of virion proteins
RLU	Relative light units
RNA	Ribonucleic acid
RNAi	RNA interference
RPMI	Roswell Park Memorial Institute medium
RT	Reverse transcriptase; can also mean room temperature
SAMHD1	Sterile α-motif and HD domain-containing protein 1
SDS-PAGE	Sodium dodecyl sulphate polyacrylamide gel electrophoresis
SERINC	Serine incorporator
shRNA	Small hairpin RNA
siRNA	Small interfering RNA
SIV	Simian immunodeficiency virus
smm	Sooty mangabey
ss	Single stranded
SSC-A	Side scatter area
TAR	Transactivation responsive region
Tat	Transactivator protein

TBS	Tris buffered saline
TCR	T cell receptor
TGN	Trans Golgi network
TRIM5α	Tripartite motif 5 alpha
UTR	Untranslated region
Vif	Viral infectivity factor
VLP	Virus-like particle
Vpr	Viral protein R
Vpu	Viral protein U
Vpx	Viral protein X
VS	Virological synapse
VSVg	Vesicular stomatitis virus glycoprotein
WHO	World health organisation

1. Introduction

1.1 HIV pathogenesis

1.1.1 Origin and classification

Acquired Immunodeficiency Syndrome (AIDS) was first diagnosed in 1981 and coincided with the discovery of the first human retroviruses infecting T cells of leukaemia patients (Poiesz et al., 1980). Given that AIDS patients also have abnormal T cell counts and dysregulated T cell function, scientists hypothesised that a T-cell tropic retrovirus may be the causative agent of AIDS. Indeed, Human Immunodeficiency Viruses type-1 and 2 (HIV-1 and HIV-2) are lentiviruses belonging to the family *Retroviridiae* and are the causative agents of AIDS. The discovery of HIV-1 (Barre-Sinoussi et al., 1983; Gallo et al., 1984; Levy et al., 1984; Popovic et al., 1984) was fuelled by the observation that a significant number of homosexual men in New York, USA were suffering from malignancies such as Kaposi's sarcoma and several opportunistic infections (Friedman-Kien, 1981) suggestive of underlying immunodeficiency in otherwise healthy individuals. Following the discovery of HIV-1, serological studies in 1986 revealed that the virus infecting the west African population was different to HIV-1, thus it was termed HIV-2 (Clavel et al., 1986). Whilst HIV-1 infection causes rapid onset of AIDS without treatment, HIV-2 is antigenically different and causes less aggressive disease progression (Drylewicz et al., 2008; Jaffar et al., 1997; Marlink et al., 1994). Since the beginning of the AIDS pandemic, HIV-1 has infected an estimated 60 million people, whereas HIV-2 has infected approximately 1 million people (*UNAIDS*, 2008).

The human immunodeficiency viruses originate from several zoonotic transmissions of Simian Immunodeficiency Viruses (SIV) into the human host. HIV-1 viruses are of chimpanzee origin and comprise of four distinct lineages named group M, N, O and P which emerged as a result of four independent cross-species transmissions (Sharp and Hahn, 2011). The first HIV-1 virus to be discovered belonged to group M (Barre-Sinoussi et al., 1983) and viruses from this group are responsible for >98% of human infections worldwide (Sharp and Hahn, 2011). By contrast, group N, which was discovered in Cameroon, resulted in only 13 cases to date (Simon et al., 1998). Groups M and N originate from direct transmissions of SIV_{cpz} into humans. On the other hand, group O and P are of gorilla origin. Phylogenetic analysis reveals that HIV-1 groups and SIV_{gor} cluster with SIV_{cpz}, thus chimpanzees are thought to be the reservoir of human and gorilla infections. Group O was discovered in 1990 (De Leys et al., 1990) and causes less than 1% of the total HIV-1 infections worldwide (Peeters et al., 1997), and group P was very recently discovered and there are only 2 known cases (Plantier et al., 2009). Exactly how humans acquired the ape strains of virus is currently unknown, however it is thought that

the transmission events occurred during bushmeat hunting exercises, whereby infected ape blood or bodily fluids entered via the cutaneous route or through mucus membranes (Peters 2002). HIV-2 is largely restricted to West Africa (de Silva et al., 2008), where it infects approximately 1-2 million people (Visseaux et al., 2016). However, surveillance data suggest that HIV-2 infections are on the decline and are being replaced by HIV-1 (Berry et al., 2002; Olesen et al., 2018; van der Loeff et al., 2006). Like HIV-1, HIV-2 is also separated into 9 distinct lineages named group A-I which result from zoonotic transmission of SIV_{smm} from sooty mangabeys (Ayouba et al., 2013). The majority of HIV-2 infections belong to groups A and B, thus they have better transmission rates compared with HIV-2 groups C-I (Visseaux et al., 2016). The sporadic nature of emergence of groups C-I suggest that these represent dead-end transmission which could not be perpetuated in the human population (Jin et al., 1994). **Figure 1.1** summarises the zoonotic events resulting in the emergence of HIV-1 and HIV-2.

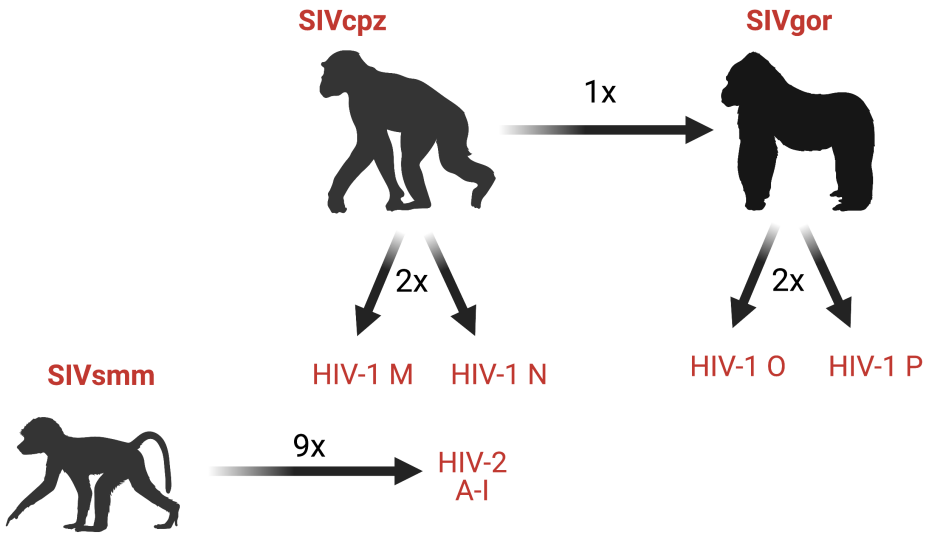

Figure 1.1 Zoonotic transmissions and origins of HIV. SIV_{cpz} was transmitted to humans on two separate occasions to give HIV-1 groups M and N, and once to gorillas to give rise to SIV_{gor}. SIV_{gor} was transmitted to humans during two separate zoonotic events to give HIV-1 groups O and P. Finally, SIV_{smm} was transmitted to humans to give HIV-2 groups A-I. Adapted from (Sauter & Kirchhoff, 2019).

1.1.2 Transmission

There are various routes of HIV transmission which facilitate exchange of contaminated bodily fluids between people. For example, sexual transmission, percutaneous inoculation and mother to child transmission, which is further divided into placental transmission, contact with contaminated maternal blood, genital secretions during birth and contaminated breastmilk. A number of virological and immunological factors affect the rate of successful person to person transmission.

Analysis of viral variability shows that HIV infected individuals have highly diverse quasi-species present in the body. However, during transmission, very few HIV strains infect the recipient host (Joseph et al., 2015; Shaw and Hunter, 2012). For example, heterosexual transmission results in only a single variant being responsible for the newly established infection, referred to as the transmitted/founder virus (T/F) (Abrahams et al., 2009; Derdeyn et al., 2004; Haaland et al., 2009; Keele and Derdeyn, 2009; Keele et al., 2008). This reduction in viral diversity is thought to be due to a transmission bottleneck. It is thought that a breach of the physical mucosal barrier allows for successful viral transmission (Kariuki et al., 2017; Tully et al., 2016). Emerging evidence also suggests that viral determinants are important in overcoming the transmission bottleneck. Comparative studies between T/F and chronic viruses reveal that there are several genotypic and phenotypic differences between them. For example, the Env glycoproteins of T/F viruses are less glycosylated (Derdeyn et al., 2004; Gnanakaran et al., 2011; Ping et al., 2013), have shorter variable loops (Curlin et al., 2010; Sagar et al., 2006), maintain a compact structure, are less sensitive to neutralising antibodies (Chohan et al., 2005; Liao et al., 2013; Nie et al., 2014) and almost exclusively use the CCR5 co-receptor (Joseph et al., 2015; Keele and Derdeyn, 2009). It is likely that Type I interferons provide a selective pressure on T/F viruses to evade early defences of the innate immune response. Therefore, T/F viruses are generally resistant to Type I Interferons, suggesting that they are able to overcome immune pressures at the point of initial infection (Fenton-May et al., 2013; Foster et al., 2016; Iyer et al., 2017; Parrish et al., 2013).

1.1.3 Clinical course of infection and pathogenesis

The primary targets of HIV and SIV infection *in vivo* are CD4 T cells, macrophages and a subset of dendritic cells (Alkhatib et al., 1996; Kaur et al., 1998; Maddon et al., 1986; Smed-Sorensen et al., 2005). HIV infection causes progressive immunodeficiency over time in untreated individuals. Laboratory tests commonly used to determine a patient's level of immunosuppression include measuring the CD4 T cell count and the patient's plasma viral load. A wide variety of viral markers are reliably used to determine the 'Fiebig Staging' of a patient (**Fig. 1.2**) (Fiebig et al., 2003). This staging system separates

the infection into six phases. Immediately after transmission, there is a time lag of 7-21 days where the virus establishes infection at the exposure site, before entering the blood, and this is known as the 'eclipse' phase. Once the virus enters the systemic circulation and the lymph nodes, an acute phase is initiated whereby rapid viral replication and spread occurs. This is when an increase in plasma viral load is observed. Here, there is an exponential increase in HIV RNA levels and as the Fiebig stages progress, other viral antigenic markers such as HIV p24 antigen begin to appear. Also, a key immunological marker of the acute phase of HIV infection is the rapid depletion of CD4 T cells. Evidence suggests that both infected and uninfected bystander cells die at this stage (reviewed by(Doitsh and Greene, 2016). When a patient's CD4 T cell count is less than 200/mm^3 they are clinically classified as having AIDS (WHO, 2005). Once HIV-1 infects a target cell, it can either establish active infection, replicate and spread or it can enter a long-lived quiescent state called viral latency. Latently infected cells contain stably integrated, replication competent proviruses that are repressed by various mechanisms (Archin et al., 2014). HIV-1 latency is preferentially established in resting memory CD4 T cells (Dahabieh et al., 2015), microglia cells (Davis et al., 1992) and monocytes/macrophages (Abbas et al., 2015), all of which have a long half-life *in vivo*. The state of HIV-1 latency is reversible, however recent evidence suggest that the majority of latent proviruses are defective and therefore cannot establish infection in the case of reactivation (Bruner et al., 2016; Bruner et al., 2019).

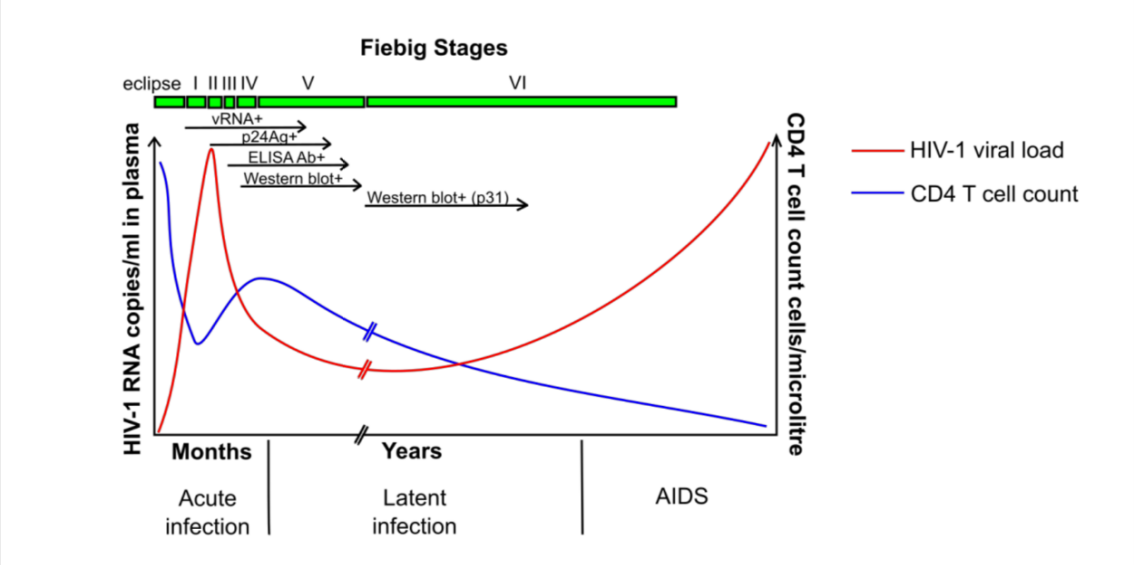

Figure 1.2 Fiebig staging of HIV-1 disease. HIV-1 infection can be classified into one of six Fiebig stages based on the appearance of viral RNA (vRNA), viral capsid (p24Ag) and virus-specific antibody detectable by ELISA (ELISA Ab) or western blot. HIV-1 infection can also be broadly divided into 3 stages, acute infection, latent infection and AIDS (Adapted from (Shaw & Hunter, 2012).

Whilst the laboratory tests are reliable and commonly used in high- and middle-income settings, the majority of infections are found in resource-limited settings where there is a lack of adequate laboratory facilities to test the entire infected population and for continued monitoring. For better surveillance in these settings, the WHO has introduced a clinical staging system which is divided into four parts and clinicians can decide the staging purely based on the patient's clinical manifestations (Jennifer et al., 2010). Stage one is an asymptomatic stage where patients have generalised lymphadenopathy. Stage two is mildly symptomatic and the patient's weight loss is equivalent to less than 10% of their total body weight. At this stage people also have recurrent respiratory and dermatological infections. Stage three is moderately symptomatic, where patients have weight loss greater than 10% of their total body weight and prolonged periods of opportunistic infections. Finally, stage four is the severely symptomatic stage where patients often manifest with HIV associated cancers such as B-cell non-Hodgkin lymphoma. HCMV infection of multiple organs is also indicative of AIDS development. Comparison of this WHO clinical staging system to the Fiebig staging system, shows that it is indeed an accurate way to manage HIV infected patients in low-income countries (Malamba et al., 1999; Lynen et al., 2006; Kagaayi et al., 2007).

1.1.4 Antiretroviral therapy

Antiretroviral Therapy (ART) was first introduced in 1987 as a monotherapy treatment, using the drug Zidovudine/AZT (Furman et al., 1986). Monotherapies were less efficacious due to the emergence of viral drug resistance (Larder et al., 1995), so in 1996, combination therapy (cART) was introduced. This strategy includes administering three antiretroviral drugs which target key viral enzymes, in order to overcome the high mutational rate of HIV-1 which leads to the emergence of viral escape mutants (Autran et al., 1997). ART is highly effective in almost completely suppressing viral replication, below the limit of detection of viral RNA in blood (<50 copies/ml of plasma) and this significantly restores the CD4 T cell numbers in infected individuals (Cihlar and Fordyce, 2016). This in turn slows down the rate of disease progression to AIDS, such that infected individuals who have access to these drugs have normal life expectancy (Trickey et al., 2017). Currently, ART can be divided into seven drug classes: nucleoside reverse transcriptase inhibitors (NRTIs); non-nucleoside reverse transcriptase inhibitors (NNRTIs); protease inhibitors (PIs); fusion inhibitors; CCR5 antagonists; post-attachment inhibitors and integrase strand transfer inhibitors (INSTIs). These drugs target multiple steps of the viral lifecycle, hence increasing the likelihood of successfully targeting the virus. First, nucleotide reverse transcriptase inhibitors (NRTIs) are dNTP analogues targeting the active site of reverse transcriptase (RT) and thus inhibiting reverse transcription by causing premature chain termination (St Clair et al., 1987).

Second, non-nucleotide reverse transcriptase inhibitors (NNRTIs) bind to RT proximal to the active site, inducing a conformational change and thus inhibiting the enzyme (Kohlstaedt et al., 1992). Third, protease inhibitors (PIs) prevent Gag polyprotein cleavage and virion maturation, thus producing non-infectious viral particles (Kempf et al., 1995). Fourth and most recent are integrase inhibitors (INIs), which inhibit DNA strand transfer reaction and thus prevent viral integration into host DNA (Espeseth et al., 2000). Fusion inhibitors and CCR5 blockers are not routinely used.

ART is also being used to prevent HIV-1 transmission. Pregnant women are prescribed specific ART regimes and drugs are used to prevent mother to child transmission in Post Exposure Prophylaxis (PEP) (Chacko et al., 2012) and as Pre-exposure prophylaxis (PrEP) to stop transmission in high-risk groups (Wilton et al., 2015). Importantly, ART does not cure infection due to the presence of a latent viral reservoir which remains undetected since active viral replication is not occurring, although some individuals do show 'blips' in which there is some detectable viral RNA in blood but this is efficiently suppressed with treatment (Pitman et al., 2018). As a result, treatment interruption results in rapid viral rebound and disease progression (Cihlar and Fordyce, 2016).

1.1.5 HIV-2 infection

HIV-2 has very similar biology to HIV-1 including mode of transmission, cell tropism and the ability to cause AIDS. However, the probability of disease progression to AIDS is much lower upon HIV-2 infection compared with HIV-1 (Marlink et al., 1994; Nyamweya et al., 2013; Olesen et al., 2018). HIV-2 also enters cells using the CD4 receptor but does have an expanded coreceptor usage by comparison with HIV-1. In addition to the CCR5 and CXCR4 coreceptors used by HIV-1, HIV-2 also exploits CCR1, CCR2, CCR3, CCR8 and CXCR6 (Shi et al., 2005). A characteristic feature of HIV-2 infection is low viral transmission rates, likely due to lower viral loads in infected individuals (Gottlieb et al., 2006; Popper et al., 2000). In line with this, HIV-2 infected individuals usually present with undetectable plasma viral loads (Popper et al., 2000; Soriano et al., 2000; van der Loeff et al., 2010), possibly reflective of better immune control. Indeed, HIV-2 infected individuals have a stronger innate, T cell and humoral immune responses which collectively suppress viral replication (Duvall et al., 2007; Duvall et al., 2008; Nuvor et al., 2006; Rodriguez et al., 2007). Together, this leads to fewer people with chronic immune activation (Hanson et al., 2005), hence fewer people with morbidity and more infected individuals become long term non-progressors (Jaffar et al., 1997; Marlink et al., 1994; Olesen et al., 2018; Thiebaut et al., 2011; van der Loeff et al., 2010). Treatment of HIV-2 infection is similar to HIV-1, however NNRTIs are not used since the drugs are inactive against HIV-2 RT (Peterson and Rowland-Jones, 2012).

1.1.6 SIV infection

Species specific strains of Simian Immunodeficiency Virus (SIV) have been infecting their natural hosts, the African non-human primates, for thousands of years. SIV infection of a natural host typically does not cause disease or progression to AIDS, despite high viral replication and neither is chronic immune activation present in infected monkeys (reviewed by (Chahroudi et al., 2012; Sharp and Hahn, 2011)). The majority of evidence for this statement comes from *in vivo* studies in the sooty mangabeys and African green monkeys. Several factors contribute to the low pathogenesis and the absence of chronic immune activation. Firstly, the number of healthy peripheral CD4 T cells remains high despite high viral loads (Silvestri et al., 2003) and T cell regeneration is unaffected (Paiardini et al., 2009), therefore there is no apparent immunodeficiency observed *in vivo*. Next, lymph nodes are important sites of viral replication and pathogenesis and histological studies of infected lymph node biopsies show that the architecture and function of SIV infected lymph nodes remain unaffected, consistent with the observation that T cell distribution is unaffected (Silvestri et al., 2003). Further, there is limited SIV infection of central memory CD4 T cells which also acts to preserve T cell homeostasis and lymphoid tissue architecture (Klatt et al., 2008; Paiardini et al., 2011). Next, the innate immune response initially established upon SIV infection is rapidly resolved and therefore there is limited immunopathology (Bosinger et al., 2009; Jacquelin et al., 2009; Lederer et al., 2009). Also, maintenance of the mucosal integrity and gut Th17 cells means that there is little to no microbial translocation, which is thought to be an important determinant of AIDS progression in HIV infection (Brenchley et al., 2008; Brenchley et al., 2006; Favre et al., 2009; Pandrea et al., 2007). Finally, the accessory protein, Nef downmodulates CD3-T cell receptor (TCR) from the cell surface to prevent excessive T cell activation and T cell death (Schindler et al., 2006). This important function of Nef is not present in the SIVcpz/HIV-1 lineage and a recent study used chimeric HIV-1 constructs expressing Nef proteins which can and cannot downmodulate CD3 from the cell surface to show that CD3 retainment leads to more efficient viral spread (Mesner et al., 2020). This is attributed to an increase in the amount of Env present at the cell surface and incorporated into virions. However, it was also shown that CD3 retention at the cell surface leads to increased T cell activation and T cell death (Mesner et al., 2020), thereby suggesting that most SIVs downmodulate CD3 in order to prevent pathogenesis.

Cross-species transmission of SIV often results in the ability of the virus to cause disease in a new host species. For example, the SIV_{mac} virus arose by infecting rhesus macaques with SIV_{smm}, which was originally found in Sooty mangabeys and does not cause disease. However, SIV_{mac} causes AIDS-like disease in the rhesus macaques, suggesting

that adaptations in the rhesus macaque host resulted in increased pathogenicity (Apetrei et al., 2005; Apetrei et al., 2006; Daniel et al., 1985). Further, natural zoonoses of SIV into the human host resulted in the emergence of HIV-1 and HIV-2 viruses, with HIV-1 group M being largely responsible for the global AIDS pandemic (Hahn et al., 2000).

1.2 HIV structure and lifecycle

This section discusses the lentiviral life cycle, using HIV-1 as an example. As shown in **Figure 1.3**, HIV-1 must complete a series of steps in its life cycle in order to replicate: (1) receptor and coreceptor binding, fusion and entry into host cell cytoplasm; (2) reverse transcription of viral genome, capsid uncoating, nuclear import and integration; (3) viral gene expression; (4) virion assembly, budding and maturation.

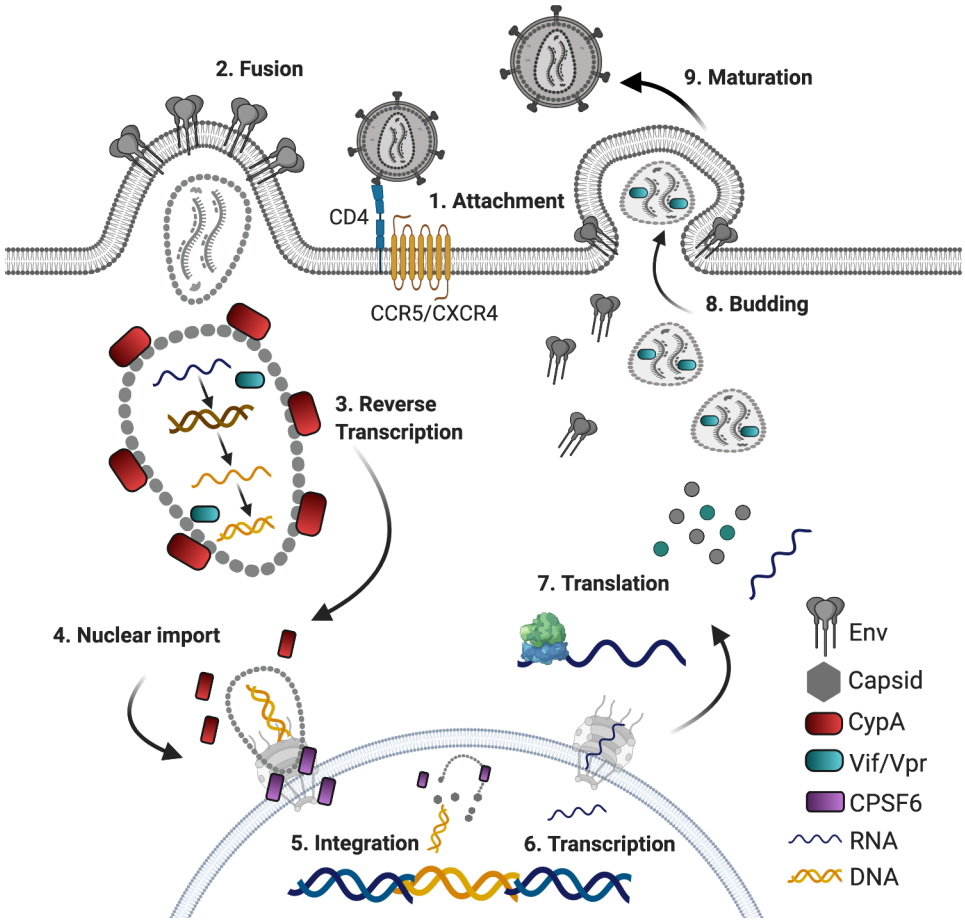

Figure 1.3 HIV-1 lifecycle. The HIV-1 life cycle is a complex series of interactions with the host cell machinery and immune evasion strategies that allow successful infection, replication and transmission. To enter cells HIV engages its envelope glycoprotein gp120 with cell surface protein CD4 and a co-receptor (CXCR4 or CCR5). Upon fusion, the capsid core is released into the cytoplasm. Capsid recruits cellular proteins cyclophilin A (red) and CPSF6 (purple), likely to prevent detection of the viral reverse transcribed products by DNA sensors. The virus reverse transcribes RNA into DNA, which is integrated into the cellular genome. Once integrated the provirus may become latent. Transcription and translation of the provirus results in viral proteins that assemble at the cell surface. Immature virions are released and incorporate envelope glycoproteins (Env) in the process. Finally, during maturation, the protease enzyme cleaves the structural polyprotein to form mature Gag proteins, resulting in the production of new infectious virions. (Created using Biorender.com)

1.2.1 Virion and genome structure

Mature HIV-1 virions are spherical particles measuring 100nm (Briggs et al., 2003) and are surrounded by 7-12 envelope glycoprotein trimers (Env) embedded within a host cell derived lipid bilayer (Chojnacki et al., 2012; Linde et al., 2013; Zhu et al., 2003). Directly under the lipid bilayer is a layer of matrix proteins (MA). Under this layer, is a conical capsid (CA) shell containing two copies of the positive sense single-stranded RNA. Each RNA molecule is 9.4kB long. The RNA molecules are bound to two essential viral enzymes: integrase (IN) and reverse transcriptase (RT). Additionally, the viral accessory protein, Vpr, is also packaged into virions (reviewed in (Freed, 2015)).

The HIV-1 genome contains 9 open reading frames that encode 14-15 viral proteins depending on viral lineage. Transcription of viral genes is driven by long terminal repeats (LTRs), which are found at the 5' and 3' ends of the genome (Burnett et al., 2009). Several transcription factors, such as NFκB, are able to bind to LTRs, leading to regulation of viral and host gene expression (Pereira et al., 2000). The structural and enzymatic genes are *gag*, *pol* and *env*, all of which are common to retroviruses. *Gag* encodes a polyprotein called p55, which is processed by the viral protease enzyme, into 6 proteins: matrix (p17/MA), capsid (p24/CA), nucleocapsid (p7/NC), p6 and spacer peptide 1 and 2. These proteins are vital for virion formation and structure. *Pol* encodes the key viral enzymes: reverse transcriptase (RT), integrase (IN) and protease (PR). A Gag-Pol precursor is formed in a 1:20 ratio to Gag, due to ribosomal frameshift and this ensures incorporation of RT, IN and PR into virions (Jacks et al., 1988). *Env* encodes the precursor protein gp160, which is proteolytically cleaved to form the surface subunit, gp120, and the transmembrane subunit, gp41 (Hallenberger et al., 1992). Further, the genome encodes two regulatory proteins, *Tat* and *rev*, which enable transcription and translation of the viral genome, as well as at least 3 accessory proteins *vif*, *vpr* and *nef*, which are necessary for efficient replication *in vivo*. Some lentiviruses also encode *vpu* or *vpx* accessory genes, as described below. Functions of all the viral proteins will be explored in detail whilst explaining the viral lifecycle.

Acquisition and loss of accessory genes, *vpu* and *vpx*, allows lentiviruses to be categorised into 3 groups (**Fig. 1.4**). The first group of viruses include HIV-1, SIVcpz, SIVgor and the SIVgsn/mon/mus lineage which encode *vif*, *vpr*, *nef* and *vpu* genes. It is thought that the *vpu* gene is in the HIV-1/SIVcpz lineage due to a recombination event between SIVrcm and the SIVgsn/mon/mus lineage (Bailes et al., 2003). The second group contains a *vpx* gene rather than *vpu* and includes two related lineages: (1) HIV-2, SIVsmm and SIVmac and (2) SIVrcm/drl infecting drills and SIVmnd2 (Etienne et al., 2013). The emergence of *vpx* has likely occurred due to a duplication event of *vpr* gene

(Tristem et al., 1990). Phylogenetic analysis shows that *vpx* emerged prior to the separation of the HIV-2/SIVsmm and SIVrcm/drl lineages and was perhaps lost in the HIV-1/SIVcpz lineage during the recombination event mentioned above. Finally, the third group of SIVs only contain *vif, vpr* and *nef* genes (Sauter and Kirchhoff, 2019).

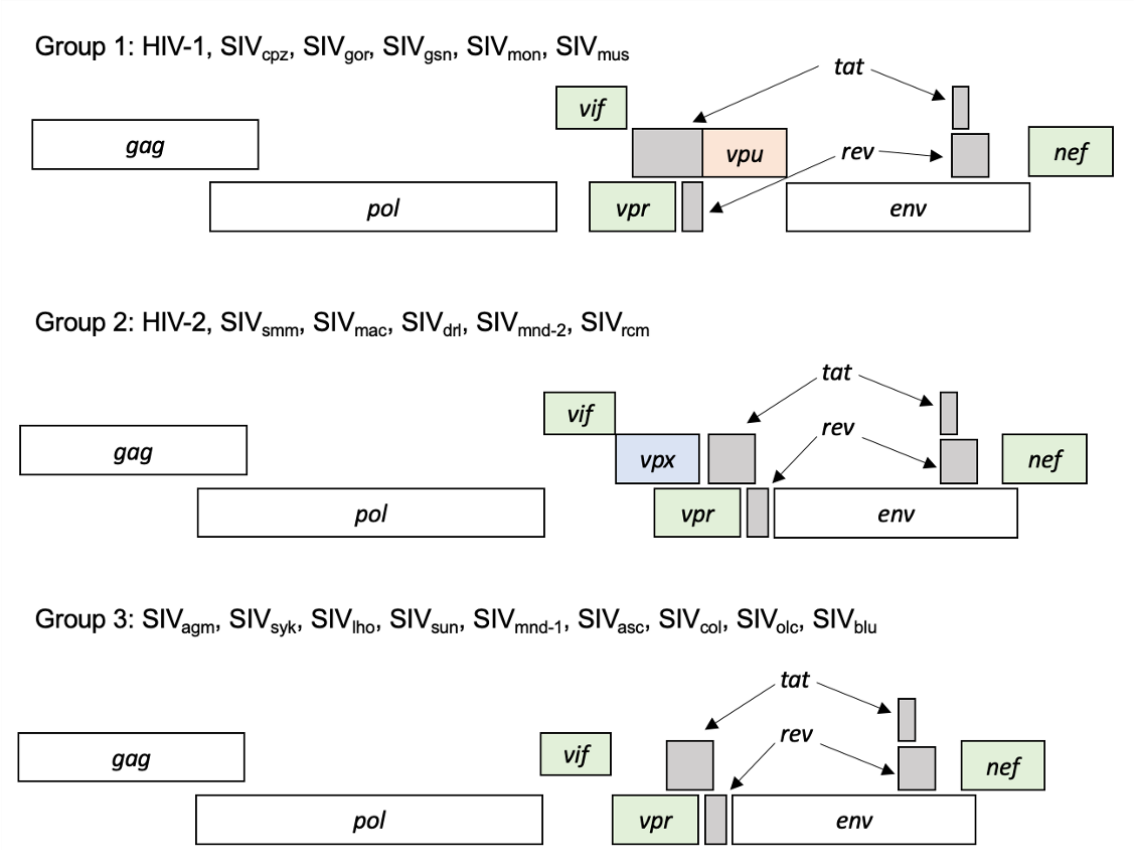

Figure 1.4 Genomic organisation of primate lentiviruses. The structural and enzymatic genes (*gag*, *pol* and *env*) are shown in white and are common to all retroviruses. The regulatory genes *Tat*and *rev* common to all primate lentiviruses are shown in grey. The accessory genes *vif*, *vpr*, and *nef* are also common to all primate lentiviruses and are shown in green. *Vpu* gene (orange) is only found in the HIV-1/SIVcpz lineage and closely related SIVgsn/mon/mus infecting Cercopithecus monkeys. *Vpx* gene (blue) is only found in the HIV-2/SIVsmm and related SIVrcm/drl/mnd2 linages. Adapted from (Sauter and Kirchhoff, 2019).

1.2.2 Entry and fusion

HIV-1 entry into target cells is a complex process. Evolving microscopy and spectroscopy techniques, as well as increasing structural data on HIV-1 Env, has aided better understanding of the process of fusion (**Figure 1.5**). The first step of viral entry is binding of Env to the CD4 receptor on target cells. Although Env exists as a trimer at the cell surface, the probability of three Env-CD4 interactions occurring simultaneously is low and this requirement would make viral entry an inefficient process. Instead, evidence suggests that a single Env-CD4 interaction may be sufficient for successful entry (Yang et al., 2005), although this remains controversial (Brandenberg et al., 2015a). Env-CD4 interactions lead to conformational changes in Env variable loops (discussed extensively in **section 1.3.2.2**), resulting in the formation of a bridging sheet, adopting a 4-stranded β sheet structure and exposure of the coreceptor binding site (Kwong et al., 1998). Next, CCR5 or CXCR4 coreceptor binds to the Env-CD4 complex. This interaction does not induce further conformational changes in gp120, although the V3 loop changes position (Shaik et al., 2019). Iliopoulou and colleagues (2018) suggest that oligomerisation of co-receptors may play an important role at this stage (Iliopoulou et al., 2019). After CD4 binding, the gp41 α-6 helix shifts away from gp120 and creates a pocket which is filled by the fusion peptide (Ozorowski et al., 2017). Intrinsic changes lead to exposure of the fusion peptide, which immediately inserts into the target cell membrane (Chan et al., 1997). It is thought that the coreceptor regulates this process, as CCR5 binding can bring the trimer closer to the target cell membrane, at a distance which is short enough for the fusion peptide to insert into the target cell membrane (Pancera et al., 2014). Concomitantly, the interactions between gp120 and gp41 weaken, leading to gp120 dissociation and shedding. The next step is 6-helix bundle formation, where the fusion peptide from three gp41 subunits fold to bring the viral and target cell membrane in close proximity. Eventually, the fusion pore is created, and the capsid core is delivered to the cell cytoplasm (Melikyan, 2008). It is thought that CCR5 may anchor and synchronise several Env-CD4-coreceptor complexes to increase the efficiency of this final step (Chen, 2019).

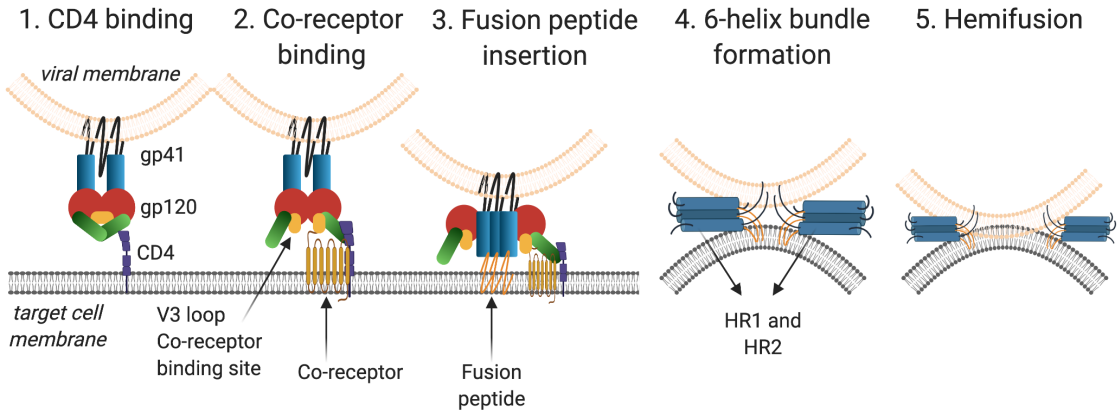

Figure 1.5 HIV-1 fusion mechanism overview. (1) CD4 binding to gp120 induces conformational changes, particularly in V1 and V2 loops, opening up the trimer and exposing the V3 loop. (2) Co-receptor binding site is exposed leading to either CCR5 or CXCR4 binding. Co-receptor binding stabilises the open CD4-bound conformation and anchors the Env in close proximity to the host cell membrane. (3) CD4 binding also induces gp41 refolding resulting in fusion peptide insertion into the host cell membrane and dissociation of gp120 subunits. (4) HR1 and HR2 domains from each trimer fold together to form a six-helix bundle. (5) The two membranes are forced into close proximity and lipid mixing results in hemifusion. Finally, the fusion pore forms and the HIV-1 capsid core is delivered into the target cell cytoplasm. Adapted from (Doms and Moore, 2000). (Created using Biorender.com).

1.2.3 Reverse transcription, integration and gene expression

Following fusion, the HIV-1 capsid (CA) core is delivered into the host cell cytoplasm. Each capsid core contains two copies of the positive sense single stranded RNA genome, as well as reverse transcriptase (RT), integrase (IN) and protease (PR) enzymes which are vital for the following steps in the viral life cycle.

1.2.3.1 Reverse transcription

The HIV-1 capsid core is a conical shape, composed of approximately 250 hexamers and 12 pentamers (Ganser et al., 1999; Pornillos et al., 2011). The process of reverse transcription is unique to the *Retroviridae* family. In 1970, two independent labs first discovered the reverse transcriptase enzyme (RT) (Baltimore, 1970; Mizutani et al., 1970). It is composed of two key enzymes called DNA polymerase II and RNase H, found in the p66 domain (Lightfoote et al., 1986). Initiation of HIV-1 transcription requires the host tRNA, Lys3, to act as a primer for the DNA Polymerase (Wayne-Hobson and Montagnier, 1986). This tRNA has a 3' end which is complementary to the 5' primer binding site on the viral RNA (Isel et al., 1996). DNA synthesis creates DNA:RNA hybrids. RNAse H recognises this hybrid structure and degrades the 5' end of the viral RNA. This leaves a newly synthesised minus-strand DNA. Next, the process of first strand transfer occurs. The 3' and 5' end of the viral RNA are repeats and so the newly synthesised DNA is transferred to the 3' end of the viral RNA for minus-strand synthesis (Panganiban and Fiore, 1988). As the DNA polymerase proceeds with DNA synthesis, RNase H concomitantly degrades the viral RNA which is no longer required as a template. Once RNase H reaches the poly purine tract (a sequence of RNA which is rich in purines), it cannot degrade this section of the RNA. Therefore, the poly purine tract acts as a primer for the synthesis of the plus strand of DNA (Hungnes et al., 1992). During DNA synthesis, the 3' $tRNA_{Lys3}$ is also copied in the DNA, hence RNase H removes the first nucleotide of this tRNA to leave just an A at the 5' end (Pullen et al., 1992; Smith and Roth, 1992; Whitcomb et al., 1990). This initiates second strand transfer. Both the plus and minus strands of DNA synthesis is completed to produce double-stranded viral DNA with LTRs on either end (reviewed by (Hu and Hughes, 2012).

1.2.3.2 Uncoating

In order for viral DNA to integrate into the host genome, it must first traverse the cytoplasm and then cross the nuclear membrane. Since lentiviruses infect non-dividing cells, nuclear envelope breakdown is not a prerequisite for infection (Yamashita and Emerman, 2006). Instead, nuclear import occurs via nuclear pore complexes (NPC), which are ring-like structures composed of proteins known as nucleoporins. The process of uncoating and reverse transcription are thought to be coupled. Atomic force

microscopy suggests that during *in vitro* transcription, the production of newly synthesised DNA can exert pressure on the inner capsid core, leading to uncoating (Rankovic et al., 2018; Rankovic et al., 2017). In 2016, Jacques and colleagues showed that the N-terminal β-hairpin structures in CA can regulate the opening and closing of a pore/channel formed at the centre of each capsid hexamer (Jacques et al., 2016). This pore is composed of six positively charged arginine residues at CA position 18. The positively charged arginine ring can attract negatively charged dNTPs and lead to their import into the CA core for initiation of reverse transcription.

The exact spatiotemporal organisation of capsid disassembly and reverse transcription remains controversial. Several models of uncoating have been proposed thus far, based on live cell, single molecule tracking of HIV-1 particles: (1) gradual uncoating with concomitant reverse transcription during cytosolic trafficking (Mamede et al., 2017); (2) reverse transcription occurs within an intact capsid core, followed by uncoating at the NPC (Francis and Melikyan, 2018) and (3) several spatially separated uncoating steps that are completed inside the nucleus (Burdick et al., 2020). Early studies suggested that the process of capsid disassembly or 'uncoating' and reverse transcription occurs in the cytoplasm, immediately following fusion and entry into target cells. This hypothesis was supported by the observation that there are low levels of CA molecules associated with the reverse transcription complex (RTC) and the pre-integration complex (Farnet and Haseltine, 1991; Fassati and Goff, 2001; Miller et al., 1997; Nermut and Fassati, 2003). Further, CA protein mutations Q63A/Q67A, result in inefficient dissociation from the RTC, which blocks infection at the level of nuclear import and integration (Dismuke and Aiken, 2006), suggesting that capsid lattice dissociation is required for successful infection. Also, live cell imaging of single viral particles in cell lines, primary macrophages and T cells revealed that uncoating takes place approximately 30 mins after entry (Mamede et al., 2017). Cytoplasmic uncoating and exposure of RT DNA was incompatible with the emerging literature on cytosolic DNA sensors such as cGAS and IFI16 (Lahaye et al., 2013; Rasaiyaah et al., 2013) that had been shown to sense HIV-1 DNA. This led to the hypothesis by a number of groups that uncoating in the cytoplasm was unlikely or disadvantageous for HIV-1. The discovery of TRIM5α and TRIM-CypA being able target capsids, suggest that the capsid must stay intact, or at least partially intact, in the cytoplasm (Forshey et al., 2005; Kutluay et al., 2013; Li et al., 2016; Sayah et al., 2004; Sebastian and Luban, 2005; Shi and Aiken, 2006; Stremlau et al., 2004; Stremlau et al., 2006).

This is in line with the second hypothesis which suggests that CA molecules are not shed from the RTC and the intact capsid core docks at the nuclear pore (Francis and Melikyan,

2018). A long-standing view with regards to capsid import into the nucleus was that the average diameter of an intact HIV-1 capsid core (60nm) is bigger than the inner diameter of an NPC (~40nm) (von Appen et al., 2015), therefore it was thought that early uncoating must precede nuclear import, in order to allow the viral genome to enter the nucleus. However, a recent study combining 3D cryoET and cryoEM revealed that NPCs in T cells can dilate enough to allow an intact capsid core to enter through the NPC (Zila et al., 2021). Indeed, nuclear import blockade studies suggest that nuclear import occurs in less than 5h and precedes the completion of reverse transcription (Dharan et al., 2020). HIV-1 remains susceptible to the capsid destabilising drug PF74, following nuclear import, suggesting that reverse transcription is completed in the nucleus (Dharan et al., 2020). In line with this, Burdick et al (2020) analysed HIV-1 uncoating by direct labelling of CA with GFP and found that intact, or partially intact, cores entered the nucleus using the host cofactor CPSF6 (Burdick et al., 2020). Kinetics of nuclear import studies suggest that uncoating occurs less that 1.5h prior to integration (Burdick et al., 2020). Taken together, it seems likely that the processes of capsid uncoating and reverse transcription are completed inside the nucleus, which provides the added benefit of keeping the viral genome shielded from innate immune responses (Lahaye et al., 2013; Rasaiyaah et al., 2013).

Capsid is an important determinant of nuclear entry and integration site selection (Achuthan et al., 2018; Lewinski et al., 2006; Schaller et al., 2011). This is partly explained by the sequential binding of HIV-1 cofactors to CA. First, Cyclophilin A (CypA) is recruited to the capsid core upon entering into the cytoplasm. CypA binds to the N-terminal domain of CA at the CypA binding loop (Gamble et al., 1996) and enhances HIV-1 infection in a cell type dependent manner (Hatziioannou et al., 2005; Kim et al., 2019; Towers et al., 2003). Whether CypA has a role in the process of capsid uncoating remains controversial. There is some evidence to suggest that CypA binding stabilises the conical capsid structure, whereas other evidence suggests that CypA binding destabilises it (Fricke et al., 2013; Liu et al., 2016). Importantly, disruption of CA-CypA binding using CA mutants (P90A) and Cyclophilin inhibitors (Cyclosporines), shows that viral genome is sensed by cytoplasmic DNA and RNA sensors (Rasaiyaah et al., 2013). This induces an innate immune sensing response. Therefore, CypA binding is thought to be an innate immune evasion strategy (Rasaiyaah et al., 2013). HIV-1 CA mutants (P90A and G89V) which cannot bind the cofactor CypA, are imported into the nucleus independently of Nup358 and Nup153, leading to integration into high gene density regions, unlike WT HIV-1 (Schaller et al., 2011).

Once HIV-1 reaches the nuclear membrane, it interacts with multiple Nups to facilitate nuclear import (Kane et al., 2018). Nup358 is a component of the NPC which interacts with CA via its cyclophilin-like domain, which provides further evidence that the capsid stays intact or at least partially intact during nuclear import as suggested above. This probably results in CypA displacement by Nup358 on CA molecules (Bichel et al., 2013). Nup358 is present on the cytoplasmic side of the NPC and binding allows HIV-1 to dock at the nuclear rim in order to undergo uncoating and/or nuclear import. On the nuclear side of the NPC, Nup153 interacts with the capsid core at an interface between two CA molecules (Price et al., 2014). Nup153 contains FG (phenylalanine-glycine) repeats which bind to the N-terminal domain of one CA monomer and binds to the hinge between the N- and C-terminal domains of the adjacent CA monomer (Matreyek et al., 2013). This suggests that some of the capsid core remains intact during nuclear import, consistent with IF and cryoEM studies (Burdick et al., 2020; Chin et al., 2015; Peng et al., 2014; Zila et al., 2021). TNPO3 is another host factor which binds CA and is required for efficient HIV-1 integration, since knockdown of TNPO3 resulted in diminished HIV-1 integration (Brass et al., 2008; Krishnan et al., 2010; Shah et al., 2013; Zhou et al., 2011). Once in the nucleus, Nup153 is displaced by cleavage and polyadenylation specificity factor 6 (CPSF6) (Price et al., 2014). CPSF6 binding was shown to be crucial for efficient nuclear import and optimal viral integration into gene-dense, transcriptionally active regions in the host chromatin (Achuthan et al., 2018; Bejarano et al., 2019; Lee et al., 2010; Price et al., 2012; Schaller et al., 2011). 3D immuno-DNA fluorescence in situ hybridization (FISH) was used to visualize gene positioning in resting and activated $CD4^+$ T cells, which revealed that the CA mutant N74D, which cannot bind CPSF6, is targeted to integration sites near the nuclear envelope, where the majority of the host genome is transcriptionally inactive. Like the CypA CA mutants, these mutants also enter the nuclear pore independently of Nup358 and Nup153. Thus, nuclear pore proteins play a crucial role in targeting HIV-1 to transcriptionally active regions of host DNA.

1.2.3.3 Integration

HIV-1 integration is the process by which newly synthesised viral DNA is inserted into the host chromatin and preferentially integrates into highly gene dense and transcriptionally active areas of chromatin. The viral IN enzyme is composed of three domains: an N-terminal zinc binding domain which is required for oligomerisation and catalytic activity; a ‘HHCC’ motif which binds to zinc ions and resembles zinc coordinating ions in a zinc finger; a central catalytic core domain (CCD) which also has catalytic activity and binds DNA and finally the C- terminal domain (CTD) which binds DNA and aids dimerisation of parallel monomers (Lusic and Siliciano, 2017).

As soon as reverse transcription is complete, the newly synthesised viral DNA binds to IN and other proteins to form a higher order structure called the pre-initiation complex (PIC), which probably has some CA molecules attached too, as discussed above. The PIC enters the nucleus through the NPC and preferentially integrates into host chromatin with high gene density and transcriptional activity (Barr et al., 2006; Demeulemeester et al., 2015; Han et al., 2004; Lewinski et al., 2006; Mitchell et al., 2004; Schroder et al., 2002; Sherrill-Mix et al., 2013). However, it might be possible for HIV-1 DNA to integrate into other areas of chromatin too. For example, the latent reservoir of HIV-1 is thought to be localised in transcriptionally silent areas of chromatin, in resting CD4 T cells (Chun et al., 1998; Chun et al., 1997; Finzi et al., 1997; Siliciano et al., 2003). Exactly how the heterochromatic status of the provirus is established is currently unknown. It is possible that the provirus directly integrates into heterochromatin, since studies in the Jurkat T cells latency model (J-LAT cells) showed that the surrounding chromatin structure regulates transcriptional control (Jordan et al., 2003). However, meta-analysis studies could not show a correlation between latency and known transcriptional regulatory genomic features when comparing different models of integration (Sherrill-Mix et al., 2013). Another possibility is that the virus initially infects an activated cell and integrates into high density and transcriptionally active regions, then the cell transitions to a resting state, due to which the integration site becomes repressed due to the deposition of histone repressive marks (reviewed by (Siliciano and Greene, 2011)). Integration site selection is determined by several factors including nuclear entry route, cell cycle stage, chromatin structure and interaction of IN with chromatin tethering factors such as LEDGF/p75 (Cherepanov et al., 2003; Koh et al., 2013; Maertens et al., 2003; Marini et al., 2015; Schaller et al., 2011).

The mechanism of integration has been extensively studied (Lusic and Siliciano, 2017). When IN binds to the viral DNA, the resulting IN-DNA complex is known as an intasome (Maertens et al., 2010). The intasome is a tetramer of IN subunits and this structure is important for IN activity. Following tetramerisation, one IN subunit in each dimer binds to the DNA and removes two nucleotides from the 3’ ends of the viral DNA (Hare et al., 2010). This generates a reactive CAOH-3’-hydroxyl group at the ends. When intasomes reach the integration site, IN docks on to the host DNA to initiate the process of strand transfer. The docked structure is called a target capture complex (TCC) (Hare et al., 2010). Then, the reactive CAOH-3’-hydroxyl groups are used by IN as nucleophiles to attack the host DNA (Brown et al., 1989; Fujiwara and Mizuuchi, 1988). The complementary strands of viral DNA are covalently joined at the 5’ end by the addition of phosphates to the ends of the host DNA (Hare et al., 2010). The strand transfer complex eventually dissociates and then the cellular repair machinery joins the single

stranded gaps which are left in the DNA recombination intermediate. This results in complete integration of the viral DNA into the host chromatin. The integrated viral DNA is termed a provirus. Consequently, the viral DNA is replicated during each cell cycle division. Viral DNA acts as a template for the production of viral RNA, which is used for viral protein synthesis and for packaging into nascent virions.

Not all viral DNA is integrated into the host genome. These unintegrated viral DNA particles circularise to form 2-LTR circles. 2-LTR circles contain LTR promoters adjacent to each other. Formation of 2-LTR circles is dependent on host-derived non-homologous end joining components: Ku70/80, ligase IV and XRCC4 (Li et al., 2001). Production of 2-LTR circles is often used as a proxy to measure nuclear import efficiency. Finally, 1-LTR circles are formed by a recombination event between the LTRs and depend on the host MRN complex (Mre11, Rad50, and NBS1) (Kilzer et al., 2003). It remains controversial whether transcription from 2 LTR circles and unintegrated DNA takes place in cells (Stevenson et al., 1990), although recent studies suggest that unintegrated HIV-1 DNA undergoes epigenetic silencing by host factors such as NP220 (Zhu et al., 2018).

1.2.3.4 Gene expression

HIV-1 gene expression is driven by the Long Terminal Repeat (LTR) regions which are found at the 5' and 3' end of the viral genome. This process is regulated by two viral proteins called Transactivator (Tat) and Rev.

The 5' LTR is 640bp in length and contains three main regions which are required for gene expression: U3, R and U5 (Klaver and Berkhout, 1994). The U3 region is found upstream of the Transcription Start Site (TSS) and is further subdivided into modulatory, enhancer and promoter regions. The modulatory region contains several transcription factor-binding sites (TFBS), including NFκB, SP1, AP-1 and NFAT, whereas the enhancer region contains specifically NFκB binding sites (Burnett et al., 2009; Rittner et al., 1995; Williams et al., 2007). Finally, the promoter region of U3 contains the TATA box sequence and three SP1 binding sites. The presence of so many TFBS indicates a crucial role that transcription factors play in the process of HIV-1 gene expression, as well as the importance of cell activation status. Next, the R region of the 5' LTR is also known as the transcription initiation site and it is composed of the Transactivating response (TAR) element, a polyadenylation signal, which is required for the addition of a 5' polyA tail, and several TFBS. The TAR element is the binding site for the regulatory protein Tat and upon binding, the process of transcription is initiated by RNA polymerase II (Berkhout et al., 1989; Wei et al., 1998).

Prior to the production of Tat protein, the 5' LTR supports basal level transcription which results in the production of short viral transcripts encoding viral proteins Tat, Rev and Nef. This process is regulated by the TFBS of the U3 and R regions of the 5' LTR. Only short transcripts are produced because initial transcription leads the production of a stem loop structure, containing the TAR element, which blocks RNA polymerase II, hence transcription elongation is prevented at the 5' end. Upon sufficient production and accumulation of Tat protein, which consequently binds to TAR, sustained viral transcription elongation occurs. This is primarily due to the recruitment of the cellular positive transcription elongation factor b (P-TEFb), which phosphorylates Negative Elongation Factor (NELF), resulting in its dissociation from the transcription complex. P-TEFb also phosphorylates serine residues in the C-terminal region of RNA polymerase II to enhance its processivity (Berkhout et al., 1989; Wei et al., 1998). Together, these events lead to a positive feedback loop of Tat production and HIV-1 transcription.

mRNA processing occurs concomitantly with transcription. mRNA processing involves 5' end capping, splicing to remove introns and the addition of a 3' polyA tail. Capping occurs when Tat phosphorylates RNA polymerase II, as mentioned above. The enzyme RNA guanylytransferase is subsequently recruited to the transcript. RNA triphosphatase cleaves the 5' triphosphate which is capped with GMP and methylated.

HIV-1 uses alternative splicing as a mechanism to regulate gene expression, using cellular splicing machinery. This is the process by which multiple (spliced and unspliced) transcripts are formed from pre-mRNA. HIV-1 produces almost 50 transcripts using different splice donor and acceptor sites from a 9.7kb pre-mRNA transcript (Purcell and Martin, 1993). These transcripts can be categorised into non-spliced, partially spliced and spliced variants. Non-spliced transcripts encode Gag and Gag-Pol polyproteins which are packaged into budding virions. Partially spliced 4kb transcripts encode Vif, Vpu, Vpr and Env. Fully spliced 2kb transcripts encode Tat, Rev and Nef. Transcripts are required to move from the nucleus to the cytoplasm for translation, protein expression and packaging into nascent virions. Initially, only fully spliced transcripts leave the nucleus to be translated and expressed. Rev, an early expressed protein, contains a Nuclear Import Signal (NIS) and a Nuclear Export Signal (NES), thus allowing the export of non-spliced and partially spliced transcripts from the nucleus (Malim et al., 1989). Rev binds to the Rev Responsive Element (RRE) on the Env coding region, which is found in both the partially- and non-spliced mRNA transcripts (Nasioulas et al., 1994).

Once the transcripts enter the cytoplasm, HIV-1 uses the cellular translational machinery to produce viral proteins. This is a cap-dependent process where the 5' cap on viral

transcripts recruits the 40S ribosomal subunit which scans towards the 3' end and recruits the 60S ribosomal subunit whenever a start codon is encountered (Bolinger & Boris-Lawrie, 2009). Other than this, HIV-1 also uses a number of different pathways to complete translation of the viral proteome. First, ribosomal frameshifting occurs at the Gag stop codon to produce the Gag-Pol precursor polyprotein at a 1:20 ratio, which is crucial for Pol production (Jacks et al., 1988). This allows the viral proteins IN, PR and RT to be incorporated into nascent virions. Second, Env and Nef genes are translated as a result of leaky scanning. The 40S ribosomal subunit scans the 5'UTR in 5' to 3' direction until it finds a start codon, however sometimes the initial start codon is bypassed and therefore translation begins at a downstream AUG start codon. Leaky scanning of the Vpu and Rev stop codons results in translation of Env and Nef, respectively (Schwartz et al., 1990). Finally, HIV-1 can also initiate translation in a cap-independent manner using structural RNA elements. For example, two Internal Ribosomal Entry Sites (IRES) are found in HIV-1 (one on the 5' UTR and another in Gag) (Vallejos et al., 2012). IRES overcome global cap-dependent translational dampening, which is a mechanism used by cells to counteract viral infection including HIV-1 (Hanson et al., 2012).

HUSH complex

Gene expression is a highly regulated process in eukaryotic cells. Epigenetic regulation of chromatin structure is one example of how cells regulate gene expression. This usually involves chemical modifications of the genome and modifications of proteins, such as histones, which are in close proximity and/or bound to the DNA (Jaenisch and Bird, 2003). This mechanism of regulation allows host chromatin to either be in an open, active, euchromatin structure or in a closed heterochromatin structure. The latter prevents transcription factor binding, hence the process of transcription is inhibited. As HIV-1 is a retrovirus which inserts its DNA into the host chromatin, it was speculated that this viral genome would also be subjected to epigenetic regulation, like the host DNA. Emerging data is beginning to provide mechanistic insight into how HIV-1 gene expression is regulated in infected cells.

The Human Silencing Hub (HUSH) complex was first described by the Lehner lab (2015), using a forward genetic screen study in the near-haploid KBM7 cell line (Tchasovnikarova et al., 2015). The three key components of this complex are TASOR, MPP8 and periphilin, all of which are located in the cell nucleus. The HUSH complex is recruited to chromatin which are rich in trimethylated Lys^9 of Histone 3 (H3K9me3). Once at the target site, HUSH recruits the H3K9 methyltransferase, SETDB1, in order to deposit more H3K9me3 marks, thus maintaining closed, heterochromatin structure. The

MORC2 ATPase is also recruited to chromatin in order to maintain a compact chromatin structure (Tchasovnikarova et al., 2017).

The HUSH complex was shown to repress over 900 genes and transposable elements (Liu et al., 2018; Tchasovnikarova et al., 2015), as well as HIV-1 proviral gene transcription (Chougui et al., 2018; Yurkovetskiy et al., 2018). Knockdown of HUSH components resulted in a rescue of GFP expression from integrated HIV-1 GFP reporter vectors, as well as reduced H3K9me3 marks on the LTR. Further, HUSH knockdown could derepress silent HIV-1 reporters in J-Lat cells, which are often used to study HIV-1 latency, suggesting a role for the HUSH complex in regulating this key process in HIV-1 biology. Intriguingly, HIV-1 does not encode a HUSH antagonist, whilst HIV-2 uses Vpx and some SIVs use either Vpx or Vpr to antagonise the HUSH complex. These accessory proteins antagonise HUSH-mediated proviral gene repression by targeting the complex for proteasomal degradation (Chougui et al., 2018; Greenwood et al., 2019; Yurkovetskiy et al., 2018). Details of this mechanism are discussed in section **1.2.6 Accessory Proteins**.

1.2.4 Assembly, Release and Maturation

1.2.4.1 Virus assembly

HIV-1 Gag protein is a crucial player in particle assembly, release and maturation. Expression of Gag alone is sufficient to produce virus-like particles which are released from the plasma membrane (Gheysen et al., 1989). Gag is produced as a polyprotein called pr55. Proteolytic processing by the viral Protease enzyme cleaves the Gag polyprotein into 4 domains: matrix domain (MA), capsid domain (CA), Nucleocapsid (NC) which is flanked by Spacer peptide (SP) 1 and SP2 and the p6 domain. As mentioned earlier, the Gagpol precursor is produced at a ratio of 1:20 to allow for viral enzymes IN, PR and RT to be incorporated into virions (Jacks et al., 1988). Both Gag and Gagpol are synthesised in the cytoplasm, after which MA directs trafficking to the plasma membrane by a currently unclear mechanism. It is thought that Gag is specifically targeted to lipid-rich microdomains called lipid rafts. Lipid rafts are thought to act as virus assembly platforms and are rich in cholesterol, sphingolipids and phosphatidylinositide-(4,5)-bisphosphate (PIP_2) (Halwani et al., 2003; Hogue et al., 2011; Mercredi et al., 2016; Nguyen and Hildreth, 2000). PIP_2 plays a key role in Gag recruitment to the plasma membrane (Mucksch et al., 2017). Studies show that Gag relocalises to endosomes and Multivesicular bodies (MVBs) when PIP_2 is deleted (Ono et al., 2004) or when the basic region of MA is mutated (Ono and Freed, 2001). NMR structures reveal that MA directly interacts with PIP_2, potentially via hydrophobic and electrostatic interactions (Saad et al., 2006). This leads to subtle conformational changes which expose the myristate attached

to MA (Saad et al., 2006). Once the myristate is released, it inserts into the plasma membrane, thereby tethering Gag to the inner leaflet of the plasma membrane (Saad et al., 2006).

Next, RNA encapsidation involves two copies of full-length viral RNA being packaged into virions (Chen et al., 2009; Moore et al., 2009; Nikolaitchik et al., 2013). Viral NC acts as a nucleic acid chaperone for this process. NC has a high affinity for RNA because it is flanked by basic residues which are electrostatically attracted to the packaging signal in the 5' UTR of the HIV-1 genome (Nikolaitchik et al., 2013). The importance of the viral 5' UTR in genome encapsidation is confirmed by observations which show that mutating this part of the genome significantly reduces RNA packaging efficiency (Lu et al., 2011c). Further, Lu and colleagues (2011) used NMR to describe that the 5' UTR undergoes an RNA structural switch to regulate multiple processes including translation, NC binding and genome packaging. Site directed mutagenesis of the AUG start codon revealed that it can adopt a hairpin conformation, which disrupts binding to the 5' UTR, thus allowing the dimer initiation site to bind to the 5' UTR and promote translation (Lu et al., 2011b). Dimerisation is induced by intramolecular U5:AUG base pairing, which destabilises the hairpin conformation and this promotes NC binding and packaging. Evidence suggests that RNA dimerisation and NC binding can occur in the cytosol and/or at the plasma membrane (Moore et al., 2009; Nikolaitchik et al., 2013). Upon reaching the plasma membrane, interactions between Gag and viral RNA initiate Gag multimerisation, nucleation of virus assembly and immature particle formation (Kutluay and Bieniasz, 2010). The CA domain encourages trimerisation of MA (Tedbury et al., 2013). Subsequently, hexamers of trimers are formed with a central cavity (Alfadhli et al., 2009).

Aside from Gag, the Env glycoprotein is also required for infectious virus production. Env is synthesised in Endoplasmic Reticulum (ER) as the gp160 precursor protein (Berman et al., 1988). During translation, gp160 is highly glycosylated and then the monomeric gp160 molecules form trimers (and occasionally dimers and tetramers) (Allan et al., 1985; Bernstein et al., 1994; Leonard et al., 1990). The resultant trimers of gp160 traffic to the Golgi network where they are extensively processed and the host protease furin cleaves gp160 to produce the gp120 surface subunit and gp41 transmembrane subunit (Hallenberger et al., 1992; McCune et al., 1988). Env trimers traffic to and associate with the outer leaflet of the plasma membrane, after which trimers are either rapidly endocytosed in an AP-2 dependent manner to avoid immune recognition (Berlioz-Torrent et al., 1999; Boge et al., 1998; Egan et al., 1996; Ohno et al., 1997; Rowell et al., 1995) or incorporated into budding virions by a currently unclear mechanism. **Section 1.3** will discuss these aspects of Env biology in further detail.

Viral assembly in macrophages can differ assembly in infected T cells since nascent viral particles have been shown to assemble at the plasma membrane and in tetraspanin-enriched vesicles known as VCCs (Deneka et al., 2007; Mlcochova et al., 2013; Pelchen-Matthews et al., 2003), which are characterised by the presence of CD63 and CD81 (Jouve et al., 2007; Ono and Freed, 2004; Orenstein et al., 1988; Pelchen-Matthews et al., 2003). 3D CryoEM and cryoET studies of HIV-1 infected macrophages show that the VCCs are connected to the extracellular space via thin channels, measuring 150-200nm in diameter, that are in continuity with the plasma membrane (Bennett et al., 2009; Deneka et al., 2007; Welsch et al., 2007). Therefore, HIV-1 assembly in macrophages occurs in a protected environment prior to viral release.

1.2.4.2 Virus release

Retroviral release is commonly regulated by late domains such as PTAP, PPXY and YPXL (Fujii et al., 2009; Garrus et al., 2001; Gottlinger et al., 1991; Huang et al., 1995; Martin-Serrano et al., 2001). In HIV-1, the N-terminus of p6 contains a PTAP motif which directly binds to TSG101, a component of the human ESCRT-I machinery (Demirov et al., 2002; Garrus et al., 2001; Martin-Serrano et al., 2001; VerPlank et al., 2001), thus HIV-1 has co-opted the host ESCRT machinery to aid budding. The ESCRT machinery is a large family of cytosolic protein complexes which are involved in membrane remodelling to allow membrane scission (Scourfield and Martin-Serrano, 2017). Protein ubiquitylation usually acts as a signal to recruit ESCRT machinery, however there is no clear evidence that this is how HIV-1 recruits the protein complexes. HIV-1 is highly dependent on ESCRT-I machinery and can also use ESCRT-II and some components of ESCRT-III, although these are dispensable for infection (Morita et al., 2011). The p6 domain also contains a second late domain, the YPXL motif, which recruits ALG2 interacting protein X (ALIX) (Fujii et al., 2009; Martin-Serrano et al., 2001). The exact mechanism of ESCRT-mediated scission is currently unknown; however, it is accepted that ESCRT-I and ALIX recruit ESCRT-III to the budding virus. ESCRT-III also recruits a cellular AAA ATPase called VPS4 which provides energy for membrane scission and is important for recycling of ESCRT components (Bleck et al., 2014; Jouvenet et al., 2008; Van Engelenburg et al., 2014). Super resolution microscopy studies have alluded to two different models by which HIV-1 budding occurs. The first model describes that ESCRT-III enters inside the budding virion (Van Engelenburg et al., 2014) and the second model describes that ESCRT-I and ALIX are inside the budding virion and ESCRT-III forms circular arrays (Hanson et al., 2009) or spirals (Shen et al., 2014) at the neck region to force scission of the immature virus particle.

1.2.4.3 Virus maturation

Virus maturation occurs concomitantly with budding and results in major morphological changes to the virion. Maturation is mediated by the viral protease enzyme (PR) which is incorporated into budding virions. PR is an aspartyl protease which functions as a dimer and cleaves multiple sites in Gag and Gag-Pol precursor proteins (Wlodawer and Erickson, 1993). PR has different efficiencies for cleaving different target sites and this leads to a sequential cleavage cascade (Kaplan et al., 1993; Pettit et al., 1994). Cleavage of Gag leads to the release of CA, which reassembles into hexamers to form the characteristic HIV-1 conical core structure (Frank et al., 2015). The MA domain remains associated with the inner leaflet of the plasma membrane and the NC domain remains associated with viral RNA (Zhao et al., 2013). Eventually the capsid core encapsidates the viral genome and viral enzymes (Zhao et al., 2013). Mutations in PR result in non-functional virion production which are either completely immature or partially immature (Kaplan et al., 1993). This can be observed by cryoET, as mature virions have a conical capsid core, whereas immature virions have uncleaved Gag attached to the inner leaflet of the viral membrane (Alfadhli et al., 2009; Tedbury et al., 2013). In immature particles, hexamers of Gag are arranged radially along the membrane and once maturation occurs, the mature CA lattice of hexamers is formed. The mature capsid lattice contains 12 pentamers which are required to close the capsid shell (Wagner et al., 2016; Zhao et al., 2013).

1.2.5 Accessory proteins

Lentiviral accessory proteins often act as virulence factors to promote viral replication and spread. Their expression is often dispensable *in vitro* but necessary for *in vivo* infection. Accessory proteins play a critical role in modulating the immune response against infection and antagonise several restriction factors, which are antiviral proteins that target multiple steps of the viral life cycle (discussed extensively in **section 1.4**). HIV-1 encodes 4 accessory proteins: Vif, Nef, Vpu and Vpr. HIV-2 and SIVs also encode an additional protein called Vpx.

Vif

The Viral Infectivity Factor (Vif) is vital for lentiviral replication *in vivo* and *in vitro,* as it counteracts the APOBEC restriction factor family, which inhibit HIV-1 infection by causing genomic hypermutation and production of defective viral particles (Gabuzda et al., 1992; Harris et al., 2003; Mangeat et al., 2003; Sheehy et al., 2003). Structural studies reveal that Vif is composed of two domains, a small α-domain and a larger $\alpha\beta$-domain, which are bound together via a Zn^{2+} ion (Guo et al., 2014). Vif acts as an adaptor protein which recruits APOBEC3 to the E3 ubiquitin ligase to produce a pentameric

complex composed of Vif, CBF-β, Cullin5, elongin B and elongin C (Sheehy et al., 2003). Interactions between Vif and the transcription factor CBF-β stabilise the conformation of this large, pentameric complex. The BC-box motif in Vif mimics the cellular SOCS-box motif which is found on SOCS proteins and this is required for Vif binding to elongin B and elongin C (Bergeron et al., 2010). Finally, the Vif zinc-finger motif HCCH is important for Cullin5 binding (Luo et al., 2005). Recruitment of this complex leads to polyubiquitination and proteasomal degradation of APOBEC3 in virus producer cells, thereby preventing virion incorporation (Jager et al., 2011; Sheehy et al., 2003). Further, Vif has also been suggested to counteract APOBEC3G in a degradation-independent manner by preventing APOBEC3G mRNA translation, virion incorporation and inhibiting the cytidine deaminase activity of APOBEC3G (Feng et al., 2013; Goila-Gaur et al., 2008; Mercenne et al., 2010). Vif is expressed by all lentiviruses and counteraction of APOBEC3 enzymes happens in a species-specific manner. Species-specificity has been mapped to a single residue in APOBEC3G at position 128, at which it is critical for a charged amino acid to be present (Schrofelbauer et al., 2004). For example, the R128K mutation renders human APOBEC3G insensitive to Vif, but not the R128A mutation (Schrofelbauer et al., 2004). The importance of Vif is highlighted by the ability of APOBEC3 enzymes to create a barrier to cross-species transmission which is then overcome by Vif to allow for efficient viral transmission. Most SIV Vif proteins are unable to antagonise chimpanzee APOBEC, however the recombination event leading to the emergence of SIVcpz, resulted in the generation of a hybrid Vif protein which is able to antagonise chimpanzee APOBEC proteins (Etienne et al., 2013). This also allowed SIVcpz to successfully transmit to the human host, as SIVcpz Vif is active against most human APOBEC proteins (Etienne et al., 2013; Zhang et al., 2017). By contrast, SIVsmm Vif is able to counteract human APOBEC, suggesting that Vif antagonism is unlikely to have caused a barrier to HIV-2 zoonoses (Letko et al., 2013).

Proteomic analysis of HIV infected cells revealed another function of Vif, which involves regulation of PP2A, a major cellular protein phosphatase (Greenwood et al., 2016). Vif expression leads to the proteasomal degradation of the phosphatase regulatory subunit of PP2A, called PPP2R5A-E, due to the recruitment of the Cullin5 ubiquitin ligase complex (Greenwood et al., 2016). This leads to reduced PP2A activity and subsequent phosphorylation of more than 200 cellular proteins (Greenwood et al., 2016; Naamati et al., 2019). PP2A regulation is a conserved feature of diverse SIV Vif proteins (Greenwood et al., 2016), although the importance of this remains to be elucidated.

Vpr and Vpx

Viral protein R (Vpr) and Viral protein X (Vpx) are closely related lentiviral accessory proteins. Whilst Vpr is conserved in all lentiviruses, Vpx is only expressed in the HIV-2/SIVsmm and SIVrcm/drl/mnd2 lineages (Schwefel et al., 2014). It is thought that a Vpr gene duplication event occurred after the HIV-2/SIVsmm and SIVrcm/drl/mnd2 lineages separated from the SIVagm lineage, giving rise to Vpx (Etienne et al., 2013; Tristem et al., 1991). Virion incorporation of Vpr and Vpx is ensured via interactions with the p6 domain of Gag (Seligmann et al., 1991) and this allows for cytoplasmic delivery of Vpr and Vpx upon viral entry into target cells. Once in the target cell cytoplasm, Vpr and Vpx target a wide range of cellular proteins for proteasomal degradation. This is achieved by a similar mechanism as described above for Vif, where they act as adaptor proteins to recruit the DCAF1-Cullin4-DDB1 E3 ubiquitin ligase complex (Le Rouzic et al., 2007; Srivastava et al., 2008).

Several roles of Vpr have been explored over time, however its primary function in enhancing viral replication *in vivo* remains to be elucidated. Some of the most well studied functions of Vpr include cell-cycle arrest in the G2-M phase (Zhang and Bienaisz, 2020), transactivation of the HIV-1 LTR and modulation of the NFκB and NFAT signalling pathways (Ayyavoo et al., 1997; Felzien et al., 1998; Jowett et al., 1995; Laguette et al., 2014; Lahti et al., 2003; Re et al., 1995; Roux et al., 2000). The cell cycle arrest function of Vpr can be attributed to its interactions with several proteins that are involved in cell cycle control, such as the SLX4 complex (Berger et al., 2015; Laguette et al., 2014; Zhou et al., 2016). The SLX4 complex is implicated in DNA damage repair, as it recruits structure-specific endonucleases (SSE) MUS81-EME1, ERCC1-ERCC4 and SLX1 to form a complex (SLX4com) that repairs DNA damage (Laguette et al., 2014). Vpr interacts with SLX4 and induces premature activation of SLX4com, which results in abnormal cleavage of DNA replication intermediates thus possibly inducing G2M cell cycle arrest.

A recent proteomics study comparing cells infected with wild type HIV-1 and a HIV-1 ΔVpr mutant suggests that Vpr promiscuously targets multiple cellular proteins and induces global cellular proteome remodelling (Greenwood et al., 2019). This results in changes in the abundance of ~2000 cellular proteins, most probably as a secondary effect of proteasomal degradation of ~38 Vpr target proteins in a DCAF-Cullin4-dependent manner. Some direct Vpr targets include the UNG2 uracil DNA glycosylase (Schrofelbauer et al., 2004), the DNA translocase HLTF (Lahouassa et al., 2016) and ZGPAT which is involved in chromatin remodelling (Maudet et al., 2013). Finally, a recent study suggests that Vpr may modulate innate immune sensing of HIV-1 infection by inhibiting nuclear translocation of NFκB and IRF3 (Khan et al., 2020).

SAMHD1 is a restriction factor that prevents HIV infection of myeloid cells and resting T cells by reducing the intracellular dNTP pool (discussed in **section 1.4**) (Goldstone et al., 2011; Laguette et al., 2011). Vpx and some lentiviral Vpr proteins target SAMHD1 to the DCAF1-Cullin4 complex for proteasomal degradation. This results in efficient infection of dendritic cells, macrophages and resting CD4 T cells. SAMHD1 antagonism by Vpx occurs in a species-specific manner, a typical feature of most HIV restriction factors. Phylogenetic studies suggest that SAMHD1 antagonism precedes the emergence of Vpx in the phylogenetic tree, as Vpr proteins from ancestor lineages, such SIVagm, can counteract SAMHD1 (Lim et al., 2012). Positive selection in SAMHD1 correlates with sensitivity to Vpr/Vpx, thus proving that these proteins are providing selective pressure on the host to evolve over time.

A recently described function of Vpx and certain Vpr proteins is antagonism of the Human Silencing Hub (HUSH) complex (Chougui et al., 2018; Yurkovetskiy et al., 2018). The HUSH complex is responsible for epigenetic silencing of cellular genes and integrated lentiviral genes (Tchasovnikarova et al., 2015). To overcome suppression, Vpx and Vpr target the TASOR component of HUSH for proteasomal degradation (Chougui et al., 2018). As described above, the mechanism for this involves recruitment of the DCAF-Culin4 complex. Whether antagonism of the HUSH complex occurs in a species-specific manner remains to be tested. It is speculated that HUSH repression is a common feature of lentiviruses, as HIV-2, but not HIV-1, Vpr proteins from diverse backgrounds are able to antagonise the HUSH complex, unlike SAMHD1 antagonism which is restricted to certain lineages.

An interesting observation is that the HIV-1/SIVcpz lineage lost the ability to, or never had the ability to antagonise both SAMHD1 and HUSH. Mlcochova *et al* (2017) show that macrophages that are in a G1-like phase will have an activated RAF-MEK-ERK pathway which deactivates SAMHD1 and provides a window of permissivity for HIV-1 infection without the need for HIV-1 to directly antagonise SAMHD1 (Mlcochova et al., 2017). SAMHD1 antagonism in *in vitro* models can achieved by delivering Vpx in *trans*, however this can be counteracted by the host via activation of DNA sensing pathways in a cGAS dependent manner (Lahaye et al., 2013). Further, knockdown of the HUSH complex results in overexpression of transposable elements and endogenous retroviruses, which possibly also activates and amplifies innate immune sensing (Robbez-Masson et al., 2018; Tunbak et al., 2020). Taken together, this suggests that the HIV-1/SIVcpz lineage may have lost the ability to antagonise these restriction factors

in order to strike a balance between the ability to infect many cell types and the ability to replicate without triggering innate immune sensing.

Vpu

Viral protein U (Vpu) is a type I transmembrane protein found in the HIV-1/SIVcpz and SIVmon/gsn/mus lentiviral lineages. Vpu is primarily localised in the endoplasmic reticulum, trans-Golgi network, endosomal pathways and the cell membrane and this subcellular localisation correlates with Vpu's ability to antagonise one of its most well-known targets, Tetherin (Dube et al., 2009; Neil et al., 2008; Van Damme et al., 2008). Vpu has an N-terminal hydrophobic transmembrane domain which is important for interactions with other membrane bound proteins and a C-terminal region composed of two α-helices that are important for binding to host endocytic machinery. For example, phosphorylation of the Vpu cytoplasmic tail leads to recruitment of the AP-1 and AP2 adaptor proteins, resulting in clathrin-mediated endocytosis of target proteins (Kueck et al., 2015).

The most recently studied function of Vpu is antagonism of the restriction factor Tetherin. Details of Tetherin restriction and mechanism of Vpu antagonism will be discussed in **Section 1.4**. Briefly, Tetherin expression at the cell membrane prevents viral release, hence significantly reducing infectivity (Neil et al., 2008; Van Damme et al., 2008). Tetherin also activates the NFκB pathway which results in induction of a Type I IFN response to eliminate infection (Galao et al., 2012). Vpu downmodulates Tetherin from the cell surface and targets it for proteasomal degradation (Goffinet et al., 2009; Van Damme et al., 2008).

As well as antagonising Tetherin-induced NFκB activation, Vpu can also directly inhibit NFκB activation which is independent of Tetherin. For example, TNF-α mediated activation of NFκB is antagonised by Vpu. This is achieved by interfering with βTrCP dependent degradation of phosphorylated IκBα (Bour et al., 2001). It is thought that Vpu sequesters βTrCP to endosomal compartments resulting in IκBα stabilisation, thus inhibition of NFκB signalling. Alternatively, a recent study shows that βTrCP interaction with Vpu is not required for NFκB antagonism (Sauter et al., 2015), suggesting that Vpu uses a multifaceted approach to antagonise a key antiviral signalling pathway in host cells.

Another key function of Vpu is downmodulation and degradation of the cellular receptor CD4. Vpu binds to CD4 in the ER and degrades CD4 via the Endoplasmic-reticulum associated degradation pathway (Binette et al., 2007; Fujita et al., 1997; Schubert et al.,

1998; Willey et al., 1992). Interactions between the cytoplasmic tails of Vpu and CD4, in the endoplasmic reticulum, recruit the SCF-β-TrCP complex to allow polyubiquitination of CD4 molecules (Bour et al., 1995; Margottin et al., 1998). Sequestration of CD4 in the ER leads to activation of endoplasmic reticulum associated degradation (ERAD) machinery and targeting for proteasomal degradation (Magadan et al., 2010; Schubert et al., 1998). It is important to prevent premature interactions between Env and CD4 during trafficking to the cell membrane for several reasons. (1) Premature CD4 binding to Env in infected cells can result in production of non-infectious virus, as it triggers conformational changes in Env which are usually required for efficient CD4 binding on target cells and successful fusion (Haim et al., 2009). (2) CD4 binding can also expose cryptic epitopes in Env which are targeted by neutralising and non-neutralising antibodies, thus increasing the likelihood of an ADCC response (Veillette et al., 2015; Veillette et al., 2014). (3) CD4-Env interactions in the infected cell may lead to tethering of virus particles at sites of virus assembly and budding. (4) CD4 downmodulation from the cell surface prevent superinfection of infected cells (Wildum et al., 2006).

Nef

The lentiviral Negative Factor (Nef) is a 27-35kDa non-enzymatic protein which is crucial for *in vivo* infection but it's requirement *in vitro* is cell-type specific (Deacon et al., 1995; Gorry et al., 2007; Kirchhoff et al., 1995). Nef is present in all lentiviral lineages. It is located in the cytosolic leaflet of membranes via a key N-myristylation found on the G2 residue in the anchor domain of Nef (Fackler et al., 1997; Geyer et al., 1999). HIV and SIV have co-opted host trafficking pathways to enhance viral replication and Nef has particularly evolved to utilise the clathrin-mediated endocytic pathway to downmodulate several target proteins from the surface of infected cells. Membrane association allows Nef to engage with host trafficking factors, such as clathrin coated vesicles, as well as membrane-associated restriction factors, such as Tetherin and SERINC5, and determinants of infection such as CD4 and MHC-I. Nef targets proteins for either sequestration or lysosomal degradation. X-ray crystallography and NMR studies show that Nef has multiple flexible regions, including the dileucine loop in the C-terminus (Geyer et al., 2001; Geyer and Peterlin, 2001). This flexibility allows for conformational changes to occur in Nef, which in turn enables the accessory protein to interact with multiple host cell proteins.

CD4 downmodulation

The first important target of Nef is CD4 which is found on the surface of HIV-1 target cells and is a critical determinant of infection. Downregulation of CD4 is a conserved feature of lentiviral Nef proteins, highlighting the importance of this function for successful

replication and transmission. Under physiological conditions, CD4 is recycled from the cell surface by clathrin mediated endocytosis. CD4 has a sorting motif ($_{408}$SQIKRLL$_{414}$) and phosphorylation of S408 is a prerequisite for endocytosis. Upon HIV infection, Nef accelerates CD4 endocytosis in an AP-2 dependent manner. Nef directly binds to both AP-2 and CD4 at the cell membrane to form a CD4-Nef-AP2 complex (Chaudhuri et al., 2009), which is internalised and CD4 is targeted to lysosomes via endosomes and multivesicular bodies (Aiken et al., 1994; daSilva et al., 2009; Rhee and Marsh, 1994). Nef binds directly to the cytoplasmic tail of CD4 and the dileucine motif in Nef is used to adapt CD4 endocytosis in the absence of S408 phosphorylation (Dalgleish et al., 1984; Garcia and Miller, 1991; Grzesiek et al., 1996; Preusser et al., 2001; Rossi et al., 1996). As mentioned in the 'Vpu' section above, CD4 downmodulation from the cell surface has multiple benefits to viral replication and transmission and therefore it is not surprising that the virus has evolved to use two different accessory proteins to target CD4.

CD3 downmodulation

Another Nef target is the CD3ζ component of the T cell receptor (TCR). CD3 is responsible for T cell signal transduction following antigen-specific TCR binding to peptide–MHC displayed on an antigen-presenting cell, resulting in T cell activation and gain of effector function. Interestingly, this Nef function was lost in the HIV-1/SIVcpz lineage. A recent study suggests that this is to allow T cell activation and increased viral replication, albeit at the cost of less effective immune evasion and increased pathogenicity (Mesner et al., 2020). This Nef function has been lost twice during evolution which coincides with the acquisition of *Vpu* (Schindler et al., 2006). This suggests that HIV-1 can afford to evolve away from CD3 downmodulation, perhaps because Vpu functions as a potent antagonist against antiviral immune responses such as NFκB activation, hence HIV-1 is balancing viral replication and immune evasion by utilising different accessory proteins.

During HIV-2 and SIV infections, downmodulation of CD3 prevents immune synapse formation between an infected CD4 T cell and antigen presenting cells, thus this function of Nef has been suggested to be an important immune evasion strategy (Arhel et al., 2009). It is also thought to disrupt TCR signalling, and therefore T cell activation, which prevents an exaggerated immune response which is typically seen in HIV-1 infected individuals but absent in HIV-2 and SIV infection (Kirchhoff, 2010). The CD3ζ chain consists of three ITAM motifs with a consensus YxxL. Nef directly interacts with the cytoplasmic tail of the ζ chain at a site which overlaps with the ITAM region, called SNID1 and SNID2 (Osman et al., 1995; Schaefer et al., 2000). Unlike CD4 downmodulation, the dileucine motif in Nef is not required for CD3 downmodulation (Swigut et al., 2003). Once

Nef interacts with CD3ζ, AP-2 is recruited, and the complex is internalised. A recent study revealed that the loss of CD3 downmodulation activity by the SIVcpz/HIV-1 lineage possibly resulted in the ability to perform enhanced cell-cell spread, due to an increase in Env surface expression and incorporation into virions (Mesner et al., 2020). However, this also leads to increased T cell activation and cell death, thus increasing viral pathogenicity.

SERINC antagonism

The discovery of SERINC3/5 as potent lentiviral restriction factors was fuelled by the observation that in the presence of Nef, viral infection is significantly enhanced in certain cell types (Chowers et al., 1994; Munch et al., 2007; Tokunaga et al., 1998; Usami and Gottlinger, 2013). It was also shown that Nef sensitises viruses to neutralisation by antibodies specifically targeting the membrane proximal external region of Env (Usami and Gottlinger, 2013). In 2015, two comparative analysis studies simultaneously discovered the SERINC family of transmembrane proteins as potent lentiviral restriction factors that are antagonised by Nef (Rosa et al., 2015; Usami et al., 2015). The mechanism and activity of SERINC restriction will be discussed in **section 1.4**. Briefly, SERINC3/5 are present at the cell membrane and are incorporated into virions, leading to inhibition of viral infectivity (Rosa et al., 2015; Usami et al., 2015).

Nef antagonises SERINC3/5 by downregulating them from the cell surface. Similar to the mechanism of CD4 endocytosis, Nef myristylation and the dileucine-based ExxxLL motif were required for Nef-mediated SERINC5 downregulation. Shi and colleagues (2018) show that the dileucine motif at positions 164 and 165 in Nef are required for relocalisation of SERINC5 from the cell membrane, as the ExxxLL motif directly interacts with the AP-2 adaptor complex and is subsequently recruited to the multivesicular body pathway. Once internalised, SERINC5 is redirected to LAMP1+ lysosomes where it is thought to undergo degradation (Shi et al., 2018). This prevents SERINC5 incorporation into nascent virions, hence viral entry is not perturbed. Alternatively, when endogenous SERINC5 was measured in an engineered Jurkat cell line, it was revealed that the steady state levels of SERINC5 did not change in the presence of both HIV-1 wild type and ΔNef infection, suggesting that under physiological conditions, Nef may sequester SERINC5 rather than targeting it for degradation (Passos et al., 2019). Interestingly, this study also reported that endogenous SERINC5 exclusion from virions is not a requirement to overcome restriction, suggesting that Nef can also antagonise this restriction factor by an alternative, unknown mechanism. This was also suggested by Trautz and colleagues (2016) who showed that Nef inhibits virion-associated SERINC5 pools using

exogenously expressed SERINC5, rather than endogenous SERINC5 (Trautz et al., 2016).

Although Nef proteins from all lentiviruses are able to antagonise SERINC5, their relative potencies against human SERINC5 vary. For example, HIV-2 Nef proteins are up to 100x less potent at antagonising SERINC5, compared with HIV-1 group M and the HIV-2 predecessor SIVsmm Nef proteins (Heigele et al., 2016). This observation suggests that perhaps HIV-2 has an alternative strategy to overcome SERINC5 restriction which is yet to be identified. Further, a study focussing on naturally occurring polymorphisms in *Nef* suggests that adaptive immune pressure *in vivo* can drive changes in the *Nef* gene, leading to an impaired ability to antagonise SERINC3/5 (Jin et al., 2019). This alludes to the idea that perhaps lentiviruses have evolved alternative strategies to overcome SERINC5 antagonism which may involve the Env glycoprotein, which is a key determinant of SERINC5 sensitivity.

1.2.6 Viral dissemination

Once retroviruses, such as HIV-1, are released from an infected cell they disseminate to infect uninfected target cells using various methods. The traditional model of dissemination is the cell-free infection model where the budded virus diffuses through the liquid phase until the Env glycoprotein attaches to the CD4 receptor on an uninfected target cell. However, retroviruses can also directly disseminate between cells via cell to cell spread (Chen et al., 2007; Jolly et al., 2004; Jolly and Sattentau, 2004, 2005, 2007; Jolly et al., 2011; Sourisseau et al., 2007). Immunofluorescence analysis of infected cells revealed that cell to cell spread, accounts for 90% of viral spread *in vitro* (Rudnicka et al., 2009). Two forms of cell-cell spread have been described. The first is via a supramolecular structure called the virological synapse (VS), which contains polarised viral and cellular proteins for efficient viral assembly and budding (Jolly and Sattentau, 2004), and the second is via filopodia and other cellular projections/nanotubes (Rudnicka et al., 2009; Sowinski et al., 2008). Two of the well-characterised modes of HIV-1 dissemination are summarised in **Figure 1.5**. HIV-1 manipulation of immune cell interaction in lymphoid tissue, where T cells are densely packed, is likely to drive efficient spread and evasion of both innate and adaptive immunity. However, the direct evidence for cell to cell spread *in vivo* is limited. This will be discussed further in **section 1.2.5.3**.

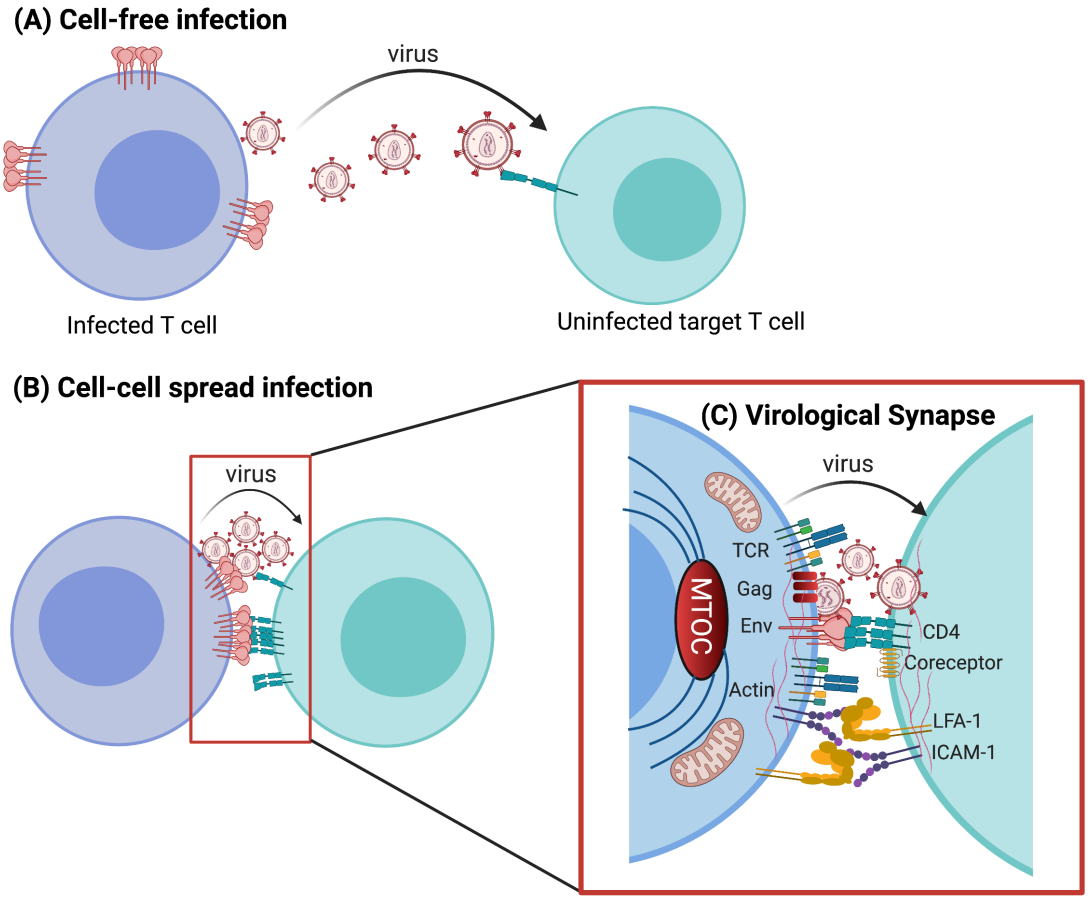

Figure 1.6 Modes of HIV-1 dissemination. (A) During cell-free infection, virions bud from infected cells into the extracellular space until the Env glycoprotein on viral particles binds to the CD4 receptor on a target cell to initiate entry. **(B)** During cell-cell spread, interactions between Env and CD4 bring the infected and uninfected target cells in close proximity to form a virological synapse (VS) within which polarised viral budding, and transfer occurs. **(C)** Diagram showing components of the VS. Once Env and CD4 bind, the interactions are further stabilised by interactions between adhesion molecules LFA-1 and ICAM-1. Env and Gag become enriched at the VS. The T cell receptor (TCR)-CD3 complex also clusters at the synapse and signalling is triggered to support efficient viral spread. Synapse formation also triggers polarisation of the microtubule-organising centre (MTOC) and mitochondria to the site of cell-cell contact to support viral budding into the synapse. Virions diffuse across the synapse to infect target cells. (Created by Biorender.com).

1.2.5.1 T cell virological synapses

Cell to cell transfer is a mode of viral dissemination which involves viral transfer upon physical contact between infected donor cells and uninfected target cells. The idea that viruses can disseminate via cell-to-cell transfer has been described in the past (Dimitrov et al., 1993; Gupta et al., 1989; Sato et al., 1992), although the exact mechanism was unknown. Discovery of the VS shed mechanistic insight on this mode of transfer between infected and uninfected T cells (Igakura et al., 2003; Jolly et al., 2004; Jolly and Sattentau, 2004). Later it was discovered that the VS is a common route of transmission between T cells and macrophages as well as T cells and dendritic cells (Duncan et al., 2014; Felts et al., 2010; Groot et al., 2008). Formation of the VS is triggered by interactions between Env on infected cells and the CD4 receptor on uninfected target cells (Jolly et al., 2004). Since the discovery of the VS, the structure and function of the VS has been extensively studied. The VS is a large, multiprotein structure that has a similar architecture to the well-described immunological synapse and is characterised by the recruitment of various cellular and viral proteins to sites of cell-cell contact (Jolly and Sattentau, 2004; Piguet and Sattentau, 2004) (**Figure 1.5**). This is an active process initiated by interactions between Env and CD4 receptor. Once the membranes of infected and uninfected cells are in close proximity, several adhesion molecules, such as ICAM-1, ICAM-3 and their receptor LFA-1, further stabilise this interaction (Chen et al., 2007; Jolly et al., 2007a; Sourisseau et al., 2007). This stable cell-cell interaction induces accumulation of actin (Jolly et al., 2004) and tubulin (Alvarez et al., 2014a; Chen et al., 2007; Haller et al., 2011; Jolly et al., 2007b) at sites of cell-cell contact. Further, mitochondria, Golgi and the microtubule organising centre (MTOC) are recruited to the VS in infected cells, as well as the induction of calcium signalling, suggesting that VS formation induces cellular remodelling of infected cells (Groppelli et al., 2015; Jolly et al., 2011; Sol-Foulon et al., 2007). Recruitment of the MTOC, actin and mitochondria contributes to trafficking of cellular and viral proteins to the VS (Chen et al., 2007; Jolly et al., 2004; Rudnicka et al., 2009). The polarised accumulation of Gag and Env at the VS is important for efficient and regulated viral assembly at sites of cell-cell contact. Viral particles are then released into the synaptic space, after which they travel a short distance to successfully infect the target cell. Loss of Gag and Env polarisation is observed when integrin inhibitors, CD4 inhibitors and nAbs are used to block cell-cell contact and VS formation, resulting in inhibition of viral spread (Chen et al., 2007; Jolly et al., 2007a; Rudnicka et al., 2009). Further, live cell imaging studies can differentiate between VS formation and temporary cell-cell contacts. Whilst VS formation remains stable for approximately 1-hour, non-specific cell-cell contacts last less than 2 minutes (Groppelli et al., 2015; Martin et al., 2010). In line with this, Gag transfer to the infected cell is also shown to take roughly 1 hour, suggesting that cell-cell contacts mediated by

the VS remain stable for long enough to allow viral transfer (Hubner et al., 2009). A possible mechanism of viral transfer upon cell-cell contact could be that cells fuse together to facilitate direct transfer of viral particles. However, immunoelectron microscopy of the VS shows mature budding virions in the synaptic space between the infected and uninfected cell (Jolly et al., 2004; Martin et al., 2010), suggesting that HIV-1 is released into the space before entering the target cell. This was further reinforced by studies showing that HIV-1 egress in T cells is trafficked via tetraspanin-enriched domains. Tetraspanin molecules CD9, CD63 and CD81 are enriched at the T cell VS (Jolly and Sattentau, 2007) and prevent syncytia formation, hence cell-cell fusion (Weng et al., 2009). Together these findings suggest that the actual mechanism of assembly, budding, attachment and entry in cell-cell spread are similar to that seen in cell free infection.

Accumulation of Env and Gag at the site of cell-cell contact is a characteristic feature of the VS. Exactly how these proteins accumulate at the VS remains elusive, however three models, which are not necessarily mutually exclusive and may depend on specific T cell types, have been suggested to describe these events. First, lipid rafts are enriched at the VS and are essential for Env and Gag recruitment to sites of viral assembly and budding (Jolly and Sattentau, 2005). Therefore, it is postulated that formation of the VS leads to plasma membrane remodelling and aids virus assembly. This is supported by the finding that lipid raft integrity is vital for VS formation, as it allows proper Env and Gag clustering (Jolly and Sattentau, 2005). Secondly, live cell imaging by Hubner and colleagues (2009) showed that there is directed Gag trafficking and polarised assembly, resulting in the formation of Gag ‘buttons’ that appear at the VS, suggesting that there is *de novo* virus production at the site of cell-cell contact. Finally, migrating T cells adopt an elongated structure with a uropod at the rear end of the cell and are hence pre-polarised. In the latter, Gag was shown to form higher order clusters at uropods in a nucleocapsid-dependent manner and the VS were enriched in uropod markers (Llewellyn et al., 2010). Gag-enriched uropods preferentially formed contacts with uninfected cells, resulting in VS formation (Llewellyn et al., 2010). Indeed, inhibition of uropod formation resulted in reduced cell-cell spread (Llewellyn et al., 2010).

Although it is yet to be elucidated exactly how Env and Gag accumulate at the VS, it was documented that HIV-1 hijacks the cell secretory network for this. Microscopy studies show that HIV-1 Env colocalises with CTLA-4 and Fas-L in secretory lysosome-related compartments at the VS, and inhibition of the regulated secretory pathway leads to reduced cell-cell spread, thus suggesting that the secretory pathway is important for Env recruitment and viral spread (Jolly et al., 2011). This is in line with recent data from Env

recycling assays using FRAP at the VS, showing that Env accumulation and incorporation into virions at the VS requires continuous Env recycling and targeted secretion to the budding virus (Wang et al., 2020). By contrast to Env, Gag is not endocytosed at the VS (Wang et al., 2020) and therefore these data suggest that there are distinct mechanisms involved in the accumulation and retainment of Env and Gag at the VS, which is also consistent with the idea that Env and Gag are independently recruited during cell-free assembly and egress. Further, Env containing vesicles were seen clustered around MTOCs and were associated with polarised Golgi apparatus and recycling endosomes at the VS (Starling and Jolly, 2016). This polarisation of cellular and virological proteins could be induced by LFA-1 engagement/crosslinking alone, in a Zap70 dependent manner, thus illustrating the importance of this integrin in cell remodelling during VS formation and cell-cell spread (Sol-Foulon et al., 2007; Starling and Jolly, 2016). Finally, polarisation of mitochondria (Groppelli et al., 2015; Jolly et al., 2011) was concomitant with Gag polarisation at the VS in a calcium-dependent manner (Groppelli et al., 2015). This resulted in an increase in intracellular Ca^{2+} levels at the VS which supports formation of a stable VS and efficient cell-cell spread. The activation of calcium signalling further reinforces the idea that Gag recruitment is an active process. As evidenced above, signalling pathways are critical in controlling cellular functions. In 2017, a phosphoproteomic study revealed that HIV-1 induces T cell receptor signalling in an antigen-independent manner and this in turn enhances viral dissemination via the VS (Len et al., 2017). Therefore, signalling in the infected donor cell triggers polarisation of proteins and cell-cell contact, as well as modulation of signalling in the uninfected targets cells. This is interesting as it indicates that cell-cell spread might influence permissivity of target cells. To conclude, these studies show that HIV-1 co-opts cellular machinery and signalling pathways in order to spread efficiently by cell to cell spread via a VS.

1.2.5.2 Macrophage and Dendritic cell virological synapses

Macrophages play an important role in HIV-1 pathogenesis and contribute to cell-cell transmission of HIV-1 (Carr et al., 1999; Duncan et al., 2014; Groot et al., 2008; Swingler et al., 2003). Viral assembly in macrophages differs to assembly in infected T cells since nascent viral particles have been shown to assemble at the plasma membrane and in tetraspanin-enriched vesicles known as VCCs (Deneka et al., 2007; Hammonds et al., 2017; Mlcochova et al., 2013; Pelchen-Matthews et al., 2003; Welsch et al., 2011). The exact mechanism of infected macrophage and target T cell VS formation remains to be elucidated (Groot et al., 2008). It is speculated that during cell-cell contact, VCCs traffic to the VS (Gousset et al., 2008) in an actin dependent manner (Duncan et al., 2014). Similar to the T cell VS, the several cellular and viral proteins are recruited to sites of

cell-cell contact, including CD4, CCR5, LFA-1, ICAM-1, Gag precursor and Env glycoproteins (Duncan et al., 2014; Groot et al., 2008). Formation of the macrophage-T cell conjugates does not dependent on gp120 (Gousset et al., 2008), contrary to the T cell VS, however the transfer of viral particles is dependent on interactions between gp120-CD4 and the adhesion molecules (Duncan et al., 2014).

Cell-cell transfer of HIV-1 can also occur via macrophage engulfment of infected T cells. Subsequently, the macrophages can become productively infected. Macrophages preferentially uptake dying, infected T cells compared with healthy, infected cells (Baxter et al., 2014). Whilst uptake of infected T cells is independent of Env-CD4 interactions, the infection of macrophages following uptake is dependent on Env-CD4 and LFA1-ICAM-1 interactions (Baxter et al., 2014), similar to the T cell VS. Also, uptake of the infected T cells is dependent on actin-cytoskeleton remodelling and this can be inhibited by amiloride (Baxter et al., 2014), therefore it suggests that the engulfment of infected T cells is via phagocytosis. Evidence for engulfment and uptake is that there is concentrated localisation of Gag in macrophages in association with the T cell specific marker, CD3 (Baxter et al., 2014). The exact mechanism by which HIV-1 infects macrophages following uptake is currently unknown. However, macrophages only get productively infected when they engulf T cells infected with CCR5-tropic viruses, not CXCR4-tropic viruses, suggesting that fusion of the viral and phagosome membranes might occur (Baxter et al., 2014). In line with this, recent *in vivo* studies using SIV infected macaque models, have suggested that SIV-infected T cells are engulfed by myeloid cells (Calantone et al., 2014; DiNapoli et al., 2017). This is because viral genome from T cells in myeloid cells was found from the spleen and lymph nodes of infected monkeys (Calantone et al., 2014; DiNapoli et al., 2017). The caveat to this is that there was no formal evaluation of phagocytosis, rather this was based on the presence of specific markers in myeloid cells which engulf infected T cells.

Dendritic cells (DC) are key players in immune surveillance. DCs express the CD4 receptor and can therefore bind to HIV-1 Env and an infectious synapse is established. Several C-type lectins including DC-specific ICAM-3-grabbing nonintegrin (DC-SIGN) receptor are also important for capturing HIV-1 (Arrighi et al., 2004; Turville et al., 2002). Capturing HIV-1 by this mechanism results in virus internalisation (McDonald et al., 2003; Sandgren et al., 2013), after which it can be presented to a CD4 T cell in lymph nodes (Manches et al., 2014). Unlike macrophages, this does not result in productive infection of DCs. Once internalised, HIV-1 is found in high concentrations within deep membrane invaginations (Felts et al., 2010; McDonald et al., 2003). Virus is then transferred in *trans* along an infectious synapse in the absence of antigen-dependent

signalling (Cameron et al., 1992; Geijtenbeek et al., 2000; Pope et al., 1994). The infectious synapse has similar characteristics to the T cell VS, whereby CD4 and coreceptors are clustered at the site of cell-cell contact (Arrighi et al., 2004; McDonald et al., 2003; Turville et al., 2004). Taken together, these alternative synapse formations provide further evidence that cell-cell spread is a highly efficient mechanism by which HIV-1 can disseminate between multiple immune cell types around the body.

1.2.5.3 Advantages of cell to cell spread

Various labs have estimated that the efficiency of cell-cell spread is 10-100 times higher than cell free infection, depending on the experimental set up and cell types used (Chen et al., 2007; Dimitrov et al., 1993; Jolly et al., 2007a, b; Martin et al., 2010; Mazurov et al., 2010; Sourisseau et al., 2007). A typical experimental set up used to investigate infection efficiency involved either coculturing infected and uninfected T cells so that they can form stable contacts or to separate infected and uninfected cells using a trans-well set up, thus preventing formation of the VS by inhibiting cell-cell contact but still allowing for viral diffusion through the trans-well membrane and thus cell-free infection.

Measuring infection kinetics and the number of infected cells revealed that cell to cell spread resulted in faster infection kinetics and an increased number of infected cells (Chen et al., 2007; Jolly et al., 2007b; Sourisseau et al., 2007). Several reasons can be given to explain this phenotype. Firstly, formation of the VS involves highly ordered polarisation of both viral and cellular proteins. This allows viral budding to occur in an ordered, unidirectional manner, towards the uninfected cell, resulting in more viral transfer, a higher multiplicity of infection (MOI) and therefore an increased likelihood of infection (Chen et al., 2007; Duncan et al., 2013; Duncan et al., 2014; Jolly et al., 2004; Sourisseau et al., 2007). In line with this, cryoEM and cryoET studies show that there are multiple virions at the virological synapse from which multiple infections can occur (Bennett et al., 2009; Jolly et al., 2004; Jolly et al., 2011; Martin et al., 2010; Welsch et al., 2007). VS formation also results in a greater number of Env, CD4 and coreceptor clusters at the cell membranes of infected and uninfected cells, respectively, thus increasing the likelihood of receptor engagement and fusion pore formation. Also, TCR signalling is triggered at the VS (Len et al., 2017), therefore it is possible that this modulates permissivity of target cells during cell-cell contact; a hypothesis which is currently being explored by Jolly and colleagues. Some evidence suggests that high MOI at the VS results in multiple HIV-1 integrations into the target cell (Del Portillo et al., 2011; Russell et al., 2013), although the idea of multiple integrations remains controversial. Single cell sequencing was used to determine the number of HIV-1 proviruses in infected cells from lymph node tissue and peripheral blood cells. This analysis revealed that less

than 10% of infected cells had multiple infections, with approximately 3.2 integrations per cell, although this remains controversial, since these events might reflect the presence of defective proviruses, as discussed above (Josefsson et al., 2011; Josefsson et al., 2013; Jung et al., 2002). Jung et al (2002) sampled cells from the spleen and increased sampling of spleen and lymph nodes may give a better estimate than the peripheral blood cells, since HIV replicates in lymphoid tissues. Further, HIV-1 infection modelling studies also suggested this to be the case, based on the amount of genetic recombination observed in chronic HIV-1 infection (Batorsky et al., 2011; Neher and Leitner, 2010).

Cell-cell spread reduces the efficacy of antiretroviral drugs against HIV-1. Firstly, HIV-1 is less sensitive to NRTIs and NNRTIs during cell-cell spread compared with cell free infection (Agosto et al., 2014; Duncan et al., 2013; Gupta et al., 1989; Mathez et al., 1993; Permanyer et al., 2012; Sigal et al., 2011; Titanji et al., 2013). This is thought to be because accumulation of virus at the VS results in a higher MOI and so a higher concentration of drugs is required to suppress infection (Duncan et al., 2013; Sigal et al., 2011; Titanji et al., 2013). Given that recent data suggest that cell-cell transmission is the primary mode of viral dissemination *in vivo* (Ladinsky et al., 2014; Schacker et al., 2000; Sewald et al., 2012), it remained unclear as to how ART was so effective at inhibiting infection based on clinical data. To better understand this, systematic testing of the effectiveness of single and combination therapies against cell-cell spread was carried out (Agosto et al., 2014; Titanji et al., 2013). These studies revealed that only some NRTIs and the protease inhibitors, were ineffective at blocking cell-cell transmission. HIV-1 was equally sensitive to protease inhibitors regardless of mode of transfer (Titanji et al., 2013; Titanji et al., 2017). This can be explained by the mechanism of action of these drugs. Protease inhibitors prevent maturation resulting in the production of non-infectious nascent virions; therefore, the mode of spread has little effect in reversing this defect. Also, resistance to the same drugs was less apparent when a primary HIV-1 isolate was tested, suggesting that the effect of ART on cell-cell spread also depends on the virus (Agosto et al., 2014). Taken together, these results have important implications in the clinical setting. It is possible that combination therapy is more effective because the drugs are targeting different stages of the life cycle, as well as different modes of HIV-1 dissemination (Agosto et al., 2014; Titanji et al., 2017).

Studies investigating sensitivity of HIV-1 to neutralising antibodies showed that transfer across a VS during cell-cell spread renders the virus less sensitive to neutralisation (Abela et al., 2012; Chen et al., 2007; Gupta et al., 1989; Malbec et al., 2013; Martin et al., 2010; McCoy et al., 2014; Zhong et al., 2013). Resistance to neutralisation varies

depending on the neutralising antibody being used. McCoy *et al* (2014) used HIV-1 infected T cell lines and primary T cells to test the effect of a panel of bnAbs on HIV-1 neutralisation sensitivity during cell-cell spread (McCoy et al., 2014). Antibodies targeting the gp41 MPER and gp120 variable loops could not inhibit cell-cell spread, whereas bnAbs targeting the CD4 binding site were able to do so (Malbec et al., 2013; McCoy et al., 2014). The resistance phenotype may be explained by the idea that during cell-cell spread, the distance a virus must travel to infect a target cell is much shorter compared with cell free infection. Therefore, there is a reduced possibility of HIV-1 being exposed and targeted by the humoural immune system. Further, since CD4-Env interactions are crucial for VS formation, the CD4 binding site antibodies will prevent virological synapse formation, thereby leading to inhibition of cell-cell spread.

Another advantage of cell-cell spread is the ability to evade restriction factors, which are antiviral proteins that target HIV-1 at multiple steps in the viral lifecycle, and will be discussed extensively in **section 1.4**. Tetherin was described to restrict HIV-1 infection by tethering virus particles to the cell membrane, thus preventing efficient budding (Giese and Marsh, 2014; Neil et al., 2008). The viral protein Vpu antagonises tetherin by targeting it for proteasomal degradation (Goffinet et al., 2009). Vpu-defective viruses were shown to be more efficient at cell to cell spread compared with WT virus and this correlated with more VS formation in the presence of Vpu-defective virus (Jolly et al., 2010). Imaging studies revealed that tetherin was enriched at the VS and this resulted in increased levels of Env accumulating at the site of cell-cell contact. Therefore, it was shown that tetherin does not inhibit infection during cell to cell spread. Instead, it was speculated that Tetherin may promote viral spread via the VS by mediating accumulation of Env and/or by providing structural integrity to the VS structure (Jolly et al., 2010). The latter was suggested based on the observation that depletion of tetherin using siRNA resulted in decreased VS formation and cell to cell spread, irrespective of the presence of HIV-1 Vpu. By contrast, one study showed that THN does inhibit cell-cell transfer of HIV-1 particles (Casartelli et al., 2010b). Discrepancies between these studies might be explained by differences in the level of Tetherin expression in different cell types, as well as differences in the mechanism of cell-cell spread between different donor and target cell types. Another restriction factor which cell-cell spread overcomes is TRIM5α. Rhesus macaque TRIM5α was shown to potently inhibit cell-free HIV-1 infection (Stremlau et al., 2004). However, when T cells that are engineered to express rhesus-TRIM5α, and cocultured with non-rhesus-TRIM5 cells, cell-cell spread is not inhibited (Richardson et al., 2008). This suggests that cell-cell spread may overcome restriction by rhTRIM5. Recently, the IFITM proteins were shown to inhibit HIV-1 infection by targeting the step of viral fusion (Lu et al., 2011a). Some studies correlate mutations in

env and *vpu* that render HIV-1 insensitive to IFITM restriction, with enhanced cell-cell spread (Ding et al., 2014). This might be explained by the observation that IFITM2 and IFITM3, in virus producer cells, interact with Env and antagonise cell-cell spread (Yu et al., 2015).

Cell-cell spread may also be disadvantageous for the virus. For example, HIV-1 cell-cell spread enhances cell death of target cells. A study using tonsil-derived T cells showed that cell-cell (but not cell-free) spread mediated non-productive or abortive infection of resting CD4 T cells leading to pyroptotic cell death (Galloway et al., 2015). During abortive infection, incomplete RT products are sensed by the IFI16 DNA sensor, which triggers pyroptosis (Doitsh et al., 2014; Monroe et al., 2014). It is possible that the high efficiency of cell-cell spread results in infection of non-permissive cells, which triggers cell death. Therefore, cell-cell spread may contribute to HIV-1 pathogenesis by trigger T cell death which is characteristic of infection. Taken together, these data suggest that cell-cell can be advantageous for HIV-1 infection in vivo due to increased efficiency of viral transmission, resistance to neutralising antibodies, ART and some restriction factors, but may also contribute to pathogenesis by inducing target cell death.

1.2.5.4 *In vivo* evidence of cell-cell spread

Although HIV-1 cell-cell spread is thought to be more efficient compared with cell-free transmission, little direct evidence exists to show that cell-cell spread occurs *in vivo*. For obvious reasons, it is difficult to perform *in vivo* studies in humans, therefore humanised mouse models have been used thus far to indirectly show that cell-cell spread is possible. For example, multiphoton intravital microscopy showed that HIV-1 infected T cells migrate to lymph nodes and establish interactions and form syncytia with neighbouring cells in a Env-dependent manner (Murooka et al., 2012), suggesting the possibility of cell-cell spread. Electron tomography of T cells from infected humanised mice revealed that they stay in close contact with uninfected cells, which are potential targets for viral dissemination (Ladinsky et al., 2014). Also, imaging of the sites of cell-cell contact show that there is polarised viral budding, as well as enriched presence of LFA-1 and ICAM-1 adhesion molecules (Ladinsky et al., 2014). This is highly suggestive of the presence of a virological synapse between infected and uninfected cells in the GALT (Ladinsky et al., 2014). Clustering of T cells was also observed using histology, in HIV-1 infected lymph nodes, suggesting that HIV-1 preferentially infects neighbouring T cells which are in close contact (Schacker et al., 2000). Finally, infection by another retrovirus, MLV, was also shown to induce stable contacts between infected and uninfected cells using intravital microscopy (Sewald et al., 2012). Initially it was shown that these cell-cell contacts form in an Env-dependent manner and that Gag polarises to sites of contact

(Sewald et al., 2012). VS formation and cell-cell spread was eventually confirmed (Sewald et al., 2015). Taken together, these data suggest that it is possible for cell-cell spread to occur *in vivo*, however the importance for viral replication remains to be elucidated.

1.2.5.5 Filopodia and Nanotubes

Cell-cell spread does not necessarily have to be mediated by a synapse between the infected and uninfected cell. Filopodia are actin-rich protrusions from the plasma membrane (Mattila and Lappalainen, 2008), which were first described for the transmission of MLV (Sherer et al., 2007). Filopodia formation has also been observed between HIV-1 laden DCs and uninfected CD4 T cells, exemplifying another cellular mechanism subverted by the virus to mediate successful transmission (Do et al., 2014; Felts et al., 2010; Nikolic et al., 2011). Engagement of DC-SIGN, results in HIV-1 mediated activation of CDC42, which is a small GTPase, and this leads to actin cytoskeleton remodelling and subsequent filopodia extension (Nikolic et al., 2011). Filopodia extend to neighbouring CD4 T cells and virus budding occurs at the tip of the filopodia, which allows HIV-1 to tether to multiple neighbouring target cells simultaneously, thereby increasing the efficiency of viral dissemination (Aggarwal et al., 2012).

HIV-1 can also transmit to target cells using nanotubes, which are longer structures compared with filopodia, and allow for rapid transmission of HIV-1 (Eugenin et al., 2009; Kadiu and Gendelman, 2011a, b; Sowinski et al., 2008). Unlike filopodia, HIV-1 does not induce/increase the number of nanotubes formed by infected cells (Sowinski et al., 2008). Nanotubes are membranous bridges that likely form after cells come into close contact and then separate (Sowinski et al., 2008)Live cell imaging revealed that HIV-1 surfs along the surface of nanotubes to transfer from an infected T cell to an uninfected target T cell (Sowinski et al., 2008). HIV-1 also disseminates via this method in macrophages (Kadiu and Gendelman, 2011a, b). The viral accessory protein Nef, is thought to be responsible for an increase in nanotube formation during HIV-1 infection of macrophages (Eugenin et al., 2009). M-sec is a key regulator of nanotube formation (Hase et al., 2009) and Nef alters its localisation to encourage nanotube formation (Hashimoto et al., 2016). This form of dissemination is independent of Env-CD4 interactions and allows for longer range transmission, although it is estimated to only account for 10% of the cell-cell spread observed *in vitro* (Rudnicka et al., 2009).

1.3 HIV Envelope biology

HIV-1 Envelope (Env) is a key determinant of infection as it binds to the CD4 receptor and coreceptors, CCR5 and CXCR4, on uninfected cells in order to initiate viral entry. **Figure 1.6** illustrates the linear structure of Env. Immature Env is produced as the gp160 polyprotein which is proteolytically cleaved into the mature form which has two functional subunits: gp120 and gp41. The gp120 subunit mediates CD4 receptor and coreceptor binding. It is heavily glycosylated, and this is thought to be a mechanism used to avoid adaptive immune recognition. The gp41 subunit regulates Env trafficking to the cell surface and incorporation into nascent virions. Each functional Env spike is a heterotrimeric structure composed of three gp120 and three gp41 subunits interacting non-covalently. The gp160 polyprotein undergoes extensive processing and traffics to the plasma membrane to get incorporated into nascent virions. Each HIV-1 virion expresses approximately 7-12 functional Env spikes on the surface, again, as another mechanism to avoid immune recognition by limiting exposure at the cell surface. It is also possible for several non-functional Env variants to be produced and incorporated into virions. For example, gp120-gp41 monomers, uncleaved gp160 monomers and oligomers and finally gp41 stumps. Incorporation of these variants significantly reduces viral infectivity, however it is thought that they act as immune decoys to induce non-neutralising antibodies, hence yet another mechanism to evade the adaptive immune system (Sanders and Moore, 2017). Despite Env incorporation being a crucial step in infectious virus production, the exact mechanism by which this event takes place is currently unknown. Several models have been proposed and will be discussed extensively in **Section 1.3.5**.

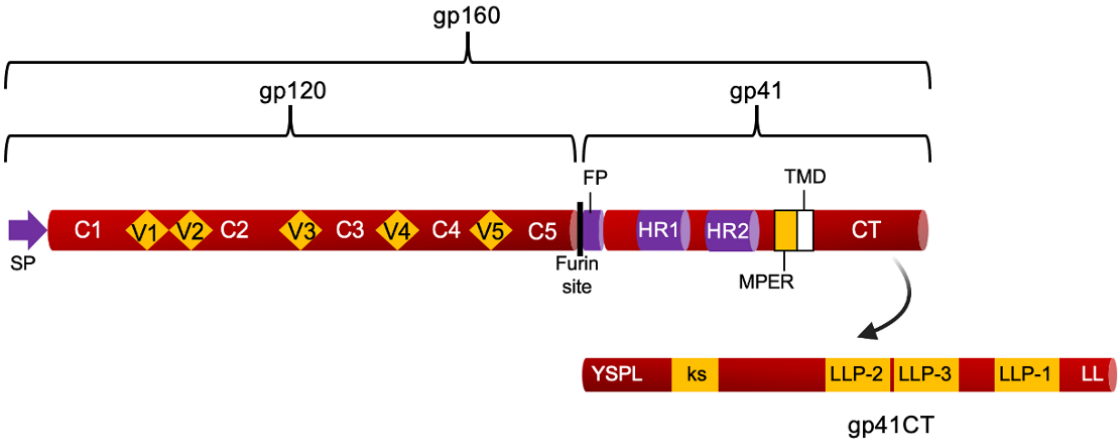

Figure 1.7 Linear structure of Env. Schematic representation of gp120 and gp41 linear structure. Shown are conserved domains (C1-C5) and variable loops (V1-V5) in the gp120 subunit. Regions containing CD4 binding site (C2, C3 and C4) are shown in orange. The gp41 subunit consists of fusion peptide, two heptad-repeat domains (HR1 and HR2) shown in purple, membrane-proximal external region (MPER), transmembrane domain (TMD) and the cytoplasmic tail (CT). Furin cleavage site is between the C5 domain and fusion peptide. The EnvCT has a conserved YxxL endocytic motif at the N-terminus (YSPL in HIV-1 NL4.3 strain) and a dileucine motif at the C-terminus which are important for Env recycling. After the N-terminal endocytic motif there is a Kennedy sequence (ks) and three a-helical structures called Lentiviral Lytic Peptides (LLP) 1-3. Adapted from (Checkley et al., 2011).

1.3.1 Env Biosynthesis

Env translation occurs in the rough endoplasmic reticulum (RER). The N-terminal region of gp160 contains an ER signal peptide which allows gp160 to insert into the RER membrane (Berman et al., 1988). Cellular peptidases cotranslationally remove this signal peptide. Haffar and colleagues (1988) performed *in vitro* analysis of gp160 in microsomal membranes and used antibody binding assays and protease protection analysis to show that gp160 remains attached to the membrane in an orientation whereby the extracellular portion of Env faces the ER lumen and the cytoplasmic tail faces the cytoplasm (Haffar et al., 1988). This results in the Env cytoplasmic tail facing inside the virus particle during Env incorporation. A stop transfer signal in the gp41 hydrophobic TMD prevents the entire polyprotein from entering the ER lumen.

The gp160 polyprotein is made from a singly spliced bicistronic *Env-Vpu* mRNA. Two models have been proposed to explain the process of Env translation: Leaky scanning and Ribosome shunting. The former model was suggested by Schwartz and colleagues when they observed that mutations in the *Vpu* initiation codon led to increased Env translation (Schwartz et al., 1992; Schwartz et al., 1990). The leaky scanning hypothesis describes that the 40S ribosome does not always scan the *Vpu* start codon as it is surrounded by a weak Kozak initiation sequence. Alternatively, Anderson and colleagues investigated the 5' UTRs of several alternatively spliced Env mRNAs and found that mutations of upstream start codons, including the *Rev* start codon, had little or no effect on Env synthesis (Anderson et al., 2007). This suggested that Env translation was a result of discontinuous ribosomal scanning and ribosome shunting is an example of this process. Ribosome shunting refers to the process in which ribosomes bypass parts of the 5' UTR in order to reach a start codon. In line with this hypothesis, Krummheuer and colleagues (2007) showed that Env translation is stimulated by a 6-nucleotide upstream ORF in the *Vpu* start codon which when mutated, led to a reduction in Env synthesis. This suggested that the upstream ORF acts as a ribosomal pause site which encourages ribosomal shunting to the Env initiation codon (Krummheuer et al., 2007).

N-linked glycosylation of gp160 takes place concomitantly with translation and O-linked glycosylation occurs in the cis-Golgi (Allan et al., 1985; Bernstein et al., 1994; Leonard et al., 1990), leaving the protein with several oligosaccharide side chains. Glycosylation is thought to trigger oligomerisation of gp160 (Earl et al., 1990; Pinter et al., 1989). Although the resultant oligomers can be of various sizes, the predominant form is a trimer of gp160 molecules. Oligomerisation and correct protein folding are thought to trigger trafficking of gp160 from the ER to the cis-Golgi and then to the Trans-Golgi network

(TGN) via the secretory pathway. Further details regarding Env glycosylation and its importance in evading adaptive immunity will be discussed in **section 1.2.2.3**

Once in the Golgi, gp160 trimers are proteolytically cleaved by the cellular protease, Furin, and other furin-like proteases (Hallenberger et al., 1992). These proteases recognise a highly conserved cleavage motif: K/R-X-K/R-R motif (Hallenberger et al., 1992; McCune et al., 1988). Mutational analysis of this motif revealed that HIV-1 particles become fusion incompetent when this motif is altered, as it alters Furin's ability to cleave gp160. This demonstrated that gp160 cleavage is essential for producing infectious virus particles with mature Env spikes. Two subunits are formed when gp160 is cleaved: a soluble gp120 surface subunit and the gp41 transmembrane subunit. A functional Env spike is characterised by a heterotrimeric structure, composed of three gp120 and three gp41 subunits. The N-terminus and the C-terminus of gp120 loop together and non-covalently interact with the gp41 subunit (Julien et al., 2013; Lyumkis et al., 2013; Pancera et al., 2014). **Figure 1.7** summarises the process of Env biosynthesis.

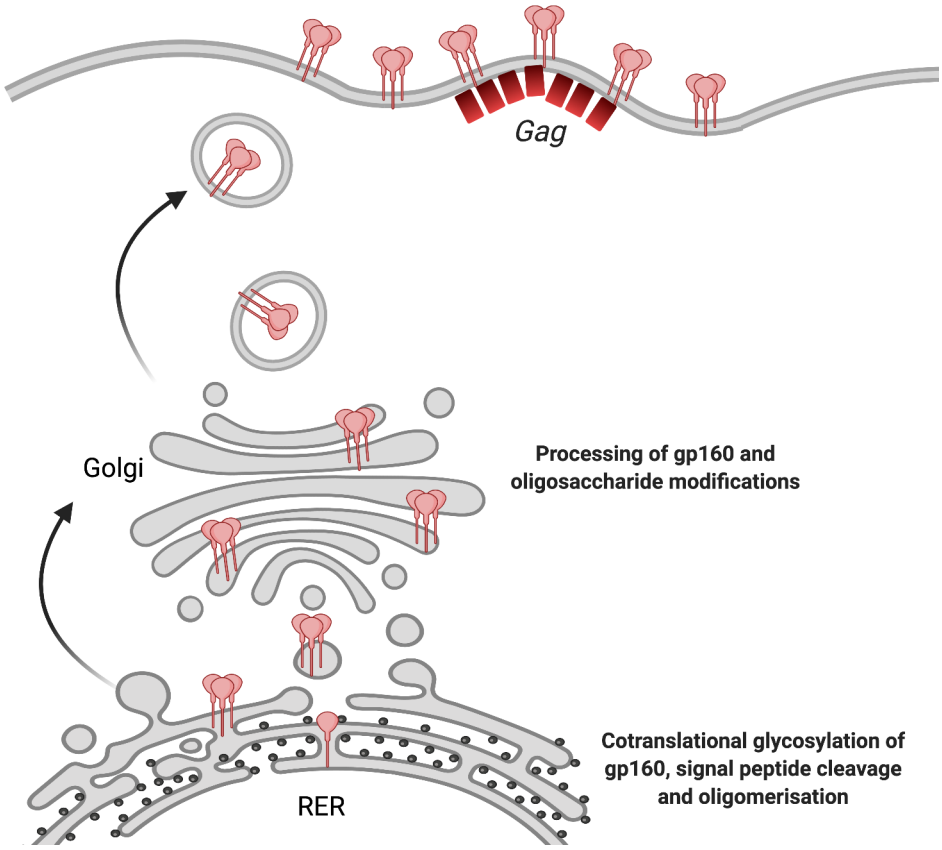

Figure 1.8 Env biosynthesis. gp160 polyprotein is synthesised in the rough endoplasmic reticulum (RER), it is glycosylated and oligomerises to form trimers. Cleavage of the signal peptide allows the newly synthesised Env trimers to leave the RER and enter the Golgi, where gp160 trimers are further processed. Finally, the trimers are trafficked to the plasma membrane, where Gag protein is also present. Adapted from (Checkley et al., 2011)(Created using BioRender.com).

1.3.2 gp120 structure and function

The gp120 subunit of Env is the only viral protein exposed to the extracellular environment (alongside gp41 MPER) and is therefore a major target for neutralising antibodies and vaccine development. Soluble gp120 protein is composed of five variable loops (V1-V5) and five constant regions (C1-C5), as depicted in **Figure 1.6** (Ward and Wilson, 2017). Understanding the 3D structure of Env is critical in aiding our understanding of HIV-1 entry mechanism, as well as designing an effective vaccine against the virus. However, this remained a challenge for many years due to high flexibility of the Env trimer, leading to technical difficulties in the process of crystallisation. In 2002, a stable Env trimer was designed and named SOSIP (Sanders et al., 2002). SOSIP Env has a disulphide bond inserted between gp120 and gp41, to allow the two subunits to be covalently linked. It also has an isoleucine to proline mutation in heptad repeat 1 (HR1) of gp41 in order to aid trimer formation (Sanders et al., 2002). SOSIP has been used to solve high resolution 3D structures of Env using crystallography and more recently, cryo-electron microscopy (cryo-EM) (Bartesaghi et al., 2013; Huang et al., 2007; Julien et al., 2013; Kwon et al., 2012; Kwong et al., 1998; Lyumkis et al., 2013). Early crystallography studies of monomeric gp120 bound to CD4 and various broadly neutralising antibodies (bnAbs) such as 17b, suggested that gp120 adopts a 'core' structure and is composed of 5 variable loops, 26 β-strands and 5 α-helices (Huang et al., 2007; Kwon et al., 2012; Kwong et al., 1998). This notion was reinforced recently using cryo-EM to show that gp120 is a globular structure that adopts a trimeric conformation via intrachain disulphide bridges (**Figure 1.9A-B**) (Bartesaghi et al., 2013; Julien et al., 2013; Lyumkis et al., 2013).

Comparisons between HIV-1 and HIV-2 Envs reveal that there is only 30% overall sequence identity and 40% overall amino acid identity between the Env glycoproteins of these viruses. However, Davenport and colleagues (2016) solved the first 3D structure of HIV-2_{ST} gp120 bound to CD4, and showed that there is very little difference in the overall structure compared with HIV-1 gp120 (**Figure 1.9C**) (Davenport et al., 2016). This is surprising because HIV-2 is known to have decreased virulence and HIV-2 infection is able to induce a robust neutralising antibody response, thus it is different to HIV-1 Env (Hahn et al., 1987; Kong et al., 2012a; Kong et al., 2012b). However, this may be explained by differences in gp120 glycosylation patterns, leading to the formation of a less effective glycan shield which exposes HIV-2 gp120 epitopes to antibodies (Shi et al., 2005).

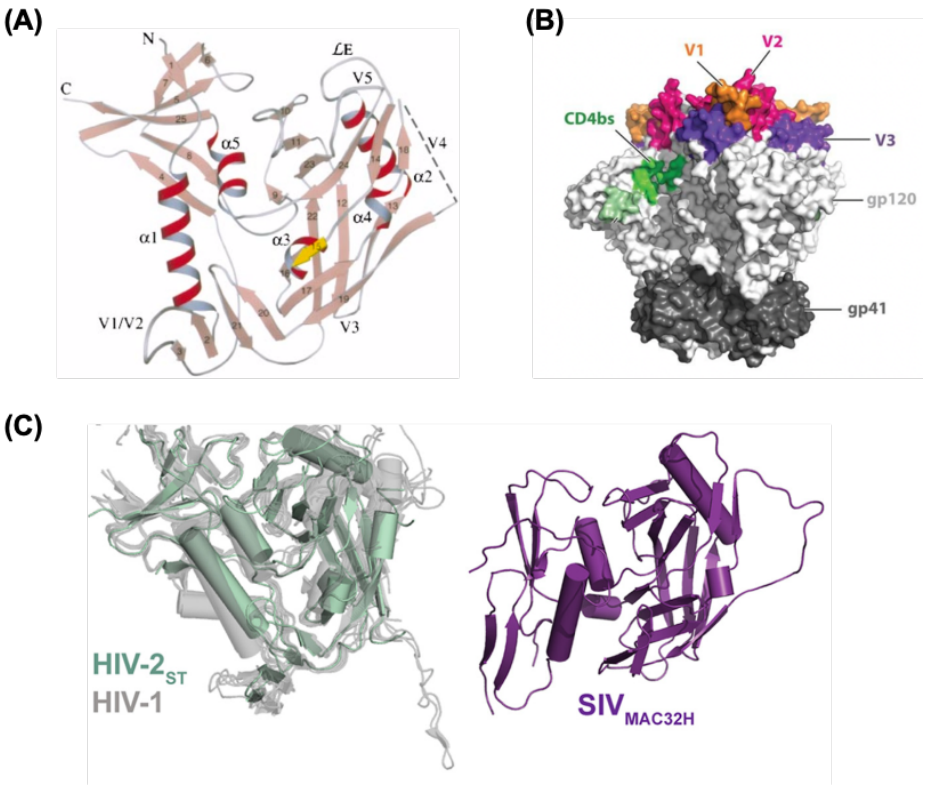

Figure 1.9 Structure of gp120 surface subunit. (A) Ribbon diagram. a-helices are depicted in red and b-strands in salmon, except for strand b15 (yellow), which makes an antiparallel b-sheet alignment with a strand of CD4. From (Kwong et al., 1998) **(B)** Crystal structure of Env trimer (PDB 4ZMJ). The gp120 subunit is shown in light grey and the gp41 subunit (ectodomain only) is shown in dark grey. V1, V2 and V3 loops are shown in orange, magenta and purple, respectively. The CD4 binding site (CD4bs) is shown in green. From (Burton and Hangartner, 2016) **(C)** Superposition of HIV-2, HIV-1, and SIV gp120 structures. (Left) Sequence-based alignment of HIV-2 ST gp120 core (green) with liganded and unliganded HIV-1 gp120 cores (grey) shows structural similarity. (Right) The SIVmac32H gp120 core from same viewpoint shows several secondary structural elements with different conformations. Taken from (Davenport et al., 2016).

Both single molecule FRET and cryo-EM studies reveal that Env is a dynamic structure, as gp120 adopts various conformations depending on the ligand bound. Details of structural rearrangements involved in viral entry and fusion will now be discussed further.

1.3.2.2 gp120 structure and viral entry mechanism

A key structural element of gp120 is the CD4 binding site (**Figure 1.9B**), which is highly conserved and essential for viral fitness (Dalgleish et al., 1984; Klatzmann et al., 1984). The CD4 binding site is a quaternary structure formed by sequences in the C2, C3 and C4 domains. Crystallography and cryo-EM studies show that CD4 binding and conformation of the CD4 binding site is highly dependent on the presence of neighbouring gp120 molecules (Kwon et al., 2012; Lyumkis et al., 2013; Stewart-Jones et al., 2016).

Single molecule FRET studies showed that Env is a highly dynamic structure which is stabilised by either CD4 binding or bnAb binding (Munro et al., 2014) and interestingly this information can be used to explain differences in sensitivity to antibody neutralisation of different Env glycoproteins. For example, the clinical isolate derived JRFL Env is more intrinsically stable compared with the lab-adapted NL4.3 Env, and JRFL is therefore less susceptible to neutralisation by bnAbs (Munro et al., 2014). Further, high resolution cryo-EM structures reveal four different conformations of gp120 (**Figure 1.10**). (**1**) The first structure is the closed conformation which is present prior to CD4 binding to gp120. Bartesaghi and colleagues (2013) used the VRC03 bnAb to determine the cryo-EM structure of Env in the prefusion state, as this bnAb was previously shown to preserve Env in a closed quaternary conformation (Tran et al., 2012). In this conformation, a 3-stranded form of the gp120 bridging sheet facilitates localisation of the V1/V2 loop region at the apex of the trimer, thus occluding the V3 loop and hiding the coreceptor binding site (Bartesaghi et al., 2013). (**2**) The next conformation was described by Ozorowski and colleagues (2017), whereby gp120 adopted an open conformation independently of CD4 binding. This conformation was induced by binding of the b12 bnAb to the CD4 binding site, which then induced rotation of gp120 cores around a fixed pivot point made up of the β-26 (C-terminal) and β-4 (N-terminal) gp120 strands (Ozorowski et al., 2017). Despite structural changes to the gp120 core. The bridging sheet remained in 3-stranded form and the V1/V2 loop region remained at the apex of the trimer, suggesting that gp120 pivoting may be a prerequisite for V1/V2 loop movement and also that further priming by CD4 binding is required for co-receptor binding site exposure and fusion. The following conformation reinforces this idea. (**3**) In this conformation, gp120 was in an open conformation when bound to CD4 and different bnAbs (Bartesaghi et al., 2013; Lyumkis et al., 2013; Ozorowski et al., 2017). gp120 cores pivoted around the β-26 and β-4 strands and the V1/V2 loop region was also displaced away from the trimer apex to reveal the V3 loop, leading to co-receptor binding site exposure (Ozorowski et al., 2017; Pancera et al., 2014). Displacement of the V1/V2 loop region was supported by the formation of a 4-stranded bridging sheet and this occurred once β-2 and β-3 of gp120

swapped positions so that they were antiparallel to one another. (**4**) The next conformation was described by Wang and colleagues (2018) as 'partially open' in a CD4- and 8ANC195-bound structure. 8ANC195 is a bnAb which recognises the gp120-gp41 interface and once bound, leads to changes in gp120 side chain arrangements compared with the fully open structure (Wang et al., 2018). This potentially leads to the gp41 fusion peptide adopting a helical conformation, ready for insertion into the target cell membrane during fusion (Wang et al., 2018). However, it is debatable whether this Env conformation exists in the absence of 8ANC195 (in which case the bnAb captured this conformation to make it more visible for structural studies) or whether 8ANC195 induced slight closure of the CD4-bound open conformation. Nevertheless, the data showed that partial closure of the open state did not reverse V1/V2 displacement, V3 exposure or the helical conformation of gp120 α0 (Wang et al., 2018). A summary of the early entry mechanism is as follows:

1. gp120 is in an equilibrium between '**closed**' and '**partially open**' conformations. The V3 loop remains occluded in both of these conformations, hence the co-receptor binding site is not exposed.
2. gp120 binds to CD4, resulting in structural rearrangements to adopt a fully '**open**', conformation, whereby the co-receptor binding site on the V3 loop is exposed.
3. The CD4-bound gp120 conformation described above may potentially undergo slight closure in order to adopt a '**partially open**' conformation. This induces helical conformation of gp41 fusion peptide, suggesting that the CD4-bound partially open conformation may lead to the next step of virus entry, which is co-receptor binding.

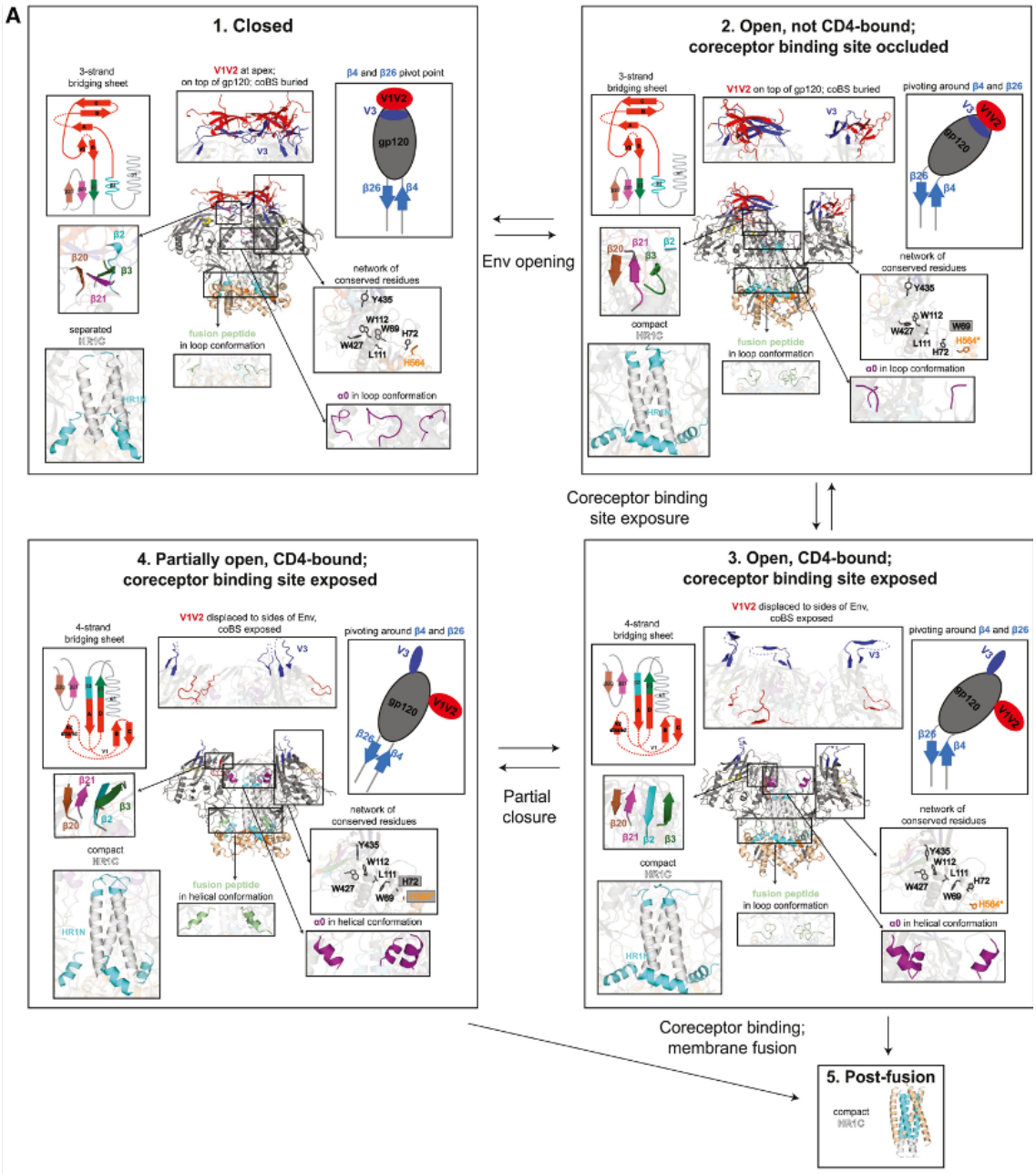

B

	gp120 conformation	V1V2	β2, β3, β20, β21	HR1C	α0	FP
closed	closed	at apex	3-strand	separated	loop	loop
open; coBS occluded	open	top of gp120	3-strand	compact	loop	loop
open; coBS exposed	open	displaced	4-strand	compact	helix	loop
partially open; coBS exposed	partially open	displaced	4-strand	compact	helix	helix
post-fusion	unknown	unknown	unknown	compact	unknown	helix

Figure 1.10 Model for order of conformational changes in Env leading to fusion. (A) Overview of the different conformations adopted by Env at various stages of fusion and viral entry. Env is a highly dynamic structure which undergoes conformational changes in several components including the variable loops in gp120 and the gp41 subunit. **(B)** Table summarising structural features shown in **(A)**. Taken from (Wang et al., 2018).

Once gp120 is bound to CD4, allosteric changes in gp120 expose the coreceptor binding site to the extracellular environment. The specificity for CCR5 or CXCR4 coreceptor binding is primarily determined by the sequence of the V3 loop, where X4-tropic viruses have more positively charged residues in the V3 loop, consistent with CXCR4 chemokine binding pocket being more negatively charged compared with CCR5 (Cocchi et al., 1996; Rosen et al., 2006; Shaik et al., 2019). Ozorowski and colleagues (2017) provided the intramolecular basis for CD4 and co-receptor induced conformational changes to HIV-1 during entry. When a dimer of CCR5 is docked on top of a trimer structure, CCR5 spans two gp120 subunits, thereby suggesting that CCR5 interacts with two co-receptor binding sites, (Ozorowski et al., 2017) however this interaction does not lead to further conformational changes in gp120 or gp41 (Ozorowski et al., 2017; Shaik et al., 2019). Later work using advanced microscopy techniques provided a detailed intermolecular basis for the conformational changes that occur prior to and during co-receptor binding(Iliopoulou et al., 2018). Iliopoulou *et al* (2019) used a combination of super-resolution microscopy and fluorescence fluctuation spectroscopy to reveal that the process of fusion initiation required formation of higher order assembly of Env-receptor-coreceptor complexes (Iliopoulou et al., 2018). Both X4- and R5-tropic envelopes undergo a three-step mechanism to initiate fusion (Iliopoulou et al., 2018). Briefly, this study showed that the X4-tropic HXB2 Env bound to 1 CD4 molecule, which induced CXCR4 dimerisation. Then CD4 engaged with 2 Envs to create a hexameric complex consisting of 1 Env molecule bound to 4 CD4 molecules and 2 CXCR4 molecules. This resulted in gp120 disassembly into an anchoring domain and a fusion domain, which would proceed to 6-helix bundle formation and fusion (Iliopoulou et al., 2018). With regards to the R5-tropic JRFL Env, it also bound to a single molecule of CD4 initially, however then it recruited 2 additional CD4 molecules. This induced CCR5 dimerisation and a complex consisting of 1 Env, 3 CD4 and 2 CCR5 molecules, leading to gp120 disassembly and fusion (Iliopoulou et al., 2018). Despite similarities in the initial step, X4- and R5-tropic envelopes had different entry kinetics and stoichiometries (Iliopoulou et al., 2018). CXCR4-mediated fusion initiation required 2 Env molecules whereas CCR5-mediated fusion required only 1 Env. Also, CXCR4 dimerisation occurred before CD4 oligomerisation, whereas CCR5 dimerisation happened after CD4 oligomerisation (Iliopoulou et al., 2018). This suggests that there are differences in the entry mechanism of X4- and R5-tropic viruses which must be considered when investigating different aspects of HIV entry and fusion, such as mechanisms of restriction factors targeting viral entry. The remainder of the Env-mediated fusion mechanism will be discussed in **section 1.3.3** as it involves crucial gp41 structure-function relationships.

1.3.2.3 gp120 glycan shield and adaptive immunity

Another important feature of gp120 is that it is heavily glycosylated, resulting in a glycocalyx-like structure called the 'glycan shield' surrounding the virus. Co-translational glycosylation of Env occurs in the ER, where N-linked glycans are added to gp160 (Bernstein et al., 1994; Leonard et al., 1990). Appropriate trimer cleavage is required to produce an Env molecule with the correct glycosylation architecture. Misfolded or poorly folded Env proteins have higher amounts of processed glycoforms and are retained in the ER.

Glycans present on HIV-1 Env account for at least half of its total mass (Doores et al., 2010; Lasky et al., 1986; Stewart-Jones et al., 2016). Using BG505 SOSIP, it was shown that there are 25-30 glycans present on each gp120 protomer and 3-5 glycans are present on gp41 (Lyumkis et al., 2013; Montefiori et al., 2018). A mixture of glycans can be found on the surface of the virus, including (1) high mannose type glycans and (2) complex type glycans, which require further processing once Env reaches the Golgi. Certain sites on Env are exclusively high mannose sites and others are exclusively complex-type, suggesting that the host processing machinery is able to distinguish between the two types of sites on HIV-1 Env and that there is differential processing at each site.

The initial cryo-EM structures of fully glycosylated Env were unable to resolve most glycans in the absence of a bnAb which stabilises the Env structure (Lee et al., 2016; Lyumkis et al., 2013). Therefore, this suggested that the glycan shield is highly dynamic. However, a crystallography study of the glycan shield suggested that the glycan shield is a stable structure as it contains a wide range of inter-glycan contacts (Stewart-Jones et al., 2016). This discrepancy in results highlights the difficulty in studying structure-function relationships of the glycan shield. Ward and colleagues (2020) recently used an integrative approach, combining Cryo-EM, mass spectrometry and computational modelling, to show that the glycan shield is indeed highly dynamic and that variation exists in the dynamics of glycans belonging to different regions of Env (Berndsen et al., 2020). This is partly due to the formation of densely packed clusters and steric hindrance. A cryo-EM structure illustrating the great mass of glycans surrounding the HIV-1 Env is shown in **Figure 1.11A**.

The glycan shield is thought to be a mechanism used by HIV-1 to evade the adaptive immune system (Burton and Hangartner, 2016). Infection of rhesus macaques with mutant SIVs lacking N-linked glycosylation in Env resulted in increased antibody binding to specific peptides from this region and increased neutralising activity (Reitter et al.,

1998). This suggests that N-linked glycosylation plays a role in limiting the neutralising antibody response against SIV. Initially it was thought that the glycan shield is impenetrable, however high resolution Cryo-EM structures of Env revealed that this is not the case. Several bnAbs, such as 2G12 and the PGT series, are able to bind to epitopes found inside the glycan shield, as well as epitopes on the surface of the V3 and V4 loops (**Figure 1.11B**).

The high mannose patch (**Figure 1.11B**) is a region of densely packed, highly homogenous glycans centred mainly around Asn332 (N332) or N334, with some interspersed at the edges of the patch (Bonomelli et al., 2011; Doores et al., 2010; Go et al., 2015; Sok et al., 2014). It was shown that due to steric hindrance caused by neighbouring glycans, this section of the glycan shield cannot undergo secondary processing in the Golgi to convert high mannose sugars into complex glycoforms using glycosidases and transferases (Bonomelli et al., 2011; Pritchard et al., 2015). Interestingly, the high mannose patch is extremely vulnerable to recognition by bnAbs and was therefore considered a prime vaccine target. However, vaccine development remains a challenge, as exposure of different epitopes is highly dependent on neighbouring glycans and the sequence of variable loops surrounding this region.

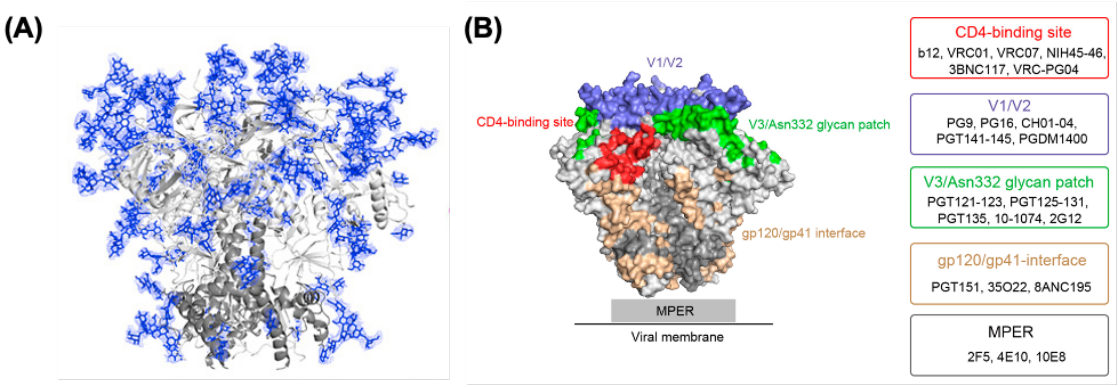

Figure 1.11 Env glycosylation. (A) A cryo-EM structure of gp120 (light grey) and gp41 (dark grey) surrounded by a large mass of glycans (blue) to make up the glycan shield. Taken from (Stewart-Jones et al., 2016) (B) Structure of Env colour coded with the epitopes recognised by different classes of broadly neutralising antibodies shown in the boxes. V1/V2 loops (purple), CD4bs (red), high mannose patch (green), gp120/gp141 interface (brown) and gp41 MPER (grey). Taken from (Zhang et al., 2016).

Vaccine development

The humoral immune system is fundamental in controlling infectious diseases. Several monoclonal antibodies (mAbs) have been identified and isolated from HIV-1 infected individuals (McCoy and Burton, 2017). These mAbs can be categorised based on their function of 'neutralising' or 'non-neutralising' infection. Neutralising antibodies (nAbs) block infection of target cells by binding to HIV-1 Env epitopes that are crucial for viral entry. During HIV-1 infection, nAbs begin to appear midway through the acute phase, once sufficient virus is circulating in the body (Wei et al., 2003). Rapid and continuous mutations in the Env sequence allows HIV-1 to escape this antibody response (Wei et al., 2003). An evolutionary arms race is thus established, whereby the virus and host immune system are constantly adapting to counteract one another.

Env proteins can be classified into different 'tiers' based on their susceptibility to nAbs (Seaman et al., 2010). Env glycoproteins belonging to tiers 1A and 1B are thought have an 'open' conformation and are easily neutralised, whereas tier 2/3 Envs have a 'closed' conformation, hence epitopes are less exposed for bnAb binding and neutralisation (Seaman et al., 2010). Generally, lab adapted strains of HIV-1 (such as NL4.3) belong to tier 1 (Seaman et al., 2010). It is thought the absence of any selective immune pressure in cell culture has allowed Env to adapt this open conformation, where the co-receptor binding site is more readily accessible, to increase infectivity (Seaman et al., 2010). On the other hand, Env from most circulating strains of HIV-1 belong to tier 2 and there are only 15 Env glycoproteins belonging to tier 3 (Seaman et al., 2010). Env undergoes dynamic structural changes at the surface of infected cells (reviewed by (Ward and Wilson, 2017)). Tiering describes the conformational state which each Env glycoprotein predominantly occupies in any given environment, in the presence of different binding partners (Seaman et al., 2010).

Broadly neutralising antibodies (bnAbs) target multiple strains of HIV-1 by binding to vulnerable epitopes on the Env trimer, therefore HIV-1 vaccine research heavily focusses on inventing strategies to induce bnAb formation in infected individuals (McCoy and Burton, 2017). *In vivo* studies have shown that passive transfer of bnAbs to rhesus macaques can protect against Simian-Human Immunodeficiency viruses (SHIV) and mice are protected against HIV-1 infection (Hessell et al., 2009; Hessell et al., 2010; Mascola et al., 2000; Moldt et al., 2012; Parren et al., 2001; Pegu et al., 2014; Rudicell et al., 2014). A recent clinical trial in sub-Saharan Africa provides proof of concept that passive administration of the mAb VRC01 can protect against susceptible virus infection (AVAC report, HIVR4P, 2021). A big hurdle in achieving this goal is the dynamic and hugely heterogenous nature of the HIV-1 Env glycan shield (Ward and Wilson, 2017).

Differences in glycosylation exist between different sites on Env and also at the same site between different Envs (Cao et al., 2017).

ADCC

Antibody-dependent cell-mediated cytotoxicity is a non-neutralising function of HIV-1 specific antibodies (Lee and Kent, 2018). ADCC refers to the process by which the antigen-binding fragment (Fab) of antibodies binds to Env expressed on infected cells (Lee and Kent, 2018). This leads to cross-linking of the Fc gamma-receptor on innate effector cells, such as NK cells, monocytes and neutrophils (Kramski et al., 2013; Smalls-Mantey et al., 2013). Effector cells subsequently release cytokines and chemokines which target infected cells (Mielke et al., 2019). Degranulation of cytotoxic granules releases perforin and granzyme B, both of which can eliminate HIV-1 infected cells (Mielke et al., 2019). Correlations between the ability of an antibody to perform ADCC and neutralise infection suggests that the two process are not mutually exclusive. Several studies have reported that bnAb binding to transmitted founder (T/F) viruses is weaker by comparison with lab-adapted strains (Bruel et al., 2016; von Bredow et al., 2016). This is likely due to the more 'open' Env conformation of the latter, as described above. The best strategy for targeting HIV-1 infection would need to be able to prevent both cell-free and cell-cell viral transmission. However, whether bnAbs can effectively block cell-cell transmission remains controversial (discussed in **section 1.2.5.1**).

The 'shock and kill' strategy that is being attempted to cure HIV-1 relies on reactivation of infected CD4 T cells which make up the latent HIV-1 reservoir (reviewed by (Deeks, 2012)). Passive transfer of ADCC-competent bnAbs in combination with a Latency Reversal Agent (LRA) may be a promising strategy, however a major problem with this is the inability to sufficiently reactivate infected CD4 T cells (to similar levels as PHA stimulation) (Deeks, 2012). A humanised mouse model study provided *in vivo* evidence that using a combination of bnAbs and a combination of different LRAs in conjunction, reduced the proportion of mice experiencing viral rebound compared with mice receiving bnAbs only or a single LRA (Halper-Stromberg et al., 2014). This strategy was successful in this study possibly because the multiple agents collectively activated the latent cells to high enough levels. Clinical trials are now required to test this the 'shock and kill' strategy in humans. Two recent studies used ART-treated humanized mice infected with HIV-1 and ART-treated, SIV-infected rhesus macaques to show that robust reactivation of latent proviruses may be possible using different methods (McBrien et al., 2020; Nixon et al., 2020). McBrien *et al* (2020) used an IL-15 activating drug in conjunction with antibody-mediated CD8 T cell depletion to show that there are high levels of virus in the blood and viral RNA is present in various tissues (McBrien et al., 2020). Nixon *et al*

(2020) administered a drug which activates the non-canonical NFkB pathway, to show that there is an increase in the viral RNA in CD4 T cells upon treatment, suggesting transcriptional activation, as well as measurable virus in the blood (Nixon et al., 2020). Whilst these studies seem promising in the context of reversing latency, they lack a component which will 'kill' the virus and therefore more research into this second step is required.

Viruses have evolved to evade antibody responses, including ADCC. The ability of an antibody to perform ADCC depends on the amount of Env antigen present. HIV-1 tightly regulates Env expression on the surface to limit exposure. Mutations in the conserved endocytic motif in the gp41 cytoplasmic tail result in increased surface Env expression, which subsequently increases susceptibility to ADCC (von Bredow et al., 2015). Also, Tetherin restricts infection by preventing viral release, hence there is an accumulation of virions at the cell membrane which can be targeted by ADCC-competent bnAbs. The viral accessory protein Vpu downregulates Tetherin from the cell surface, which avoids this outcome (Alvarez et al., 2014b; Arias et al., 2014). Finally, the accessory proteins Vpu and Nef downmodulate CD4 from the surface of infected cells which reduces the likelihood of CD4 binding to Env and exposing CD4 inducible epitopes that are often targeted by bnAbs (Veillette et al., 2015; Veillette et al., 2014).

1.3.3 gp41 structure and function

The gp41 subunit of Env can be subdivided into an extracellular domain, a transmembrane domain and the cytoplasmic tail (**Figure 1.7**). This section will discuss the structure-function relationship of different parts of the gp41 subunit.

1.3.3.1 gp41 extracellular domain

The extracellular domain of gp41 is important in the process of fusion, as it contains the fusion peptide, two alpha helical coiled-coil heptad repeats called HR1 and HR2 and a membrane proximal external region (MPER). Lyumkis and colleagues (2013) used PGV04 (a CD4-binding site antibody) complexed with BG505-SOSIP to create the first cryoEM structure of Env at ~5.8Å resolution (Lyumkis et al., 2013). This study highlights that gp41 forms the base of the Env trimer and confirmed that HR1 is a three-helix bundle found in the trimer core and HR2 is an alpha helix which wraps around the base of the trimer (**Figure 1.12**). Ozorowski and colleagues (2017) further revealed the structure of the gp41 fusion peptide in a CD4-17b bound state (Ozorowski et al., 2017). From this study it was evident that CD4 binding to gp120 and 17b binding to the coreceptor binding site in gp120, results in major structural changes within gp41, which primes Env for fusion. For example, the N-terminus of the HR1 domain moves away from the centre of

the trimer and concomitantly there is stabilisation of a helix in the fusion peptide proximal region. Further changes in gp120 and the gp41 HR2 domain produce a new pocket at the core of the trimer where the fusion peptide inserts itself and subsequently undergoes large conformational changes to stabilise in a fusion intermediate state (Ozorowski et al., 2017). It is hypothesised that coreceptor binding induces further structural changes to allow the fusion peptide to 'spring out' of this pocket and insert into the target cell membrane. Following this, interactions between gp120 and gp41 weaken, resulting in gp120 shedding. Then, extensive structural rearrangements in gp41 lead to the formation of a 6-helix bundle, which is a highly stable structure (Shu et al., 2000). It contains a hairpin turn (residues 597 to 609) between HR1 and HR2. Mutations in residues around this hairpin loop structure can result in loss of 6-helix bundle formation by interfering with HR1-HR2 interactions and inhibit fusion (Markosyan et al., 2009). Crystal structures of the 6-helix bundle reveal that the three N-terminal HR1 domains of gp41 form a triple stranded coiled coil α-helical structures, whereas the three C-terminal HR2 units are packed antiparallel and fit into the grooves of HR1. 6-helix bundle formation is complete once the viral and cellular membranes fuse to produce a fusion pore (Markosyan et al., 2003). Once fusion pore formation and enlargement is complete, the viral capsid core is delivered into the target cell cytoplasm marking the completion of HIV-1 entry.

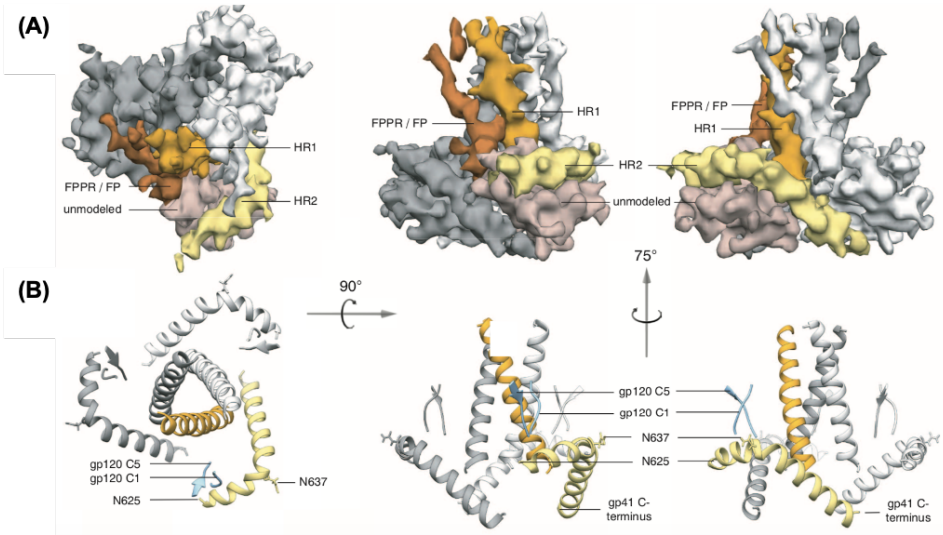

Figure 1.12 gp41 structure. (A) Segmented EM density map of the gp41 trimer. The C-terminal half of HR1 (rust) forms a three-helix bundle at the centre of the trimer; the C-terminal half of HR2 (yellow) forms a helical structure that wraps around the trimer base. Additional density that is not assigned in the model (beige) likely corresponds to the intervening region between HR1 and HR2, including the disulfide loop, as well as C1 and C5 from gp120. Density parallel to HR1 (brown) likely corresponds to the N-terminal half of HR1, the fusion peptide proximal region (FPPR), and the fusion peptide (FP). **(B)** Modelled portion corresponding to the same views of the EM density maps in (A). Taken from (Lyumkis et al., 2013).

1.3.3.2 gp41 transmembrane domain

Next, the transmembrane domain (TMD) of gp41 is a conserved region which anchors Env to the lipid bilayer and is important in Env-mediated membrane fusion and infectivity (reviewed by (Checkley et al., 2011)). It forms a well-ordered trimer which has a positively charged residue at the centre of the trimer, typically an arginine (Chen and Chou, 2017). NMR studies by Chen and Chou (2017) further reveal that the C-terminus forms a coiled-coil trimer containing a GxxxG motif and is held together by polar contacts to produce a hydrophilic core. The N-terminal coiled coil is in a helical wheel representation and forms the hydrophobic core. Typically, GxxxG motifs are involved in oligomerisation of proteins (MacKenzie et al., 1997), however only G690 is important in the HIV-1 Env TMD (Dev et al., 2016). Mutating the second Glycine (G694A) does not impact TMD trimerisation. G690 is important as it facilitates interactions with V689 on neighbouring TMD helices (Dev et al., 2016). Further, mutations in the TMD which result in destabilisation of the hydrophilic core, often resemble cytoplasmic tail-deleted virus with regards to sensitivity to neutralising antibodies (Dev et al., 2016). This is like due to the fact that changes in the TMD and EnvCT lead to global conformational changes in the Env ectodomain. Finally, the importance of the TMD in maintaining Env stability is highlighted by the observation that soluble Env proteins, which do not have an intact TMD, are often unstable and highly heterogenous; a major problem in HIV-1 vaccine design thus far.

1.3.3.3 gp41 cytoplasmic tail

The gp41 cytoplasmic tail (EnvCT) is the least well characterised domain of Env. Molecular biology and structural studies reveal that the EnvCT is crucial in Env trafficking and incorporation into nascent virions (Bowers et al., 2000; LaBranche et al., 1996; Sauter et al., 1996). A recent NMR structure reveals that the EnvCT is primarily embedded within the lipid bilayer, however the N-terminal region is unstructured (**Figure 1.13**) (Murphy et al., 2019). This region contains the highly conserved Y_{712}SPL endocytic motif which binds to cellular proteins such as the AP-2 adaptor protein for clathrin-mediated endocytosis of Env from the plasma membrane. The EnvCT also contains three lentiviral lytic peptides, LLP-1, LLP-2 and LLP-3 (**Figure 1.13**). LLP-1 and LLP-2 are positively charged due to the presence of arginine residues and LLP-3 is located between LLP-1 and LLP-2. Their name was derived from the observation that LLPs can perturb membranes (Chen et al., 2001; Chernomordik et al., 1994; Gawrisch et al., 1993), resulting in cytolysis (Miller et al., 1993). These highly conserved amphipathic alpha helical structures have been implicated in several Env properties including fusogenicity (Kalia et al., 2003), stability (Lee et al., 2002a), cell surface expression (Bultmann et al., 2001) and Env incorporation into nascent virions (Bultmann et al., 2001; Murakami and Freed, 2000). Finally, the Kennedy sequence is a highly immunogenic

region containing 3 consecutive epitopes that are recognised by SR1 nAbs: $P_{728}DRPEG_{732}$, $I_{733}EEE_{736}$ and $E_{739}RDRD_{743}$ (Buratti et al., 1998). These nAbs are able to inhibit cell-free infection, as well as cell-cell spread of HIV-1 by inhibiting the process of fusion (Cheung et al., 2005; Heap et al., 2005; Reading et al., 2003).

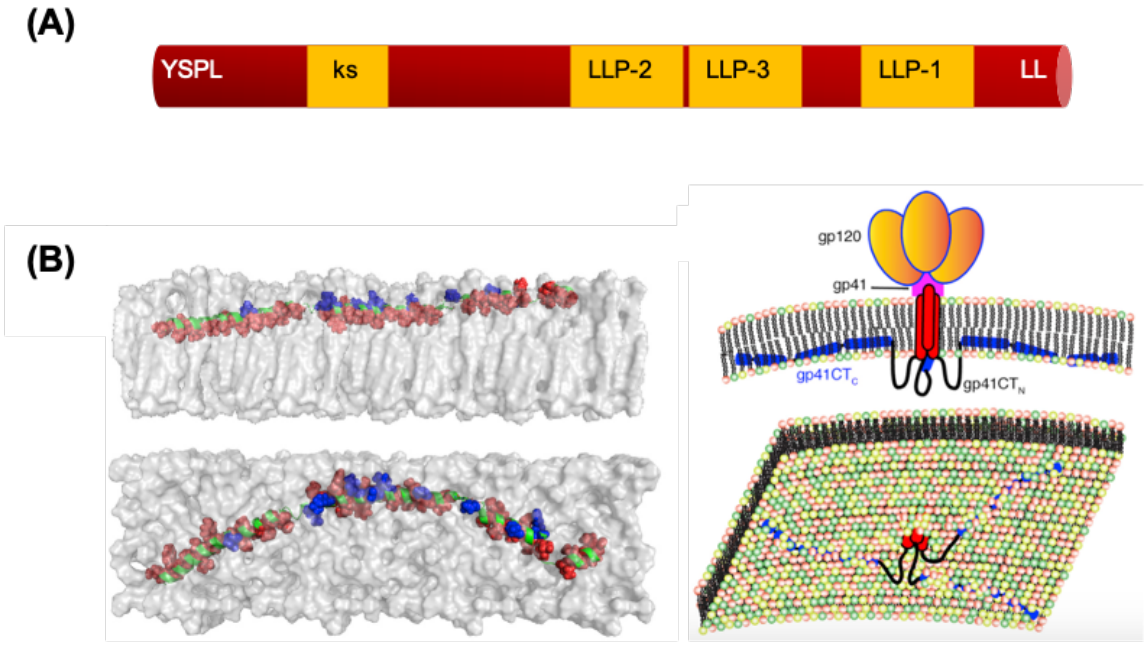

Figure 1.13 gp41 cytoplasmic tail. (A) Schematic showing the linear structure of the HIV-1 EnvCT containing a conserved, N-terminal YxxL (YSPL in HxB2 consensus sequence) endocytic motif, Kennedy sequence (ks), Lentiviral Lytic Peptides (LLP) 1-3 and a C-terminal dileucine motif important for Env trafficking. **(B)** Top panel: A model depicting the gp120 and gp41 proteins on the surface of HIV-1 particles. The EnvCT C-terminal domain is penetrating deeply in the inner leaflet of the membrane. Lower panel: An expanded view of the inner leaflet of the membrane showing EnvCT penetrating the bilayer. Taken from (Murphy et al., 2019).

1.3.4 EnvCT and Env trafficking

Once mature, heterotrimeric Env spikes reach the plasma membrane, they are either incorporated into nascent viral particles or rapidly recycled via clathrin-mediated endocytosis (Berlioz-Torrent et al., 1999; Egan et al., 1996; Rowell et al., 1995). Internalisation of Env is regulated by the EnvCT. In the EnvCT there are two tyrosine-based sorting motifs which can be recognised by the AP-2 complex (YSPL and YHRL), however mutational analysis revealed that the Y_{712}SPL motif (Egan et al., 1996) was important for endosomal sorting of Env (Boge et al., 1998). This is a highly conserved motif among HIV and SIV strains, suggesting that Env internalisation is crucial in the viral lifecycle, possibly to evade the adaptive immune response by limiting exposure on the cell surface. The Y_{712}SPL motif is recognised and predominantly bound by the μ2 chain of the AP-2 adaptor protein, as shown using coimmunoprecipitation and GST-pull down assays (Boge et al., 1998; Ohno et al., 1997). If this sequence is mutated to produce the Y712A mutant, AP-2 no longer binds to Env, resulting in less efficient Env recycling kinetics. Further, CD4-SIV Env constructs have been used to show that the SIVmac239 Env it remains at the plasma membrane for less than 5 minutes prior to internalisation via endocytosis (Bowers et al., 2000). Infection of Rhesus macaques with SIVmac239 mutants containing a mutation or deletion in this motif, resulted in attenuated SIV pathogenicity *in vivo,* as indicated by no clinical symptoms of disease and survival until the end of the study at 120-139 weeks post inoculation (Fultz et al., 2001). This suggests that the YxxΦ motif has important implications *in vivo*. Furthermore, the C-terminal dileucine motif in EnvCT, L855L856, also regulates Env trafficking via interactions with the AP-1 (Wyss et al., 2001) and AP-2 adaptor proteins (Byland et al., 2007). Byland *et al* (2007) used chimeric proteins in which HIV-1 Env was fused to the CD4 luminal and transmembrane domains, and the HxB2 Env, to assess the role of the YxxΦ endocytic motif and the c-terminal dileucine motif (Byland et al., 2007). Expression of these constructs in HeLa cells revealed that the dileucine motif is responsible for Env endocytosis, independent of the YxxΦ motif, since the L855L856/AA and Y712I mutants were able to recycle Env appropriately and there was only a significant increase in Env surface expression when both L855L856/AA and Y712I mutations were present in the same construct. This suggests that the two HIV-1 endocytic motifs are redundant and do not have any additive effects when expressed together in wild type Env. By contrast, SIV Env endocytosis is not dependent on the C-terminal dileucine motif (Bowers et al., 2000), suggesting that there are differences in the SIV and HIV Env trafficking which require further investigation. Such differences might explain the phenotype that SIV truncates its EnvCT when passaged in human cells (Kodama et al., 1989; Luciw et al., 1998), as discussed in **section 1.3.6**.

Once endocytosis occurs and Env enters an early endosome, there are three possible fates for the glycoprotein: 1. Lysosomal degradation; 2. Retromer-dependent retrograde trafficking to the Trans-Golgi network (TGN) or 3. Rab11-FIP1C and Rab14-dependent trafficking to the plasma membrane for incorporation into nascent virions (**Figure 1.14**)

1. Lysosomal degradation

One possible fate of Env is to enter endosomes which mature into lysosomes, resulting in degradation of Env trimers. Enhanced lysosomal degradation of Env has been observed upon manipulation of the gp120 glycan shield. For example, deletion of a conserved glycan at Env position 260 leads to lower levels of gp160 proteolytic cleavage into functional trimers, as well as enhanced lysosomal degradation of Env which could be rescued in the presence of the lysosome inhibitor chloroquine (Mathys et al., 2014). Further, infection of macrophages with HIV-1 ΔVpr virus leads to enhanced lysosomal degradation of Env by comparison with wild type HIV-1 (Mashiba et al., 2014). Pulse chase analysis in the presence of ammonium chloride (a lysosome inhibitor) rescued Env expression in the absence of Vpr (Mashiba et al., 2014). This suggests that Vpr protects Env from lysosomal degradation in macrophages.

2. Retromer-dependent retrograde trafficking to the TGN

Another fate of Env is to undergo retrograde transport from the cell membrane in a Retromer-dependent manner (Groppelli et al., 2014). The human retromer complex is hetero-pentameric structure, composed of a trimer of vacuolar protein sorting molecules (Vps26- Vps29- Vps35) and a membrane bending complex consisting of two sorting nexins (SNX1/2 with SNX5/6) (Swarbrick et al., 2011). This complex is an important member of the endosomal sorting machinery, as it recognises specific membrane proteins (cargo) and sorts them from maturing endosomes into nascent endosomal tubules (Arighi et al., 2004; Seaman, 2004, 2012). Then, cargo often undergoes retrograde transport to the Golgi complex. Some evidence also suggests that retromer can transport cargo proteins from endosomes to the plasma membrane (Seaman, 2012; Temkin et al., 2011). Retromer is responsible for endosomal sorting of physiologically important cargo proteins such as the cation independent mannose-6-phosphate receptor (CIMPR) (Arighi et al., 2004; Seaman, 2004); the iron transporter DMT1-II (Tabuchi et al., 2010), Wntless/MIG-14 (Eaton, 2008) and an amyloid precursor protein binding protein (Fjorback et al., 2012; Nielsen et al., 2007). Groppelli and colleagues (2014) show that siRNA-mediated depletion of retromer, in Hela TZM-BL reporter cells and in Jurkat T-cells, results in increased HIV-1 Env surface expression and incorporation into virions. Further, immunofluorescence microscopy was used to show that Env and Vps26, a crucial member of the retromer complex, colocalise and that upon retromer depletion,

Env is not retrieved in the Golgi apparatus from endosomes (Groppelli et al., 2014). Coimmunoprecipitation of Env and retromer components revealed that the Vps35 and Vps26 interact with the EnvCT. Using EnvCT truncation mutants, the group show that this phenotype is dependent on the C-terminal 100 amino acids of the EnvCT. Given that the EnvCT and Gag colocalise at sites of viral budding, one might speculate that retromer affects Gag localisation. Interestingly, retromer depletion has no effect on Gag, suggesting that Retromer specifically targets Env (Groppelli et al., 2014).

3. Rab11-FIP1C and Rab14 dependent trafficking to the plasma membrane

The Spearman lab have conducted extensive microscopy studies to understand the role of cellular trafficking proteins in Env trafficking to the plasma membrane. They elucidated the requirement of FIP1C and Rab proteins in this process (Kirschman et al., 2018; Qi et al., 2015; Qi et al., 2013). Rab11-FIP1C is a large hetero-tetrameric trafficking complex composed of the following proteins: Rab11, Rab14, Rab4 and FIP1C. shRNA-mediated depletion of FIP1C diminishes HIV-1 infectivity and reduces Env incorporation, whereas overexpression of FIP1C enhances infectivity and Env incorporation in a cell-type dependent manner (Qi et al., 2013). Qi and colleagues (2013) used TIRF microscopy to show that FIP1C, which is normally localised in perinuclear compartments with Rab11a (Jin and Goldenring, 2006), is re-localised to the plasma membrane in the presence of HIV-1 Env. Later studies further elucidated that the YW_{795} motif on alpha helix 2 of the EnvCT is important for Rab11-FIP1C mediated Env trafficking. Mutating the YW_{795} motif results in reduced Env incorporation in viruses produced from T cell lines, reduced infectivity and loss of FIP1C relocalisation to the plasma membrane (Qi et al., 2015). These results indirectly suggest that the Rab11-FIP1C complex interacts with the YW_{795} motif in EnvCT to mediate Env trafficking to the plasma membrane. Finally, in 2018 they provided the first piece of direct evidence to show that Env traffics through the endosomal recycling compartment (ERC) prior to FIP1C-mediated Env trafficking (Kirschman et al., 2018). A dominant negative mutant of FIP1C ($FIP1C_{560-649}$) was used to show that whilst wild-type HIV-1 Env becomes trapped in ERCs, the YW_{795} mutant is resistant. Further, super resolution microscopy and transmission electron microscopy was used to show that Rab11a and Rab14 are sequestered in the presence of $FIP1C_{560-649}$. Thus, Rab sequestration may lead to Env sequestration in the ERC. In support of this hypothesis, immune-EM studies reveal that Env is localised on ERC tubular membranes in the presence of $FIP1C_{560-649}$. This may be the site at which Rab14-FIP1C complexes interact with EnvCT prior to Env trafficking to the plasma membrane. Alternatively, the authors hypothesise that mutant FIP1C in complex with Rab14 and Env is unable to recruit an essential motor protein required for trafficking. Currently, there is no evidence to prove this hypothesis.

Other EnvCT potential interactions with host trafficking factors:

Other host factors have also been proposed to traffic Env after endocytosis from the plasma membrane. For example, TIP47 is a late endosome-Golgi recycling protein is thought to bind the Y802W803 residues in the EnvCT and facilitate retrograde trafficking of Env to the TGN (Blot et al., 2003). Mutating these residues resulted in loss of interaction with TIP47, as well as reduced trafficking to the Golgi (Blot et al., 2003). Further, TIP47 is implicated in ensuring appropriate Env incorporation, HIV-1 assembly and virion infectivity, due to its interactions with the MA domain of Gag and the EnvCT (Lopez-Verges et al., 2006). NMR studies confirmed that TIP47 interacts with MA, however no interactions were determined between EnvCT and TIP47 (Checkley et al., 2013), thus the role of this host protein remains controversial.

Mass spectrometry analysis of proteins bound to the HIV-1 EnvCT revealed that the host proteins Prohibitin1 and Prohibitin2 interact with the EnvCT (Emerson et al., 2010). Env residues L799L800 were required for interactions and mutating this motif resulted in resulted in diminished binding to Prohibitins, which also correlated with reduced infectivity (Emerson et al., 2010). However, this was a cell-type dependent phenotype in which lack of Prohibitin binding allowed viral replication in permissive MT4 cells but not in non-permissive H9 cells (Emerson et al., 2010). Therefore, the importance of this interaction for viral replication remains uncertain.

To conclude, rapid recycling and gp120 shedding, due to weak interactions with gp41, results in low levels of Env on the surface of virions and infected cells. It is thought that this is a strategy to evade the adaptive immune response and to reduce the cytopathic effects of HIV infection. Hence, Env trafficking is critical in the HIV-1 replication cycle and transmission.

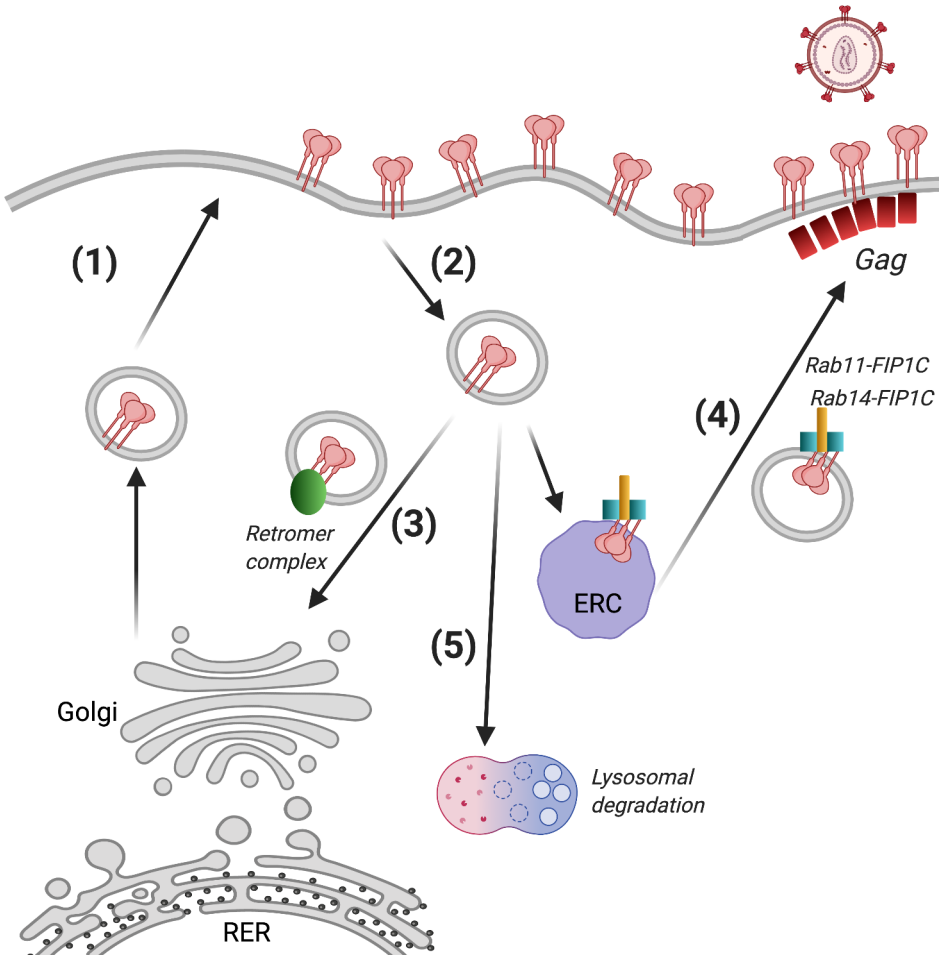

Figure 1.14 Env trafficking. Diagram showing different Env trafficking pathways and possibly fates after biosynthesis in the Rough endoplasmic reticulum (RER). **(1)** Env trimers enter the secretory pathway to traffic to the plasma membrane. **(2)** Env trimers internalised via clathrin mediated endocytosis and interaction of the EnvCT with AP-2 adaptor proteins. **(3)** Retromer binds to the EnvCT and mediates retrograde transport to the Golgi, where Env can re-enter the secretory pathway. **(4)** Trafficking to the endosomal recycling compartment (ERC) upon internalisation, where Env trimers bind to Rab-FIP1C complexes in a EnvCT-dependent manner to traffic to sites of virus assembly and budding. **(5)** Degradation of Env trimers via lysosomal degradation. (Created using BioRender.com)

1.3.5 EnvCT and Env incorporation

Env incorporation is a key step in producing infectious virus and the EnvCT is important in recruitment of Env to sites of virus assembly and budding (Akari et al., 2000; Freed and Martin, 1995; Mammano et al., 1995; Murakami and Freed, 2000; Muranyi et al., 2013). Given that only 7-14 trimers are incorporated into virions (Zhu et al., 2003) this suggests that Env incorporation is a tightly regulated process or that there are few functional trimers due to endocytosis from the cell membrane. The exact mechanism of Env incorporation remains to be elucidated, however four models have been suggested thus far: (**1**) Passive incorporation, (**2**) Gag-Env co-targeting. (**3**) Indirect Gag-Env interactions and (**4**) Direct Gag-Env interactions. Emerging data suggests that these models are not mutually exclusive and that these models may have oversimplified the process of Env incorporation. Here, as I discuss these below, I will also suggest a fifth model, based on recent super resolution microscopy and alternative interpretations to existing data, which emphasises the independent roles of the EnvCT and the Matrix domain (MA) of Gag. Whilst the EnvCT is responsible for appropriate *trafficking* of Env to sites of virus assembly and budding, the role of MA is to *retain* Env at these sites, and together these independent functions of EnvCT and MA allow for appropriate Env incorporation into virions. **Figure 1.15** summarises the different Env incorporation models.

(1) Passive incorporation

The passive incorporation model argues that plasma membrane associated Env is incorporated when HIV acquires the plasma membrane lipid bilayer during budding, thus Env is incorporated simply because it is present in the membrane. Evidence supporting this model includes the observation that mutating the conserved endocytic motif in the EnvCT can result in increased surface Env levels, leading to increased Env incorporation (Boge et al., 1998; Byland et al., 2007; Day et al., 2004; Groppelli et al., 2014; Qi et al., 2013). Also, many cellular proteins are passively incorporated into budding HIV-1 virions if present at sites of budding (Arthur et al., 1992; Lusso et al., 1990; Ott, 2008). The non-specificity of this process suggests that Env incorporation is also randomly incorporated. Next, HIV-1 can be pseudotyped with a variety of retroviral and non-retroviral Env proteins which produce infectious virus, thus suggesting that there is little specificity for Env incorporation (Cronin et al., 2005; Page et al., 1990). Finally, truncation of the EnvCT does not prevent Env incorporation in permissive cell lines such as HEK293T cells and HeLa cells (Freed and Martin, 1995; Murakami and Freed, 2000; Qi et al., 2015). However, presence of the EnvCT is necessary for HIV-1 Env incorporation into virions produced in primary CD4 T cells, many T cell lines and monocyte-derived macrophages, arguing against this model (Akari et al., 2000; Groppelli et al., 2014; Murakami and

Freed, 2000; Qi et al., 2015). This cell-type dependence on the requirement for a long HIV-1 EnvCT suggests that cellular factors, present in some cells and not others, may play a role in Env incorporation. This idea is proposed in two incorporation models: Gag-Env co-targeting and indirect Gag-Env interactions.

(2) Gag-Env co-targeting

The Gag-Env co-targeting model suggests that both viral proteins are targeted to the same plasma membrane microdomain leading to Env incorporation during virion budding. Lipid rafts are microdomains that have been implicated as sites of HIV-1 assembly and budding (Halwani et al., 2003; Hogue et al., 2011; Jolly and Sattentau, 2005; Mercredi et al., 2016; Nguyen and Hildreth, 2000). These microdomains are enriched in cholesterol and sphingolipids. Biochemical and super resolution microscopy studies have shown that HIV-1 Env clusters in microdomains at the plasma membrane, which are thought to be lipid rafts (Bhattacharya et al., 2006; Muranyi et al., 2013; Ono and Freed, 2001; Rousso et al., 2000; Yang et al., 2010). Therefore, Gag-Env co-targeting to lipid rafts probably plays a part in Env incorporation. Env recycling from the plasma membrane to endosomal compartments and/or the trans-Golgi network is important for Env incorporation, as disrupting Env endocytosis leads to differences in incorporation into virions (Kirschman et al., 2018; Qi et al., 2013). This may be explained by the fact that recycling allows Env to be targeted to the correct site of virus budding. Finally, co-expressing HIV-1 Env and a non-retroviral Env, such as the Ebola virus glycoprotein with HIV-1 Gag resulted in both Env glycoproteins localising separately at the plasma membrane and virus particles produced from these cells had either one but not a mix of both Envs incorporated (Leung et al., 2008).

(3) *Indirect Gag-Env interactions*

The indirect Gag-Env interactions model suggests that cellular proteins act as bridging factors between Env and Gag, allowing both proteins to colocalise at sites of viral assembly and budding. Although several host proteins have been suggested to interact with the EnvCT, such as TIP47, Dlg1 and α-catenin (Checkley et al., 2013; Kim et al., 1999; Lopez-Verges et al., 2006; Perugi et al., 2009), no mechanistic insight has been gained regarding their function in Env incorporation or Gag interactions. Therefore, evidence in support of this model is weak.

(4) Direct Gag-Env interactions

Biochemical, genetic and a few microscopy studies have suggested that a direct interaction occurs between MA and the EnvCT to allow Env incorporation, although this remains controversial (Alfadhli et al., 2016; Alfadhli et al., 2019; Cosson, 1996; Hourioux

et al., 2000; Wyma et al., 2004). For example, GST-tagged EnvCT was used in coimmunoprecipitation assays to show that it binds directly to the MA protein (Alfadhli et al., 2016; Alfadhli et al., 2019). A major criticism of this interpretation for the relevant data is that the binding events being observed may be a result of non-specific gp41 binding. Emerging evidence using super resolution microscopy suggests that the observations used as evidence for direct Gag-Env interactions may have an alternative interpretation, which is that Gag lattices accommodate the long EnvCT to allow Env incorporation, which does not necessarily require a direct interaction between the two proteins.

(5) EnvCT accommodation by Gag lattice

Early crystallography studies revealed that both HIV (Hill et al., 1996) and SIV (Rao et al., 1995) MA proteins form trimeric structures. A 2D structure of myristylated Gag, in a synthetic lipid bilayer, further showed that the MA trimers form a higher order, hexameric structure with a central cavity, which could possibly be occupied by EnvCT (Alfadhli et al., 2009). The presence of MA trimers in replication competent virus was confirmed using biochemical assays (Tedbury et al., 2016). Several mutations in the MA trimer apex result in loss of Env incorporation (Tedbury et al., 2013). It was suggested that these mutations cause steric hindrance, leading to the inability of EnvCT to insert into the MA hexamer cavity. This is supported by the observation that a CT-deleted HIV-1 mutant (Δ144) can incorporate Env, suggesting that it overcomes the steric hindrance, although this could also be explained by passive incorporation of Δ144 mutant Env into virions. It is important to note that this phenotype is cell-type specific and rescue of infection is only seen in cell lines such as HEK293T and HeLa cells, not T-cell lines such as Jurkats and primary CD4 T cells or monocyte-derived macrophage, as discussed above. A matrix mutant, Q62R, results in a global rescue of defects in Env incorporation (Tedbury et al., 2013). The arginine residue is longer and more positively charged, compared with glutamine, suggesting that it can interact with side chains of neighbouring MA molecules within the trimer configuration. This mutation is found at MA trimer interfaces, suggesting that it modulates trimer interactions to allow Env incorporation. However, crystal structures of MA show that Q62 is not likely to be exposed to the plasma membrane, hence a direct interaction between MA Q62 and EnvCT is unlikely.

MA hexamers were observed in live cells using cryoET and this study suggested that upon cleavage, the mature CA lattice is formed directly from the Gag lattice and gradually rolls away from the membrane to wrap around the NC and form a core structure (Frank et al., 2015). In order to correlate MA trimerisation with Env incorporation, Tedbury and colleagues (2016) investigated the T69R MA mutant. This mutant prevents Env incorporation and is situated at the MA trimer interface, in close proximity to Q62 on

neighbouring MA molecules. Therefore, it may sterically hinder MA trimerisation. By testing a range of T69 mutants, it was revealed that polar, hydrophobic residues had little effect on Env incorporation, whereas charged residues prevented incorporation. Further, the latter mutations resulted in loss of MA trimerisation, thus correlating the two phenotypes (Tedbury et al., 2016). This suggests that interactions between MA trimers within the lattice structure are important for appropriate Env incorporation, however it does not prove that there is a direct interaction between MA and Env.

Live single molecule imaging of Env, particularly the Y712A mutant which undergoes a slower rate of endocytosis, revealed that efficient Env incorporation requires the EnvCT to be trapped in a MA lattice (Pezeshkian et al., 2019). In the absence of a MA lattice, i.e., no virus assembly site, Y712A mutant Env molecules freely diffuse around the plasma membrane. By contrast, the presence of a MA lattice drastically reduced Env mobility. Similarly, when Y712A Env encounters the MA mutant, L12E, which is deficient of MA trimerisation, Env is no longer trapped in the lattice. Further, the importance of the EnvCT in Env trapping was demonstrated in this study by calculating the rate of diffusion of ∆144 Env within the MA lattice. This revealed that the ∆144 mutant was significantly more mobile within the lattice, compared with Y712A Env, suggesting that Env is not trapped and can diffuse out. This could explain why ∆144 Env has an incorporation defect in non-permissive cells, despite increased surface expression compared with WT Env (Murakami and Freed, 2000).

In line with this hypothesis, Van Engelenberg and colleagues (2018) used super resolution microscopy to interrogate spatiotemporal dynamics of Env at sites of viral assembly and budding (Buttler et al., 2018). Single molecule tracking of HIV-1 Env trimers revealed that WT Env and ∆144 Env had similar diffusion kinetics along the plasma membrane, however significantly more WT Env was immobilised in the Gag lattice, compared with ∆144 Env. Further, HIV-1 WT Env showed a biased distribution at the neck of budding particles, whereas HIV-1 ∆144 Env showed an unbiased distribution in the CEM-A T cell line. The unbiased distribution of ∆144 Env suggests that the mutant is probably recruited to the plasma membrane at the same time as MA recruitment, whereas WT Env is recruited later. Importantly, this suggests that MA lattice formation and membrane curvature occurs prior to Env recruitment and that the EnvCT is important in regulating timely recruitment of Env during budding. Interestingly, this study also provides insight into an additional layer of regulation of Env incorporation, other than lattice trapping and plasma membrane diffusion, as discussed above. The EnvCT is important for Env recycling from the plasma membrane. Pulse chase analysis of Env revealed that significantly more WT Env is trapped in transferrin-positive intracellular

compartments, as previously described (Roy et al., 2013), compared with Δ144 Env. This is a cell type specific observation, as equal levels of WT and mutant Env were recovered in COS7 cells. This may be explained by differences in host cell trafficking machinery which are important for Env recycling. Therefore, this study suggests that regulation of Env incorporation occurs at two levels. First, Env recycling from the plasma membrane and retainment in endosomal compartments, before being trafficked back to sites of budding, results in a delay between MA lattice formation and Env recruitment. The process of budding begins prior to Env recruitment, thus the large EnvCT is sterically relegated to the neck of budding virions and only a limited number of Env trimers can be incorporated.

Taken together, these recent studies describe a complex model of Env incorporation which involves multiple regulatory factors including MA, EnvCT and host cell factors (especially cellular trafficking machinery). They allude to the importance of MA trimerisation in Env retainment, which in turn is dependent on the EnvCT. MA is recruited to lipid raft microdomains on the plasma membrane and begins trimerisation and lattice formation. Late during the budding process, Env trimers are recruited to budding virions, possibly using host trafficking machinery such as FIP1C and other unidentified proteins. Recruitment of Env trimers allows EnvCT to encounter MA at the neck of budding virions after which Env is incorporated. It remains to be elucidated as to whether this encounter results in direct interactions between MA and EnvCT.

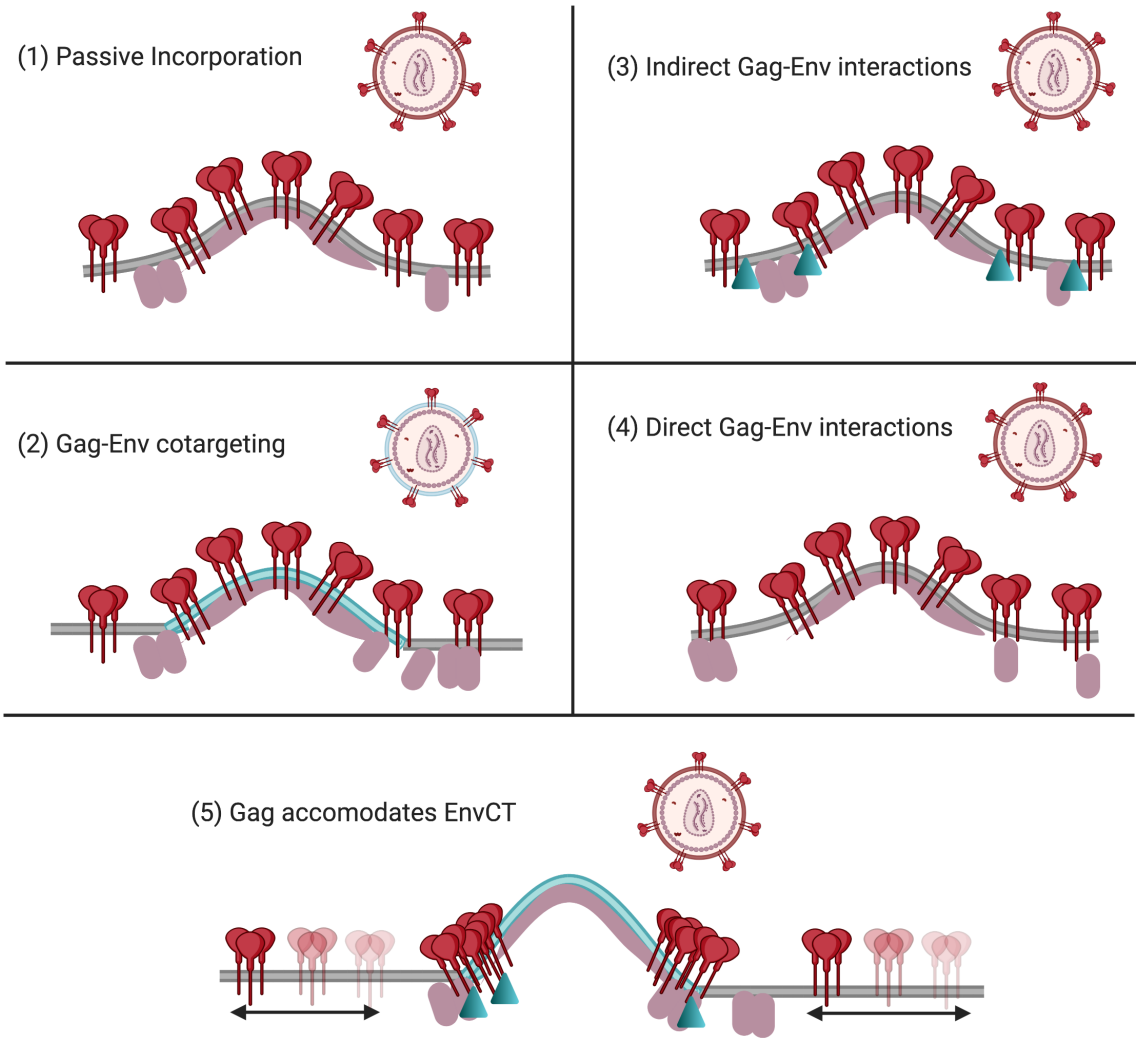

Figure 1.15 Env incorporation models. (1) The passive incorporation model argues that Env (red trimers) is randomly incorporated into budding virions. **(2)** The Gag-Env cotargeting model argues that Gag (pink) and Env are targeted to the same microdomains, specifically lipid rafts (blue) on the plasma membrane. **(3)** The indirect Gag-Env interaction model argues that a cell host factor (blue triangle) acts as a bridge between Gag and Env to ensure both essential proteins traffic to the sites of viral assembly. **(4)** The direct Gag-Env interactions model suggests that Env and Gag directly interact during trafficking to and at sites of viral assembly and budding. **(5)** The Gag accommodates EnvCT model argues that Gag forms a lattice structure under the plasma membrane and begins inducing membrane curvature. This is followed by Env recruitment to the neck of the budding virion using host factors such as FIP1C. Env is trapped via direct or indirection interactions with the Gag lattice. Those Env trimers which are not trapped at the Gag lattice are dynamic at the plasma membrane. Adapted from (Checkley et al., 2011). (Created using BioRender.com).

1.3.6 Retroviral EnvCT truncations

A unique feature of lentiviral EnvCTs is their long length (**Figure 1.16**). For example, the HIV-1 EnvCT is 150 amino acids long, whereas other retroviruses have tails which are approximately 50 amino acids long. Although there is little conservation in the amino acid sequence of lentiviral EnvCTs, the secondary structures and various trafficking motifs are highly conserved. For example, the YxxΦ endocytic motif, which is responsible for AP2 binding, is found in the majority of lentiviral EnvCT sequences (Berlioz-Torrent et al., 1999; Boge et al., 1998; Byland et al., 2007). Conservation of the length of lentiviral EnvCTs suggests the presence of key determinants within the cytoplasmic tail that are essential for efficient viral replication and spread. This is demonstrated by the observation that when HIV-1 EnvCT is truncated, the virus is unable to spread in T cell lines and primary CD4 T, cells due to an Env incorporation defect (Akari et al., 2000; Murakami and Freed, 2000). These cells, in which HIV-1 EnvCT truncation cannot be tolerated, are termed 'non-permissive' compared with 'permissive' cells in which truncation does not impact the production of infectious HIV-1 virus (Checkley et al., 2011). Examples of permissive cell lines include 293T cells, HUT78 cells, MT4 cells and HeLa cells (Checkley et al., 2011). In trying to decipher the role of different motifs within the HIV-1 EnvCT, truncations and mutational analyses revealed that manipulation of the EnvCT has varying effects on viral infectivity and Env biology, depending on the length of the EnvCT that is removed and the cell type. Generally, truncations which remove the C-terminal LLP-1 motif and the dileucine motif, which is important for Env recycling (Byland et al., 2007), resulted in reduced infectivity of HIV-1 virions due an Env incorporation defect (Dubay et al., 1992; Kalia et al., 2003; Piller et al., 2000; Yu et al., 1993). Truncation of the entire EnvCT or downstream of LLP3 resulted in alterations in the ability of Env to carry out fusion of mature (Jiang and Aiken, 2007) and immature virions (Wyma et al., 2004). These observations will be explored in further detail below.

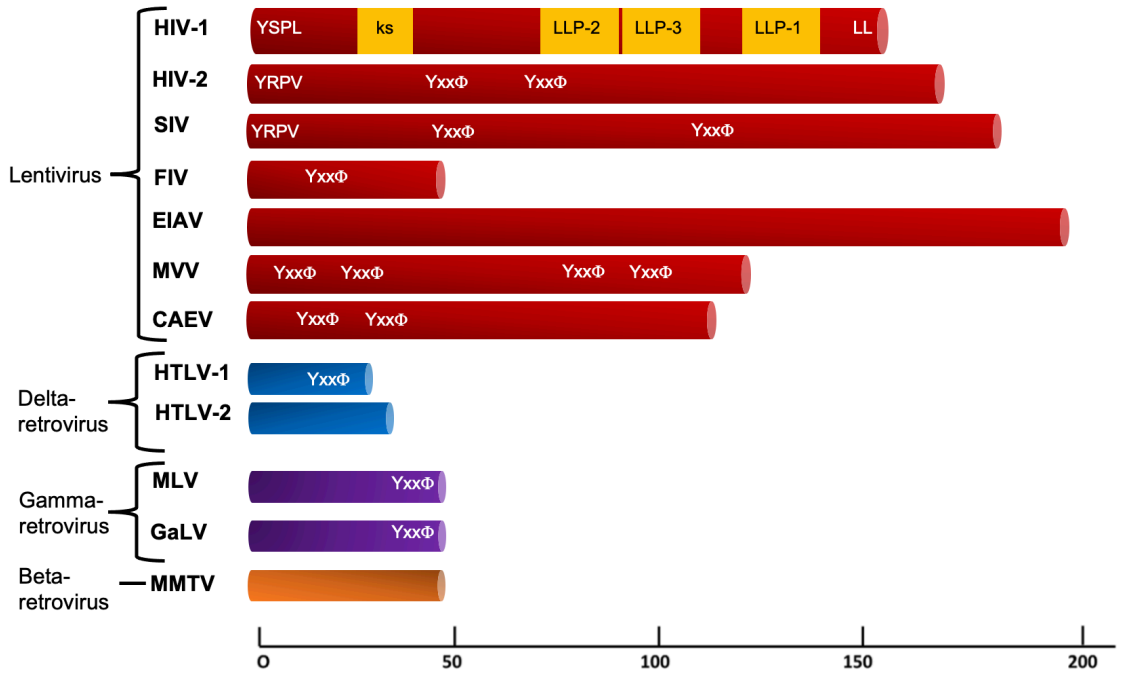

Figure 1.16 Retroviral EnvCT lengths. Comparison of the lengths of the EnvCT of Human Immunodeficiency Virus type 1 (HIV-1), HIV-2, Simian Immunodeficiency Virus (SIV), Feline Immunodeficiency Virus (FIV), Equine Infectious Anemia Virus (EIAV), Maedi-Visna Virus (MVV), Caprine Arthritis Encephalitis Virus (CAEV), Human T-lymphotropic Virus type I (HTLV-1), HTLV-2, Mouse Mammary Tumor Virus (MMTV), Murine Leukemia Virus (MLV) and Gibbon Ape Leukemia Virus (GaLV); conserved YxxΦ motifs (where Φ represents a hydrophobic residue) are in white text. Adapted from (Santos da Silva et al., 2013).

Contrary to HIV-1, HIV-2 and SIV viruses are often reported to truncate their EnvCT. Initial studies which reported the discovery of some HIV-2 and SIV patient isolates, suggested that the viruses had truncated their EnvCT *in vivo* (Albert et al., 1987; Chakrabarti et al., 1987; Evans et al., 1988; Hahn et al., 1987; Hirsch et al., 1987; Hirsch et al., 1989a; Hirsch et al., 1989b; Kong et al., 1988), however this is now questionable, since the truncation may in fact be a cell culture adaptation. The method of virus isolation used in these studies involved coculturing infected cells with uninfected, mitogen stimulated cells from a healthy donor, after which the resultant virus was propagated in cell lines, such as HUT-78 cells, to produce high titre virus stocks. There is little data regarding how long this isolation process took and therefore it is highly likely that the presence of a premature stop codon in the EnvCT sequence was a cell culture adaptation. Alternatively, it is possible that the patient samples contained a viral quasispecies in which some viruses had a full length (FL) and others had a truncated (ΔCT) EnvCT. A change in the viral niche, hence the selective pressure exerted on the virus during cell culture, may have provided the ΔCT viruses with a replicative advantage

over the FL viruses over time. However, later studies with SIV and HIV-2 infectious molecular clones, such as SIVmac316 and SIVmac1A11, confirmed that during *in vitro* propagation in human cells, amino acid substitutions arise in the EnvCT which create a stop codon, resulting in the emergence of EnvCT truncated mutants (Bonavia et al., 2005; Hirsch et al., 1989a; Kodama et al., 1989; Mori et al., 1992; Vzorov et al., 2005). Subsequent analysis of HIV-2 and SIV ΔCT viruses revealed that EnvCT truncation can affect viral replication and Env biology. Aspects of Env biology that are altered upon lentiviral EnvCT truncation include: Env expression and incorporation, Env-mediated fusion and susceptibility to neutralisation by antibodies. This will be discussed later in the thesis.

Effect of EnvCT truncation on Env incorporation

Expression of Env on the cell surface is regulated by the EnvCT and truncation of this region can increase Env expression on virus producer cells and incorporation into nascent virions, which might impact viral infectivity in different cell types (reviewed by (Postler and Desrosiers, 2013)). Increased Env incorporation has been observed in studies with SIV (Kuwata et al., 2013; Manrique et al., 2001; Yuste et al., 2004; Zhu et al., 2003; Zingler and Littman, 1993). Yuste *et al* (2004) truncated the SIVmac239 EnvCT by substituting two amino acids downstream of the conserved YxxF endocytic motif to stop codons (Q738*/Q739*). These mutations were initially reported to arise in a number of SIVs upon passage in human cells (Chakrabarti et al., 1987; Hirsch et al., 1989a; Kodama et al., 1989). Immunoblot analysis of this mutant virus produced in 293T cells revealed that there is 13-fold more ΔCT Env incorporated compared with WT Env (Yuste et al., 2004). Flow cytometry analysis of transfected 293T cells showed that there is more ΔCT Env expressed on the surface of the cells, which could explain an increase in Env incorporation (Yuste et al., 2004). However, infection of CEMx174 cells showed that the Q738*/Q739* mutant did not have any significant replicative advantage due to the EnvCT truncation (Yuste et al., 2004). Kuwata *et al* (2013) also used a similar SIVmac316 mutant (Q733*) to show that EnvCT truncation resulted in 12-44 times more Env incorporation into virions produced in 293T cells, however this could not be explained by an increase in Env production in 293T cells. Discrepancies between these two studies maybe explained by the fact that different SIV strains were used, as the position of the stop codon is analogous in both studies. Spreading infection of SIVmac316 ΔCT virus in human and macaque cells quantified by flow cytometry analysis revealed that 100% of human cells were infected by 10 days post infection, compared with only 20% infection observed in macaque cells. This might be explained by EnvCT truncation greatly enhancing infection which leads to increased cell death, because when cells were infected with lower MOI, replication over 10 days was enhanced and reached 45%.

Finally, cryoET studies have further corroborated these findings by showing that SIV virus particles have increased Env trimers density compared with wild type HIV-1 viruses with a full length EnvCT (Zhu et al., 2003; Zhu et al., 2006). By contrast, a recent study compared three SIVsmE660 isolates derived from the same parental clone, with EnvCT truncations (analogous to the previous studies mentioned thus far) and showed that there was no significant increase in Env incorporation (White et al., 2018). This correlated with no differences in viral infectivity between viruses with a full length and truncated EnvCT in rhesus PBMCs and the human CEMx174 cell line (White et al., 2018). Taken together, SIV EnvCT truncation often leads to increased Env incorporation, however it is unclear whether this provides a replicative advantage, likely due to differences in the requirement for the EnvCT in different cell types, as has been observed for HIV-1. The strain of SIV used can also determine the effect of EnvCT truncation on Env incorporation and infectivity.

The effect of EnvCT truncation on HIV-1 Env incorporation and infectivity is cell type dependent. Truncation of the HIV-1 EnvCT can result in reduced Env incorporation into virions (Dubay et al., 1992; Piller et al., 2000; Yu et al., 1993). Piller *et al* (2000) inserted stop codons to remove 6 or 19 amino acids from the C-terminus of the EnvCT. Infectious molecular clones were produced in 293T cells, which are permissive for HIV-1 EnvCT truncation, and resultant viruses were used to infect H9 and CEMx174 cells. Infectivity of mutant viruses was determined by measuring RT activity in virus containing supernatant, which revealed that ΔCT mutants had delayed replication kinetics in a spreading infection assay (Piller et al., 2000). This correlated with reduced Env incorporation when viruses were produced in H9 cells (Piller et al., 2000). Similarly, when larger truncations were made in the HIV-1 EnvCT, including removal of the LLP-2 domain, resultant viruses were non-infectious in H9 cells and primary PBMCs due to a reduction in Env incorporation (Dubay et al., 1992; Yu et al., 1993). By contrast, when HIV-1 EnvCT truncation mutant Δ144, which has a stop codon upstream of the YxxL endocytic motif, was used to infect MT4 cells, which are a permissive cell line, no differences in Env incorporation were observed by comparison with the WT virus (Akari et al., 2000; Murakami and Freed, 2000; Wilk et al., 1992). Finally, little data is available on the effects of HIV-2 EnvCT truncation on Env incorporation. Whilst immunoblot and sequence analyses revealed that HIV-2 viruses incorporate a truncated TMD protein (Albert et al., 1987; Evans et al., 1988; Kong et al., 1988; Kumar et al., 1990), direct comparison to virus with full length EnvCTs are rarely reported, therefore it was difficult to decipher whether there is a relative change in the amount of Env incorporation and infectivity. One study compared replication of a primary isolate, HIV-2ST, with a EnvCT truncated mutant called HIV-2 ST#2 and found that EnvCT truncation resulted in

enhanced replication in SupT1 cells (Hoxie et al., 1991), however Env incorporation data was not reported, thus it is unclear whether this contributes to increased infectivity.

EnvCT truncation and ectodomain conformation and function

One common feature reported for HIV-1, HIV-2 and SIV ΔCT viruses is an increase in Env fusogenicity (Abrahamyan et al., 2005; Edwards et al., 2001; Edwards et al., 2002; Hoxie et al., 1991; Johnston et al., 1993; Mulligan et al., 1992; Ritter et al., 1993; Wyss et al., 2005; Zingler and Littman, 1993). Interaction between Env and CD4 and coreceptors results in a series of conformational changes that eventually lead to gp120 dissociation from gp41 and fusion of viral and target cell membranes (Melikyan, 2014). Increased fusogenicity could be advantageous as it is likely to enhance the virus' ability to potentiate entry into target cells and enhance viral spread. Env-mediated fusion was primarily tested using cell-cell fusion assays. A comparison between cell-cell fusion upon infection of SIVmac239 with a long and short EnvCT revealed that the ΔCT virus was able to induce larger syncytia in HUT78, COS-1 and HeLa T4 cells compared with SIVmac239 FL virus (Ritter et al., 1993). Further, Zingler and Littman (1993) used SIVmac239 (originally FL virus) and SIVmac1A11 (originally ΔCT virus) viruses to investigate the role of EnvCT truncation in fusion (Zingler and Littman, 1993). COS7 cells were transfected with DNA encoding the envelope glycoproteins of these viruses and syncytia formation was assessed by overlaying the transfected cells on to HUT-78 cells. SIVmac239 virus produced 9-fold less syncytia compared with SIVmac1A11 virus. Next, chimeric gp160 proteins were produced by swapping the EnvCT region between these viruses and testing syncytia formation (Zingler and Littman, 1993). SIVmac239 with 1A11 EnvCT (ΔCT) resulted in a 5-fold increase in fusogenicity, whereas SIVmac1A11 with 239 EnvCT (FL) resulted in a 3-fold reduction in fusogenicity (Zingler and Littman, 1993). Similar results have been reported for HIV-2 (Mulligan et al., 1992). By contrast, investigation of the primary isolate HIV-2 ST showed that Env does not bind to CD4 receptor efficiently and is unable to induce syncytium formation between SupT1 cells effectively, suggesting reduced fusogenicity (Kong et al., 1988; Kumar et al., 1990; Mulligan et al., 1990). Upon prolonged culture in SupT1 cells, a new variant of HIV-2 ST emerged, containing 5 mutations, one of which was a premature stop codon in the EnvCT at Env position 713, resulting in a truncated EnvCT (Mulligan et al., 1992). The EnvCT truncated variant, ST#2, was more efficient at syncytium formation (Hoxie et al., 1991; Mulligan et al., 1992) and became highly cytopathic due to increased viral replication (Hoxie et al., 1991). A spreading infection assay in SupT1 cells showed that 80% of target cells were Gag-positive when infected with ST#2, compared with only 10% infection by HIV-2 ST with a full length EnvCT on day 7 post infection (Hoxie et al., 1991). Further, a panel of HIV-1 HXBc2 EnvCT truncation mutants, including the Q733* mutant,

were expressed in QT6 cells and syncytium formation was tested in a cell-cell fusion assay (Wyss et al., 2005). EnvCT truncated mutants showed increased syncytia formation compared with the full-length virus. Fusion kinetics of the mutants was assessed using a dye-transfer assay. Briefly, HeLa cells were transfected to express the Env glycoproteins and mixed with dye labelled target SupT1 cells and incubated for up to 2h. Fusion was determined as the ratio between Env-expressing HeLa cells that became dye-labelled and the total number of Env-expressing cells in contact with target cells counted from microscopic images (Wyss et al., 2005). This experiment revealed that EnvCT truncation increases HIV-1_{HXBc2} fusion kinetics (Wyss et al., 2005). Taken together these data suggest that truncation of the primate lentiviral EnvCT can lead to increased fusogenicity, which may result in more efficient viral replication. It has been suggested that this effect on fusogenicity is a result of inside-out regulation by the EnvCT i.e., truncation of the cytoplasmic tail may induce conformational changes in the gp41 ectodomain and the gp120 subunit to impact fusogenicity (Affranchino and Gonzalez, 2006; Edwards et al., 2002; Jiang and Aiken, 2007; Kalia et al., 2003; Spies et al., 1994; Wyma et al., 2004; Wyss et al., 2005). Further, biochemical studies using synthetic peptides found that infectivity of viruses depends on interactions between LLP-1 and LLP-2 with the plasma membrane and/or with the gp41 ectodomain, particularly the 6-helix bundle (6HB) (Abrahamyan et al., 2005; Lu et al., 2008). Lu *et al* (2008) showed that antibodies targeting LLP-1 and LLP-2 are able to inhibit Env-mediated cell-cell fusion at cold temperatures when gp41 refolding is slowed down. This may suggest that the LLP-2 region becomes transiently surface exposed and interacts with the gp41 ectodomain to regulate fusion (Lu et al., 2008). Peptide inhibitors of fusion, such as C34 and T-20, were used to show that EnvCT truncation leads to increased fusion kinetics in a cell-cell fusion assay and ΔCT virus is less sensitive to fusion inhibition (Abrahamyan et al., 2005; Gallo et al., 2001). Also, probing for fusion kinetics using fusion inhibitors suggested that the EnvCT slows down 6HB formation and therefore truncation leads to an increase in fusogenicity and rate of fusion (Abrahamyan et al., 2005). Collectively, these data suggest that truncation of the EnvCT can impact the gp41 ectodomain, particularly during late stages of fusion. This hypothesis is supported by recent structural studies which revealed that the LLP-2 region of the EnvCT adopts an amphipathic helical structure which wraps around the gp41 TMD and acts as a baseplate to stabilise the Env trimer (Piai et al., 2020), therefore LLP-2 may not 'flip out' of the membrane to interact with gp41 ectodomain as suggested previously (Abrahamyan et al., 2005; Lu et al., 2008), but instead regulate via the TMD. Further, NMR dynamics suggest that the EnvCT is physically coupled to the Env ectodomain via the gp41 TMD (Piai et al., 2020). Therefore, it is plausible to suggest that truncation of the EnvCT, particularly removal or

disruption of the LLP-2 baseplate, will have a global impact on Env conformation and function.

Another piece of indirect evidence to suggest that the cytoplasmic tail regulates Env conformation, is that truncation of the EnvCT often leads to altered antigenicity and sensitivity of HIV and SIV to neutralising antibodies (Chen et al., 2015; Edwards et al., 2001; Edwards et al., 2002; Kuwata et al., 2013; Puffer et al., 2002; White et al., 2018; Wyss et al., 2005; Yuste et al., 2005). EnvCT truncation alters accessibility of antibodies targeting epitopes including the CD4 binding site on gp120 (Edwards et al., 2002) and the MPER in gp41 (Durham et al., 2012). The HIV-1HXBc2 8x mutant contains a frame shift mutation in the cytoplasmic tail, resulting in the production of a truncated protein (Edwards et al., 2001; Edwards et al., 2002). This 8x mutant and a range of other HIV-1 X4 and R5-tropic Envs containing a similar frame shift mutation, were expressed in 293T cells and binding to 17b and 42d antibodies was tested. 17b and 42d bind to epitopes on gp120 which are usually exposed upon CD4 binding, such as the coreceptor binding site. Antibody binding assays showed that HXBc2 8x and all other truncation mutants had increased binding to 17b and 42d, suggesting that the epitopes are more accessible (Edwards et al., 2002), hence gp120 is perhaps in a more open conformation. This also resulted in increased sensitivity of HXBc2 8x to neutralisation by HIV-1 positive human sera (Edwards et al., 2001). Importantly, the amount of Env on the surface of 293T cells revealed that there are no differences in surface exposure between ΔCT Env compared with WT Env (Edwards et al., 2001). Therefore, it is most likely that the differences in antigenicity and sensitivity to neutralisation are due to conformational changes rather than just an increase in the amount of Env available for antibodies to bind to. Further, Durham *et al* (2012) tested the neutralisation sensitivity of HIV-1 ΔCT virus with a range of bnAbs and found that ΔCT infection was 4-fold more sensitive to MPER targeting bnAbs, 4E10 and 2F5, but not to 2G12 which recognises gp120 (Durham et al., 2012). Finally, studies

Therefore, these data suggest that the gp41 ectodomain can be altered to expose epitopes and increase neutralisation sensitivity.

Turning to SIV, the first reports of SIVmac239 EnvCT truncation in human cells, showed that the position of the stop codon is at Q733 (Chakrabarti et al., 1987; Hirsch et al., 1989a; Kodama et al., 1989). Based on these reports, infectious molecular clones of SIV were created to have a truncation in their EnvCT by introducing stop codons at positions analogous to those found in SIVmac239 and their sensitivity to antibody neutralisation was tested (Kuwata et al., 2013; Puffer et al., 2002; Vzorov et al., 2005; White et al.,

2018; Yuste et al., 2005). There are a lot of discrepancies in the literature regarding the effect of EnvCT truncation on sensitivity to neutralising antibodies (Bonavia et al., 2005; Puffer et al., 2002; Vzorov et al., 2005), whilst others reported a decrease (Kuwata et al., 2013; White et al., 2018; Yuste et al., 2005). These discrepancies might be explained by genetic differences between the different SIV strains tested thus far. For example, Vzorov *et al* (2005) compare SIVmac239 and SIVmac1A11, which originally have full length and truncated EnvCTs, respectively. Truncation of the SIVmac239 EnvCT increased resistance to neutralisation by different polyclonal antisera from infected macaques (Vzorov et al., 2005). By contrast, the tail truncated SIVmac1A11 virus was highly sensitive to neutralisation and a chimeric virus which contains the ectodomain of SIVmac1A11 and CT of SIVmac239 was unable to rescue infection in the presence of antibodies (Vzorov et al., 2005). Therefore, this suggests that the genetic makeup of the virus and probably the gp120 subunit dictates the effect of EnvCT truncation. To overcome these discrepancies which may be arising as a result of different genetic backgrounds, a study investigated the effect of EnvCT truncation on sensitivity to neutralisation, using three SIVsmE660 isolates that were derived from the same parental strain, but had different neutralisation profiles, hence their Envs were categorised as Tier 1, Tier 2 and Tier 3 (White et al., 2018). Truncating the EnvCT of all three isolates resulted in increased resistance to neutralisation by sera from infected macaques. Further, this result was verified using a panel of monoclonal nAbs that target the various epitopes in gp120, including V2 loop, V3 loop and the CD4 binding site. IC50 values for all three EnvCT truncated mutants were > 50ug/ml which means infection could not be neutralised (White et al., 2018). Western blot analysis of virus made in A66-R5 T cells revealed that this phenotype is not due to a change in Env incorporation levels (White et al., 2018). Taken together, these data suggest that the effect of EnvCT truncation on lentiviral sensitivity to neutralising antibodies is complex and multifactorial, giving rise to discordance in the literature, however it is clear that alterations in the EnvCT can impact Env conformation, leading to changes in functionality.

EnvCT truncation *in vitro* and *in vivo*

HIV-1

Although an intact EnvCT is crucial for efficient HIV-1 replication in primary CD4 T cells, which are the main targets of HIV-1 infection *in vivo* (Maddon et al., 1986), previous studies have reported that HIV-2 and several SIVs truncate their cytoplasmic tail when passaged in human T cell lines and PBMCs, in order to replicate efficiently (Edmonson et al., 1998; Kanki et al., 1986; Mulligan et al., 1992; Vzorov and Compans, 1996). Whilst it is obviously difficult to extrapolate the importance of *in vitro* observations to the situation encountered *in vivo* for HIV-2, it is worth noting that HIV-2 isolates from patients

in West Africa, have been described to have a premature stop codon in EnvCT (Albert et al., 1987; Evans et al., 1988; Kong et al., 1988). As discussed at the beginning of this section, it is unclear whether the EnvCT truncated mutants were present in the viral quasispecies that were isolated from infected individuals, or if the premature stop codon emerged as an adaptation to cell culture. If the former is correct, it would suggest that perhaps EnvCT truncation results in a fitness defect for the virus, as the occurrence of this variant is rare *in vivo*. In line with these discussions, a recent study reported that a HIV-1 patient isolate, HIV-1 92UG046-T8, contains a premature stop codon in the EnvCT sequence (Saha et al., 2005; Zerhouni et al., 2004). This isolate is thought to have been a part of the viral quasispecies, rather than a cell culture adaptation, because the parental 92UG046-infected primary CD8+ lymphocytes were in short term (2-3 weeks) cocultures, during which it is unlikely to have developed the stop mutation. Secondly, the 92UG046-T8 variant was never propagated in any cell lines, unlike the HIV-2 examples present above. Finally, approximately 10% of the RNA pool in the parental 92UG046 viral quasispecies had the 92UG046-T8 sequence present (Saha et al., 2005), which suggests that the EnvCT truncation mutant existed as a minority variant in the viral quasispecies of the patient. Based on these findings, it is possible for HIV-1 and HIV-2 ΔCT variants to be present in infected individuals.

Whether HIV-2 ΔCT viruses exist *in vivo* remains unclear. Some early reports suggested that HIV-2 ΔCT virus were isolated from infected individuals because western blot analysis revealed the presence of a protein at 30-32kDa (Albert et al., 1987; Evans et al., 1988; Kong et al., 1988). However, these western blots do not directly measure the virus from patient derived PBMCs. Instead, the viruses were passaged in vitro to produce high titre stocks, which were then subjected to immunoblot analysis to identify key viral proteins, including Env. Moreover, there is often a lack of information on the phenotype of the original virus swarm which was isolated from the infected individuals. A common method of virus isolation was used, in which PBMCs from infected donors were co-cultivated with PBMCs from healthy donors and then high titre virus stocks were produced by infecting and propagating isolated viruses in T cell lines. Exactly how long this process was carried out for remains unclear in many early studies. It is possible that ΔCT variants emerged during prolonged propagation of virus, as an adaptation to *in vitro* cell culture conditions, and this is what was detected by western blot and genetic analysis (Albert et al., 1987; Evans et al., 1988; Kong et al., 1988). On the contrary, it is also possible that both FL and ΔCT viruses exist *in vivo*, as viral quasispecies, with the ΔCT virus possibly existing as a minority variant, which may explain why HIV-2 ΔCT variants are rarely discovered from patient samples.

Early *in vivo* studies of SIV infection revealed that importance of the long EnvCT for SIV, similar to HIV-1. A Rhesus macaque was inoculated with SIVmac239 ΔCT virus and at 58 weeks post inoculation, virus was recovered from CD4 T cells (Kodama et al., 1989). Sequencing of virus from infected cells revealed that the virus was exclusively SIVmac239 with a full length EnvCT (Kodama et al., 1989), suggesting that a full length SIV EnvCT is required for viral replication *in vivo*. Further, in Rhesus macaque PBLs, the virus replicated and spread during 80 days of serial passage, with no ΔCT variants arising (Kodama et al., 1989).

Taken together, multiple reports of *in vitro* EnvCT truncations revealed a consistent selective advantage for lentiviruses *in vitro* that with further study may reveal new biological insight into the role of the EnvCT in the viral lifecycle. For example, whether this phenotype can be explained by the actions of any known species-specific antiviral factors or whether these viruses simply do not interact appropriately with the host trafficking machinery, thus mutate to bypass such interactions, warrants further investigation.

Other retroviruses

A conserved function of retroviral EnvCTs is to inhibit membrane fusion and syncytium-induced apoptosis of virus producer cells using various mechanisms (Bobkova et al., 2002). The Murine Leukaemia Virus (MLV) Env is produced as a precursor protein which is proteolytically cleaved to produce a surface subunit (SU) and a transmembrane subunit (TM), similar to HIV-1 Env. Whilst the SU is involved in receptor engagement, the TM subunit regulates fusion. The TM subunit influences conformational changes that occur in the SU once receptor is bound. This involves a disulphide bond that bridges the SU and TM subunits (Aguilar et al., 2003). Particularly, the TM domain contains a C-terminal 16-amino acid R-peptide, which acts as a 'safety catch' to prevent premature, irreversible post fusion Env conformations in producer cells. Structural studies of the MLV Env protein reveal that the TM subunit has an open structure with separated legs (Forster et al., 2005; Wu et al., 2008) and the R-peptide ties the legs together to prevent activation of Env (Loving et al., 2012). During viral maturation, the R-peptide is cleaved by viral protease and this enables Env to initiate fusion of viral and cellular membranes (Green et al., 1981; Henderson et al., 1984). The importance of this cleavage event is emphasised by the observation that MLV containing the R-peptide have significantly reduced infectivity (Kiernan and Freed, 1998; Kubo and Amanuma, 2003; Kubo et al., 2007). The HIV-1 EnvCT is not cleaved during maturation and budding, it has been implicated in regulating fusogenicity of Env. This is primarily due to potential EnvCT and

Gag interactions which are thought to lock Env in a prefusion conformation until maturation occurs. During maturation, Gag precursor protein is cleaved into MA and CA subunits (Gottlinger et al., 1989; Kohl et al., 1988; Peng et al., 1989). This maturation event possibly relieves the inhibitory effect of gp41 and activates Env for fusion (Jiang and Aiken, 2007; Murakami et al., 2004; Wyma et al., 2004). This idea is reinforced by the observation that deleting the HIV-1 EnvCT renders HIV-1 infectious, even if there is a defect in Gag and Gag-Pol cleavage (Murakami and Freed, 2000; Wyma et al., 2000). This suggests that removal of the EnvCT eliminates interactions between Gag and the EnvCT to allow for fusion to proceed (Murakami et al., 2004; Wyma et al., 2000).

1.4 Innate immune restriction of HIV

The host cell cytoplasm is a hostile environment for invading pathogens, including lentiviruses such as HIV-1. Restriction factors are cellular proteins with the ability to counteract viral replication and act as the first line of defence against infections. They are typically upregulated by Type I Interferons (IFN), mainly IFN-α and IFN-β. Once IFN binds to its cell-surface IFN receptor, complex signalling cascades are activated. This leads to nuclear translocation of transcription factors, NF-kB and IRF3, which upregulate expression of interferon stimulated genes (ISGs). Ultimately, an antiviral state is established, and viral infection is controlled.

Well characterised proteins and families of restriction factors against HIV-1 and related lentiviruses include: the APOBEC family; IFITM family; SERINC family; Tetherin; MxB; TRIM5α and SAMHD1. Each of these cellular proteins are responsible for blocking different parts of the viral life cycle (**Figure 1.17**). A common feature of restriction factors is that they act in a species-specific manner which prevents cross-species transmission of the virus. In accordance with the 'Red Queen hypothesis' of evolution, lentiviruses have evolved several mechanisms to evade restriction. Viral accessory proteins play a critical role in this. Studies suggest that the acquisition of viral genes encoding accessory proteins, has been driven by strong selective pressure exerted by restriction factors. Interestingly, some of these accessory proteins also downmodulate cell surface proteins which are involved in immune activation, hence evading antiviral immunity (discussed in Genome structure section).

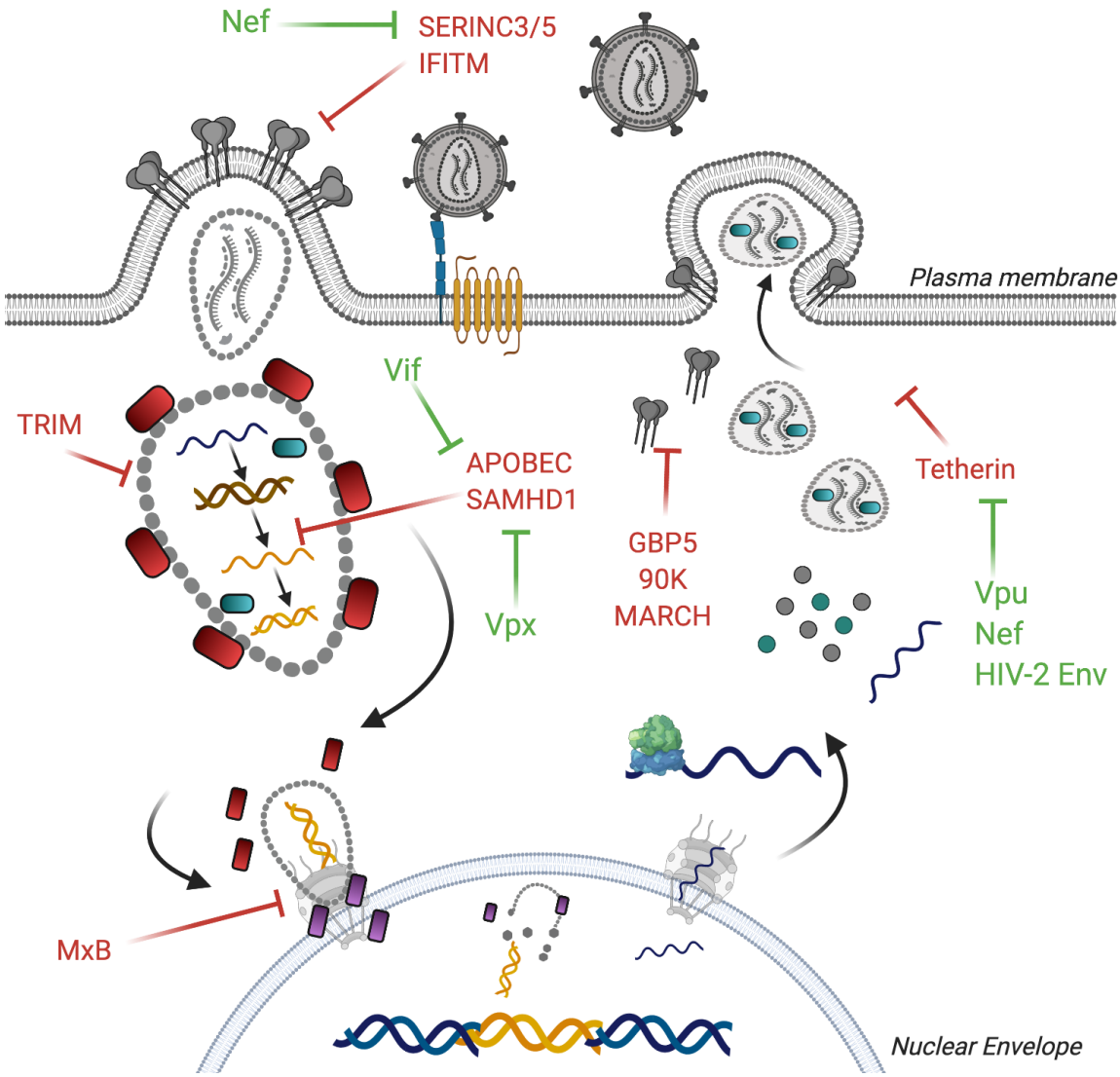

Figure 1.17 HIV restriction factors. Diagram showing different stages of the HIV lifecycle which are targeted by various restriction factors (red). HIV has evolved to have several mechanisms to counteract restriction factors and one way it to encode accessory proteins (green). These accessory proteins directly antagonise the restriction factors. (Created using BioRender.com)

1.4.1 Antiviral factors with an Env-dependent phenotype

SERINC

Serine Incorporator Proteins (SERINC) are large proteins consisting of 10-12 transmembrane domains. There are five human paralogues named SERINC 1-5, and they are encoded by five individual SERINC genes. These genes are highly conserved among eukaryotes (Grossman et al., 2000). SERINC3/5 expression levels vary in different cell types, with the highest expression in Jurkat cells and PBMCs that are both stimulated and unstimulated (Usami, Wu and Göttlinger, 2015). The exact physiological role(s) of these proteins remain to be elucidated. Initial evidence suggested that SERINCs are involved in phospholipid biosynthesis, as they act as carrier proteins and

aid serine incorporation (Inuzuka, Hayakawa and Ingi, 2005). However, recent mass spectrometry studies show that removing SERINC1 (Chu et al., 2017) and SERINC5 from cell membranes (Trautz et al., 2017) does not alter the lipid composition of either viral or cellular membranes.

The discovery of SERINC3 and SERINC5 as antiviral factors (Rosa et al., 2015; Usami et al., 2015) was guided by the observation that the lentiviral Nef protein (Kim et al., 1989; Miller et al., 1994; Spina et al., 1994) and MLV Glycogag (Pizzato, 2010) enhance HIV-1 replication in primary macrophages and T cells and some non-permissive T cell lines, such as H9 and Jurkats. However, there are some permissive cell lines that allow HIV-1 infection. Transcriptomic (Rosa et al., 2015) and phospho-proteomic (Usami et al., 2015) analyses, comparing *Nef* positive and *Nef* negative viruses, revealed that expression of SERINC3/5 varied greatly between the two comparators. SERINCs also antagonise the equine infectious anaemia virus, which uses its S2 accessory protein to counteract the restriction factor (Chande et al., 2016), thus it has broad activity against retroviruses. SERINC3/5 restrict infection at the step of viral entry. They are present on the cell membrane at sites of virus maturation and budding, hence are incorporated into nascent virions. In the absence of Nef or in the presence of a non-functional Nef protein, HIV-1 virions are significantly less infectious. Some evidence suggests that reduced infectivity is due to less efficient Env-mediated fusion of the viral and target cell membranes (Usami et al., 2015; Sood et al., 2017). Sood and colleagues further suggest that the step of small fusion pore formation is manipulated by SERINC5, however the exact mechanism remains to be elucidated. The viral accessory protein Nef counteracts SERINC5 restriction by directly interacting with SERINC5 and downmodulating its expression from the cell membrane in an AP2 dependent manner. This downmodulation results in less SERINC3/5 incorporation into virions, hence no significant impact is seen on infectivity (Rosa et al., 2015; Usami et al., 2015).

Different members of the SERINC family of proteins have varying potency against HIV-1. SERINC2 has no antiviral activity, whereas SERINC5 is the most potent antiviral protein and SERINC1/4/3 have moderate antiviral activity (Rosa et al., 2015; Schulte et al., 2018; Usami et al., 2015). This is in accordance with transcriptomic studies which show that SERINC5 transcripts are highly expressed in many lymphoid and myeloid tissues (Rosa et al., 2015). Hence, SERINC5 potently restricts lymphotropic and myelotropic viruses, including HIV and MLV. Dai and colleagues (2018) show that whilst SERINC5 orthologues from various species (human, mouse, zebrafish and frog) can restrict HIV-1 infection, frog SERINC5 is insensitive to Nef counteraction. Hence, adding Nef in trans does not rescue HIV-1 infection in the presence of frog SERINC5. Therefore,

the function of restriction and sensitivity to Nef can be separated. Mutational analysis and production of chimeric SERINC5 proteins reveal that the intracellular loop 4 (ICL4) of SERINC5 determines its sensitivity to Nef, but not its ability to restrict HIV-1 infection (Dai et al., 2018).

SERINC proteins do not exhibit features which are typical of restriction factors. For example, analysis of the proportion of positively selected sites in SERINC genes do not show any evidence of positive selection (Murrell et al., 2016). This suggests that SERINCs have not been involved in a strongly selective evolutionary arms race, which is surprising given its direct interaction with Nef and broad antiviral activity against distantly related viruses. However, Murrell and colleagues (2016) discuss potential explanations for this finding. Firstly, it is possible that the rare sites, within SERINC genes, which are under positive selection are important for interacting with viral antagonists. Alternatively, the arms race may not have had a direct effect on the gene at the codon level, similar to *BST2/tetherin* (amino acid deletion leads to loss of interaction with Nef) and *TRIM* (gene fusion to produce TRIM-Cyp). Finally, the authors suggest that the physiological function(s) of SERINCs may make it impossible for the gene to undergo changes through an evolutionary arms race. Another atypical feature of SERINC3/5 is that they do not act in a species-specific manner. Human, mouse, zebrafish and frog SERINC5 proteins are able to significantly restrict HIV-1 infection (Dai et al., 2018). Finally, SERINC3/5 gene expression is not induced by IFN-α in several cell types that are typically infected by HIV-1, including monocyte-derived dendritic cells and primary CD4 T cells (Rosa et al., 2015).

One possible mechanism for SERINC5 restriction is that it induces conformational changes in HIV-1 Env, resulting in inefficient fusion. This has been explored using neutralising antibodies which target specific, well characterised epitopes on Env. The presence of SERINC5 in pseudotyped NL4.3 virions renders them more sensitive to neutralisation by MPER targeting antibodies but not gp120 specific antibodies (Beitari et al., 2017; Sood et al., 2017). This suggests that the structure of gp41 is altered by SERINC5, specifically the MPER. The exact molecular mechanism of how SERINC5 might induce conformational changes in Env remains to be solved. One hypothesis is that SERINC alters the lipid profile of membranes, particularly within the lipid rafts, where both SERINC and Env localise. This would explain indirect effects of SERINC5 on HIV-1 infectivity. In line with this hypothesis, a recent study used super resolution fluorescence microscopy to look at single virions and found that Env clusters and SERINC5 clusters do not colocalise on viral membranes, thus SERINC5 has an indirect effect on Env clustering (Chen et al., 2020). This study also highlights that presence of

SERINC5 in viral particles reduces Env clustering, suggesting that perhaps Env mobility along the lipid bilayer is compromised. The importance of the lipid composition of membranes in Env clustering has been studied and cholesterol sequestration is shown to rigidify membranes to prevent later movement of Env trimers (Schulte et al., 2018). SERINC5 may be involved in cholesterol sequestration, although there is little evidence to support this as yet.

On the other hand, direct interacts have also been suggested in light of recent data. A structural study by Pye and colleagues (2020) shows that SERINC5 is almost completely embedded within the membrane, and that the only external region of Env it could interact with is the gp41 MPER (Pye et al., 2020). This provides an alternative mechanism by which SERINC5 can alter neutralisation profiles of HIV-1 in the presence of MPER targeting antibodies. The study further explores potential functional sites within SERINC5 and finds that there are two classes of mutants that are unable to restrict HIV-1 infection. The first class cannot localise to the cell membrane and are thus excluded from virions. The second class of mutations do not prevent membrane localisation, allowing SERINC5 to be incorporated into virions. Despite incorporation, mutant SERINC5 proteins are unable to restrict infection. Further, these mutants are unable to alter the sensitivity of HIV-1 to neutralising antibodies targeting the MPER region. Interestingly, several mutations belonging to Class 2 are found in extracellular loop 5 (ECL5) and ECL3 of SERINC5. By modelling HIV-1 Env trimer and SERINC5 in a lipid bilayer, the authors suggest that the distance between ECL5 and ECL3 of SERINC5, is the same as the distance between MPER regions on Env trimers. This suggests that these regions are potentially interacting and allowing inhibition of fusion and increased sensitisation to neutralisation (Pye et al., 2020). The involvement of ECL5 and ECL3 further suggests that SERINC5's restrictive activity is occurring on the external surface of the virion. Further research is required to better understand the molecular mechanism of SERINC5 restriction and its interactions with the viral Env glycoprotein.

Interestingly, SERINC5 restriction has an Env-dependent phenotype (Beitari et al., 2017; Rosa et al., 2015; Usami et al., 2015). Beitari and colleagues (2017) show that NL4.3 virus pseudotyped with CCR5-tropic Env proteins are less sensitive to SERINC3/5 restriction. By contrast, CXCR4-tropic Env proteins from lab adapted strains render the virus sensitive to restriction. This pattern of sensitivity also correlates with the virus' requirement for Nef. X4-tropic viruses, such as NL4.3 and HxB2, require a functional Nef protein for enhanced replication in T cell lines. However, YU-2 and ADA viral infectivity is unaffected by the presence of Nef (Usami and Gottlinger, 2013). Mutational analysis reveals that the V3 loop of Env is the determinant for viral sensitivity to SERINC3/5

(Beitari et al., 2017). However, it is yet to be determined why and how Env proteins determine sensitivity to SERINC5. Both SERINC5 and Env are large proteins embedded in lipid-rich membranes, making structural studies to identify direct interactions very difficult. Recent studies suggest that the conformation of Env is crucial for sensitivity to SERINC5. BiFC assays show that sensitive Envs (e.g., NL4.3) bind to SERINC5 better compared with resistant Envs (e.g. AD8) in a CD4-negative cell line. However, in the presence of CD4, both envelopes bind to SERINC5 equally as well and the AD8 virus becomes more sensitive to SERINC5 restriction (Zhang et al., 2019a). CD4 binding is known to induce conformational changes in Env, leading to an open conformation. Of note, X4-tropic envelopes most belong to chronic viruses and highly lab adapted strains which have a tier 1 Env and are inherently in a more open conformation compared with R5-tropic envelopes, prior to CD4 binding (Montefiori et al., 2018). Therefore, these results suggest that SERINC5 binds better to envelopes with an open conformation which eventually leads to premature gp120 dissociation (Zhang et al., 2019a). Ultimately, what is clear thus far is that SERINC5 can affect conformation, clustering ability, stability and sensitivity of Env trimers to neutralising antibodies, although mechanistic details remain to elucidated. Further investigations are required to better understand the relationship between Env and SERINC5, in order to gain an understanding of SERINC5 restriction mechanism.

IFITM

The Interferon Inducible Transmembrane proteins (IFITM) target a wide range of enveloped viruses including Influenza A virus, Dengue virus, Ebola virus, Hepatitis C virus and HIV (Brass et al., 2009; Huang et al., 2011; Lu et al., 2011a). There are five loci on human chromosome 11, which encode the proteins IFITM1, 2, 3, 5 and 10 (Bailey et al., 2014). IFITM1, 2 and 3 are IFN-inducible, have antiviral activity and are under positive selection (Zhang et al., 2012). IFITM5 is expressed exclusively in osteoblasts and lacks antiviral activity (Farber et al., 2014). IFITM10 function remains to be elucidated. All IFITM proteins are targeted to the plasma membrane after synthesis. However, IFITM2 and IFITM3 have a Yxxθ endocytic motif which enables internalisation into endosomes (Jia et al., 2012; Jia et al., 2014). IFITM1 lacks this motif, hence is primarily localised to the plasma membrane. IFITMs belong to the Dispanin group of transmembrane proteins (Sallman Almen et al., 2012). They have a conserved intracellular loop which is palmitoylated to increase the stability of the large structure. The intracellular loop is flanked by hydrophobic domains on the N- and C-terminus (Bailey et al., 2013; Weston et al., 2014). The N-terminal domain contains two alpha helices which are embedded in the inner leaflet of the membrane, a feature which is thought to regulate membrane curvature (Ling et al., 2016).

An ISG siRNA screen identified IFITM1, 2 and 3 as HIV-1 restriction factors (Lu et al., 2011a). Lu and colleagues (2011) discovered that IFITM proteins in the target cells were important for blocking HIV-1 cell-free infection, although cell-cell transmission could overcome this block (Lu et al., 2011a). Two subsequent studies argued that the IFITM proteins present in virus producer cells are important for restriction (Compton et al., 2014; Tartour et al., 2014). Once incorporated into nascent virions, these proteins reduce HIV-1 infectivity without affecting virus production. In line with this, an overexpression system was used to show that IFITM proteins impair Env processing and incorporation into virions (Yu et al., 2015), although this observation is yet to be replicated in more physiologically relevant experimental systems.

Despite this evidence that IFITM1/2/3 can restrict HIV-1 infection, the exact molecular mechanism of restriction remains to be elucidated. Similar to SERINC5-mediated restriction, IFITM-restriction may have multiple facets. First, experiments investigating IAV restriction suggest that IFITMs block formation of fusion pores once viral and target cell membranes have undergone hemifusion, thereby reducing viral infectivity but not production (Desai et al., 2014; Li et al., 2013). The Blam-Vpr assay has been used to show that IFITMs disrupt fusion of HIV-1 with the target cell membrane (Wang et al., 2017). Next, the C terminal domain of IFITM3 has a transmembrane alpha helix which is responsible for IFITM oligomerisation (John et al., 2013). The resultant higher order structures may influence membrane fluidity, thus preventing movement and clustering of receptors which are required for efficient viral fusion and entry into target cells (Amini-Bavil-Olyaee et al., 2013; Desai et al., 2014; Feeley et al., 2011; Li et al., 2013; Lin et al., 2013).

Foster and others show that, similar to SERINC5, Env is a determinant for IFITM restriction, particularly the V3 loop (Foster et al., 2016; Tartour et al., 2014; Wang et al., 2017; Wu et al., 2017). Some evidence suggests that viral coreceptor usage determines sensitivity to different IFITM proteins, for example R5-tropic HIV-1 viruses are sensitive to IFITM1 but not IFITM2/3 (Foster et al., 2016). On the other hand, X4-tropic chronic viruses are sensitive to IFITM2/3, which are located on endosomal membranes. Mislocalisation of IFITM2/3 via mutagenesis of residues Y19/Y20, is able to abolish restriction, as seen by a rescue of HIV-1 infection (Foster et al., 2016). To note, virion incorporation of IFITM proteins was unaffected in these experiments, suggesting that the primary mode of restriction is not via virion incorporated IFITMs, but rather by IFITM proteins on target cells. Further, R5-tropic viruses are resistant to a putative splice variant of IFITM2 called Δ20 (Wu et al., 2017). However, by inserting the C-terminus of the X4

receptor into the R5 receptor, R5-tropic viruses become sensitive to IFITM2 Δ20. Thus, further validating that coreceptor usage explains why the V3 loop of Env is a determinant of IFITM sensitivity. Alternatively, Wang and colleagues (2017) show that although the V3 loop determines sensitivity, this is not explained by coreceptor usage. Several R5-tropic viruses were assessed for their sensitivity to IFITM3 and swapping the V3 loops to make chimeric viruses, showed that viruses had varying sensitivities to IFITM3, despite the same coreceptor usage (Wang et al., 2017). In line with this, R5 viruses were tested for their sensitivity to Maraviroc, a CCR5 inhibitor, and this sensitivity profile did not correlate with IFITM3 sensitivity (Wang et al., 2017). Interestingly, this same study probed for conformational differences between IFITM3 sensitive and insensitive Envs using a panel of HIV-1 nAbs. This showed that IFITM3-sensitive viruses were more susceptible to soluble CD4 and 17b (binds to a CD4 inducible epitope) neutralisation, by comparison with IFITM3-resistant viruses. Also, the presence of IFITM3 in resistant and sensitive virus particles, does not alter their sensitivity to sCD4 and 17b neutralisation. Therefore, these data suggest that conformation of the CD4-binding site and the inherent propensity of Env to adopt 'open', CD4-bound-like conformations determines sensitivity to IFITM3 (Wang et al., 2017).

In order to assess the importance of IFITM restriction on chronic and acute HIV-1 infection, Foster and colleagues (2016) compared IFITM sensitivity of different viruses to show that Transmitted/Founder (T/F) viruses are resistant to IFITM restriction, whereas chronic viruses are sensitive (Foster et al., 2016). Another interesting finding from this study is that there is a correlation between viruses becoming sensitive to IFITM restriction and the gain of escape mutations to avoid neutralising antibodies. This evidence suggests that IFITM proteins are indeed a barrier to viral transmission, hence avoiding IFITM-mediated restriction is crucial. Interestingly, despite the selective pressure exerted on HIV-1 by IFITM proteins, no known HIV accessory proteins have been shown to antagonise IFITM proteins directly.

GBP5, 90K and MARCH proteins

Guanylate Binding Protein 2 and 5 (GBP2/5) are part of the IFN-inducible GTPase family of proteins. Their expression is upregulated by HIV-1 infection and Type I IFNs, resulting in reduced HIV-1 and SIV infectivity (Krapp et al., 2016). Western blot analysis shows that GBP2/5 target Env processing and incorporation (Braun et al., 2019; Krapp et al., 2016). The Env precursor gp160, undergoes mannose trimming and proteolytic cleavage in the Golgi apparatus. Therefore, it was hypothesised that GBP2/5 directly target the accessible EnvCT during this process. In the presence of overexpressed GBP2/5, a EnvCT truncated mutant shows equal levels of Env downmodulation from the cell

surface, compared with the WT Env protein (Braun et al., 2019). This suggests that GBP2/5 are not directly antagonising Env. Further investigation by this group revealed that the mechanism of GBP2/5 restriction is indirect. The antiviral proteins interfere with Env processing and maturation by targeting the key protease, furin (Braun et al., 2019). Furin is responsible for the proteolytic cleavage of gp160, to produce mature Env proteins, composed of the gp120 and gp41 subunits (Dubay et al., 1995; Moulard and Decroly, 2000). Co-immunoprecipitation assays in HEK293T cells and macrophages showed that GBP2/5 directly bind to the cytoplasmic domain of furin and reduce the efficiency of furin maturation (Braun et al., 2019). Maturation is crucial for producing proteolytically active furin (Denault et al., 2002; Plaimauer et al., 2001; Thimon et al., 2006). Krapp and colleagues (2016) also show that GBP5 does not require its GTPase activity to restrict, rather its Golgi localisation determines the phenotype. It is known that isoprenylation of GBP5 is a determinant for Golgi localisation. This may explain why a GBP5 isoprenylation mutant (C583A) is unable to restrict HIV-1 infection. Interestingly, some HIV-1 strains have mutations in Vpu which allow for increased Env production, which allows the virus to overcome GBP5 restriction (Krapp et al., 2016), suggesting that GBP proteins are providing a selection pressure on HIV-1.

90K is a secreted scavenger receptor with species specific, antiviral activity against HIV-1 (Lodermeyer et al., 2018). This protein is upregulated by Type I and II IFNs and upon HIV infection. Overexpression of 90K in HEK293T cells produce viral particles with an infectivity defect (Lodermeyer et al., 2013). Western blot analysis of these particles shows defective Env processing and flow cytometric analysis confirms that 90K reduces surface Env levels, similar to GBP2/5. However, this is not likely due to interference with furin cleavage, as other furin dependent viral envelopes are cleaved appropriately in the presence of overexpressed 90K (Lodermeyer et al., 2013). Also, there is no direct evidence to suggest that 90K interacts with HIV-1 Env in the secretory pathway. Therefore, the exact mechanism by which 90K is restricting HIV-1 infection remains to be elucidated. Finally, siRNA-mediated depletion of 90K in T cells and macrophages confers a replicative advantage to HIV-1, suggesting that it is active against HIV-1 infection in relevant cell types.

The Membrane Associated Ring CH proteins (MARCH) are a family of RING-finger E3 ubiquitin ligases. There are 11 members, of which three have antiviral activity against HIV-1: MARCH 1, MARCH 2 and MARCH 8 (Tada et al., 2015; Zhang et al., 2018; Zhang et al., 2019b). MARCH1/2/8 are primarily localised at cellular and endosomal membranes; a common feature of antiviral factors that target Env glycoproteins (Zhang et al., 2019b). Their mechanism of action is not specific to HIV-1 Env, as VSV-G Env is

also affected by overexpression of MARCH1/2/8 in cell lines (Tada et al., 2015; Zhang et al., 2019b) (Tada et al., 2015; Zhang et al., 2019). mRNA analysis shows that all three are highly expressed in monocyte-derived macrophages, and MARCH 1 and 2, but not MARCH 8, are also highly upregulated by Type I IFNs (Zhang et al., 2019b). Expression of these proteins leads to a viral entry defect due to inefficient Env incorporation into nascent virions. Immunofluorescence and flow cytometry analyses of HIV-1 infected cells show that MARCH 1/2/8 downregulate Env from the cell surface but do not degrade it (Zhang et al., 2018; Zhang et al., 2019). This is by contrast to VSV-G Env which undergoes lysosomal degradation (Tada et al., 2015). This suggests that MARCH proteins restrict different envelopes by using different molecular mechanisms, the exact details of which are yet to be elucidated. It is yet to be determined whether these proteins can directly bind to Env at the cell surface to downregulate it or whether this is an indirect mechanism, using other host factors involved in endocytosis.

1.4.2 Other antiviral factors targeting HIV-1 replication

Tetherin

Tetherin (also known as BST2) is the most prominent antiviral factor targeting the final stage of HIV-1 replication – viral release. It was first discovered as a target of the Vpu accessory protein, which is known to enhance release of virions (Neil et al., 2008). Tetherin is an example of a prototypic HIV-1 restriction factor as it is an ISG, functions in a species-specific manner and is directly antagonised by viral proteins. Tetherin targets a multitude of enveloped viruses including HIV-1, Ebola virus, Nipah virus and Lassa virus (reviewed by (Neil, 2013)).

Tetherin is a small (20kDa), glycosylated type II transmembrane protein which is primarily localised at the cell membrane. The structure is composed of an N-terminal domain, an alpha helical transmembrane domain, a coiled coil ectodomain and a C-terminal GPI anchor (Hinz et al., 2010; Schubert et al., 2010). Tetherin is synthesised in the ER after which it continuously traffics between the plasma membrane, endosomes and the trans-Golgi network. Whilst in the ER, the C-terminus of tetherin is cleaved and a GPI anchor is added to the S161 residue (Cole et al., 2012). Localisation to the plasma membrane is controlled by two asparagine residues in the ectodomain which are N-linked glycosylated. This together with the GPI anchor, allows Tetherin to anchor in apical membranes (Kupzig et al., 2003). Specifically, the GP1 anchors targets Tetherin to lipid rafts and removal of the GPI anchor leads to mislocalisation at the cell membrane (Kupzig et al., 2003). At the cell membrane, tetherin exists as dimers held together by disulphide linkage, which is mediated by cysteine residues in the coiled coil ectodomain (Kupzig et al., 2003). The transmembrane domain has also been implicated in tetherin

homodimerisation (Cole et al., 2012). Finally, the N-terminal domain regulates trafficking as it contains a conserved dual tyrosine motif which binds to the clathrin adaptor proteins AP-1 and AP2, resulting in clathrin-mediated endocytosis from the cell membrane (Rollason et al., 2007).

Localisation to lipid rafts is essential for tetherin's ability to restrict HIV-1 infection, as this is the site of viral assembly and budding. Tetherin restricts infection by a multifaceted approach. First, it retains nascent virions to the cell surface. Specifically, the GPI anchor is embedded within the viral membrane, whilst the N-terminus is embedded within the cell membrane (Hammonds et al., 2010). This orientation results in viral particles being tethered to the surface of producer cells and to each other during ESCRT-mediated scission of viral and cellular membranes (Hammonds et al., 2010; Neil et al., 2008; Venkatesh and Bieniasz, 2013). Some evidence suggests that viral transmission via cell-cell spread overcomes this tetherin-mediated restriction (Jolly et al., 2010), which is thought to be the primary mode of HIV-1 transmission. Further, Tetherin also acts as a PRR and activates an innate immune response by activation of the NFkB signalling pathway (Cocka and Bates, 2012; Galao et al., 2012). Finally, tethered virions are exposed to the adaptive immune system, thus increasing the potential to induce ADCC (Alvarez et al., 2014b).

Tetherin antagonism is a conserved attribute amongst primate lentiviruses (Sauter et al., 2009), highlighting the importance of this restriction factor in providing a barrier to cross-species transmission. As tetherin targets a part of the virus which the virus cannot afford to mutate, lentiviruses encode proteins to directly counteract tetherin. Lentiviruses have evolved to counteract tetherin using different viral proteins, for example HIV-1 uses Vpu, HIV-2 uses Env and most SIVs use the Nef accessory protein (Jia et al., 2009; Sauter et al., 2009; Zhang et al., 2009). The exception to this is that SIV_{mus}, SIV_{mon} and SIV_{gsn} all use Vpu to counteract tetherin (Sauter et al., 2009). Interestingly, SIV_{cpzPtt} and SIV_{gor} also encode a Vpu protein, however in these viruses Vpu has lost the ability to downmodulate tetherin, although CD4 downmodulation function remains intact (Sauter et al., 2009). Instead, Nef antagonises tetherin by binding to the AP-2 adaptor protein, leading to clathrin-mediated endocytosis from the site of virus assembly. From this, it seems that lentiviruses which encode two antagonists of tetherin, lose tetherin-counteractivity in one of their proteins.

The cytoplasmic tail of human tetherin has a 5 amino acid deletion (G/DIWKK) which renders it insensitive to SIV Nef-mediated counteraction (Dube et al., 2011; Jia et al., 2009; Sauter et al., 2009; Zhang et al., 2009). Therefore, viruses which have successfully

undergone zoonotic transmission into humans, have adapted their strategy to counteract human tetherin, as discussed below.

(1) HIV-1 group M Vpu potently counteracts tetherin by inducing degradation and mislocalising tetherin in the endosomal pathway. Endosomal localisation of Vpu allows it to interact with both newly synthesised and recycling tetherin. Mutagenesis and NMR studies of the transmembrane alpha helices (TMD) of Vpu and tetherin reveal that interactions between the two proteins are facilitated by the highly conserved A14, W22 and A18 residues found in the Vpu TMD (Skasko et al., 2012; Vigan and Neil, 2010). Mutating these residues resulted in appropriate localisation of Vpu, however the ability to interact with tethering by coimmunoprecipitation and to downregulate tetherin from the cell surface was abolished (Vigan and Neil, 2010). Physical interactions between Vpu and tetherin are necessary but insufficient for antagonism and instead the cytoplasmic tail of Vpu has been shown to be responsible for tetherin counteraction. Phosphorylation of the Vpu cytoplasmic tail recruits the AP-1 and/or AP-2 adaptor proteins to form a ternary complex consisting of tetherin:Vpu:AP-1/2 which undergoes clathrin-mediated endocytosis (Jia et al., 2014; Kueck et al., 2015; Stoneham et al., 2017). Concomitant phosphorylation of a dual serine phosphorylation motif, DSGxxS, in Vpu recruits SCF E3 ubiquitin ligase via interactions with β-TrCP (Mangeat et al., 2009; Margottin et al., 1998; Mitchell et al., 2009; Schmidt et al., 2011). Consequently, the Vpu cytoplasmic tail is ubiquitinated (Douglas et al., 2009; Tokarev et al., 2011) and ESCRT-mediated lysosomal degradation of tetherin occurs (Mitchell et al., 2009).

(2) Vpu proteins belonging to HIV-1 Group O are relatively poor antagonists of tetherin by comparison with Group M Vpu. This is overcome by the use of Nef. Unlike SIV Nef proteins, HIV-1 Group O Vpu targets an alternative region of tetherin, which does not involve the 5 amino acid deletion in the cytoplasmic tail (Kluge et al., 2014).

(3) SIV Nef proteins recognise and bind to the G/DWIKK motif, whilst simultaneously interacting with AP-2. Thereby resulting in tetherin downmodulation from the cell surface (Serra-Moreno et al., 2013; Zhang et al., 2011).

(4) HIV-2 has evolved to use a different protein to antagonise tetherin. The HIV-2 Env glycoprotein, specifically the highly conserved GYxxΦ endocytic motif in the gp41 cytoplasmic tail, is essential for this role (Le Tortorec and Neil, 2009). However, interactions between the extracellular domains of Env and Tetherin interact, leading to the downmodulation of Tetherin from the cell surface in an AP-2 dependent manner (Abada et al., 2005; Le Tortorec and Neil, 2009). A key

difference between HIV-1 Vpu and HIV-2 Env-mediated antagonism is that HIV-2 Env does not induce degradation of tetherin, rather just sequestration from virus budding sites (Le Tortorec and Neil, 2009).

Leaky scanning of tetherin mRNA produces two isoforms, long and short, both of which can dimerise and restrict HIV-1 infection. The shorter isoform lacks the N-terminal initial 12 amino acids that contain the tyrosine motif required for activation of innate signalling pathways (Cocka and Bates, 2012). Further studies revealed that the ability of Tetherin to retain virions on the cell surface and the ability to activate NFkB signalling could be genetically uncoupled. This is due to the differential requirement for the GPI anchor. Whilst the anchor is indispensable for viral restriction, it is not required for activation of signalling (Tokarev et al., 2013). Tetherin's ability to activate the NFkB pathway is dependent on a di-tyrosine motif found in the cytoplasmic tail that functions as a hemi-immunoreceptor tyrosine-based activation motif (hemITAM). Signalling is induced by viral particle retention at the cell membrane. Interactions of Tetherin with the cortical actin skeleton via RICH2 adaptor protein results in phosphorylation of hemITAM by Syk kinase and propagation of downstream signalling via TRAF2, TRAF6 and TAK1 which ultimately results in NFkB activation (Galao et al., 2014). Taken together, tetherin provides a high level of selection pressure on HIV-1 due to its ability to restrict infection, activate innate signalling pathways and thereby modulate the adaptive immune response to infection by increasing exposure of viral particles.

TRIM5α

TRIpartite Motif 5α (TRIM5α) is a species-specific lentiviral restriction factor which is upregulated by Type I and II IFN and acts an innate immune sensor (Keckesova et al., 2006; Pertel et al., 2011b; Stremlau et al., 2004; Ylinen et al., 2006). It was discovered as a HIV-1 restriction factor using a cDNA screen from macaque and owl monkey cells (Sayah et al., 2004; Stremlau et al., 2004). HIV-1 infection is potently restricted by TRIM5α by preventing viral reverse transcription post viral entry into target cells (Wu et al., 2006). The structure of TRIM5α consists of an N-terminal RING finger zinc binding protein, a B-box zinc binding domain and a coiled coil region (Grutter and Luban, 2012; Meroni and Diez-Roux, 2005). The C-terminus also contains a PRY-SPRY domain which binds to capsid (CA) molecules, forming a hexagonal lattice around the capsid core (Fletcher and Towers, 2013; Stremlau et al., 2006). Formation of these higher order lattice structure is dependent on the B-box domain. Mutating residues within this domain, that are important for lattice formation, leads to loss of restrictive activity (Diaz-Griffero et al., 2007; Li and Sodroski, 2008). Formation of this lattice structure around the capsid core triggers TRIM5α autoubiquitination via the E3 ligase RING domain. Consequently,

the NFκB and AP-1 pathways are activated in a TAK-1 dependent manner (Pertel et al., 2011b)and capsid cores are targeted for proteasomal degradation (Kim et al., 2019; Lascano et al., 2016; Pertel et al., 2011a). Interestingly, mutating the RING domain relieves the block to reverse transcription but not infection, suggesting that TRIM5a restricts infection by two separate mechanisms (Javanbakht et al., 2005; Roa et al., 2012).

The first mechanism of restriction involves the E3 ligase activity of the RING domain. This model inhibits reverse transcription and infectivity. The second mechanism involves forming a lattice structure around the capsid core which can stabilise the capsid structure or lead to premature capsid uncoating to reveal HIV-1 genome and restrict infection.

SAMHD1

The Sterile Alpha Motif and Histidine-aspartate Domain containing protein 1 (SAMHD1) was initially identified as a target of the SIV accessory protein Vpx in myeloid cells, such as dendritic cells, macrophages and resting CD4 T cells (Descours et al., 2012; Goldstone et al., 2011; Hrecka et al., 2011; Laguette et al., 2011). The Vpx protein recruits DCAF1 which polyubiquitinates SAMHD1 and targets it for proteasomal degradation by (Hrecka et al., 2011; Laguette et al., 2011). By contrast, HIV-1 does not encode a Vpx protein and does not directly antagonise SAMHD1. Therefore, SAMHD1 restriction may explain why HIV-1 preferentially infects dividing cells, such as activated CD4 T cells. SAMHD1 restricts HIV-1 infection in resting CD4 T cells by blocking reverse transcription and this can be overcome by providing Vpx in HIV-1 and HIV-2 viral particles (Baldauf et al., 2012). Interestingly, it was suggested there is another block to reverse transcription in resting primary CD4+ T cells (but not in macrophages) that is SAMHD1-independent (Baldauf et al., 2017). Therefore, the exact mechanism of restriction remains to be elucidated. The structure of SAMHD1 is composed of an N-terminal domain, a catalytic core HD domain and a C-terminus (Goldstone et al., 2011). The HD domain has dNTPase activity which is important for HIV-1 restriction as it reduces the amount of nucleotides available for reverse transcription and viral DNA synthesis and mutations in this region prevent viral restriction (Goldstone et al., 2011; Laguette et al., 2011). Further, depletion of SAHMD1 correlates with an increase in dNTP levels and increased HIV-1 replication (Arnold et al., 2015).

The activity of SAMHD1 is regulated by cell cycle dependent phosphorylation and local dNTP levels. Activation of SAMHD1 initiates when GTP binds to the first allosteric site in a SAMHD1 monomer which results in conformational changes and dimerisation. Then, dNTPs bind to the second C-terminal allosteric site and catalytic site to produce active

SAMHD1 tetramer structures (Goldstone et al., 2011; Ji et al., 2013; Yan et al., 2013). In cycling cells, CDK1 and CDK2 phosphorylate SAMHD1 in a Cyclin A-dependent manner to inactivate the restriction factor (Cribier et al., 2013; Pauls et al., 2014). Phosphorylation occurs on residue T592, leading to destabilisation of the tetramer structure and the production of catalytically inactive SAMHD1 dimers and monomers (Arnold et al., 2015). Oligomerisation of SAMHD1 is a requisite for HIV-1 restriction and this can be explained by the observation that SAMHD1 monomers and dimers are unable to reduce dNTP levels enough to prevent reverse transcription (Arnold et al., 2015; Yan et al., 2013).

SAMHD1 is widely expressed in a range of human tissues, however HIV-1 restriction is only observed in non-dividing cells. This may be explained by the fact that non-dividing cells have low levels of dNTP which is maintained at low levels by SAMHD1 and because SAMHD1 is inactivated in dividing cells. In activated T cells, SAMHD1 phosphorylation (inactivation) is mediated by T cell receptor mediated T cell activation or by common gamma chain cytokines which relieve the block and allow HIV-1 infection of these cells (Coiras et al., 2016; Manganaro et al., 2018). Mlcochova and colleagues (2017) provide insight into the mechanism by which HIV-1, which does not encode a SAMHD1 antagonist, evades SAMHD1 restriction in primary macrophage cells by exploiting a window of opportunity during which SAMHD1 is turned off. They show that primary macrophages cycle between G1-like and G0-like states. In the G1-like state macrophages express the marker MCM2 indicative of cell cycle entry, but they do not proceed to DNA replication (S phase) and cell division (M phase). MCM2 expression correlates with SAMHD1 phosphorylation, thus deactivation, and results in SAMHD1 inactivation, allowing for dNTP levels to rise and fuel the process of reverse transcription. In the G0-like state, the cell cycle marker, MCM2, is not expressed by the cell and therefore SAMHD1 is dephosphorylated and HIV-1 infection is restricted (Mlcochova et al., 2017).

APOBEC3

The first HIV-1 restriction factor family to be identified were Apolipoprotein B mRNA editing enzyme catalytic polypeptide 3 proteins (APOBEC3 → A3), which are constitutively expressed in cells but also further upregulated upon interferon induction and they target HIV-1 at a post entry step in the viral lifecycle (Koning et al., 2009). APOBEC3 was discovered in a comparative study in which HIV-1 ΔVif virus was used to infect permissive (CEM) and non-permissive (CEM-SS) cells, after which RNA extraction from these cells identified the presence and absence of APOBEC, respectively (Sheehy et al., 2003).

The APOBEC3 family consists of 7 cytidine deaminase members called APOBEC3A-H, of which A3G is the most potent inhibitor of HIV-1 infection in CD4 T cells and macrophages (Chaipan et al., 2013; Gillick et al., 2013). Packaging of A3G is a determinant of viral restriction and this is achieved by interactions with viral RNA and the nucleocapsid protein of Gag (Bogerd and Cullen, 2008). A3G dimerisation occurs in an RNA-dependent manner and this is crucial for A3G packaging into virions, as well as HIV-1 restriction mechanism (Huthoff et al., 2009). Two mechanisms of restriction have been described thus far: hypermutation of viral genome and inhibition of reverse transcription.

A3G acts at the step of reverse transcription where is deaminates cytidine residues in the newly synthesised negative strand of DNA and this results in G to A hypermutations in the positive sense DNA (Bishop et al., 2004). Consequently, proviruses accumulate stop codons and missense mutations resulting in non-functional proteins and defective viral particles. The level of G to A hypermutation has been correlated with low levels of viremia in HIV-1 infected individuals, as well as an increased CD4 T cell count. However, it was shown that only 6% and 10% of the guanosines in HIV-1 infected CD4 T cells and macrophages were hypermutated, respectively (Koning et al., 2011). This suggests that *in vivo*, the dominant mode of restriction is probably not hypermutation, but instead inhibition of reverse transcription.

Several mechanisms have been proposed to explain how A3G inhibits the process of reverse transcription. Initially it was suggested that a reduction in the amount of RT products was observed because the hypermutated DNA is recognised by the cellular uracil DNA glycosylases which are a part of the uracil base excision pathway, leading to degradation of RT products (Yang et al., 2007). However, inhibition of the UBER pathway does not rescue viral DNA levels (Langlois and Neuberger, 2008). Also, it was shown that a reduction in viral DNA by A3G was independent of the deaminase activity of the enzyme (Iwatani et al., 2007). Further studies suggested that A3G targets multiple steps of reverse transcription, including tRNA binding to the primer binding site, minus and plus strand transfer and also tRNA processing and DNA elongation (Bishop et al., 2008; Guo et al., 2007; Li et al., 2007; Nowarski et al., 2014). A recent study also suggested that A3G directly binds to the RT enzyme (Pollpeter et al., 2018).

Studies in mice reveal that A3G is able to module the innate and adaptive response to HIV-1 infection. First, by inhibiting reverse transcription, A3G reduces the amount of viral DNA available to be sensed by the intracellular DNA sensor cGAS, thereby reducing the

possibility of activating an IFN response (Stavrou et al., 2015). Some sublethal mutations induced by A3G are beneficial for the virus as they allow escape from immune responses, for example CTL escape could occur if the region recognised by the CD8 T cell is hypermutated (Kim et al., 2010). Resistance to antiretroviral therapy can also arise (Sato et al., 2014). Conversely, hypermutation can result in the production of non-functional proteins that are processed and presented to MHC-I molecules, thereby increasing the CTL response (Casartelli et al., 2010a). Also, activation of the DNA damage response can lead to an increase in NK cell activation which results in cell lysis (Norman et al., 2011).

MxB

There are two human and two mice myxovirus (Mx) resistance genes named MxA/B and Mx1/2, respectively. These proteins belong to the GTPase superfamily. Whilst MxA has broad antiviral activity against DNA and RNA viruses (Haller and Kochs, 2011), MxB targets specific retroviruses such as HIV-1 (Goujon et al., 2013). Whilst the majority of HIV-1 subtypes and transmitted/founder viruses are sensitive to restriction (Liu et al., 2015), HIV-2 and some SIVs are less susceptible to MxB (Kane et al., 2013). MxB has characteristics of typical restriction factors. Orthologues of this protein show species specificity, as indicated by differences in their patterns of restriction (Busnadiego et al., 2014).

Mx proteins are composed of a GTPase domain, a Bundle Signal Element (BSE) and a C-terminal stalk region (Fribourgh et al., 2014), which together form higher order oligomers (Alvarez et al., 2017). Dimerisation of MxB and oligomerisation are important for HIV-1 restriction, although assembly of larger helical structures are thought to be dispensable (Alvarez et al., 2017; Buffone et al., 2015; Fricke et al., 2014). MxB has an additional 25 amino acids at the N-terminus (NTD), which contains a nuclear localisation signal (King et al., 2004). Acquirement of these extra 25 amino acids suggested that the NTD is important in HIV-1 restriction and it has been shown that transfer of this region of MxB to the non-restrictive MxA protein results in HIV-1 restriction. These observations would suggest that the nuclear localisation, which is dictated by the NTD, is important in MxB restriction mechanism (Busnadiego et al., 2014; Goujon et al., 2014). However, genetic manipulation of MxB revealed that a single point mutation at position 20 (K20) can abrogate nuclear localisation, but not HIV-1 restriction (Schulte et al., 2015).

The exact mechanism of MxB restriction remains to be elucidated. Current evidence suggests that MxB prevents HIV-1 nuclear entry, as suggested by a reduction in the production of 2-LTR circles but no effect on reverse transcription and DNA synthesis

(Kane et al., 2013; Li et al., 2001). The NTD of MxB has been suggested to bind capsid hexamers *in vitro*, however the importance of this remains controversial, as capsid mutations which allow MxB evasion, do not result in loss of interaction between the two proteins (Fribourgh et al., 2014; Fricke et al., 2014; Liu et al., 2013; Wei et al., 2016). Recently it was shown that MxB interacts with components of the nuclear pore complex via the NTD. Particularly, interactions between the triple arginine motif in MxB NTD and Nup214 and TNPO1 were required for MxB nuclear localisation and HIV-1 restriction (Dicks et al., 2018). Consistent with these findings, a second study showed that changes in the nucleoporin levels using siRNA, altered MxB activity (Kane et al., 2018). This suggests that MxB restricts HIV-1 nuclear entry by manipulating the nuclear pore complex.

Two papers hypothesise that MxB targets HIV-1 capsid in a cofactor-dependent manner (Goujon et al., 2014; Kane et al., 2013). Mutational analysis of capsid has shown that binding to different cofactors, such as CPSF6 and CypA, commits HIV-1 to different nuclear import pathways. It has also been shown that repeated passage of HIV-1 in MxB expressing cells results in capsid mutations in the CypA binding loop, rendering the virus resistant to MxB (Liu et al., 2013). Further, preventing CypA recruitment to capsid rescues infection in the presence of MxB (Goujon et al., 2013; Kane et al., 2013). Together these data suggest that cofactors play a role in MxB restriction, although the exact details remain unclear. A recent study by Miles and colleagues (2020) suggests that MxB sensitivity is determined by capsid surface dynamics which can be altered by cyclophilin A binding and the capsid sequence. Cyclophilin A binding provides conformational flexibility to HIV-1 capsid thus facilitating evasion of restriction factors (Miles et al., 2020). Therefore, this suggests that HIV-1 cofactors themselves may not be a determinant of MxB sensitivity, rather it is the viral capsid that is important.

1.4 Aims of the project

The EnvCT can regulate various aspects of Env biology, which have implications on Env function and ultimately viral replication. The aims of this study are as follows:

1. To use a comparative biology approach to better understand whether HIV-1 and HIV-2 have a differential requirement for a long EnvCT and why this is the case.
2. With emerging literature describing the presence of lentiviral restriction factors that operate in an Env-dependent manner, I hypothesise that the EnvCT can regulate sensitivity to restriction factors such as SERINC3, SERINC5 and the IFITMs.
3. SIV and HIV-1 EnvCTs are capable of activating the NFκB signalling pathway which is beneficial during early stages of the viral lifecycle. I will investigate whether HIV-2 can also activate NFκB signalling and whether the lentiviral EnvCTs are able to activate other proinflammatory signalling pathways, such as AP-1 signalling, as well as antiviral signalling via IRF3.

2 Materials and Methods

2.1 **Cell culture**

HEK293T/17 (Pear et al., 1993), HEK293T/JL, HEK293T SERINC5 knock out cells (provided by Massimo Pizzato, Trento University, Italy) and HeLa TZM-bl reporter cells were grown in Dulbecco's Modified Eagle's Medium (DMEM; Gibco) supplemented with 10% foetal calf serum (FCS; Gibco) and 50 µg/ml penicillin-streptomycin (Gibco). HEK293T cells were obtained from American Type Culture Collection (ATCC) and HeLa TZM-bl cells (Wei et al., 2002) were obtained from Centre for AIDS Reagent (CFAR, NIBSC, Potters Bar, UK). HeLa TZM-bl reporter cells are a derivative of HeLa cells that have been engineered to express CD4 and CCR5, and naturally express CXCR4. They contain a luciferase reporter gene under the control of a Tat inducible promoter. When HIV infects the HeLa TZM-bl cells, the Tat protein drives expression of luciferase, which is proportional to the amount of infection. Human glioblastoma U87-MG cells were modified to express CD4 and either CCR5 or CXCR4 (Goujon et al., 2013) (provided by Greg Towers, UCL, UK). IFITM proteins were overexpressed in U87-MG and HeLa TZM-bl reporter cells by lentiviral transduction. IFITM overexpressing U87-MG cells were grown in DMEM supplemented with 10% FCS, 50 µg/ml penicillin-streptomycin, 2 µg/ml puromycin (Sigma) and 100 µg/ml G418 (Sigma). TZM-bl cells overexpressing IFITM proteins were grown in DMEM supplemented with 10% FCS, 50 µg/ml penicillin-streptomycin and 2 µg/ml puromycin. Cells were passaged every 3 days (until reaching 70-80% confluency) using trypsin (Gibco) to detach cells and diluted (1:4-1:10) in fresh culture medium.

H9 and Jurkat CE6.1 T cell lines were obtained from ATCC and grown in Roswell Park Memorial Institute (RPMI 1640; Gibco) medium supplemented with 10% FCS and 50 µg/ml penicillin-streptomycin. Cells were passaged once a week when cells had reached 1-2x10^6 cells/ml by diluting in fresh medium (diluted to a density of 1x10^5 cells/ml).

All cells were grown in a humidified 5% CO_2 incubator at 37°C.

2.2 **Proviral constructs**

Proviral constructs expressing full length, replication competent viruses:

HIV-1 NL4.3 donated by Dr. Malcolm Martin, obtained from CFAR, NIBSC, Potters Bar, UK. Accession code: MN685337

HIV-1 NL4.3 ΔNef is a molecular clone derived from NL4.3 WT with termination codons in the first and third codons of the *nef* gene, producing infectious virus without a functional Nef protein (Sloan et al., 2011). Obtained from R. Sloan, Edinburgh University, UK.

HIV-1 NL4.3 ΔCT ΔNef mutant was made by inserting a stop codon in the EnvCT of the HIV-1 NL4.3 ΔNef construct using primers described in **section 2.4**.

HIV-1 NL4.3 ΔVpu is a molecular clone derived from the NL4.3 WT as described previously (Klimkait et al., 1990). Obtained from Klaus Strebel, NIH, US.

HIV-2 ST donated by Dr. Beatrice Hahn and Dr. George. M. Shaw. Obtained from CFAR, NIBSC, Potters Bar, UK. Accession code: M31113

HIV-2 7312A donated by Dr. Feng Gao and Dr. Beatrice Hahn. Obtained from CFAR, NIBSC, Potters Bar, UK. Accession code: L36874

HIV-2 ROD10 donated by Dr. Ryan-Graham. Obtained from CFAR, NIBSC, Potters Bar, UK. Accession code: MH541055

2.3 Plasmid constructs

pMDG is a vector containing the vesicular stomatitis virus glycoprotein (VSV-G) under the control of a cytomegalovirus promoter for expression in mammalian cells.

pcDNA3.1 is an empty vector control that was used to insert genes of interest and to equalise total DNA transfected into cells in relevant experiments.

pcDNA-SERINC5 is a construct expressing human SERINC5 which is dually tagged with an external FLAG tag and an internal HA-tag. This construct was obtained from Massimo Pizzato (Trento University, Italy).

pcDNA-SERINC3 is a construct expressing human SERINC5 which is dually tagged with an external FLAG tag and an internal HA-tag. This construct was obtained from Massimo Pizzato (Trento University, Italy).

pcDNA-Tetherin is a construct which expresses human Tetherin with a HA-tag in the ectodomain (Gupta et al., 2009). This construct was obtained from Greg Towers (University College London, UK).

CMS28 is a retroviral expression vector. The BglII/XhoI/HpaI/EcoI polylinker has been replaced with EcoRI/NotI/XhoI (a gift from M.Malim King's College London).

CMS28-CD8-STOP is a construct that expresses the CD8 ectodomain and transmembrane domain. A stop codon is located at the end of the CD8 transmembrane domain so that the CD8 ectodomain and transmembrane domain are expressed but not lentiviral EnvCTs (Groppelli et al., 2014).

CMS28-CD8-EnvCT are a set of constructs that express the EnvCT of different lentiviruses (HIV-1 NL4.3, HIV-1 Rbf, HIV-2 ROD10, SIVsmm, SIVpbj, SIVtan) fused to the CD8 ectodomain and transmembrane domain (Groppelli et al., 2014).

Thymidine kinase renilla is a reporter construct containing a promoter that is constitutively active and expresses renilla luciferase. This construct was obtained from Greg Towers (University College London, UK).

IgK NFκB luciferase is a reporter construct under control of the natural promoter of the immunoglobulin kappa light chain (IgK) gene, used to measure NFkB activation, as it is sensitive to NFκB subunits p50 and p65 and contains three repeat kB sequences. Activation of this reporter leads to the expression of firefly luciferase. This construct was obtained from Greg Towers (University College London, UK).

NFκB luciferase is a reporter construct containing a promoter that is specifically activated by the canonical NFkB subunits (Promega). Activation of this reporter leads to the expression of firefly luciferase.

AP-1 luciferase is a reporter construct that contains a promoter that is activated upon binding of AP-1 subunits. Activation of this reporter leads to the expression of firefly luciferase. This construct was obtained from Greg Towers (University College London, UK).

IFNβ luciferase is a reporter construct that contains a promoter that is sensitive to IFNβ secretion. Activation of this reporter leads to the expression of firefly luciferase. This construct was obtained from Greg Towers (University College London, UK).

ISG56 luciferase is a reporter construct that contains a promoter that is sensitive to ISG56 expression. Activation of this reporter leads to the expression of firefly luciferase. This construct was obtained from Greg Towers (University College London, UK).

pcRVI Vpu expresses HA-tagged HIV-1 Vpu in the CMS28 backbone construct (Pickering et al., 2014). Obtained from Stuart Neil (Kings College London, UK).

pCMV-BlaM-Vpr vector expresses BlaM-Vpr which is incorporated into newly formed virus particles upon transfection (Invitrogen, Carlsbad, CA).

pAdVAntage is a vector which is cotransfected with the pCMV-BlaM-Vpr construct to increase protein expression by increasing translation initiation (Invitrogen, Carlsbad, CA).

2.4 Plasmid preparation

Proviral plasmids were produced in *E. coli* JM109 competent cells (>10^8cfu/µg, Promega). JM109 cells (20 µl) were incubated with 100 ng of plasmid DNA on ice for 30 min. The bacteria were transformed by heat-shock at 42°C for 45 s and then incubated on ice for 5 min. Bacteria were then plated on Luria Bertani (LB) agar plates containing 100 µg/ml ampicillin and incubated overnight (16 h). The next day, 3 ml starter culture of LB broth (containing 100 µg/ml ampicillin) was inoculated with a single colony from the overnight plate and incubated at 30°C with shaking for 8 h. The starter culture was transferred (1:1000 dilution) into 200 ml LB (with ampicillin) and incubated at 30°C with shaking overnight (16 h). Cultures were then centrifuged at 6000 x g for 20min at 4°C to pellet the bacteria. To produce all other plasmids, overnight shaking cultures were incubated at 37°C. Plasmid DNA was extracted using Qiagen Plasmid Maxiprep kit according to manufacturer's instructions. Purified plasmid DNA was resuspended in 300 µl nuclease- free water. DNA concentration was measured using the NanoDrop 2000 Spectrophotometer (Thermo Fisher) according to the manufacturer's instructions.

2.5 Site Directed Mutagenesis

The following primers were designed to make viruses with truncated envelope cytoplasmic tails using the QuikChange Primer Design tool (Agilent). A stop codon was added in the centre of the primers.

HIV-1 NL4.3 (P722stop) and NL4.3 ΔCTΔNef mutant
Forward: 5'-tgtcgggtcccctctagattgggaggtggg-3'
Reverse: 5'-cccacctcccaatctagaggggacccgaca-3'

HIV-2 ROD10 (stop719Q)
Forward: 5'-cccggttatatccaacagatccatatccag-3'
Reverse: 5'-gtggatatggatctgttggatataaccggg-3'

HIV-2 ST and HIV-2 7312A (Q713stop)
Forward: 5'-cccccccgcttacttctaacagatccatatccac-3'
Reverse: 5'-gtggatatggatctgttagaagtaagcgggggggg-3'

All reactions were performed using the QuikChange Lightning Site-Directed Mutagenesis Kit (Agilent) using the following reaction set up:

	Vol (μL)
10x reaction buffer	5
dsDNA template (10ng/ul)	5
Forward primer (125ng)	1.25
Reverse primer (125ng)	1.25
dNTP mix (1mM)	1
QuikSolution reagent	1.5
ddH2O	35
TOTAL VOLUME	50

PCR conditions for these reactions are summarised below:

Segment	**Cycles**	**Temperature**	**Time**
1	1	95	2 mins
2 (x12 cycles)	18	95	20 sec
		60	10 sec
		68	30 sec/kb plasmid length
3	1	68	5 mins

Following the PCR reaction, products were incubated with 1uL DpnI enzyme to digest methylated/hemi-methylated parental DNA, for 1 hour at 37°C. DNA was then ethanol precipitated and re-suspended in 5μl H_2O. The DNA was transformed into XL-10 ultracompetent cells (Agilent), as directed by the QuikChange Lightning Site-Directed Mutagenesis Kit (Agilent). XL-10 clones were cultured, and the DNA was purified by Miniprep (Qiagen). DNA carrying the desired mutation was confirmed by sequencing (Eurofins genomics).

2.6 Virus production, release and infectivity

2.6.1 Virus Production

$5.5x10^6$ HEK293T/17 cells were plated in T-75 flasks overnight to reach 70-80% confluency. On the following day, cells were transfected with 4µg full length viral plasmid. Alternatively, to generate VSV-G pseudotyped infectious virus, cells were transfected with 4µg full length viral plasmid and 4 µg pMDG using 15 µl FuGENE 6 (Promega) and 500 µl Opti-MEM (Promega). Media was replaced 24 hours post-transfection. Supernatants were harvested at 48- and 72-hours post-transfection, centrifuged for 10 mins at 2000*g* and filtered through a 0.45 µm filter and then aliquoted and stored in liquid nitrogen.

2.6.2 Virus release

Virus-containing cell culture supernatants were harvested and centrifuged to remove cell debris at 2000*g* for 10 mins. Then, supernatants were filtered through a 0.45 µm filter, aliquoted and then stored in -80°C. Virus budding was quantified by reverse transcriptase activity using the SG-PERT RT-qPCR assay (Pizzato et. al., 2009). Virus was thawed and lysed using 2x lysis buffer and then the reaction was set up as below. Recombinant HIV RT (Applied Biosystems) was used to create standards for quantitation. A 7900HT Real-Time PCR machine (Applied Biosystems) was used to run the programme shown in **Table 2.1**.

Table 2.1: SG-PERT PCR cycling programme.

Step	Temperature (°C)	Time	No. of cycles
Reverse transcription	42	20 mins	1
Taq initial heat inactivation	95	15 mins	
Denaturation	95	10 sec	40
Annealing	60	30 sec	
Extension	72	15 sec	

SG-PERT measurements were converted into mU/mL of RT activity.

2.6.3 Virus infectivity

Infectivity of viruses was measured by infecting the HeLa TZM-BL reporter cell line, which contains a firefly luciferase reporter gene. Expression of luciferase is under the control of a Tat inducible promoter. HIV infection and expression of viral Tat protein drives expression of the luciferase reporter gene. This is proportional to the amount of HIV-1 infection. For infectivity assays, HeLa TZM-BL cells were seeded in 96-well plates at a concentration of $1x10^5$ cells/ml in 100uL per well for 24 h. After 24 h, 4-fold serial dilutions of virus stock were prepared in culture media and immediately added to seeded cells. Infected cells were incubated at 37°C for 48 h. After 48 h, all the supernatant was removed from each well and cells were lysed with 50 µL 1x lysis buffer (Promega). After 5 mins, 50 µL diluted BrightGlo solution (Promega) was added to each well and incubated for 2 mins before taking luciferase readings. Luciferase activity was measured using the Pherastar or GloMax (Promega) luminometer. TCID50 values were calculated using an Excel macro (available at http://www.hiv.lanl.gov/content/nab-reference-strains/html/TCID501.xls). Where necessary, the infectivity from the HeLa TZM-BL assay was normalised to viral budding from the SG-PERT assay by dividing the RLU units (per mL) by the SG-PERT units (mU/mL). This produced an infectivity ratio expressed as RLU/RT throughout the thesis, as a proxy to measure the infectivity of each virus particle.

2.7 H9 spreading infection

H9 cells were seeded in 12-well plates at a concentration of $1x10^6$ cells/mL and infected with VSV-G pseudotyped viruses at an initial dose of 10 mU of RT per $1x10^6$ cells. Individual wells were seeded for each time point per virus. Supernatants were collected at 1-, 2-, 4-, 7- and 9-days post infection. Cells were pelleted by centrifugation at 500 x g for 5 mins and lysed in RIPA buffer for immunoblot analysis. Virus containing supernatant was used for SG-PERT analysis to measure viral release. Virus containing supernatants were centrifuged at 500 x g to remove cell debris. Virions were further purified and concentrated by placing on top a 20% sucrose cushion and centrifuged for 1.5 h at 500 x g. After centrifugation, sucrose was removed and viral pellets were resuspended in culture medium and frozen in -80°C until SG-PERT analysis.

2.8 Immunoblot analysis

Cells were centrifuged for 5 mins at 1200 x g and washed in ice cold PBS before transferring to clean Eppendorf tubes. Cells were lysed in 100µL RIPA buffer (50mM Tris pH 8, 150mM NaCl, 1% (v/v) NP-40, 0.5% (w/v) deoxycholate, 0.1% (w/v) SDS (Sigma), 1mM phenylmethylsulphonyl fluoride (PMSF)) and kept on ice for 10mins until lysates

were clear. Lysates were centrifuged at 6000 x g for 10mins. Supernatants were transferred to clean Eppendorf tubes and 2X Laemmli sample buffer (50mM Tris-HCl pH 6.8, 2% (w/v) SDS, 10% (v/v) glycerol, 0.1% (w/v) bromophenol blue, 100mM 2-mercaptoethanol) was added before storing samples at -20°C. To prepare viruses for western blot analysis, supernatant was spun through a 25% sucrose cushion at 6000 x g for 90mins. After the spin, liquid was removed from the tubes and virus pellets were resuspended in 2X Laemmli sample buffer (50 mM Tris-HCl pH 6.8, 2% (w/v) SDS, 10% (v/v) glycerol, 0.1% (w/v) bromophenol blue, 100 mM β-mercaptoethanol) before storing at -20°C. To blot for SERINC proteins, cell lysates and viral pellets were resuspended in sample buffer containing 50mM TCEP (rather than β-mercaptoethanol).

For Sodium dodecyl sulphate – polyacrylamide gel electrophoresis (SDS-PAGE) analysis cell lysates and virus samples were heated at 100°C for 5 min. SERINC containing lysates and viruses were heated at 37°C for 1h to avoid protein aggregation. Samples were loaded on an appropriate polyacrylamide gel and proteins were separated by electrophoresis at 100V in NuPage MOPS SDS running buffer (Thermoscientific).

For immunoblotting, the proteins were transferred to a Hybond nitrocellulose membrane (Amersham biosciences) in transfer buffer (25 mM Tris- HCl, 250 mM glycine, 20% [v/v] methanol), using a wet transfer system. After protein transfer, membranes were blocked for non-specific protein binding in 5% (w/v) milk protein solution (Sigma) in 0.01% (v/v) Tween-20 in PBS (PBST) for 1 h. The membranes were then incubated at 4°C with primary antibody diluted in PBST milk for 1 h. Membranes were then washed 3 times in PBST and then incubated with secondary antibody containing a near-infrared fluorescent dye (LI-COR Biosciences) diluted in PBST milk for 30 mins at room temperature. The membranes were washed 3 times in PBST and finally in PBS before imaging using the Odyssey infrared imager (LI-COR Biosciences). Antibodies used are summarised in **Table 2.2**.

Table 2.2 Antibodies used for immunoblotting.

Target	Antibody clone	Fluorophore	Supplier	Stock Conc	Dilution
Env gp120	Rabbit antisera ARP3051	Unconjugated	CFAR		1:1000
Env gp41	Human mAb 246-D	Unconjugated	CFAR		1:500
HIV-2 Env gp105	Rabbit ARP418	Unconjugated	CFAR		1:1000
Gag	Mouse mAb 183-H12-5C	Unconjugated	CFAR	1.44mg/ml	1:3000
Anti-Tubulin	Mouse mAb DM1A	Unconjugated	Sigma	1mg/ml	1:1000
Anti-HA	Mouse 16B12	PE	Biolegend	0.2mg/ml	1:2000
Anti-CD8	Mouse mAb UCHT-4	Unconjugated	Sigma	1mg/ml	1:1000
Rabbit IgG	ab216773	IRDye 800CW	Licor	1mg/ml	1:10,000
Mouse IgG	ab216772	IRDye 800CW	Licor	1mg/ml	1:10,000
Human IgG	925-68078	IRDye 680RD	Licor	1mg/ml	1:10,000

2.9 Immunofluorescence analysis

For Env staining, $5x10^4$ HEK293T cells were transfected for 48 h on coverslips (VWR). After 48h, cells were fixed with 4% formaldehyde 1% BSA in PBS (1 ml/well) for 45 min at 4°C and washed thrice with 1 ml of 1% bovine serum albumin (BSA; Sigma) in PBS solution (BSA/PBS). Cells were then permeabilised for 1 h with 5% FCS 1% BSA 0.1% Triton X-100 (Sigma) and washed thrice with BSA/PBS. Samples were stained in 200 μl of BSA/PBS with anti-Env antibody for 1 h at RT and washed thrice in BSA/PBS. Primary antibodies were detected with fluorescent secondary antibodies in 200 μl BSA/PBS for 30 min at RT and washed thrice in BSA/PBS and once in water. Antibodies used are summarised in **Table 2.3**. After washing, coverslips were dried and mounted on microscope slides with ProLong Gold Antifade mounting solution without DAPI (Thermo Fisher Scientific). Images were acquired on DeltaVision Elite image restoration microscope (Applied Precision) with softWoRx 5.0 software. Image processing was performed using Huygens Professional 4.0 and Adobe Photoshop 7 software.

Table 2.3 Antibodies used for immunofluorescence microscopy.

Target	Antibody clone	Fluorophore	Supplier	Stock Concentration	Dilution
Env gp120	2G12	Unconjugated	CFAR[1]	50ug/mL	1:13000
Env gp105	ARP3083	Unconjugated	CFAR[2]	Culture fluid	1:50
Rat IgG	Polyclonal	FITC	Bethyl		1:200
Human IgG	Polyclonal	FITC	Bethyl		1:200

[1]Donated by Dr. H. Kattinger [2] Donated by Dr. A. McKnight

2.10 Flow cytometry

For detection of intracellular antigens, $5x10^5$ cells were first washed in PBS and then stained with cell viability dye Zombie UV or NIR (1:500 dilution; Biolegend) for 30 mins at RT to detect dead cells. Cells were then permeabilised with 200 μl Permeabilization Wash Buffer (Biolegend) for 20 min at RT, after which they were stained with antibodies in 50 μl of the permeabilisation buffer for 30min at 4°C, washed twice in permeabilisation buffer and resuspended in FWB before flow cytometry. Antibodies used in this thesis (and their dilution factors) are listed in **Table 2.4**.

Alternatively, for detection of FLAG-tagged SERINC5 surface expression, cells were first washed in PBS and then stained with antibody against the FLAG-tag in 50 μl PBS, for 30min at 4°C. Cell viability dye Zombie UV or NIR (1:500 dilution; Biolegend) was included in all stains to detect dead cells. Next, cells were washed in FACS wash buffer (FWB; 1% FCS and 0.1% sodium azide in PBS) and fixed in 100 μl of 4% methanol-free formaldehyde (Thermo Fisher) for 30min at 4°C. Cells were then washed and resuspended in FWB and analysed by flow cytometry.

Flow cytometry analysis was performed using LSR Fortessa X-20 cytometer (Becton Dickinson, BD) or the BD FACSCalibur Becton Dickinson, BD). Compensation was performed using single stained cells. Compensation was calculated by FACSDiva software (BD). Data was analysed using FlowJo V10 software (BD).

Table 2.4 Antibodies used for flow cytometry.

Target	Antibody clone	Fluorophore	Supplier	Stock Concentration	Dilution
FLAG-tag	L5	PE/Cy7	Biolegend	0.2mg/ml	1:150
Gag-p24	KC57-RD1	PE	Beckman Coulter		1:200
HA-tag	16B12	PE	Biolegend	0.2mg/ml	1:200

2.11 Buffers and solutions

Phosphate-buffered saline (PBS) (Gibco)

Luria Bertani (LB) medium (made in-house). A solution of LB powder (Sigma Aldrich) dissolved in distilled water (20g/L) and then autoclaved at 121°C for 15 mins to sterilise. Used for the growth of liquid cultures of E. coli.

LB agar (made in-house). LB agar powder (40g/L) (Sigma Aldrich) was melted into water using a microwave and then autoclaved at 121°C for 15 mins to sterilise. This was used to make LB agar ampicillin plates for the growth of E. coli.

Ampicillin sodium salt (Sigma Aldrich) solution. A stock solution of ampicillin salt was made in water at 100mg/ml, filter sterilised and stored in aliquots at -20°C. This was used at a final concentration of 100μg/ml in LB broth or LB agar as an antimicrobial and selection agent.

Tris-acetate-EDTA (made in-house). To make a 10X buffer, 48.5g of Trizma base (Sigma Aldrich) was dissolved in 800ml distilled water, 11.4ml glacial acetic acid and

20ml 0.5M EDTA at pH 8.0 were added and solution made up to 1L with distilled water. A 1X working solution was made by diluting 100ml 10X buffer with 900ml distilled water.

PBS-Tween 0.1% (PBST) (made in-house). Used for western blot washes. 100ml 10x DPBS, 900ml distilled water and 1ml Tween-20 (Sigma Aldrich).

Radioimmunoprecipitation assay (RIPA) buffer (made in-house). This buffer was used to lyse cells before running the lysates by SDS-PAGE and western blotting to detect protein. A 5X buffer was composed as follows: 750mM NaCl; 5% NP-40 detergent; 2.5% Deoxycholate (DOC); 0.5% SDS; 250mM Tris pH 8. A 1X buffer was made on the day of use by diluting 5X buffer in distilled water (final concentration = 1X) and adding Phenylmethylsulphonyl fluoride (PMSF, stock solution is 100mM in isopropanol, final concentration = 1mM) and protease (Protease inhibitor cocktail tablets, Roche) and phosphatase (PhosSTOP tablets, Roche) inhibitors.

5X SDS sample buffer for SDS-PAGE (made in-house). Containing: 1.5 M Tris- HCl pH 6.8, 4ml; Glycerol, 10ml; β-mercaptoethanol, 5ml; SDS, 2g; 1% bromophenol blue, 1ml. Used for denaturing cell lysates for SDS-PAGE.

Tris-glycine running buffer (made in-house). 3g of Trizma base and 14.4g of glycine were dissolved in 990ml distilled water and 10ml of a 10% SDS solution was added. This running buffer was used to run SDS-PAGE gels poured in-house.

NuPAGE® MOPS SDS Running Buffer (20X) (Novex). A running buffer system for Bis-Tris based pre-cast gels. Diluted 1/20 with distilled water to get a working solution.

Methanol transfer buffer (made in-house). 3g of Trizma base and 14.4g of glycine were dissolved in 800ml distilled water and 200ml methanol added. This buffer was used to transfer proteins from SDS-PAGE gels to nitrocellulose.

Flow cytometry buffer (made in-house). Dulbecco's Phosphate-Buffered Saline (DPBS) containing 5% foetal bovine serum (FBS) as a blocking agent and 0.05% sodium azide to prevent bacterial growth. Used as a wash buffer when preparing cells for flow cytometry analysis.

Fixing buffer (made in-house). This is a solution of 4% paraformaldehyde (Sigma Aldrich) diluted in either flow cytometry wash buffer (if cells are to be analysed by flow cytometry analysis) or in 1% bovine serum albumin (BSA)/PBS (if cells are to be

analysed by immunofluorescence (IF) microscopy). This buffer reacts with primary amines on proteins and nucleic acids to form partially-reversible methylene bridges.

Perm/wash buffer (BD Biosciences). A buffer used to permeabilise cells before staining for intracellular components and analysing by flow cytometry.

Immunofluorescence Perm buffer (made in-house). A buffer composed of 0.1% Triton-X100 detergent (Sigma Aldrich) diluted in 1% bovine serum albumin (BSA) in DPBS. Used to permabilise cells before staining for intracellular components and analysing by immunofluorescence microscopy (IF).

Immunofluorescence wash buffer (made in-house). 1% BSA in PBS. Used to wash cells whilst staining for IF microscopy.

2.12 Restriction factor assays

2.12.1 Tetherin

293T/17 cells were seeded in 6-well plates ($8x10^5$cells/well in 1.5 ml culture medium). After 24 h cells were transfected with 600 ng proviral DNA, 0-200 ng Tetherin DNA and empty pcDNA vector to equalize DNA content using 6 ul Fugene 6 and 200 ul Opti-MEM medium (Gibco). Transfected cells and virus containing supernatants were collected at 48h post-transfection (Gibco). Cells were washed in PBS and lysed for immunoblot analysis and supernatants were ultracentrifuged for 10 mins at 1200 x g to remove cell debris, filtered through a 0.45 μm filter and then frozen in -80°C. Virus release in the supernatant was measured using the SG-PERT assay.

2.12.2 SERINC3/5

293T/17 cells were seeded in 6-well plates ($8x10^5$cells/well in 1.5 ml culture medium). After 24 h cells were transfected with 600 ng proviral DNA, 0-200 ng SERINC DNA and empty pcDNA vector to equalize DNA content using 6 μl Fugene 6 and 200 μl Opti-MEM medium. Transfected cells and virus containing supernatants were collected at 48h post-transfection. Cells were washed in PBS and lysed for immunoblot analysis and supernatants were ultracentrifuged for 10 mins at 1200 x g to remove cell debris, filtered through 0.45 μm filter and then frozen in -80°C. Virion infectivity was measured using the SG-PERT and HeLa TZM-bl reporter assays. Single particle infectivity was calculated by dividing the RLU/mL values from the HeLa TZM-bl assay by the SG-PERT units (mU/mL). Single particle infectivity is expressed as RLU/RT throughout this thesis. 1 mL supernatant was lysed for immunoblot analysis, as described in **section 2.8**.

2.12.3 IFITM

U87-MG $CD4^+$ $CXCR4^+$, U-87 $CD4^+$ $CCR5^+$ and HeLa TZM-bl cells overexpressing IFITM1, IFITM2 and IFITM3 were produced by lentiviral transduction as previously described (Foster et al., 2016; Qian et al., 2015). IFITM proteins were HA-tagged and overexpression was confirmed using flow cytometry or immunoblot analysis using the HA tag.

For infectivity studies, $4x10^5$ U87 or HeLa cells were plated in a 48-well plate and infected with equivalent RT units of indicated viruses. Infected cells and virus containing supernatants were collected at 48h post infection. Virion infectivity was measured using the SG-PERT and HeLa TZM-BL reporter assays, as described in section 2.4.3. Cells were also analysed by flow cytometry to calculate the percentage of infected cells.

2.13 **BlaM-Vpr assay**

BlaM-Vpr containing viruses were produced by co-transfecting HEK293T cells with full length proviral constructs and plasmid encoding BlaM-Vpr. The BlaM-Vpr assay was performed using the Invitrogen kit (K1085). $2.5x10^5$ HeLa TZM-BL cells per well were plated in 48-well plates. 24h later the cells were infected with indicated BlaM-Vpr viruses by spinoculation for 2h at 5000 x g. The fusion inhibitor T20 (CFAR) control wells were incubated with the 10nM drug for 10 mins before infection and during spinoculation. Immediately after spinoculation cells were incubated at 37°C for 2h. Following the incubation, cells were washed with CO_2-independent media and incubated with 1x loading solution at room temperature in the dark. Then, cells were washed twice with development media and incubated in development media at room temperature, in the dark for 16h. After this final incubation, cells were harvested using warm EDTA solution, stained with the UV live-dead FACS stain (Biolegend) and fixed for flow cytometry analysis using 4% PFA for 15mins. Cells were washed in PBS and stained for flow cytometry analysis.

2.14 **Coimmunoprecipitation**

To investigate the interaction of SERINC5 and Env WT and ΔCT, 5 x 10^6 293T/17 cells were co-transfected with 4 ug pNL4.3 (ΔEnv, WT or ΔCT) and 1ug pcDNA-flag-SERINC5-HA using Fusion 6 transfection reagent (Promega). 48 h post transfection, culture media was removed, and cells were washed once in PBS and lysed in ice cold Pierce IP lysis buffer (Thermo scientific). The soluble fraction was recovered and incubated with anti-FLAG M2 magnetic beads (Sigma) overnight at 4°C to pulldown flag-

SERINC5-HA. FLAG beads were magnetically separated from the lysate and washed four times with ice cold IP buffer. Flag-SERINC5-HA was eluted from FLAG beads using 50uL of 3x-FLAG peptide (Sigma) in IP buffer (500µg/ml) for 30mins rotating at 4°C. The input cell lysate and eluted samples were prepared for immunoblot analysis as described above. Flag-SERINC5-HA was detected using anti-HA.11 epitope tag-PE (16B12, Biolegend) and Env detected by anti-HIV-1 gp120 rabbit antisera.

2.15 **Neutralisation assays**

Virus stocks were titrated on HeLa TZM-BL cells as mentioned above (section 2.4.3). The lowest viral dose which gives luciferase readings that are 50 times higher than background are selected for the neutralisation assays.

For neutralisation assays, HeLa TZM-BL cells were plated at a concentration of $1x10^5$ cells/mL in a 96-well plate overnight. Virus stocks were thawed, and a fixed viral dose (determined above) was incubated with titrations of different HIV-1 neutralising antibodies or T20 fusion inhibitor in a 96-well plate for 1h at 37°C. After the incubation period, media from the HeLa TZM-BL cells was removed and replaced with the virus-antibody/inhibitor mix for 48h at 37°C. After 48h all media from TZM-bl cells was removed and 50 µL BrightGlo solution (Promega) was added to cells. Luciferase activity was measured using the Pherastar luminometer.

Neutralisation was calculated as percent decrease in luciferase activity compared with the corresponding virus only control. The half maximal inhibitory concentration (IC50) values were calculated by non-linear regression analysis (sigmoid curve interpolation) using Prism software (GraphPad).

Table 2.5 Antibodies used for neutralisation assays.

Antibody	**Source**
PGT151	Gift from Laura McCoy (UCL)
VRC01	Gift from Laura McCoy (UCL)
17b	NIH Centre for AIDS Reagents
10E8	NIH Centre for AIDS Reagents
4E10	NIH Centre for AIDS Reagents
2F5	NIH Centre for AIDS Reagents

2.16 **Kinetics of viral entry**

HeLa TZM-bl cells were plated at a concentration of $1x10^5$ cell/well in a 96-well plate for 24h prior to infection. Equal RT units of virus were added to cells and 20 μg/ml T20 inhibitor was added at 0, 1, 2, 4, 6 and 24 hours post-addition of virus. Viral infection was quantified after 48h by measuring luciferase activity. To analyse the data, the percentage viral entry was determined by normalising infectivity at each time point to the untreated (no T20) control from three independent experiments.

2.17 **Thermostability assay**

HeLa TZM-bl cells were plated in a 96-well plate 24 h prior to infection. At indicated time points, viruses were thawed and incubated at 37°C for different durations. After 6 hours, freshly thawed virus was used to infect cells (Time point 0 h) and previously incubated virus were also used to infect cells. Cells were lysed after 48h in BrightGlo (Promega) and luciferase measurements were taken using the Glomax (Promega).

2.18 **Dual Glo luciferase assay**

Reporter gene constructs encode firefly luciferase, which is expressed downstream of various stimuli, as described in **section 2.3**. HEK293T/JL cells were plated at a concentration of $2x10^4$ cells/well in a 48-well plate. After 24h, cells were transfected with different doses (0-200ng) of CD8-EnvCT fusion plasmid or pcDNA-gp160 plasmid, indicated reporter gene (5ng/well), and pcDNA3.1 to balance the total DNA transfected per well, along with 2.5ng/well TK Renilla luciferase plasmid. Luciferase activity was measured after 48h using the Dual-Luciferase reporter assay system (Promega). Firefly Luciferase and TK remilla luciferase readings were measured using the GloMax Luminometer (Promega). Relative luciferase activity was calculated by dividing the firefly luciferase values by the Renilla luciferase values (FF/TK). Then, fold change over 'pcDNA only' control was calculated by dividing the FF/TK values for each dose of CD8-EnvCT and CD8-STOP expression by the pcDNA FF/TK. Finally, fold change over CD8-STOP was measured. Three independent transfection experiments were performed in triplicates. In indicated experiments, TNF-α (Peprotech) was added to cells as a positive control for NFκB activation at a dose of 10 ng/mL for 6 h prior to cell lysis. For drug inhibitor assays, cells were incubated with the NFκB inhibitors TPCA1 (Sigma) and NBP2 (Novus Biotech), for 30 mins prior to transfection. In relevant experiments, Vpu plasmid was cotransfected with reporter plasmids and CD8-constructs.

2.19 **Statistical analysis**

Statistical significance was calculated using paired or unpaired Student's *t* test, since the data are normally distributed. For multiple comparisons, 2-way analysis of variance (ANOVA) with Sidak's multiple comparisons test was performed. Statistical significance was assumed when $p<0.05$. All statistical analyses were calculated using Prism 6 software (GraphPad).

3 Role of the HIV EnvCT in lentiviral replication

3.1 Introduction

The HIV-1 Env cytoplasmic tail (EnvCT) is crucial for Env trafficking to sites of virus assembly at the plasma membrane and for Env incorporation into virions (Akari et al., 2000; Murakami and Freed, 2000). Although an intact EnvCT is essential for efficient HIV-1 replication in CD4 T cells, previous studies have reported that HIV-2 and several SIVs truncate their cytoplasmic tail when passaged in human T cell lines and PBMCs (Albert et al., 1987; Chakrabarti et al., 1987; Evans et al., 1988; Franchini et al., 1989; Hirsch et al., 1987; Hirsch et al., 1989a; Hirsch et al., 1989b; Kong et al., 1988; Kumar et al., 1990; Mulligan et al., 1992; Naidu et al., 1988; Ohta et al., 1988; Tsujimoto et al., 1988). In the case of SIV_{mac239}, truncation of the EnvCT results in a replicative advantage in human cells (Kodama et al., 1989). Specifically, Kodama et al used human and Rhesus macaque peripheral blood lymphocytes (PBL) transfected with a proviral construct encoding SIV_{mac239} with a full length EnvCT (Kodama et al., 1989). In Rhesus macaque PBLs, the virus replicated and spread during 80 days of serial passage, with no ΔCT variants arising (Kodama et al., 1989). However, in human PBLs wild type SIV_{mac239} with a full length EnvCT displayed delayed replication until passage 3, which coincided with the emergence of ΔCT variants in the supernatant (Kodama et al., 1989), suggesting that EnvCT truncation is selected for *in vitro*. Further, when a Rhesus macaque was inoculated with SIVmac239 ΔCT virus and virus recovered from CD4 T cells and sequenced at 58 weeks post inoculation, the virus was exclusively SIVmac239 with a full length EnvCT (Kodama et al., 1989), suggesting this ΔCT virus reverted and thus that a full length SIV EnvCT is required for viral replication *in vivo*. To my knowledge, only one previous study has compared replication of HIV-2 FL and ΔCT side by side (Hoxie et al., 1991), no other direct comparison of HIV-2 replication with a full length and truncated EnvCT has been measured *in vitro*, thus it is unclear whether EnvCT truncation provides a replicative advantage for HIV-2 in vitro, like it does for SIV. Nonetheless, it has been observed that HIV-2 viruses with a truncated EnvCT can replicate in various T cell lines and primary CD4 T cells (Evans et al., 1988; Kong et al., 1988; Kumar et al., 1990). The long length of the lentiviral EnvCT is considered unique and unusual given that other retroviruses have a shorter EnvCT which ranges from approximately 10-60 amino acids in length (reviewed by (Postler and Desrosiers, 2013)). This suggests that the presence of a long EnvCT is important in viral replication *in vivo*, otherwise we might expect that viruses would evolve to lose this feature over time. However, a caveat to this is that HIV-2 EnvCT truncation predominantly arises during repeated passage in cell culture (Franchini et al., 1989; Kong et al., 1988; Kumar et al., 1990; Mulligan et al., 1992), therefore it is difficult to speculate the effect of EnvCT truncation *in vivo*. In light

of these observations, important questions arise regarding the presence of a long lentiviral EnvCT: Why do lentiviruses have a long EnvCT? Do HIV-1 and HIV-2 viruses have the same requirements for a long EnvCT? In this chapter, I will directly compare the requirement of a long EnvCT in HIV-1 and HIV-2 during viral replication *in vitro*.

3.2 Results

3.2.1 Single round infectivity of FL and ΔCT viruses produced in 293T cells.

In order to investigate the role of the EnvCT in lentiviral replication, it was first necessary to create a panel of lentiviruses with a full length EnvCT and an EnvCT deleted counterpart, referred to hereon as ΔCT viruses. Figure 3.1 shows an alignment of HIV-1 and HIV-2 EnvCT sequences and suggests that the EnvCT sequence is largely conserved, with the exception of some insertions and/or deletions in HIV-2 sequences. Site-directed mutagenesis was used to replace an amino acid with a stop codon downstream of the highly conserved YxxΦ endocytic motif to produce lentiviruses with a deleted EnvCT (ΔCT) (Table 3.1). The position of the stop codons which were inserted in the lentiviral EnvCTs for this study correspond to the position at which several SIVs have been reported to insert stop codons during cell culture (Johnston et al., 1993; Zingler and Littman, 1993). The HIV-2_{ROD10} infectious molecular clone has a pre-existing stop codon within the EnvCT and therefore this stop codon was reverted to create HIV-2_{ROD10} with a full length EnvCT (referred to as FL virus). Characterisation and exploration of the HIV-2_{ROD10} EnvCT will be discussed exclusively from **section 3.2.6**, as I have discovered that this clone does not behave in a similar way to other HIV-2 primary isolates, such as HIV-2_{ST} and HIV-2_{7312A}.

```
HIV-1_NL4.3      --NRVRQGYSPLSF-------QTHLPIPRGPDRPEGIEEEGGERDRDRSIRLVNGSLALI   51
HIV-2_ROD10      MLSRLRKGYRPVFSSPPGYI*QIHIHKDRGQPANEETEEDGGSNGGDRYWPWPIAYIHFL   59
HIV-2_ST         MLSRLRKGYRPVFSSPPAYFQQIHIHKDREQPAREETEEDVGNSVGDNWWPWPIRYIHFL   60
HIV-2_7312A      MIGRLRRGYRPVFSSPPAYFQQIHIHKDREQPAREETEEDVGNSVGDNWWPWPIRYIHFL   60
                   .*:*:** *:         * *:   *     *  **: *.   *.        : ::

HIV-1_NL4.3      WDDLRSLCLFSYHRLRDLLLIVTRI---VELLGRRGWEALKYWWNL----LQY---WSQE   101
HIV-2_ROD10      IRQLIRLLTRLYSICRDLLSRSFLTLQLIYQN-------LRDWLRLRTAFLQYGCEWIQE   112
HIV-2_ST         IRQLIRLLNRLYNICRDLLSRSFQTLQLISQSLRRALTAVRDWLRFNTAYLQYGGEWIQE   120
HIV-2_7312A      IRQLIRLLNRLYNICRDLLSRSFQTLQLISQSLRRALTAVRDWLRFNTAYLQYGGEWIQE   120
                   :*  *    *   ****         :          :: * .:    ***   * **

HIV-1_NL4.3      LKNSAVNLLNATAIAVAEGTDRVIEVLQAAYRAIRHIPRRIRQGLERILL     151
HIV-2_ROD10      AFQA---AARATRETLAGACRGLWRVLERIGRGILAVPRRIRQGAEIALL     159
HIV-2_ST         AFRA---FARATGETLTNAWRGFWGTLGQIGRGILAVPRRIRQGAEIALL     167
HIV-2_7312A      AFRA---FARATGETLTNAWRGFWGTLGQIGRGILAVPRRIRQGAEIALL     167
                   .:     .**  ::: .   .  .*    *.*  :******* *  **
```

Figure 3.1 EnvCT sequence alignments. HIV-1 NL4.3 and multiple HIV-2 EnvCT sequences were aligned using the Clustal Omega software (EMBL-EBI).

Table 3.1 Mutated HIV-1 and HIV-2 envelope cytoplasmic tail sequences. Amino acids were replaced with a stop codon in HIV-1 NL4.3, HIV-2 ST and HIV-2 7312A sequences. In HIV-2 ROD10, a premature stop codon at position 719 was replaced with a glutamine residue (shown in bold and underlined).

Lentivirus	Mutated EnvCT sequence	
HIV-1 NL4.3	NRVRQGYSPLSFQTHLPI*RGPDRPEGIEEEGGERDRDRSIRLVNGSLALIWDDL RSLCLFSYHRLRDLLLIVTRIVELLGRRGWEALKYWWNLLQYWSQELKNSAVNL LNATAIAVAEGTDRVIEVLQAAYRAIRHIPRRIRQGLERILL	P722*
HIV-2 ST	MLSRLRKGYRPVFSSPPAYF*QIHIHKDREQPAREETEEDVGNSVGDNWWPWP IRYIHFLIRQLIRLLNRLYNICRDLLSRSFQTLQLISQSLRRALTAVRDWLRFNTAYL QYGGEWIQEAFRAFARATGETLTNAWRGFWGTLGQIGRGILAVPRRIRQGAEIA LL	Q713*
HIV-2 7312A	MIGRLRRGYRPVFSSPPAYF*QIHIHKDREQPAREETEEDVGNSVGDNWWPWPI RYIHFLIRQLIRLLNRLYNICRDLLSRSFQTLQLISQSLRRALTAVRDWLRFNTAYL QYGGEWIQEAFRAFARATGETLTNAWRGFWGTLGQIGRGILAVPRRIRQGAEIA LL	Q713*
HIV-2 ROD10	MLSRLRKGYRPVFSSPPGYIQ**Q**IHIHKDRGQPANEETEEDGGSNGGDRYWPWP IAYIHFLIRQLIRLLTRLYSICRDLLSRSFLTLQLIYQNLRDWLRLRTAFLQYGCEWI QEAFQAAARATRETLAGACRGLWRVLERIGRGILAVPRRIRQGAEIALL	*719Q

To test the single round infectivity of HIV-1 (NL4.3) compared with HIV-2 (ST and 7312A), 293T cells were transfected with plasmids encoding infectious molecular clones and 48h post transfection the virus-containing supernatants were harvested, cell debris removed by centrifugation, and virions further purified by ultracentrifugation over a 25% sucrose cushion. In order to characterise the viruses produced from 293T cells, the SG-PERT assay was used to measure viral reverse transcriptase activity in supernatants and therefore acts a surrogate for the amount of budding viral particles. The virus-containing supernatants were also titrated on to the HeLa TZM-bl reporter cell line, in which luciferase expression is under a tat-inducible promoter. Luciferase activity is arbitrarily measured using Relative Light Units (RLU). The SG-PERT results were first expressed as mU/mL of RT activity and the infectivity was determined by calculating RLU/mL. In order to determine single particle infectivity, the SG-PERT value was normalised to RLU and this infectivity ratio is referred to as the RLU/RT measurement throughout the thesis. Figure 3.2 shows that truncating the EnvCT of HIV-1 and HIV-2 viruses does not significantly impact viral budding from 293T cells (Fig. 3.2A-C), nor does it impact viral infectivity when titrated on HeLa TZM-bl reporter cells (Fig. 3.2D-F). Thus, the normalised infectivity ratios reveal that truncation of the long EnvCT is tolerated by both HIV-1 and HIV-2 in 293T cells (Fig. 3.2G-I). This is consistent with published data showing that HIV-1 ΔCT viruses that are produced in 293T cells can infect HeLa cells (Akari et al., 2000; Murakami and Freed, 2000). The ability of 293T cells to produce virus that can infect HeLa TZM-bl cells is consistent with the notion that 293T cells are permissive for EnvCT truncation, as discussed in **Chapter 1, section 1.3**.

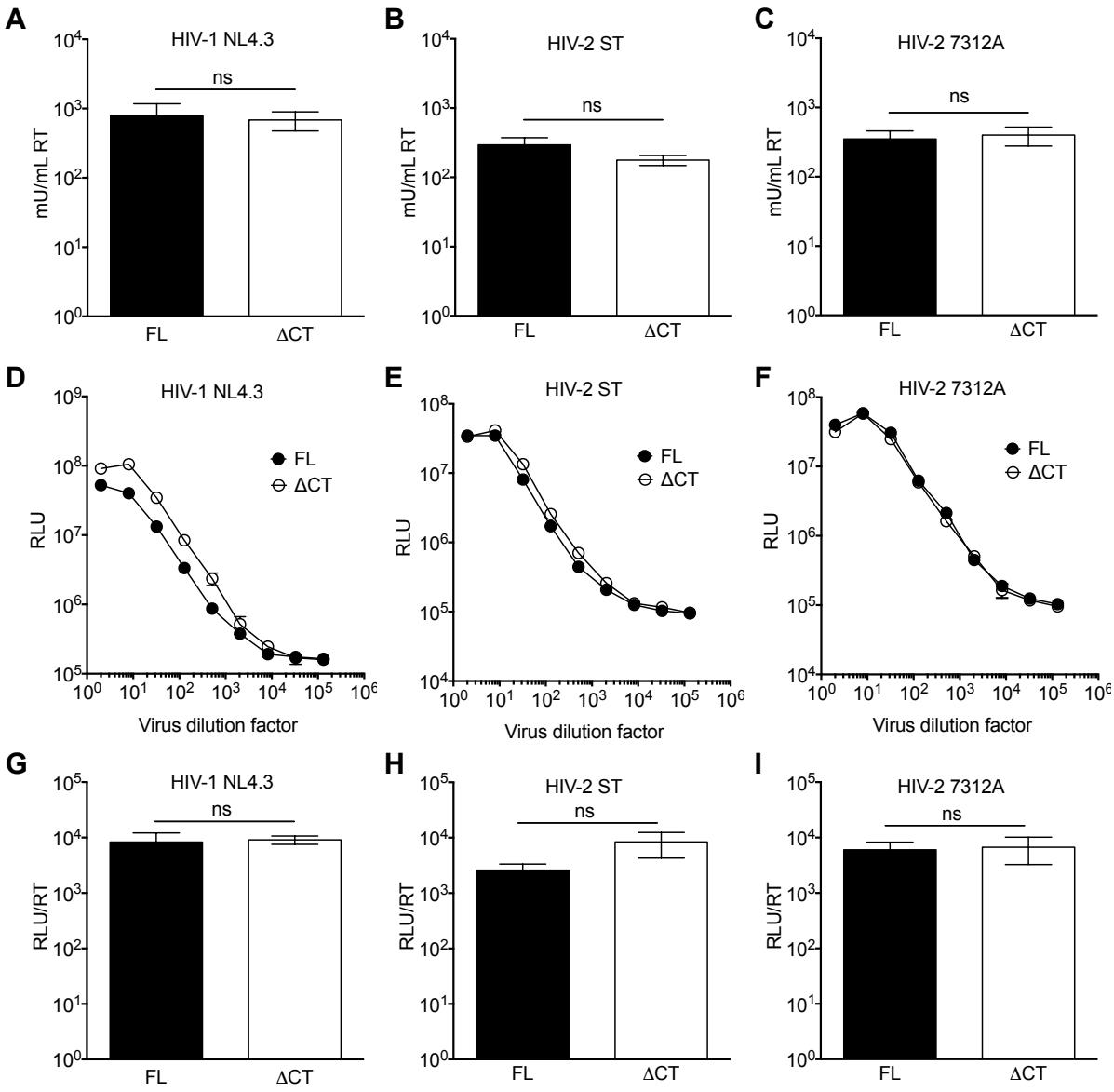

Figure 3.2 Production of lentiviruses in 293T cells and infectivity in HeLa TZM-bl cells. 293T cells were transfected with proviral constructs encoding full-length replication competent WT and ΔCT viruses. Virus containing supernatant was purified after 48h for **(A-C)** SG-PERT analysis which is used as a surrogate to measure the amount of budding particles and **(D-F)** relative light units (RLU) produced upon titration of viruses on HeLa TZM-bl reporter cell lines, as a measure of infectivity. These are representative titration curves. **(G-H)** Infectivity was normalised to the number of budding viral particles in order to determine the infectivity of single virus particles (RLU/RT). Bar charts represent data from 6 independent experiments. Bars represent mean and error bars represent mean ± SEM. Groups were compared using two-tailed unpaired *t*-test. (ns, P>0.05).

3.2.2 Env incorporation into HIV FL and ΔCT virions produced in 293T cells.

Env incorporation is required for viral infectivity. To investigate whether there are differences in Env incorporation between HIV-1 and HIV-2 viruses with a FL or ΔCT Env,

supernatant from 293T cells were purified on a 25% sucrose cushion for subsequent SDS page and immunoblot analysis. Quantification of the amount of HIV-1 Env relative to cellular p55 levels show that there is equivalent Env synthesis in 293T cells, regardless of EnvCT length (Fig. 3.3A). However, the amount of HIV-1 ΔCT Env relative to p24 in virions is significantly less by comparison with WT Env incorporation (Fig. 3.3A). By contrast, HIV-2 ST and 7312A isolates consistently show a trend towards increased ΔCT Env incorporation into virions (3.5 fold and 2 fold for ST and 7312A, respectively), despite quantification of Env normalised to cellular p55 showing equivalent amounts of ΔCT and WT Env production in cell lysates (Fig. 3.3B,C).

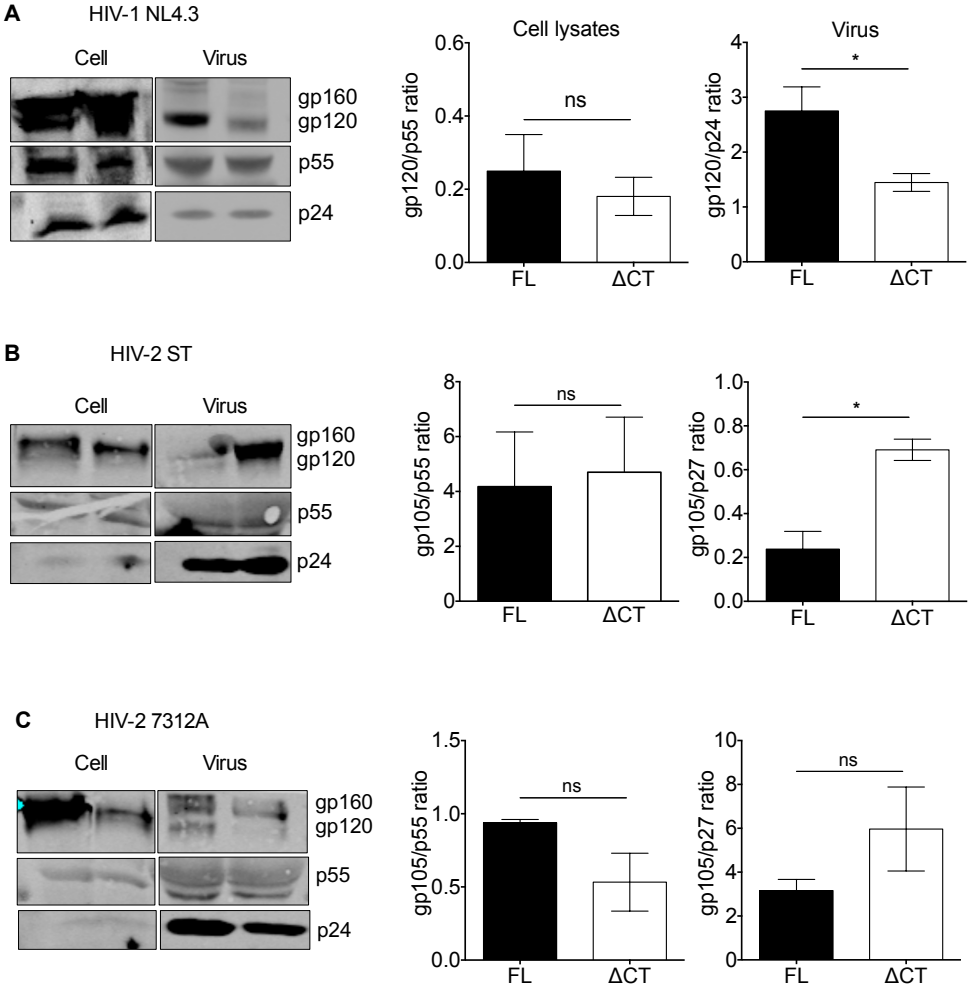

Figure 3.3 Env production and incorporation in 293T cells. (A-C) Representative immunoblots from 293T cells that were transfected with proviral constructs and 48h after transfection, cell lysates and purified virions were analysed for expression of Env (gp120 or gp105) and Gag (p55 and p24 or p27). Quantification of Env incorporation was calculated by dividing the band intensity of Env by Gag from three independent experiments. Bars represent mean and error bars represent mean ± SEM. Groups were compared using two-tailed unpaired *t*-test (ns, p>0.05; *, p<0.05).

3.2.3 Single round infectivity of FL and ΔCT viruses produced in H9 cells.

Having shown that virus made in 293T cells have no infectivity defect, I next assessed the effect of EnvCT truncation of these viruses in H9 T cells. H9 T cells were used because they express the CD4 receptor and both co-receptors, CXCR4 (X4) and CCR5 (R5) (Lazzarino et al., 2000). Usage of H9 T cells is fundamental in this study, as it allows investigation of Env biology of HIV-1 (X4-tropic) and HIV-2 (R5 tropic) viruses in the same cell type. This is important because several studies have highlighted the cell-type dependence of the long lentiviral EnvCT (Akari et al., 2000; Murakami and Freed, 2000). Thus, using H9 cells overcomes any confounding factors which could arise if different T cell lines were used for HIV-1 and HIV-2 infections. Finally, several EnvCT truncation mutants were reported to arise when passaged in H9 cells (Hirsch et al., 1989a; Jones et al., 2002; Spies et al., 1994), providing further precedence for using this cell line.

$1x10^6$ H9 cells were infected using an equal input dose of VSV-G pseudotyped FL and ΔCT virus particles (200mU/mL RT units) using gravity infection for 4h. Input virus was washed off from H9 cells after 4h and replaced with fresh media for a further 24h. Then, virus containing supernatant was harvested and purified for SG-PERT measurements. VSV-G pseudotyped virus was used to account for potential entry defects into H9 cells when the EnvCT is truncated and to normalise infection levels. As expected, Figure 3.4A shows that there is no significant difference between in HIV-1 ΔCT virus budding when compared with HIV-1 FL, indicative of equivalent infection of H9 cells using the VSV-G pseudotyped virions. Further, HIV-2 viruses also do not have a budding defect from T cells when the EnvCT is truncated (Fig. 3.4B,C). By contrast, titration of H9 viruses on to the HeLa TZM-bl reporter cell line revealed that HIV-1 ΔCT viruses were up to 5-fold less infectious by comparison with HIV-1 FL virus (Fig. 3.4D). By contrast, HIV-2 viruses with a long and short EnvCT were equally infectious (Fig. 3.4E,F).

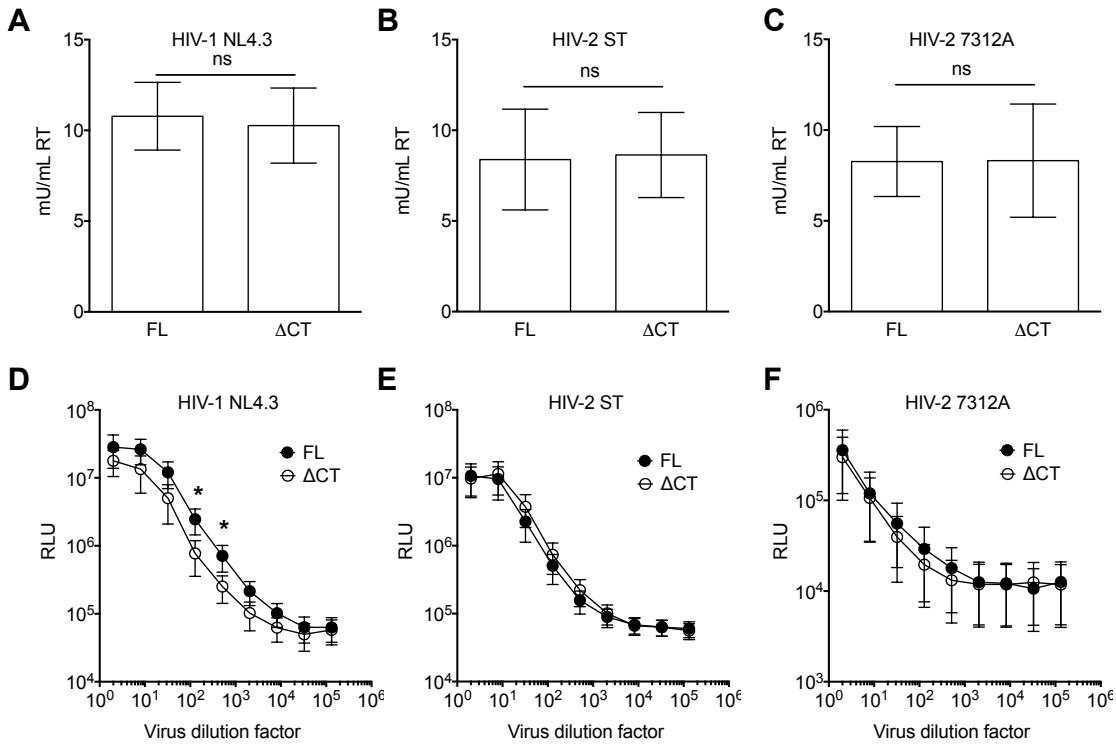

Figure 3.4 HIV-1 and HIV-2 replication in H9 T cells. H9 cells were infected with equal dose of VSV-G pseudotyped full-length replication competent viruses for 4h by gravity infection. VSV-G viruses were removed from cells after 4h and replenished with fresh media for an additional 24h. After 24h, virus containing supernatant was purified for **(A-C)** SG-PERT analysis which is used as a measure of the number of budding particles and **(D-F)** relative light units (RLU) produced upon titration of viruses on HeLa TZM-bl reporter cell lines, as a measure of infectivity from 6 independent experiments. Bars represent Mean and error bars represent mean ± SEM. Groups were compared using the two-tailed unpaired *t*-test (ns, P>0.05; *, P<0.05).

3.2.4 Spreading infection in H9 cells.

Next, I performed a spreading infection assay to test viral replication over time in H9 cells. To my knowledge, this is the first report showing a direct comparison of viral replication between HIV-2 FL and ΔCT viruses. Results from this experiment will determine whether HIV-2 EnvCT truncation confers a replicative advantage, like SIV (Kodama et al., 1989), and will highlight differences in the requirement for a long EnvCT between HIV-1 and HIV-2. To this end, I tested the ability of HIV-1 and HIV-2 FL and ΔCT mutant virus to spread in H9 T cells over a period of 9 days. To generate virus for this study, proviral constructs (FL and ΔCT mutants) and VSV-G plasmid were cotransfected into 293T cells to generate pseudotyped virions. VSV-G pseudotyped viruses were used to normalise initial infection. $1x10^6$ H9 cells were infected with 10 mU/mL of VSV-G pseudotyped virus to achieve 10% initial infection, which is a low dose of virus and will therefore allow detection of viral spread into target cells over a time course. To monitor viral replication and spread over time, cell culture supernatants were collected for 9 days and virus production was quantified using the SG-PERT assay and percentage of Gag-positive infected cells was measured by flow cytometry. As expected, HIV-1 FL replicates and spreads well over time, infecting up to 75% of H9 cells by Day 9 (Fig. 3.5A-B). By contrast, truncation of the EnvCT completely blocked HIV-1 replication and spread (Fig. 3.5A-B), which is consistent with previous studies showing that the EnvCT is required for HIV-1 replication in most T cell lines and primary T cells, and that truncated HIV-1 viruses are non-infectious in a spreading assay (Dubay et. al., 1992; Wilk et. al., 1992; Gabuzda et. al., 1992; Murakami et. al., 2000; Akari et. al., 2000). Conversely, truncation of the EnvCT did not block HIV-2 replication and spread over time (Fig. 3.5C,D) and HIV-2 ST and 7312A ΔCT viruses replicated as well as their respective FL counterparts. Of note, HIV-2 7312A SG-PERT values increased 3-fold from Day 1 to Day 9, whereas HIV-2 ST SG-PERT values increased by 56-fold (Fig. 3.5C,D), suggesting that HIV-2 7312A does not replicate as robustly as HIV-2 ST in H9 cells. In this study, I was unable to measure the percentage of HIV-2 FL and ΔCT infected cells using the KC57 monoclonal antibody (Beckman Coulter) which was used to measure HIV-1 infectivity because this antibody did not efficiently detect HIV-2 Gag (data not shown).

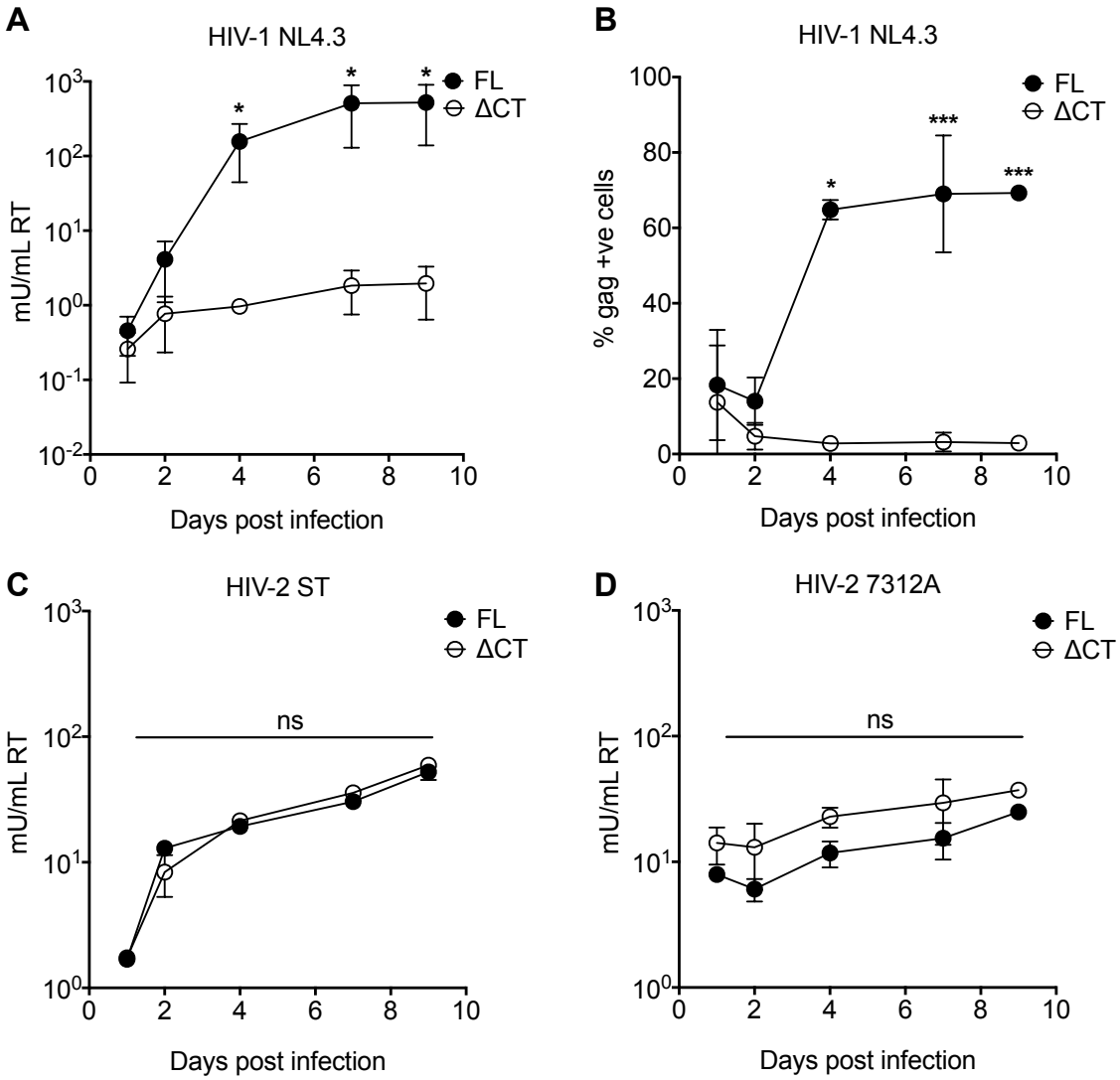

Figure 3.5 HIV-1 and HIV-2 spreading infection in H9 T cells. H9 cells were infected with 10mU/mL of VSV-G pseudotyped full-length replication competent viruses. Virus containing supernatant was collected at indicated time points and purified for **(A,C,D)** SG-PERT analysis and **(B)** HIV-1 NL4.3 infected cell lysate was used for measuring the percentage of Gag positive cells by flow cytometry from three independent experiments. Error bars represent mean ± SEM. Groups were compared using two-tailed unpaired *t*-test (ns, P>0.05; *, P<0.01; ***, P<0.001).

3.2.5 Env incorporation into HIV FL and ΔCT virions produced in H9 cells.

Next, I analysed the amount of Env incorporation in virions produced from H9 cells. To do this, H9 cells were infected with a high dose (200 mU/mL) of VSV-G pseudotyped FL or ΔCT virus, in order to produce high titre virus stocks. Figure 3.6A shows that NL4.3 FL and ΔCT Env are synthesised to similar levels in H9 cells, but like in 293T cells, there is significantly less ΔCT Env incorporated into virions. Quantification of multiple immunoblots revealed that there was 5-fold less ΔCT Env incorporated into HIV-1 virions compared with FL Env (Fig. 3.6A). Defective Env incorporation thus correlates with the

production of less infectious virus and fewer infected H9 cells (Fig. 3.5A,B). Figure 3.6B-C show that equivalent amounts of HIV-2 ST and 7312A FL and ΔCT Env are synthesised in H9 cells. Also, the amount of FL and ΔCT Env incorporated into virions is comparable, which correlates with the spreading infection in H9 cells (Fig. 3.5C,D).

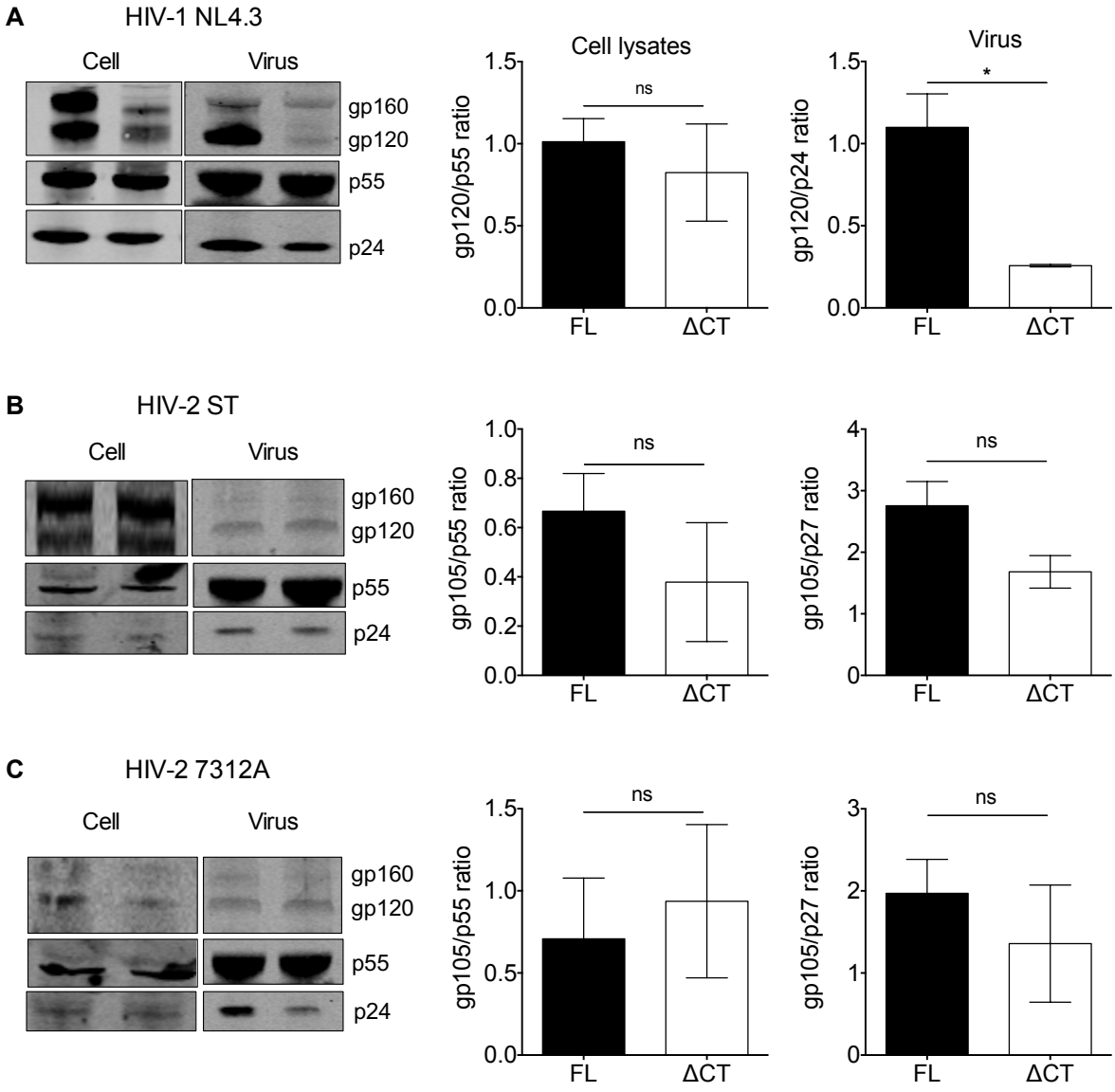

Figure 3.3 Env production and incorporation in H9 T cells. (A-C) Representative immunoblots from H9 T cells infected with equivalent RT units of VSV-G pseudotyped FL and ΔCT virus for 24h. Infected cell lysates and virus containing supernatant was analysed for expression of Env (gp120 or gp105) and Gag (p24 or p27). Quantification of Env incorporation was calculated by dividing the band intensity of Env by Gag from three independent experiments. Bars represent mean and error bars represent mean ± SEM. Groups were compared using two-tailed unpaired *t*-test (ns, p>0.05; *, p<0.05).

3.2.6 HIV-2 ROD10 FL and ΔCT infectivity analysis.

HIV-2 ROD10 is a commonly used lab-adapted strain of HIV-2. Sequencing of HIV-2 ROD10 EnvCT revealed that there is a pre-existing stop codon at position 719 of Env, and so this virus is originally a ΔCT virus. This is different to HIV-2 ST and 7312A primary isolates which have a full length EnvCT. In this section, I assess whether HIV-2 ROD10 FL and ΔCT viruses replicate similarly to the non-lab-adapted HIV-2 isolates HIV-2 ST and 7312A. For functional analysis, the stop codon at Env position 719 was reverted back to a glutamine residue in order to produce the HIV-2 ROD10 FL virus (Table 3.1).

First, single round infectivity of HIV-2 ROD10 FL and ΔCT viruses was measured by transfecting 293T cells with infectious molecular clones and virus-containing supernatant was collected after 48h. Figure 3.7A shows that the SG-PERT units for both HIV-2 ROD10 FL and ΔCT viruses are similar, hence virus production and budding is unaffected by reversion of the stop codon to produce HIV-2 ROD10 with a full length EnvCT. Titrating these viruses on HeLa TZM-bl reporter cells shows that the original HIV-2 ROD10 ΔCT virus is infectious, however the revertant HIV-2 ROD10 FL virus is non-infectious and in fact cannot produce RLU readings above the background RLU readings (Fig. 3.7B-C). This is in stark contrast to HIV-2 ST and 7312A FL viruses, which were comparable in the presence and absence of a full-length EnvCT in the same assays. Next, the infectivity of HIV-2 ROD10 FL and ΔCT viruses were tested on the H9 T cell line. As previously described, equal RT units of VSV-G pseudotyped HIV-2 ROD10 FL and ΔCT viruses were added to H9 cells for 4h, after which VSV-G viruses were replaced with fresh media and spreading infection was observed over a 9-day period. In line with the 293T and HeLa TZM-bl data, HIV-2 ROD10 FL was unable to spread in the H9 T cell line, whilst the HIV-2 ROD10 ΔCT virus spreads over the 9-day period, producing over 100mU/mL of viral particles by Day 9 (Fig. 3.7D).

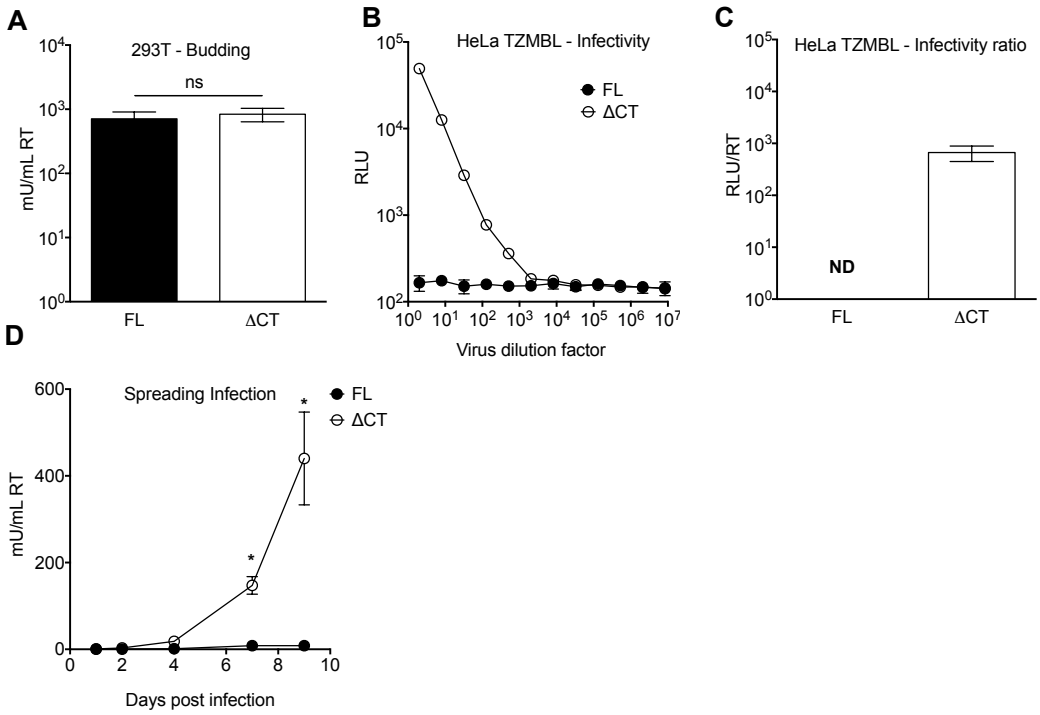

Figure 3.7 Characterisation of HIV-2 ROD10 FL and ΔCT infectivity. 293T cells were transfected with infectious molecular clones encoding HIV-2 ROD10 FL and ΔCT virus for 48 h, after which supernatant was collected for **(A)** SG-PERT analysis and **(B)** titration on to HeLa TZM-BL reporter cells. **(C)** The infectivity ratio of viral particles was calculated using (A) and (B) from three independent experiments. Due to non-infectious nature of the HIV-2 ROD10 FL virus, no RLU values were detected above background RLU activity of TZM-bl cells, therefore an infectivity ration could not be calculated, hence labelled 'ND', not detected **(D)** Spreading infection in H9 cells. H9 cells were infected with a low dose (10mU/mL RT units) of VSV-G pseudotyped FL and ΔCT virus for 4h by gravity infection. After 4h the input virus was removed and replaced with fresh media. Infected cells were cultured for up to 9 days and supernatants were collected at indicated time points to measure the amount of virus produced and released using the SG-PERT assay from three independent experiments. Bars represent mean and error bars represent mean ± SEM. Groups were compared using unpaired *t*-test (ns, $p>0.05$; *, $p<0.05$).

3.2.7 HIV-2 ROD10 FL and ΔCT Env expression and incorporation into virions.

In an attempt to explain the infectivity defect of HIV-2 ROD10 FL virus, I next tested Env incorporation levels in virions. 293T cells were transfected as described above, and virus containing supernatant was purified for immunoblotting. Quantification of HIV-2 ROD10 Env (gp105) normalised to cell-associated p55, reveals that there is significantly less FL Env produced in transfected 293T cells, by comparison with ΔCT Env (Fig. 3.8A). Analysis of virions reveals that FL Env incorporation is highly inefficient and 3 independent immunoblots showed FL Env bands that were below the level of detection by the Image Studio Lite software used to quantify the intensity of bands on a western blot. This is perhaps unsurprising given that there are low levels of FL Env in producer cells. By contrast, ΔCT Env was incorporated to high levels, corresponding to the ability of the ΔCT virus to infect HeLa and H9 cells. Importantly, the amount of cell associated p55 and virion associated p27 in cell is equivalent between HIV-2 ROD10 FL and ΔCT virions (Fig. 3.8A), therefore there appears to be a specific defect in Env production and/or turnover in transfected cells, rather than a global defect in virion production.

To further corroborate these findings, I transfected 293T cells with equivalent RT units of HIV-2 ROD10 FL and ΔCT constructs in order to perform immunofluorescence (IF) microscopy and observe Env expression. Figure 3.8B shows that there is no detectable FL Env signal, whilst there is bright ΔCT Env staining colocalising with Rab7 staining. In line with this, infected HeLa TZM-bl had no FL Env staining (Fig. 3.8B), possibly explained by the fact that this virus cannot infect HeLa TZM-bl cells (Fig. 3.7B,C). By contrast, ΔCT Env signal is detected in infected HeLa TZM-bl cells, particularly localised around the nucleus, suggesting localisation in the endoplasmic reticulum, which is the site of Env synthesis.

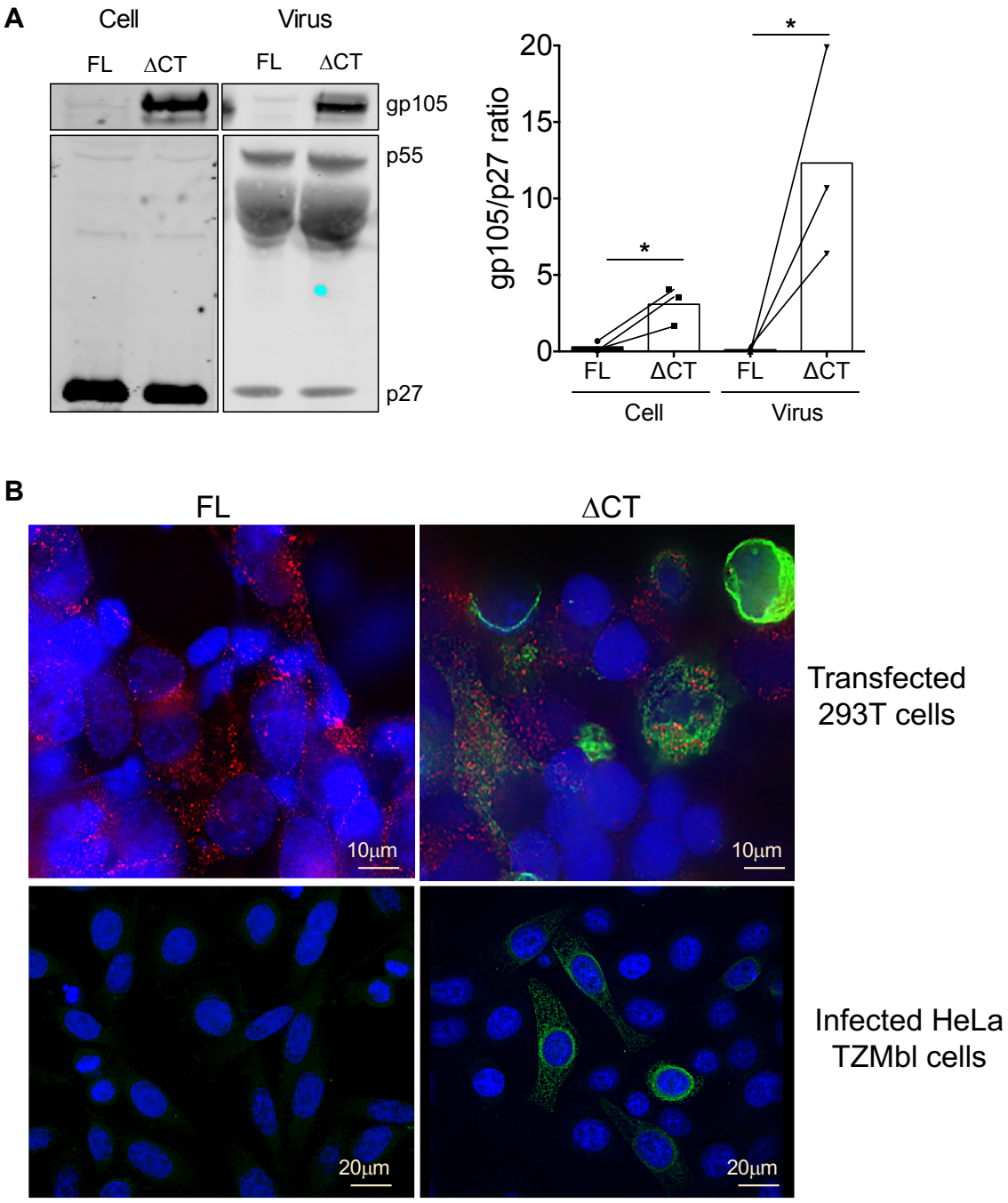

Figure 3.8 HIV-2 ROD10 Env production and incorporation. (A) 293T cells were transfected with proviral constructs encoding HIV-2 ROD10 FL and ΔCT virus. After 48 h, transfected cell lysates and purified virions were lysed for immunoblot analysis to detect Env (gp105) and p27 proteins. (left) This is a representative immunoblot. The intensity of Env and p27 bands were calculated using the Image Studio Lite software and (right) normalised values from multiple experiments are shown in the bar chart. N=3 **(B)** Top panels are representative IF images (single xy slice) of transfected 293T cells and bottom panels show infected HeLa TZM-bl cells. DAPI nuclear stain is shown in blue, Env is shown in green and Rab7 positive compartments are shown in red (Rab7 staining only present in transfected 293T cells, not HeLa cells). Bars represent mean and error bars represent mean ± SEM. Groups were compared using two-tailed unpaired *t*-test (ns, p>0.05).

3.3 Discussion

The results from this chapter reveal differences in the requirement for a long EnvCT between the two human immunodeficiency viruses. Here I have directly compared the requirement for the EnvCT by HIV-1 and HIV-2 viruses. The key finding from this Chapter is that truncation of the HIV-2 EnvCT does not impact on viral replication nor Env incorporation into virions for the HIV-2 primary isolates ST and 7312A.

To investigate the differential requirements of human immunodeficiency viruses for a long EnvCT in viral replication, I created a panel of HIV-1 and HIV-2 viruses with a full-length or truncated EnvCT. H9 cells were infected with HIV-2_{ST} and HIV-2_{7312A} primary isolates with a long (FL virus) and short (ΔCT virus) EnvCT. This revealed that FL and ΔCT viruses have comparable spreading infection curves, suggesting that the long EnvCT is dispensable for HIV-2 infection and spread in this T cell line. In line with my results, previous studies have reported that HIV-2 truncates its EnvCT and ΔCT variants are replication competent in various cell types (Albert et al., 1987; Evans et al., 1988; Franchini et al., 1989; Kong et al., 1988). Franchini and colleagues (1989) reported the first HIV-2 replication competent proviral clone called SBL-6669. This virus has a truncated EnvCT and is able to infect and replicate in multiple human cell types including H9, HUT78 and Jurkats (Franchini et al., 1989). Infectivity was measured by counting the number of viable cells and syncytia at different time points post infection, with the assumption that increased infectivity will lead to increased cell death and syncytia formation. Only 50% of viable H9 cells remained after 12 days of infection, suggestive of ongoing viral replication (Franchini et al., 1989). Further, Evans and colleagues (1989) isolated HIV-2_{UC1} from an individual from the Ivory coast by cocultivation of infected cells with uninfected PBMCs (Evans et al., 1988). Immunoblot analysis of virus pellets, using serum from the infected individual, revealed that the EnvCT was 32kDa rather than 40kDa, suggestive of a truncated protein (Evans et al., 1988). HIV-2_{UC1} infected various cell types including primary PBMCs and macrophages and replication was comparable to HIV-1 virus with a full length EnvCT (Evans et al., 1988). An infectious molecular clone was derived from this primary isolate and named UC1mc (Barnett et al., 1993). This became the first fully sequenced HIV-2 subtype B virus. Immunoblot analysis of the initial virus sample revealed the presence of transmembrane proteins that are 32 and 40kDa (Barnett et al., 1993), suggesting that the patient was infected with a mixture of FL and ΔCT viruses. Repeated passage of this pool of virus in the MOLT4/8 cell line gave rise to a virus population containing only ΔCT variants (Barnett et al., 1993), suggesting that the ΔCT virus outgrew the FL virus and therefore had a replicative advantage. Finally, the HIV-2_{ST} virus was isolated from a patient in Senegal and, similar to the above, western blot analysis revealed the presence of virus with a FL and ΔCT EnvCT (Kong et

al., 1988). This swarm of virus could successfully replicate in the SupT1 T cells and human PBLs (Kong et al., 1988). The viruses present in the supernatant of infected SupT1 cells and human PBLs were not characterised in that study, however a later study showed that repeated passage of these viruses in SupT1 cells resulted in the emergence of a viral population consisting of ΔCT virus only (Kumar et al., 1990). This suggests that the ΔCT variant in the initial pool of virus isolated from the infected individual may have had a replicative advantage in SupT1 cells (Kong et al., 1988), similar to UC1mc virus in MOLT4/8 cells (Barnett et al., 1993). Taken together, this data and the results from this Chapter suggest that EnvCT truncation does not prevent HIV-2 replication in permissive (MOLT4, SupT1, 293T) and non-permissive cells (H9, Jurkats, primary T cells and macrophages), unlike HIV-1, and therefore the two human immunodeficiency viruses have a differential requirement for a long EnvCT. According to the results in this Chapter, HIV-2 gains no replicative advantage upon EnvCT truncation, contrary to previous reports (Hoxie et al., 1991). It remains unclear why this discrepancy exists, however it is possible that if spreading infection in this study was allowed to proceed for longer than 9 days, I may have started to see the ΔCT viruses replicate better in H9 cells.

Efficient Env incorporation is necessary for the production of infectious viral particles and this process is regulated by the EnvCT in a cell type dependent manner for HIV-1 (Akari et al., 2000; Murakami and Freed, 2000). In this Chapter, I have shown that HIV-2 viruses that are produced in 293T and H9 cells have no Env incorporation defect, by contrast to HIV-1. This suggests that there are key differences in the process of Env trafficking, Env incorporation and viral assembly between HIV-1 and HIV-2 viruses. It is possible that HIV-2 is less dependent on interactions between the cytoplasmic tail and host proteins that regulate Env trafficking, thereby overcoming a block to Env incorporation. Alternatively, HIV-2 EnvCT may utilise a different set of cofactors compared with HIV-1, the expression of which do not differ significantly between permissive and non-permissive cells, or which enable HIV-2 Env to use a different mechanism of Env incorporation and viral assembly. There is currently no data exploring HIV-2 Env trafficking and incorporation mechanisms and whether HIV-2 has the same cofactor usage as HIV-1 in different cell types. These differences may be attributed to the fact that HIV-2 belongs to a different lineage to HIV-1 and has therefore evolved a different mechanism of virus production based on the biology of its ancestor SIVsmm. Comparison of the HIV-1 and HIV-2 EnvCT sequences does not reveal any striking differences which might explain differences in Env incorporation. In light of the data presented in this chapter, I propose a comparative study between HIV-1 and HIV-2 assembly and budding should be performed in order to provide further insight into the

differential cytoplasmic tail-dependent Env incorporation phenotype seen in the two human lentiviruses.

An Env incorporation defect was characteristic of HIV-1 ΔCT virus made in 293T and H9 cells, however an infectivity defect was only observed in viruses made in H9 cells. This could be explained by two possibilities. First, it is possible that the defect seen in 293T cells is not as potent as that seen in H9 cells, meaning the nascent virus particles have enough Env to be able to infect HeLa TZM-bl cells as successfully as the HIV-1 virus with a full length EnvCT. Alternatively, this observation may suggest that the amount of CD4 receptor and coreceptors present on target cells influences the ability of the mutant virus to successfully infect cells. HeLa TZM-bl cells have been engineered to overexpress CD4 receptor, thereby increasing the likelihood of receptor engagement with Env on virions. By contrast, H9 cells have lower levels of CD4 and coreceptor expression, thus decreasing the likelihood of receptor engagement and initiation of fusion and entry. This would explain why HIV-1 ΔCT infects HeLa cells but not H9 T cells in this study. A future experiment to investigate this hypothesis would be to infect 293T affinofile cells (Johnston et al., 2009), which can be treated with different doses of minocycline and Ponasterone A to alter the expression of CD4 receptor and determine whether infectivity of HIV-1 ΔCT virus increases as the amount of CD4 expression increases. This might be particularly important if the HIV-1 ΔCT Env binds poorly to the CD4 receptor and/or coreceptors, in which case increasing the amount of these cellular proteins at the surface of target cells increases the likelihood of ΔCT Env binding with higher avidity. This hypothesis will be discussed further in the next chapter of this thesis.

Another intriguing result from this chapter is that there is a striking difference between the primary HIV-2 isolates (ST and 7312A) and the infectious molecular clone HIV-2_{ROD10} (GenBank: M15390), which was previously constructed using fragments of ROD27 and ROD35 in the pSPE5 backbone. The original sequence of HIV-2 ROD10 has a premature stop codon at Env position 719, resulting in a truncated EnvCT, by contrast to HIV-2 ST and 7312A which have a full length EnvCT. Immunoblot analysis and immunofluorescence microscopy of infected cells and purified virions revealed that there is less HIV-2 ROD10 FL Env expression in both producer cells and virions. A reduction in the amount of cell associated Env in part explains why less Env is incorporated into virions, although there may be an additional block to Env incorporation too. Lower expression of HIV-2 ROD10 FL Env compared with ΔCT Env in cell lysates suggests that perhaps the FL Env glycoprotein is not produced as efficiently as ΔCT Env or that it has an increased turnover rate. These hypotheses can be tested by measuring the amount of HIV-2 Env mRNA and by assessing HIV-2 Env protein turnover using a cycloheximide

chase assay. Host cofactors that regulate Env expression may have altered interactions with the HIV-2 ROD10 FL Env resulting in dysregulated expression. For example, a large proportion of Env glycoproteins that are produced in the endoplasmic reticulum get targeted for Endoplasmic reticulum associated degradation (ERAD) (Meusser et al., 2005; Zhou et al., 2014; Zhou et al., 2015) and so it is possible that the HIV-2 ROD10 FL Env is more susceptible to entering this degradative pathway for reasons we do not completely understand. Blocking the ERAD pathway using a small molecule inhibitor, Kifunensine, might rescue viral infectivity by increasing the amount of HIV-2 ROD10 FL Env available for incorporation into nascent virions.

Exploring the genomic structure of HIV-2 Env may provide insight into why we observe reduced HIV-2 ROD10 FL Env in cells. The 3' end of the HIV-2 *env* gene contains the nucleotide sequences that encode Tat, Rev and the start of Nef in overlapping open reading frames (ORF) within the sequence of the EnvCT (Bakouche et al., 2013). Therefore, it is possible that mutating residues within the HIV-2 EnvCT can impact *tat*, *rev* and/or *nef* sequences, resulting in dysregulated expression and function of these proteins, thereby impacting expression of Env. However, upon sequencing the HIV-2 ROD10 FL EnvCT, no mutations were found to have impacted the ORFs of these proteins. Alternatively, because HIV-2ROD10 is a chimera of ROD27 and ROD35, it is possible that there is mismatch between accessory proteins, resulting in increased susceptibility to certain antiviral proteins, resulting in reduced infectivity. Perhaps HIV-2_{ROD10} EnvCT truncation overcomes this block. In Chapter 4, I will investigate how HIV-1 and HIV-2 EnvCT truncation allows viral evasion of two potent entry targeting restriction factors, SERINC5 and IFITM1, thereby highlighting the possibility that lentiviral EnvCT truncation occurs due to a selective pressure exerted by cell intrinsic antiviral factors. Given that HIV-2_{ROD10} virus with a full length EnvCT has a significant infectivity defect, I will be using HIV-2_{ST} and HIV-2_{7312A} to explore SERINC5 and IFITM restriction.

Whether HIV-2 ΔCT viruses exist *in vivo* remains unclear. Some early reports suggested that HIV-2 ΔCT virus were isolated from infected individuals because western blot analysis revealed the presence of a protein at 30-32kDa (Albert et al., 1987; Evans et al., 1988; Kong et al., 1988). However, these western blots do not directly measure the virus from patient derived PBMCs. Instead, the viruses were passaged in vitro to produce high titre stocks, which were then subjected to immunoblot analysis to identify key viral proteins, including Env. Moreover, there is often a lack of information on the phenotype of the original virus swarm which was isolated from the infected individuals. A common method of virus isolation was used, in which PBMCs from infected donors were co-cultivated with PBMCs from healthy donors and then high titre virus stocks were

produced by infecting and propagating isolated viruses in T cell lines. Exactly how long this process was carried out for remains unclear in many early studies. It is possible that ΔCT variants emerged during prolonged propagation of virus, as an adaptation to *in vitro* cell culture conditions, and this is what was detected by western blot and genetic analysis (Albert et al., 1987; Evans et al., 1988; Kong et al., 1988). On the contrary, it is also possible that both FL and ΔCT viruses exist *in vivo*, as viral quasispecies, with the ΔCT virus possibly existing as a minority variant, which may explain why HIV-2 ΔCT variants are rarely discovered from patient samples. This hypothesis also gives rise to the possibility that HIV-1 ΔCT variants might exist *in vivo*. Indeed, a HIV-1 ΔCT variant called 92UG046-T8 was discovered when patient derived viruses were stringently isolated in order to find minority variants that enter cells in a CD4-independent manner (Zerhouni et al., 2004). This variant was unlikely to have emerged during the isolation process for several reasons. First, the 92UG046-T8 strain was isolated from the parental 92UG046-infected primary CD8+ lymphocytes in short term culture (2-3 weeks) cocultures, during which it is unlikely to have developed the stop mutation. Secondly, the 92UG046-T8 variant was never propagated in any cell lines, unlike the HIV-2 examples present above. Finally, a heteroduplex tracking assay (HTA) was used to detect the stop codon in EnvCT sequence of 92UG046-T8 (Saha et al., 2005). Results from this experiment revealed that approximately 10% of the RNA pool in the parental 92UG046 viral quasispecies had the 92UG046-T8 sequence present (Saha et al., 2005), which suggests that the EnvCT truncation mutant existed as a minority variant in the viral quasispecies of the patient. Based on these findings, I believe that it is possible for HIV-1 and HIV-2 ΔCT variants to be present in infected individuals, and we might capture the presence of more EnvCT truncated mutants if there were an increase in sampling and isolation specifically for this phenotype. Based on this, I next explore the following question: Given that HIV-2 ΔCT viruses are replication competent and sometimes have a replicative advantage over their FL counterpart, why are they only present as minority variants, if they exist at all *in vivo*? One possibility is that EnvCT truncation leads increased susceptibility to humoral immunity and targeting by neutralising antibodies. This idea will be discussed further in Chapter 4 and Chapter 6.

It is plausible to suggest that the lack of an adaptive immune system, hence the absence of this strong selection pressure in cell culture, may give rise to ΔCT mutant viruses. I have already discussed this is the context of HIV-2, however there is also evidence that HIV-1 viruses truncate their EnvCT during prolonged passage in cell culture (Jones et al., 2002; Shimizu et al., 1990). For example, HIV-1_{RF} was grown in H9 cells and adapted by mutating a tryptophan residue at position 227 to a stop codon (Jones et al., 2002). This truncated mutant had increased fusogenicity and was able to infect primary PBMCs

and several T cell lines. By contrast, a 133 amino acid truncation in the clinical isolate, HIV-1_{KB-1}, rendered the virus unable to infect PBMCs (Shimizu et al., 1990). However, this mutant was able to infect permissive T cell lines such as MOLT-4 and MT4 (Shimizu et al., 1990). Finally, when the HIV-1_{IIIB} isolate was passaged in a CD4- cell line called BC7, a premature stop codon resulted in a 30 amino acid long EnvCT (LaBranche et al., 1999). This virus was termed 8x and inserting this EnvCT into a HIV-1_{HxB2} background resulted in a 3-fold increase in fusogenicity compared with the wild type HIV-1_{HXB2} virus (LaBranche et al., 1999). Therefore, these data suggest that the adaptive immune system probably exerts a strong selection pressure for lentiviruses to maintain a long EnvCT, and as soon as the virus is in a different niche, where there is no adaptive system, it truncates to become more fusogenic and perhaps spread better by cell-cell transmission. In the future, it would be interesting to formally compare the ability of ΔCT and FL viruses to perform cell-cell spread, using a specific cell-cell spread assay as described previously (Groppelli et al., 2015; Jolly et al., 2007b; Martin et al., 2010).

Another possibility is that EnvCT truncation may broaden HIV tropism. For example, the HIV-1 8x and 92UG046-T8 EnvCT truncation mutants adapted to infect CD4 negative cells (Edwards et al., 2001; LaBranche et al., 1999; Saha et al., 2005; Zerhouni et al., 2004). In line with this, a wide range of CD4 negative cells *in vivo* are thought to become susceptible to HIV-1 infection during disease progression, indicating the emergence of HIV-1 variants which could possibly have EnvCT truncations (Bhattacharya et al., 2003; Fauci, 1996). Taken together, this suggests that HIV-1 EnvCT truncation might occur *in vivo,* resulting in increased fusogenicity and broadened cellular tropism. However, these viruses probably remain a minority variant as they are more susceptible to antibody neutralisation and have an Env incorporation defect, resulting in a fitness cost and are therefore predominantly selected against *in vivo*.

4 Role of the EnvCT in evasion of HIV restriction factors

4.1 Introduction

The evolutionary arms race between HIV-1 and host cells has allowed for efficient viral replication and transmission. Host cells are naturally hostile environments for invading pathogens and have evolved to express an arsenal of antiviral proteins, collectively referred to as restriction factors that target different steps of the viral life cycle to block replication. Restriction factors act as the first line of defence against viral infections and are often a component of the cell intrinsic innate antiviral immune system (Malim and Bieniasz, 2012). Common features of restriction factors include upregulation by type I IFNs, undergoes positive selection and species-specific activity (Malim and Bieniasz, 2012). In response to these antiviral proteins, viruses including pandemic HIV-1 and related lentiviruses, have evolved to evade or directly antagonise host restriction factors, often by encoding viral accessory proteins (Reviewed in (Foster et al., 2017; Sumner et al., 2017)), illustrating the Red Queen Hypothesis of evolution.

The most recently described family of lentiviral restriction factors are the Serine Incorporator proteins (SERINCs) (Rosa et al., 2015; Usami et al., 2015). HIV-1 is most potently restricted by SERINC5, and to a lesser extent by SERINC3, but not by SERINC2 (Rosa et al., 2015; Usami et al., 2015). SERINC3/5 expression levels vary in different cell types, with the highest expression in Jurkat cells and PBMCs (Usami, Wu and Göttlinger, 2015). The exact physiological role(s) of these proteins remain to be elucidated. Initial evidence suggested that SERINCs are involved in phospholipid biosynthesis, as they act as carrier proteins and aid serine incorporation (Inuzuka, Hayakawa and Ingi, 2005). However, recent mass spectrometry studies show that removing SERINC1 (Chu et al., 2017) and SERINC5 from cell membranes (Trautz et al., 2017) does not alter the lipid composition of either viral or cellular membranes. HIV-1 inhibition is a conserved feature of several SERINC5 species including mouse, frog and zebrafish SERINC5 (Dai et al., 2018). In addition to human and simian lentiviruses, SERINC5 has broad antiviral activity against other retroviruses, such as Equine Infectious Anaemia Virus (Ahi et al., 2016; Chande et al., 2016) and Murine Leukaemia Virus (Rosa et al., 2015; Usami et al., 2015).

SERINC5 is composed of 10 transmembrane domains and is primarily localised at the plasma membrane (Pye et al., 2020) where it is incorporated into budding virions and inhibits viral entry (Rosa et al., 2015; Sood et al., 2017; Usami et al., 2015). The lentiviral accessory protein Nef antagonises SERINC5, excluding it from incorporation into nascent viral particles (Rosa et al., 2015; Sood et al., 2017; Usami et al., 2015) by

removing SERINC5 from the plasma membrane via AP-2 dependent endocytosis (Shi et al., 2018). This relocalises SERINC5 to the endosomal pathway, particularly into $Rab5^+$ early endosomes, $Rab7^+$ late endosomes and eventually LAMP1+ compartments, for subsequent lysosomal degradation (Shi et al., 2018). Although anti-HIV-1 activity is a conserved feature of divergent SERINC5 proteins, their sensitivity to Nef is not (Dai et al., 2018). Whilst human SERINC5 is highly sensitive to Nef-mediated counteraction, frog SERINC5 is resistant. Swapping the ICL4 regions between human and frog SERINC5 also swaps their responsiveness to Nef, therefore the ICL4 determines sensitivity to Nef (Dai et al., 2018).

Although the exact mechanism of how SERINC5 restricts lentiviruses remains incompletely understood, it is clear that the Envelope glycoprotein (Env) is crucial in determining sensitivity to SERINC5 (Beitari et al., 2017; Chen et al., 2020b; Sood et al., 2017; Zhang et al., 2019a). HIV-1 enters target cells by fusing with the host cell plasma membrane after the gp120 subunit engages entry receptors CD4 and co-receptor, which is usually either CXCR4 or CCR5. Biochemical studies suggest that SERINC5 acts to inhibit small fusion pore formation, thereby reducing the efficiency of fusion (Sood et al., 2017), but whether SERINC5 directly interacts with Env to inhibit fusion, or whether indirect effects mediate restriction remains an open question (Chen et al., 2020b; Sood et al., 2017; Zhang et al., 2019a). Modelling of Env trimers and SERINC5 in the lipid bilayer suggests that SERINC5 extracellular loops 3 and 5 potentially interact with the membrane proximal external region (MPER) of Env gp41 to mediate restriction (Pye et al., 2020). By contrast, a recent study investigating the effect of SERINC5 on Env clustering on virions, indicated that SERINC5 clusters do not colocalise with Env clusters in the viral membrane (Chen et al., 2020b), suggesting an indirect mechanism of restriction.

The majority of the EnvCT is believed to be embedded within the plasma membrane (Murphy et al., 2017) similar to SERINCs (Pye et al., 2020), where the EnvCT has been shown to influence Env mobility in membranes (Muranyi et al., 2013; Pezeshkian et al., 2019). However, whether this critical region of Env interacts with SERINC5 and what role the EnvCT plays in SERINC5-mediated restriction remains unknown. Here I examine the role of the EnvCT in determining sensitivity to SERINC5-mediated restriction, with the goal of better understanding the complex relationship between Env and SERINC5. Furthermore, I investigate how EnvCT truncation impacts sensitivity to Interferon Inducible Transmembrane proteins (IFITM) proteins which are another family of potent lentiviral membrane-bound restriction factors that target viral entry. IFITMs also target a wide range of enveloped viruses including Influenza A virus, Dengue virus, Ebola virus,

Hepatitis C virus and HIV (Brass et al., 2009; Huang et al., 2011; Lu et al., 2011a). Similar to SERINC5, Env is a determinant for IFITM restriction, particularly the V3 loop (Foster et al., 2016; Tartour et al., 2014; Wang et al., 2017; Wu et al., 2017), although the exact mechanism of restriction remains to be elucidated. Given that several features of SERINC5 and IFITM sensitivity overlap, I hypothesise that EnvCT truncation have a similar effect on viral sensitivity to both SERINC5 and IFITMs. Finally, I test whether truncation of the HIV-1 and HIV-2 EnvCT alters sensitivity to Tetherin, which prevents budding and is antagonised by HIV-2 Env (Le Tortorec and Neil, 2009).

4.2 Results

4.2.1 Truncating the HIV-1 EnvCT overcomes SERINC5 restriction.

To determine the consequence of EnvCT truncation for SERINC5 restriction, I used an established co-transfection assay previously described to interrogate SERINC5 restriction (Beitari et al., 2017; Rosa et al., 2015; Sood et al., 2017; Usami et al., 2015). 293T cells were co-transfected with replication-competent HIV-1 NL4.3 molecular clone encoding either a full-length (FL) or truncated (∆CT) EnvCT alongside increasing doses of plasmid encoding SERINC5 with an internal HA-tag and external FLAG tag. At 48h post-transfection, supernatants were harvested, and viral budding was quantified using the SG-PERT assay for reverse transcriptase (RT) activity (Fig. 4.1A), and infectivity quantified by titrating virus-containing supernatants onto HeLa TZM-bl luciferase reporter cells (RLU) (Fig. 4.1B). To calculate single particle infectivity, RLU values were normalised to RT units from the SG-PERT assay and labelled as RLU/RT measurements (Fig. 4.1C). As a control, HIV-1 ∆Nef virus, which cannot antagonise SERINC5, was used to show that SERINC5 can potently restrict infection in a dose dependent manner (Fig. 4.1B-D). This is consistent with previous reports (Beitari et al., 2017; Rosa et al., 2015; Sood et al., 2017; Usami et al., 2015). As HIV-1 FL virus encodes a *Nef* allele, infection was not significantly inhibited at low doses of SERINC5 overexpression (Fig. 4.1B-D). However, at high doses (50-200ng) SERINC5 was capable of inhibiting FL in a dose dependent manner, explained by SERINC5 overexpression overwhelming Nef activity (Fig. 4.1B-D). Of note, when no SERINC5 protein was overexpressed, i.e., at 0ng, HIV-1 ∆Nef was less infectious compared with HIV-1 FL and this can be explained by the presence of endogenous SERINC expression in 293T cells. Strikingly, truncation of the EnvCT rendered HIV-1 ∆CT completely resistant to SERINC5 restriction (Fig. 4.1B-D). Even at the highest dose where I observed a 100-fold reduction in FL virus infectivity, the infectivity of ∆CT virus remained unaffected (Fig. 4.1C,D). Western blot analysis of cell lysates from transfected 293T cells confirmed SERINC5 expression (Fig. 4.1E). I also assessed the cell surface levels of SERINC5 on 293T cells using flow cytometry

(stained for an external FLAG-tag) to confirmed that both HIV-1 FL and ΔCT viruses similarly downregulated SERINC5, since both viruses contain a Nef allele (Fig. 4.1F).

It has been previously shown that truncating the HIV-1 EnvCT, particularly by removing the YxxL endocytic motif and the C-terminal dileucines (commonly referred to as Δ144 virus), can result in increased surface expression of the Env glycoprotein due to reduced Env endocytosis, which may lead to increased Env incorporation into nascent virions (Boge et al., 1998; Byland et al., 2007; Day et al., 2004). Also, the P722* ΔCT mutant in this study contains an intact YxxL endocytic motif, however the C-terminal dileucine motif is removed, which is important for Env endocytosis (Byland et al., 2007) and therefore might affect Env incorporation. Therefore, to test whether truncation of the HIV-1 EnvCT resulted in increased Env incorporation into virions that might overcome SERINC5 restriction, western blot analysis of purified HIV-1 virions was performed. Figure 4.1G shows that both HIV-1 FL and ΔCT viruses incorporated similar levels of Env into virions produced by 293T cells in the presence and absence of SERINC5. From these data I conclude that HIV-1 ΔCT virus is resistant to SERINC5 restriction by a mechanism that is independent of increased Env incorporation into virions.

Given that the HIV-1 ΔCT Env was able to potently overcome SERINC5 restriction, I next asked whether this was a dominant effect and whether the ΔCT Env can rescue HIV-1 ΔNef infectivity in the presence of SERINC5. A HIV-1 ΔCTΔNef double mutant was generated by substituting amino acid residue P722 with a stop codon (as described above for ΔCT) in the NL4.3 ΔNef proviral construct. This virus was produced in 293T cells without overexpressing SERINC5, for initial characterisation. NL4.3 ΔCTΔNef virus has a significant budding and infectivity defect in the absence of SERINC5 overexpression by comparison with NL4.3 FL, ΔCT and ΔNef viruses (Fig. 4.1H, I). Based on this data, the HIV-1 ΔCTΔNef double mutant is completely defective and therefore cannot be used to determine the effect of SERINC5 on viral infectivity. As the RLU values for NL4.3 ΔCTΔNef infectivity were in the same range as the background RLU activity of HeLa TZM-bl cells, it was not possible to assess the effect of SERINC5 on this mutant.

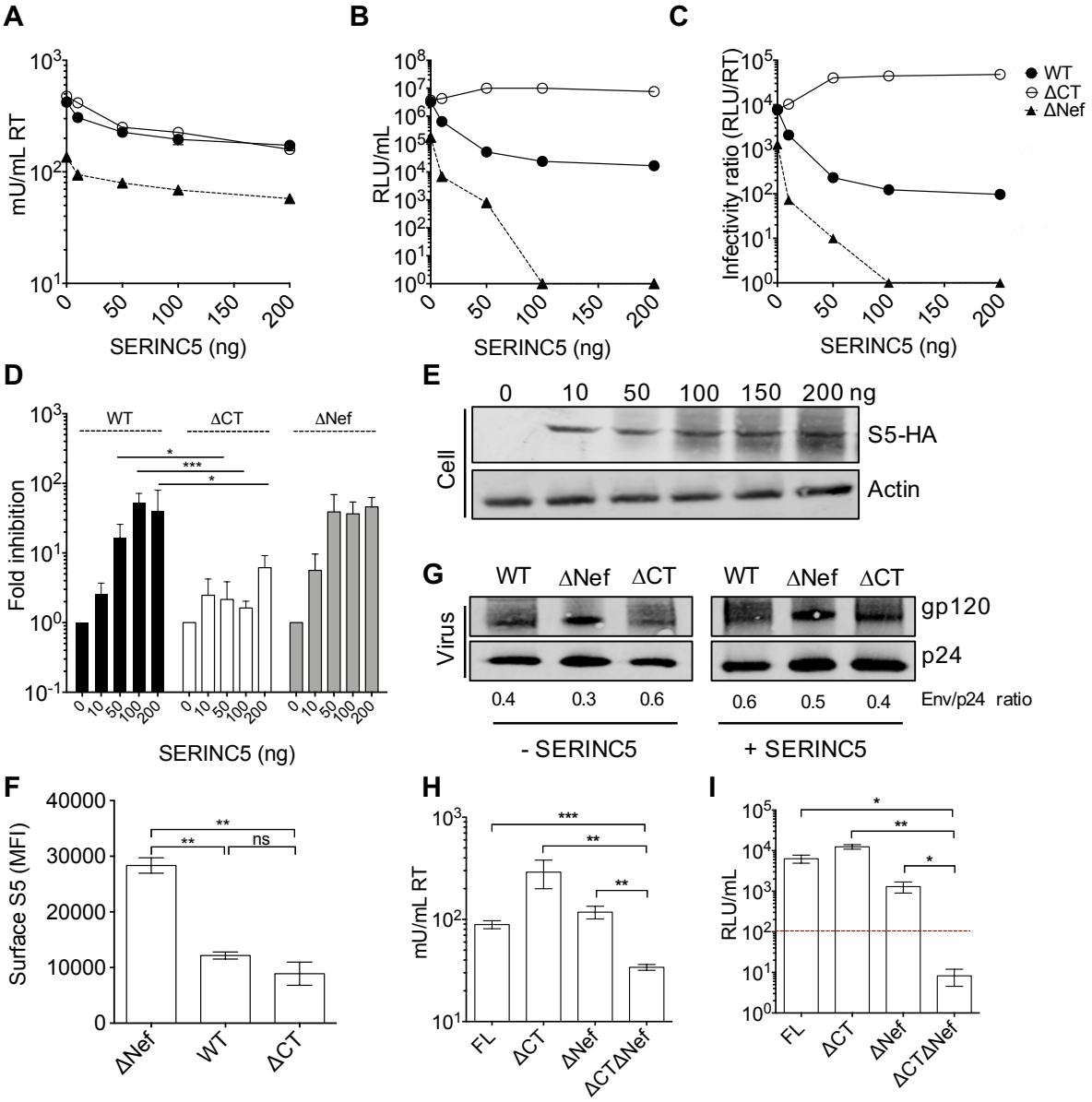

Figure 4.1 HIV-1 EnvCT truncation overcomes SERINC5 restriction. 293T cells were cotransfected with molecular clones encoding full-length HIV-1 NL4.3 WT, ΔNef or ΔCT virus alongside increasing doses of pcDNA-based tagged SERINC5 plasmid (Flag-SERINC5-HA). Virus containing supernatants were harvested after 48h. **(A)** Budding was measured by quantifying RT activity in supernatants by SG-PERT assay. **(B)** Infectivity was measured by titrating supernatant on to HeLa TZM-bl reporter cells and measuring luciferase activity (RLU). **(C)** Particle infectivity was calculated by normalising infectivity RLU (B) to RT activity measured (A). A-C are data from a representative experiment. **(D)** Fold inhibition of viral infectivity was calculated by normalising RLU/RT measurements to 0ng SERINC5. Bar graphs represent fold inhibition from three independent experiments. HIV-1 WT (black), HIV-1 ΔCT (white) and HIV-1 ΔNef (grey). **(E)** Representative immunoblot of transfected 293T cell lysates confirming SERINC5 overexpression detected using antibody against HA-tagged SERINC5 (S5-HA). **(F)** Plasma membrane SERINC5 levels were quantified by surface staining transfected 293T cells for the external Flag-tag of SERINC, the intracellular HA-tag of SERINC5 and Gag. Surface SERINC5 MFI is shown for cells gated on HA-SERINC5 and Gag. **(G)** Representative immunoblot of purified

virions produced in the presence and absence of overexpressed SERINC5 and probed for Env gp120 and Gag p24. The ratio of Env incorporation was calculated by measuring the intensity of gp120 bands and normalising to the intensity of the corresponding p24 bands. Bars show mean and error bars represent mean +/- SEM. Fold inhibition at each dose of SERINC5 was compared using two-way ANOVA testing (ns, $p>0.05$; *, $p<0.05$; **, $p<0.01$; ***, $p<0.001$). **(H)** Budding of indicated virions measured by SG-PERT in the absence of SERINC5 overexpression. **(I)** Infectivity of indicated viruses measured using the HeLa TZM-bl reporter assay. Red dotted line represents the limit of detection for the Glomax luminometer (Promega). Bars show mean and error bars represent mean +/- SEM. Fold inhibition at each dose of SERINC5 was compared using two-way ANOVA testing (ns, $p>0.05$; *, $p<0.05$; **, $p<0.01$; ***, $p<0.001$).

4.2.2 Truncating the HIV-2 EnvCT overcomes SERINC5 restriction.

Next, I tested whether truncation of the HIV-2 EnvCT also conferred resistance to SERINC5 restriction. HIV-2 Nef is reportedly less active against SERINC5 compared with HIV-1 Nef (Heigele et al., 2016). A similar 293T cotransfection assay was used to determine the potency of Nef to counteract SERINC5, however this was in the context of chimeric HIV-1 NL4.3 encoding a HIV-2 *nef* allele, rather than in the context of full-length HIV-2 virus in which there is no mismatch of viral genetics (Heigele et al., 2016). Figure 4.2A-B shows that SERINC5 does not impact budding of HIV-2 strains ST and 7312A. However, infectivity of both FL viruses is restricted up to 10-fold by SERINC5 overexpression, whereas HIV-2 ΔCT viruses remain fully infectious even at high doses of SERINC5 overexpression (Fig. 4.2). Taken together, this shows that EnvCT truncation of both HIV-1 and HIV-2 confers resistance to SERINC5.

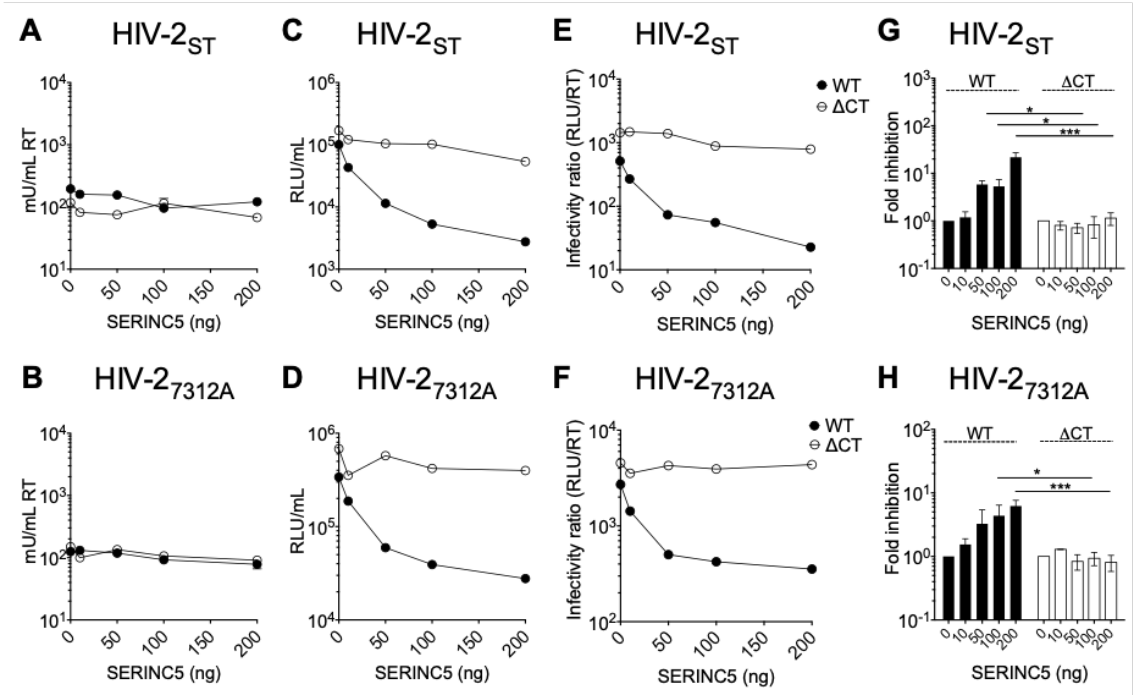

Figure 4.2 Truncating the HIV-2 EnvCT confers resistance to SERINC5 restriction. 293T cells were cotransfected with molecular clones encoding full-length HIV-2 WT isolates and ΔCT mutants alongside increasing doses of pcDNA-based SERINC5 plasmid. Virus containing supernatant was harvested after 48h for analysis. **(A-B)** Budding was measured by quantifying RT activity in supernatants by SG-PERT assay. **(C-D)** Infectivity was measured by titrating supernatant on to HeLa TZM-bl reporter cells and measuring luciferase activity (RLU). **(E-F)** Particle infectivity was calculated by normalising infectivity RLU to RT activity. A-F are data from a representative experiment. **(G-H)** Fold inhibition of viral infectivity was calculated by normalising RLU/RT measurements to 0ng SERINC5. Bar graphs represent fold inhibition from three independent experiments. Bars show mean and error bars represent mean +/- SEM. Fold inhibition at each dose of SERINC5 was compared using two-tailed unpaired t-test (*, $p<0.05$; ***, $p<0.001$).

4.2.3 Truncating the HIV EnvCT overcomes SERINC3 restriction

Several studies have shown that SERINC3 also has the ability to restrict HIV-1 infection, albeit less potently (Rosa et al., 2015; Usami et al., 2015). To test if HIV-1 and HIV-2 EnvCT truncation enables viral evasion of SERINC3 restriction, FL and ΔCT mutant viruses were produced in 293T cells by co-transfection of infectious molecular clones and increasing doses of HA- and FLAG-tagged SERINC3 plasmid. Viral budding and infectivity was measured as described above. Figure 4.3A shows that budding of NL4.3 FL and NL4.3 ΔCT viruses are unaffected by SERINC3 overexpression, similar to SERINC5. However, NL4.3 FL virus shows a dose-dependent reduction in infectivity with increasing doses of SERINC3 and is inhibited up to 5-fold at the highest dose of

SERINC3 overexpression (Fig. 4.3B-D). Conversely, NL4.3 ΔCT virus remains insensitive to SERINC3 overexpression (Fig. 4.3B-C).

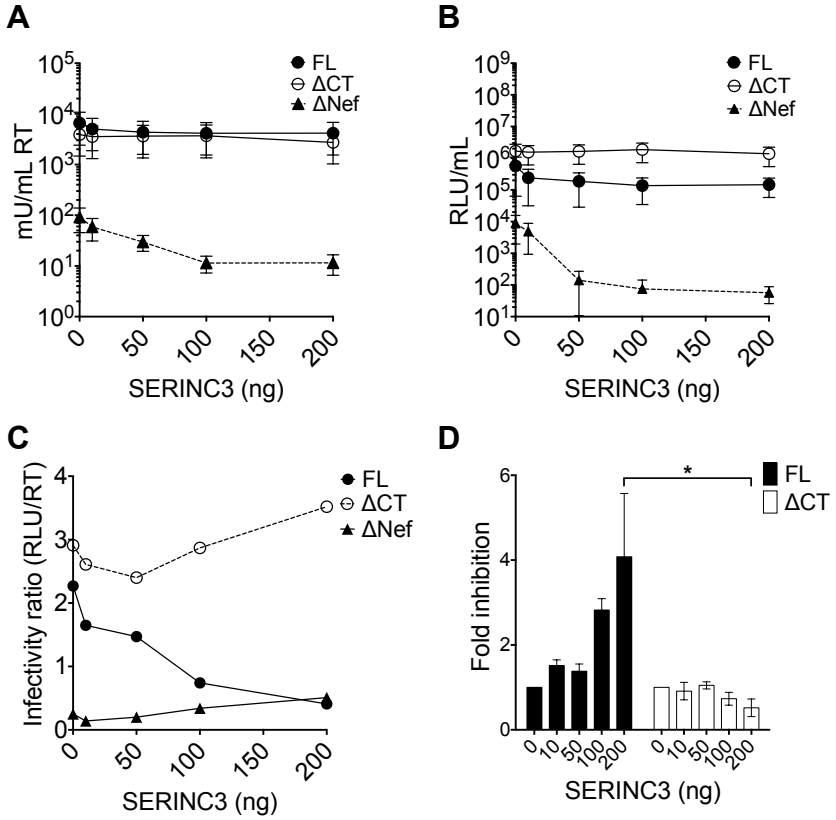

Figure 4.3 Truncating the HIV-1 EnvCT confers resistance to SERINC3 restriction. 293T cells were cotransfected with molecular clones encoding full-length HIV-1 NL4.3 FL isolates and ΔCT mutants alongside increasing doses of pcDNA-based SERINC5 plasmid. Virus containing supernatant was harvested after 48h for analysis. **(A)** Budding was measured by quantifying RT activity in supernatants by SG-PERT assay. **(B)** Infectivity was measured by titrating supernatant on to HeLa TZM-bl reporter cells and measuring luciferase activity (RLU). **(C)** Particle infectivity was calculated by normalising infectivity RLU to RT activity. A-C are data from a representative experiment. **(D)** Fold inhibition of viral infectivity was calculated by normalising RLU/RT measurements to 0ng SERINC5. Bar graphs represent fold inhibition from three independent experiments. Bars show mean and error bars represent mean +/- SEM. Fold inhibition at each dose of SERINC5 was compared using two-tailed unpaired t-test (*, $p<0.05$).

Turning to HIV-2, Figure 4.4A-B shows that budding of full-length replication competent HIV-2 FL and ΔCT viruses is unaffected by SERINC3 overexpression, similar to SERINC5. However, unlike SERINC5, SERINC3 overexpression did not inhibit HIV-2 infectivity, irrespective of EnvCT length (Fig. 4.4C-H). To confirm SERINC3 was expressed in these experiments, transfected 293T cell lysates were lysed for immunoblot analysis and probed for HA-tagged SERINC3 (Fig. 4.4I).

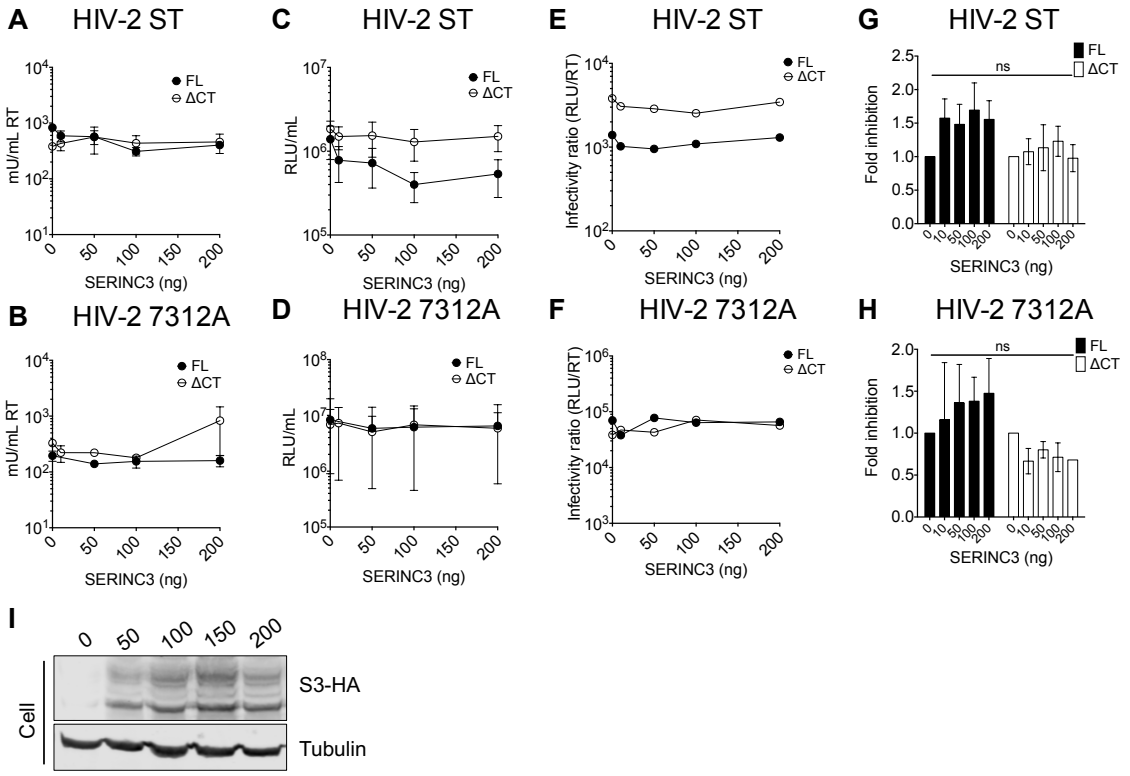

Figure 4.4 Truncating the HIV-2 EnvCT confers resistance to SERINC3 restriction. 293T cells were cotransfected with molecular clones encoding full-length HIV-2 FL isolates and ΔCT mutants alongside increasing doses of pcDNA-based SERINC3 plasmid. Virus containing supernatant was harvested after 48h for analysis. **(A-B)** Budding was measured by quantifying RT activity in supernatants by SG-PERT assay. **(C-D)** Infectivity was measured by titrating supernatant on to HeLa TZM-bl reporter cells and measuring luciferase activity (RLU). **(E-F)** Particle infectivity was calculated by normalising infectivity RLU to RT activity. **(G-H)** Fold inhibition of viral infectivity was calculated by normalising RLU/RT measurements to 0ng SERINC5. **(I)** Representative immunoblot of transfected 293T cell lysates confirming SERINC5 overexpression detected using antibody against HA-tagged SERINC3 (S3-HA). Bar graphs represent fold inhibition from three independent experiments. Bars show mean and error bars represent mean +/- SEM. Fold inhibition at each dose of SERINC5 was compared using two-tailed unpaired t-test (ns, $p>0.05$).

4.2.4 SERINC5 depletion does not rescue HIV-2 ROD10 FL infectivity.

In Chapter 3 I showed that the HIV-2ROD10 FL virus had a significant infectivity defect, in the absence of a budding defect, in HeLa cells and H9 cells (Fig. 3.7). One explanation for this might be that the long HIV-2 ROD10 EnvCT is recognised by an antiviral protein, which the virus is not adapted to antagonise directly, hence tail truncation is an evasion strategy. Sensitivity to SERINC5 restriction is dependent on the Env glycoprotein (Beitari et al., 2017; Rosa et al., 2015; Usami et al., 2015; Zhang et al., 2019a) and in the case of HIV-1, lab-adapted strains such as NL4.3 are more sensitive to restriction compared with primary isolates such as JRFL which are resistant (Beitari et al., 2017; Pye et al., 2020; Sood et al., 2017). Therefore, lab adaptation might explain differences in infectivity of HIV-2 ROD10 (lab-adapted) compared with HIV-2 ST and HIV-2 7312A (primary isolates) viruses with a full length EnvCT, whereby ST and 7312A FL viruses can replicate and spread but ROD10 FL cannot, possibly due to SERINC5 restriction. To test this hypothesis, I tested whether depletion of SERINC5 from virus producing 293T cells can rescue HIV-2 ROD10 FL virus infectivity. 293T SERINC3/5 CRISPR knockout cells were kindly gifted by Massimo Pizzato (University of Trento, Italy). SERINC KO cells were transfected with plasmid encoding HIV-2 ROD10 with a full length and truncated EnvCT, as explained previously. Figure 4.5A shows that there is no significant difference in the amount of HIV-2 ROD10 FL and ΔCT virions budding from SERINC5 KO cells. However, HIV-2 ROD10 FL virus remained non-infectious when titrated on to HeLa TZM-bl reporter cells (Fig. 4.5B), similar to observations reported in Chapter 3. This suggests that SERINC5 is not the dominant factor inhibiting HIV-2 ROD10 FL infectivity.

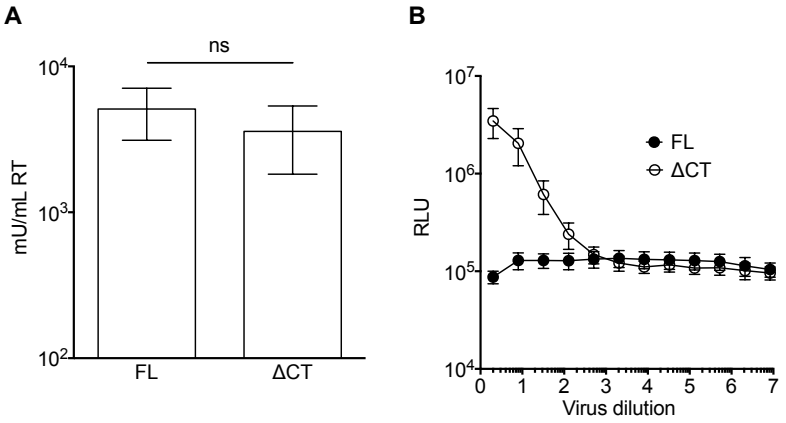

Figure 4.5 Effect of SERINC5 depletion on HIV-2 ROD10 infectivity. 293T SERINC5 knock out cells were transfected with infectious molecular clone HIV-2 ROD10 with a full length and truncated EnvCT for 48h. Virus containing supernatant was collected and purified to determine **(A)** the number of viral particles released by SG-PERT and **(B)** infectivity of virions when titrated on HeLa TZM-bl reporter cells from three independent experiments. Bars represent mean and error bars represent mean ± SEM. Groups were compared using two-tailed unpaired *t*-test (ns, p>0.05).

4.2.5 EnvCT truncation overcomes SERINC5 mediated inhibition of fusion.

Although the exact mechanism of SERINC5 restriction remains enigmatic, it has been shown that SERINC5 blocks fusion of viral and cellular membranes (Rosa et al., 2015; Sood et al., 2017; Usami et al., 2015) by preventing fusion pore expansion, rather than initiation of fusion (Sood et al., 2017). The BlaM-Vpr assay measures the delivery of β-lactamase (BlaM) into target cells following fusion (Fig. 4.6A). BlaM-Vpr is incorporated into virions and used to infect target cells. Target cells are loaded with a CCF2 dye, which is the substrate for BlaM, and therefore entry is detected by enzymatic cleavage of CCF2. The CCF2 substrate is added to cells 16h after infection and subsequent cleavage of CCF2 leads to a change in fluorescence which can be measured by flow cytometry. The percentage of cleaved CCF2 substrate is therefore a proxy for the fusion efficiency of the viral and target cell membranes. Here, the BLAM-Vpr assay was used to assess whether HIV-1 ΔCT virus is able to overcome the ability of SERINC5 to prevent fusion. Viruses were produced in 293T cells by co-transfection of full-length FL or ΔCT infectious molecular clones and 100ng SERINC5, a dose which potently inhibits HIV-1 FL but not NL4.3 ΔCT infectivity.

Figure 4.6B and 4.6C show that 40-50% of HeLa TZM-bl target cells contain BLAM-Vpr when infected with HIV-1 FL and ΔCT viruses in the absence of SERINC5 incorporation into virions at 16h post infection. To note, there was a consistent trend showing that ΔCT Env is more fusogenic than FL Env, although this did not reach statistical significance (Fig. 4.6B,C). Consistent with the notion that SERINC5 targets the step of viral fusion, a significant 6.5-fold reduction in fusion of HIV-1 FL virus was observed when virions were produced in the presence of SERINC5 (Fig. 4.6B,C). Notably, fusion of the HIV-1 ΔCT Env was unaffected by SERINC5 overexpression (Fig. 4.6B,C) consistent with this virus evading S5 restriction and inhibition of infection. As a negative control, HIV-1 ΔEnv viruses do not fuse with the target cell membrane, as Env is the viral fusion machinery which is absent in this virus (Fig. 4.6B,C). Also, treatment of infected cells with the T20 fusion inhibitor (Enfuvirtide), resulted in loss of fusion of all viruses as expected (Fig. 4.6D). These data reveal a mechanism for HIV-1 ΔCT Env overcoming SERINC5-mediated inhibition at the step of viral fusion.

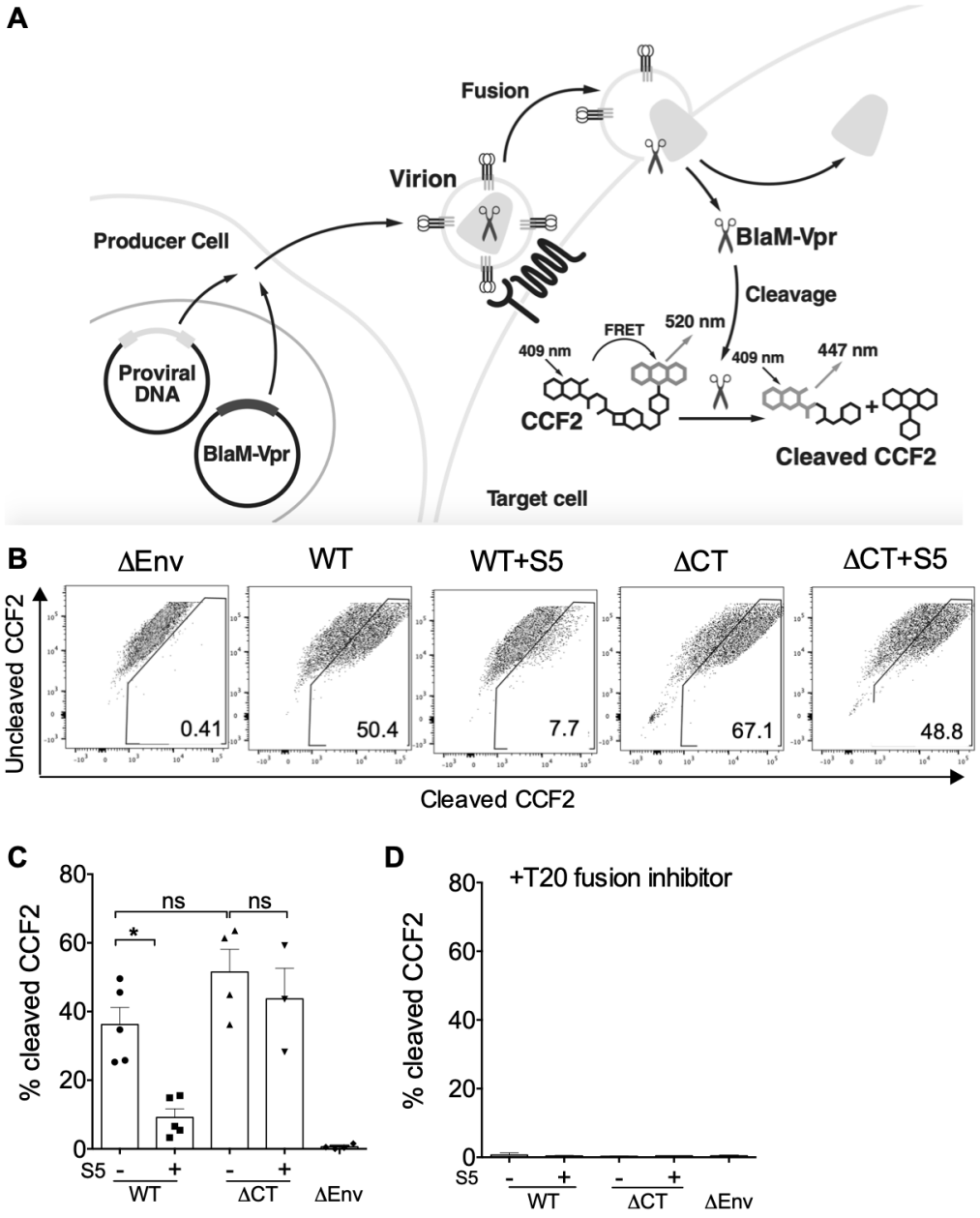

Figure 4.6 EnvCT truncation allows evasion of SERINC5-mediated inhibition of fusion. Viral fusion was measured by Blam-Vpr assay on HeLa TZM-bl cells using HIV-1 FL and ΔCT virions made in the presence or absence of 100ng SERINC5. **(A)** Schematic showing the BlaM-Vpr assay (Cavrois et al., 2002). Virus is produced by co-transfecting 293T cells with constructs encoding proviral DNA and BlaM-Vpr. Equal dose of BlaM-Vpr containing virions used to infect target HeLa TZM-bl cells for 16h. CCF2 substrate added to infected cells after 16h and CCF2 cleavage measured by a change in fluorescence using flow cytometry. **(B)** Representative flow cytometry dot plots indicating the percentage of CCF2 substrate cleavage. **(C)** Pooled data from five independent experiments. ΔEnv virus used as a negative control. **(D)** Pooled data from experiments carried out in the presence of 20 ug/mL T20 fusion inhibitor as another negative control. Bars represent mean and error bars represent SEM. Groups were compared using 2-way ANOVA multiple comparison analysis (ns, $P>0.05$; *, $P<0.05$).

4.2.6 Failure to incorporate SERINC5 into virions does not explain ΔCT resistance to SERINC5 restriction.

Virion incorporation of SERINC5 is likely to be a prerequisite for SERINC5 mediated restriction of fusion and infectivity (Rosa et al., 2015; Usami et al., 2015). Therefore, I explored the possibility that truncating the EnvCT perturbed SERINC5 incorporation into HIV-1 ΔCT virions, leading to evasion of restriction. To explore this hypothesis, HIV-1 virions were produced in 293T cells in the presence of 100ng SERINC5. Virus containing supernatants were harvested after 48h and purified for immunoblot analysis.

Figures 4.7A and 4.7B show that HIV-1 FL, ΔNef and ΔCT viruses all package SERINC5, despite differences in sensitivity to SERINC5-mediated restriction (Fig. 4.7C). Of note, HIV-1 ΔNef consistently incorporates more SERINC5, which can be explained by the absence of a functional Nef protein to downmodulate SERINC5 from the cell membrane (Fig. 4.7B). To investigate potential differences in the level of SERINC5 incorporation in FL and ΔCT virions, SERINC5 band intensity on western blots were normalised to that of p24 using the Image Studio Lite software and no significant differences were observed between FL and ΔCT virion incorporation of SERINC5 (Fig. 4.7B). SERINC5 is a transmembrane protein which recycles in vesicles during endocytosis and exocytosis, thus it is possible to detect contaminating vesicle associated SERINC5 in viral supernatants. To confirm that I was not detecting pelleted SERINC5 containing vesicles, 293T cells were transfected with plasmid encoding SERINC5 and supernatant was collected after 48h to be purified over a sucrose cushion and analysed by immunoblotting (S5 mock). Figure 4.7A shows that the S5 mock condition does not contain any SERINC5, therefore ΔCT virions do indeed incorporate SERINC5, despite being resistant to its effects on fusion and infectivity. Therefore, the resistance of HIV-1 ΔCT virus to SERINC5 restriction of virion fusion cannot be explained by failure to package SERINC5 into nascent virions, supporting the notion that SERINC5 incorporation is likely necessary but not sufficient for restriction.

4.2.7 EnvCT truncation does not prevent potential SERINC5-Env interactions.

Whether SERINC5 and Env physically interact on the plasma membrane of infected cells or in virions remains unclear (Chen et al., 2020b; Sood et al., 2017; Zhang et al., 2019a), but has important implications for understanding mechanism of SERINC5 restriction and viral evasion. Coimmunoprecipitation of Env and SERINC5 suggested that there is perhaps a direct interaction between the two surface proteins (Zhang et al., 2019a), however super resolution imaging of infected cells expressing SERINC5 revealed that Env and SERINC5 do not co-cluster on the cell surface (Chen et al., 2020b), questioning the presence of a direct interaction.

To investigate whether SERINC5 binds to HIV-1 Env, and if so whether this is EnvCT dependent, I performed a co-immunoprecipitation (Co-IP) assay. Briefly, 293T cells were cotransfected with Flag-tagged SERINC5 and plasmid encoding either HIV-1 FL, ΔCT, or ΔEnv, and SERINC5 was pulled down using α-FLAG antibody. Figure 4.7D shows that both the FL and ΔCT Env glycoproteins co-immunoprecipitated with SERINC5. Of note, the gp160 protein of HIV-1 ΔCT is smaller than FL Env and is therefore shifted lower on the immunoblot. As expected, no band was detected using α-gp120 serum in the ΔEnv condition (Fig. 4.7D). This data is suggestive of an interaction between SERINC5 and Env mediated by domains upstream of residue 722 in the EnvCT. Furthermore, evasion of SERINC5 restriction by ΔCT cannot be explained by a loss of any putative interaction between Env and SERINC5.

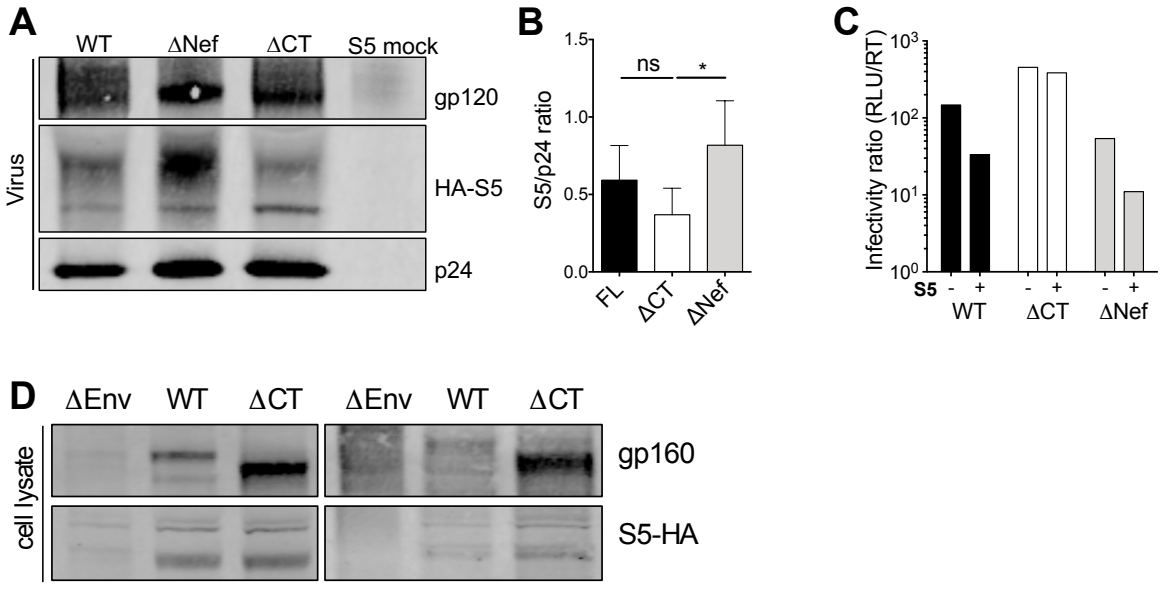

Figure 4.7 EnvCT truncation does not prevent SERINC5 incorporation into HIV-1 ΔCT virions. (A) Immunoblot analysis of purified virions probed for Env gp120, HA-tagged SERINC5 (S5-HA) and Gag p24. Supernatant from 293T cells that were transfected with SERINC5 plasmid only, was purified and probed to confirm that SERINC5 is expressed due to incorporation into virions rather than in endocytic and exocytic vesicles (S5 mock). **(B)** Quantification of SERINC5 incorporation normalised to Gag p24 from five independent experiments. **(C)** Infectivity of virions from the corresponding immunoblot in (A) to enable correlation between restriction and SERINC5 incorporation. **(D)** 293T cells cotransfected with FLAG-tagged SERINC5 (Flag-S5-HA) and plasmid encoding either HIV-1 FL, ΔCT and ΔEnv virus. Flag-SERINC5 was immunoprecipitated and proteins transferred to nitrocellulose and probed for HA-tagged SERINC5 and Env. Left panels of the immunoblot are the input and right panels are the immunoprecipitation. This is a representative immunoblot is shown. Bars represent mean and error bars represent SEM. Groups were compared using 2-way ANOVA multiple comparison analysis (ns, P>0.05; *, P<0.05).

4.2.8 EnvCT truncation dysregulates Env conformation and functionality.

The results presented in this chapter thus far demonstrate that EnvCT truncation allows for virion fusion in the presence of SERINC5, suggesting that truncation of the cytoplasmic tail confers functional changes on the extracellular domains of Env. This would suggest a mechanism of evasion in which EnvCT truncation alters the conformation of Env, thereby dysregulating the steps of viral entry, such that SERINC5 cannot inhibit this process. Therefore, I investigated whether the ΔCT mutation, which is associated with SERINC5 escape, is also associated with conformational changes to the extracellular domains of Env, that may contribute to SERINC5 evasion. To do this, neutralisation assays were performed using a panel of well-characterised broadly neutralising antibodies (bnAbs) against HIV-1. Neutralisation curves for VRC01 (recognises the CD4 binding site) (Zhou et al., 2010) and PGT151 (recognises the gp120:gp41 interface and functional trimers) (Falkowska et al., 2014) revealed that ΔCT virus was more susceptible to neutralisation by these gp120 targeting antibodies (IC50 of 0.02 and 0.04 μg/ml) compared with FL virus (IC50 of 0.31 and 0.46 μg/ml) (Fig. 4.8A,B). Conversely, ΔCT viruses were significantly more resistant to gp41 MPER targeting bnAbs 10E8 and 2F5 compared with FL (IC50 for ΔCT of 0.43 and >50 μg/ml versus FL of 0.04 and 1.5 μg/ml) (Fig. 4.8C,D).

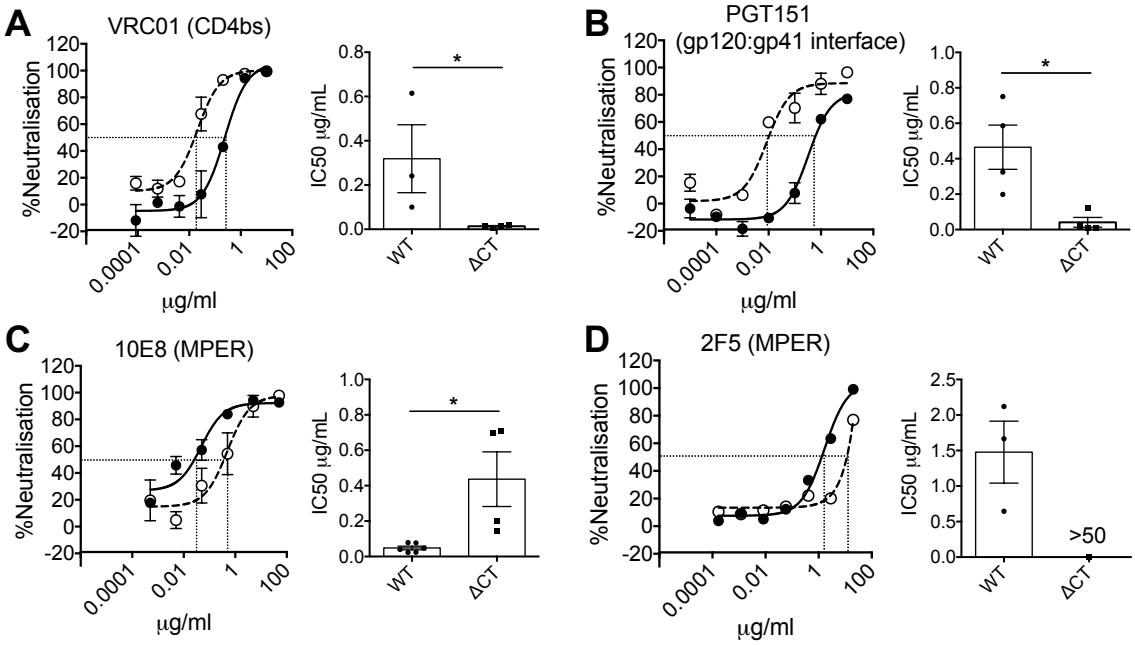

Figure 4.8 EnvCT truncation alters Env conformation in the absence of SERINC5. Equal infectious doses of virus were incubated with indicated broadly neutralising antibodies for 1h before infecting HeLa TZM-bl reporter cells. RLU measurements were taken using the luciferase assay and % neutralisation was calculated by normalising to highest concentration of bnAbs resulting in 100% neutralisation. **(A-D)** Neutralisation of HIV-1 FL (solid lines, black symbols) and ΔCT viruses (dotted lines, white symbols) by broadly neutralising antibodies. Representative neutralisation curves are shown. Bar charts show IC50 values from pooled independent experiments. Bars represent mean and error bars represent mean +/- SEM. Groups were compared using two-tailed unpaired t-tests (*, $p<0.05$).

Next, SERINC5 incorporated virions were tested in this assay to determine the effect of SERINC5 on susceptibility to bnAbs. Incorporation of SERINC5 into FL and ΔCT virus particles did not alter sensitivity to VRC01 and PGT151 (Fig. 4.9A-D). However, there was a trend towards altered sensitivity to MPER targeting antibodies, although most results were not statistically significant (Fig. 4.9E-H). These results are consistent with the hypothesis that truncation of the HIV-1 EnvCT alters the conformation of Env, allowing evasion from SERINC5.

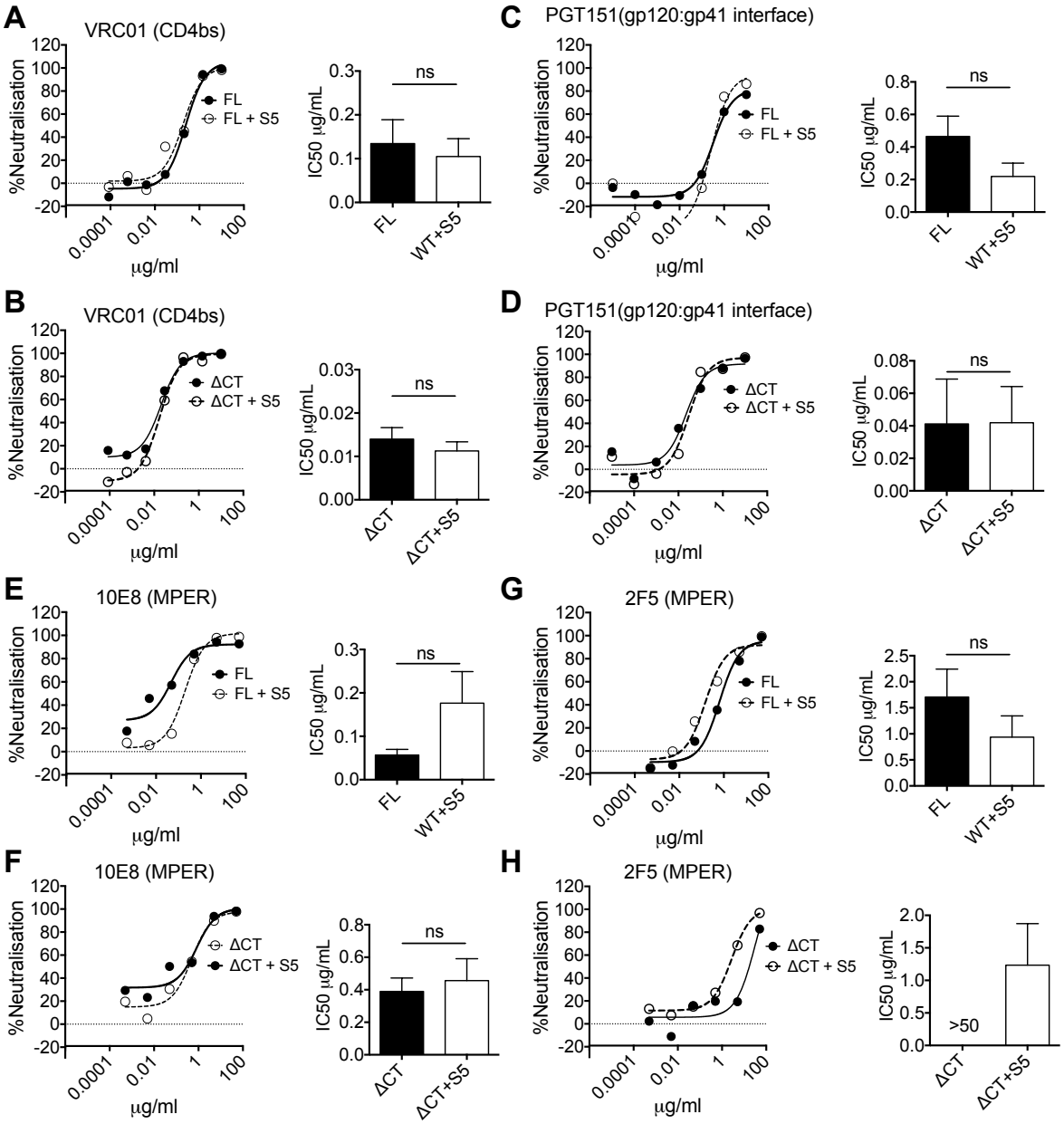

Figure 4.9 SERINC5 incorporation alters sensitivity to MPER targeting bnAbs. HIV-1 FL and ΔCT viruses were made in presence of 100ng SERINC5. Equal infectious doses of virus were incubated with indicated broadly neutralising antibodies for 1h before infecting HeLa TZM-bl reporter cells. **(A-H)** Neutralisation of HIV-1 FL and ΔCT viruses in the presence (solid lines, black symbols) and absence (dotted lines, white symbols) of SERINC5 in virus particles by broadly neutralising antibodies. Representative neutralisation curves are shown. Bar charts show IC50 values from three independent experiments. Bars represent mean and error bars represent SEM. Groups were compared using two-tailed unpaired t-test (ns, $p>0.05$).

Next, I tested neutralisation by 17b, which recognises a CD4-inducible epitope and is a coreceptor blocking antibody (Sullivan et al., 1998). Most strikingly, 17b neutralised HIV-1 FL with an IC50 of 0.25μg/ml, by contrast to HIV-1 ΔCT virus which was completely resistant to neutralisation (Fig. 4.10A). Pre-incubation of virus with soluble CD4 (sCD4) is expected to induce conformational changes in gp120 to open Env trimers and further expose cryptic epitopes including that recognised by 17b. To test if this would sensitise HIV-1 ΔCT to 17b, I first performed a neutralisation assay with sCD4 to determine a sub-inhibitory dose of sCD4. I selected 1μg/ml that resulted in approximately 25% neutralisation of both viruses (Fig. 4.10B), however even in the presence of sCD4, HIV-1 ΔCT virus remained completely resistant to 17b neutralisation (Fig. 4.10C). Interestingly, the sCD4 neutralisation curves (Fig. 4.9B) suggested that ΔCT Env required more sCD4 for neutralisation compared with FL (IC50 values >50 μg/mL and 5.3 μg/mL, respectively), consistent with EnvCT truncation influencing Env conformation and function.

Having shown that ΔCT virus is resistant to SERINC5 inhibition of fusion and that EnvCT truncation alters the conformation of the Env extracellular domains, I hypothesised that EnvCT truncation may also alter the processivity of Env-mediated fusion, especially given the knowledge that SERINC5 interferes with virus fusion and that ΔCT was fusion-competent in the presence of SERINC5. To test this, I performed a neutralisation assay with the fusion inhibitor T20. Fig. 4.10D shows that ΔCT virus was more sensitive to neutralisation by the T20 fusion inhibitor by comparison with FL virus (IC50 of FL 0.4μg/mL vs ΔCT 0.02μg/mL). Next, entry kinetics of HIV-1 FL and ΔCT virus was measured by performing a T20 chase assay. To do this, virus was incubated with cells and T20 added at various time points post-infection to determine at which point entry became resistant to fusion inhibition. Figure 4.10E shows that by 6h post-addition of virus, T20 was no longer able to inhibit HIV-1 FL fusion and block infection, indicating entry is complete. By contrast, at this same time point, only 50% of ΔCT infection was blocked, indicating that the ΔCT virus has altered entry kinetics (Fig. 4.10E). By 24h post-infection both FL and ΔCT viruses became resistant to T20 inhibition, suggesting that the process of entry was complete. It was intriguing that the HIV-1 ΔCT virus displayed slower entry kinetics than FL virus during the first 6hrs of entry, but eventually caught up with completion of entry between 16h (BLAM-Vpr assay) and 24h (T20 chase). To explore this further, I incubated HIV-1 FL and ΔCT viruses at 37°C for various times and measured Env-dependent viral infectivity. Figure 4.10F shows that ΔCT virus was significantly more stable than FL virus, the latter showing a time-dependent reduction in thermostability. Taken together, these data suggest that truncation of the HIV-1 EnvCT

confers conformational changes on Env that are reflected by altered neutralisation and viral fusion kinetics that may collectively contribute to evasion of SERINC5 restriction.

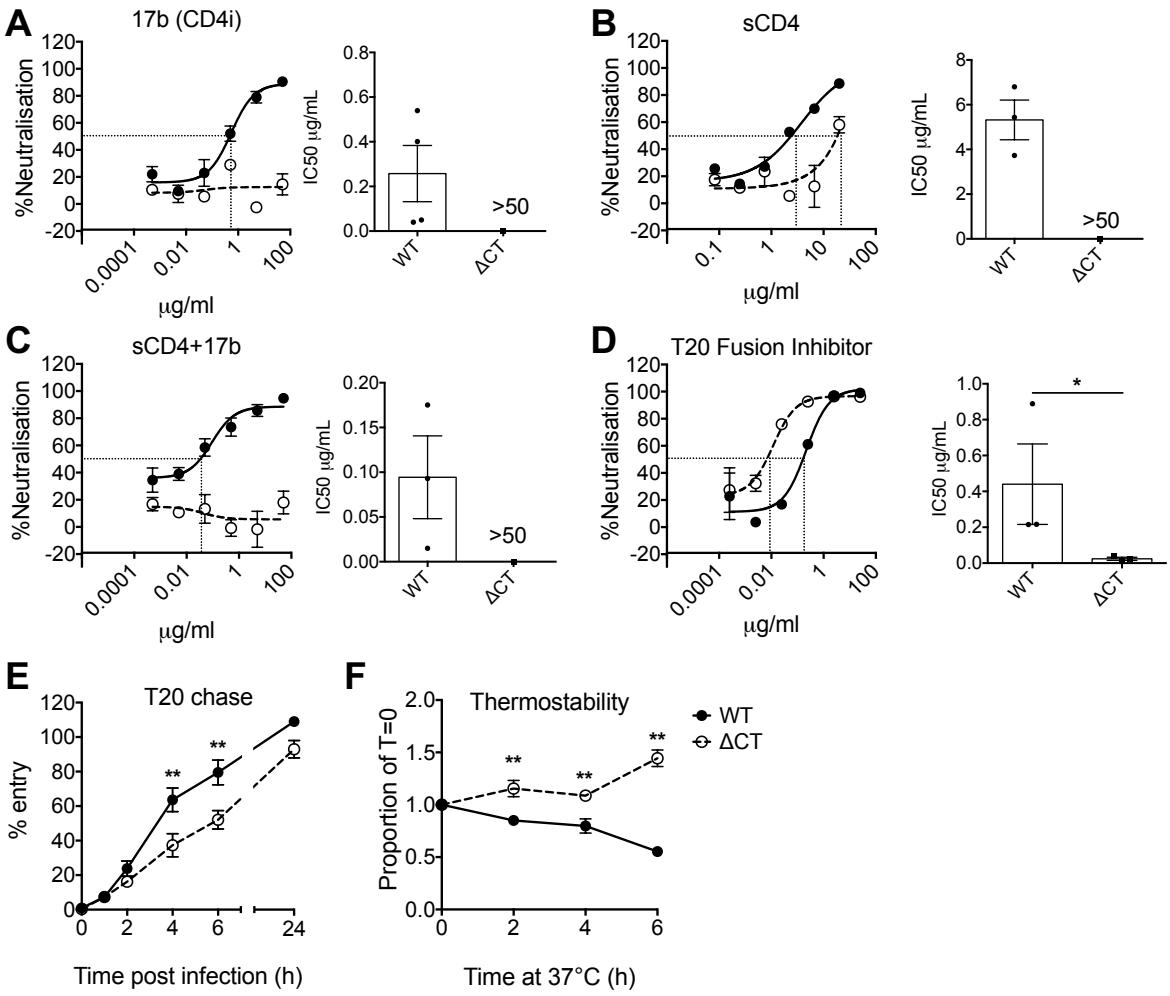

Figure 4.10 EnvCT truncation dysregulates Env functionality. (A-C) Neutralisation of HIV-1 FL (solid lines, black symbols) and ΔCT viruses (dotted lines, white symbols) by (A) 17b and **(B)** soluble CD4 (sCD4). **(C)** Viruses were preincubated with a subinhibitory dose of sCD4 for 1h before further incubation with 17b. Representative neutralisation curves are shown. Bar charts show IC50 values from pooled independent experiments. **(D)** A representative T20 neutralisation curve is shown, bar chart shows IC50 values from four independent experiments. **(E)** T20 chase assay. Virus was added to HeLa TZM-bl cells and T20 added after indicated times. Viral infection was measured after 48h by luciferase assay. Data shown as the percentage virus entry normalised to the untreated (no T20) control from three independent experiments. **(F)** Thermostability of Env measured by incubating virus at 37ºC for indicated time periods prior to infection of HeLa TZM-bl cells. Viral infection was measured 48h post infection by luciferase assay. Data are from three independent experiments. Bars represent mean and error bars represent mean +/- SEM. Groups were compared using two-tailed unpaired t-tests (ns, $p>0.05$; *, $p<0.05$; **, $p<0.01$).

4.2.9 Truncating the HIV-1 and HIV-2 EnvCT confers resistance to IFITM restriction.

So far in this chapter it has been established that HIV-1 and HIV-2 EnvCT domains modulate sensitivity to SERINC5-mediated restriction of fusion and viral entry. The IFITM proteins are another potent entry-targeting restriction factor family that can inhibit HIV-1 infection when present in producer and target cells (Foster et al., 2016; Lu et al., 2011a; OhAinle et al., 2018; Qian et al., 2015; Yu et al., 2015). Whether HIV-2 is similarly sensitive to IFITMs is less well understood. Here I investigated the effect of IFITMs in target cells on full length, replication competent HIV-2 viral infectivity. I also tested whether SERINC5 in virions can sensitise HIV-1 and HIV-2 viruses to IFITM proteins in the target cell, thereby investigating potential interplay between the two restriction factors which target the same stage of the viral life cycle. To do this, HA-tagged IFITM 1, 2 and 3 were expressed in the U87 cell line, expressing CD4 and either CXCR4 or CCR5 coreceptor, using lentiviral transduction. U87 cells were infected with equal RT units of HIV-1 FL and ΔCT mutants, made in the presence and absence of 100ng SERINC5 in 293T cells, for 24h before measuring infectivity by flow cytometry and viral output by SG-PERT. Figure 4.11A shows that HIV-1 FL virus infects 25% of control U87 cells, that do not overexpress IFITM proteins, and incorporation of SERINC5 does not significantly reduce infectivity by flow cytometry analysis. By contrast to HIV-1 FL virus, HIV-1 ΔCT viruses cannot infect U87 control cells in the presence and absence of SERINC5 in viral particles (Fig. 4.11A), suggesting that U87 cells are non-permissive for EnvCT truncation and therefore are not a suitable model to investigate restriction factors in. Figure 4.11B further reveals that whilst HIV-1 FL infection results in release of viral particles, HIV-1 ΔCT viral particles are not released explained by the lack of initial infection in Figure 4.11A. Turning to the effect of IFITMs on viral infectivity, HIV-1 FL infection was potently inhibited by IFITM1 but not IFITM2/3 and this pattern of IFITM restriction did not change in the presence of SERINC5 (Fig. 4.11C,D). Intriguingly, HIV-1 ΔCT viruses could not infect control or IFITM1 overexpressing U87 cells but could infect up to 13% of IFITM2 and IFITM3 overexpressing cells in the presence and absence of SERINC5 (Fig. 4.11E). However, SG-PERT analysis reveals that no ΔCT virus particles were released into the supernatant (Fig. 4.11F). Next, I tested HIV-2 infectivity in this system using U87-R5 cells. Surprisingly, Figure 4.11G and H show that HIV-2 FL and ΔCT viruses are restricted in U87-R5 as there is no detectable SG-PERT measurements above the background no RT controls. IFITM overexpression was confirmed by immunoblot analysis (Fig. 4.11I).

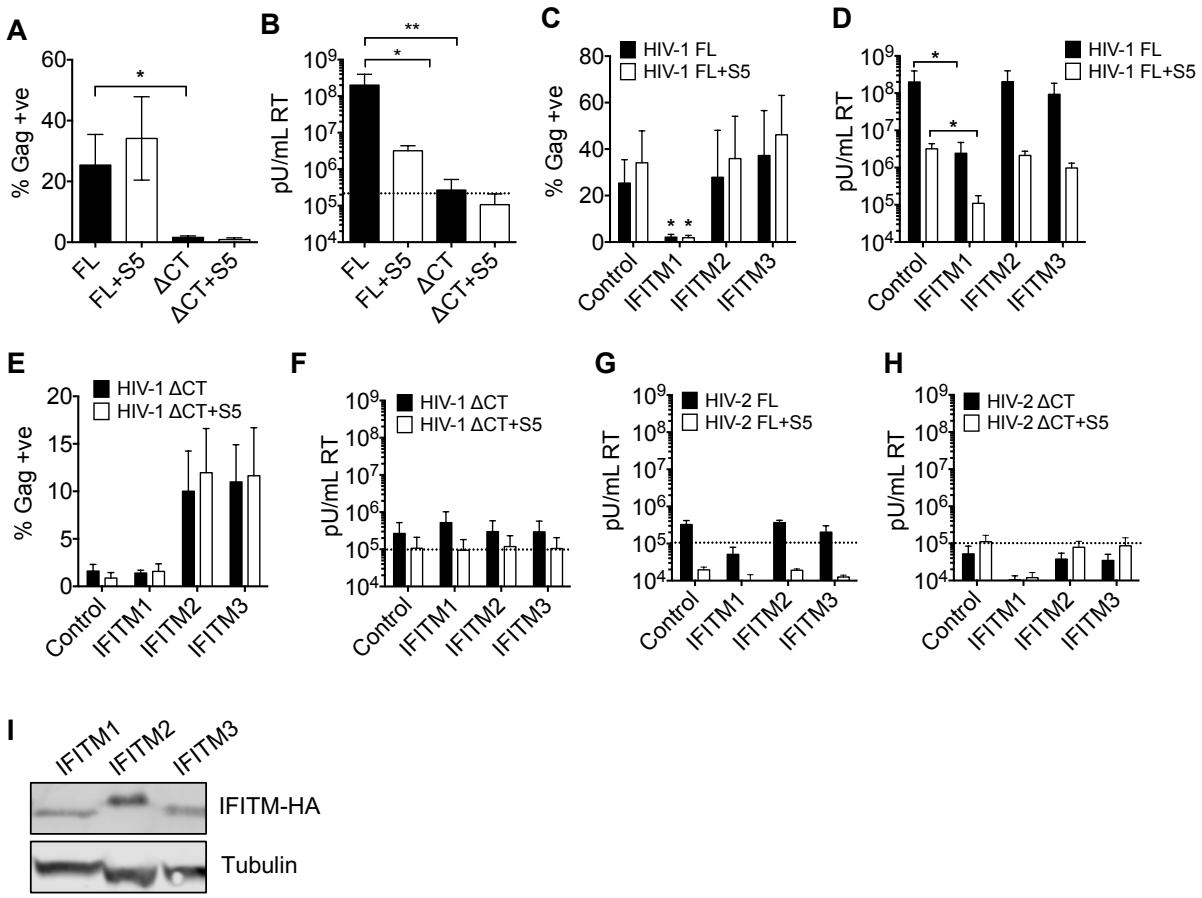

Figure 4.11 Effect of IFITM overexpression in U87 cells on HIV-1 and HIV-2 infectivity. U87-X4 and U87-R5 cells were transduced with pSIN vectors expressing IFITM1, IFITM2 or IFITM3 and selected using puromycin. To assess the effect of IFITM inhibition, viruses were produced in 293T cells in the presence and absence of 100ng SERINC5 plasmid. Equal RT units of virus were used to U87 cells for 24h and infection was measured by flow cytometry to detect Gag and by measuring the amount of budding viral particles using SG-PERT. **(A)** Percentage of infected U87-X4 cells not overexpressing IFITM proteins (control). **(B)** SG-PERT results from same experiments as A. Percentage of infected U87-X4 cells overexpressing IFITMs and SG-PERT measurements for **(C-D)** HIV-1 FL and **(E-F)** HIV-1 ΔCT viruses in the presence and absence of SERINC5 incorporated into virions. **(G-H)** Budding of HIV-2 virions from U87-R5 IFITM overexpressing cells. **(I)** IFITM overexpression was confirmed by immunoblot analysis of transduced cells. Dotted lines represent background RT activity determined by no RT control. Bars show mean and error bars represent mean +/- SEM from three independent experiments. Infectivity and SG-PERT inhibition was compared using 2-way ANOVA test (*, $p<0.05$; **, $p<0.01$).

HIV-1 ΔCT virus was restricted in control U87 cells, suggesting that this cell line is non-permissive for EnvCT truncation, thus not a tractable model for investigating the effect of restriction factors. Therefore, I tested the effect of IFITM overexpression in HeLa TZM-bl reporter cells, where I have already established that HIV-1 ΔCT and HIV-2 viruses do not have an infectivity defect. HA-tagged IFITM 1, 2 and 3 were expressed in the HeLa TZM-bl reporter cell line using lentiviral transduction and expression of HA-tagged IFITMs were measured by flow cytometry (Fig. 4.12A). To validate this assay, I showed that the transmitted/founder virus HIV-1 CH058 was resistant to IFITM proteins as reported previously (Fig. 4.12B) (Foster et al., 2016) and that VSV-G pseudotyped HIV-1 ΔEnv virus is restricted by IFITM3 (Fig. 4.12C), also as previously described (OhAinle et al., 2018; Qian et al., 2015). Next, IFITM-expressing cells were infected with equal RT units of HIV-1 and HIV-2 FL or ΔCT viruses and infection measured. Figure 4.12D shows that HIV-1 FL virus was potently restricted up to 50-fold by IFITM1 but not IFITM2/3, the former being plasma membrane localised and the latter mainly located in early and late endosomes (Foster et al., 2016; Weston et al., 2014), consistent with HIV-1 entering by fusion at the plasma membrane. No difference in IFITM inhibition was observed when HIV-1 FL virus was produced in the presence of SERINC5, (Fig. 4.12E), demonstrating that SERINC5 does not alter HIV-1 sensitivity to IFITM proteins. Notably, HIV-1 ΔCT virus was completely resistant to IFITM 1, 2 and 3 (Fig. 4.12D) similar to what was observed for SERINCs, and SERINC5 did not sensitise ΔCT virus to IFITM restriction (Fig. 4.12E). Turning to HIV-2, Figure 4.12F shows that HIV-2 FL was also restricted by IFITM1, and again SERINC5 incorporation did not alter sensitivity of this virus to IFITMs (Fig. 4.12G). Like HIV-1, I found that EnvCT truncation allowed HIV-2 ΔCT virus to evade IFITM1-mediated inhibition (Fig. 4.12F) and incorporation of SERINC5 into HIV-2 ΔCT virions did not alter sensitivity to IFITM proteins (Fig. 4.12G).

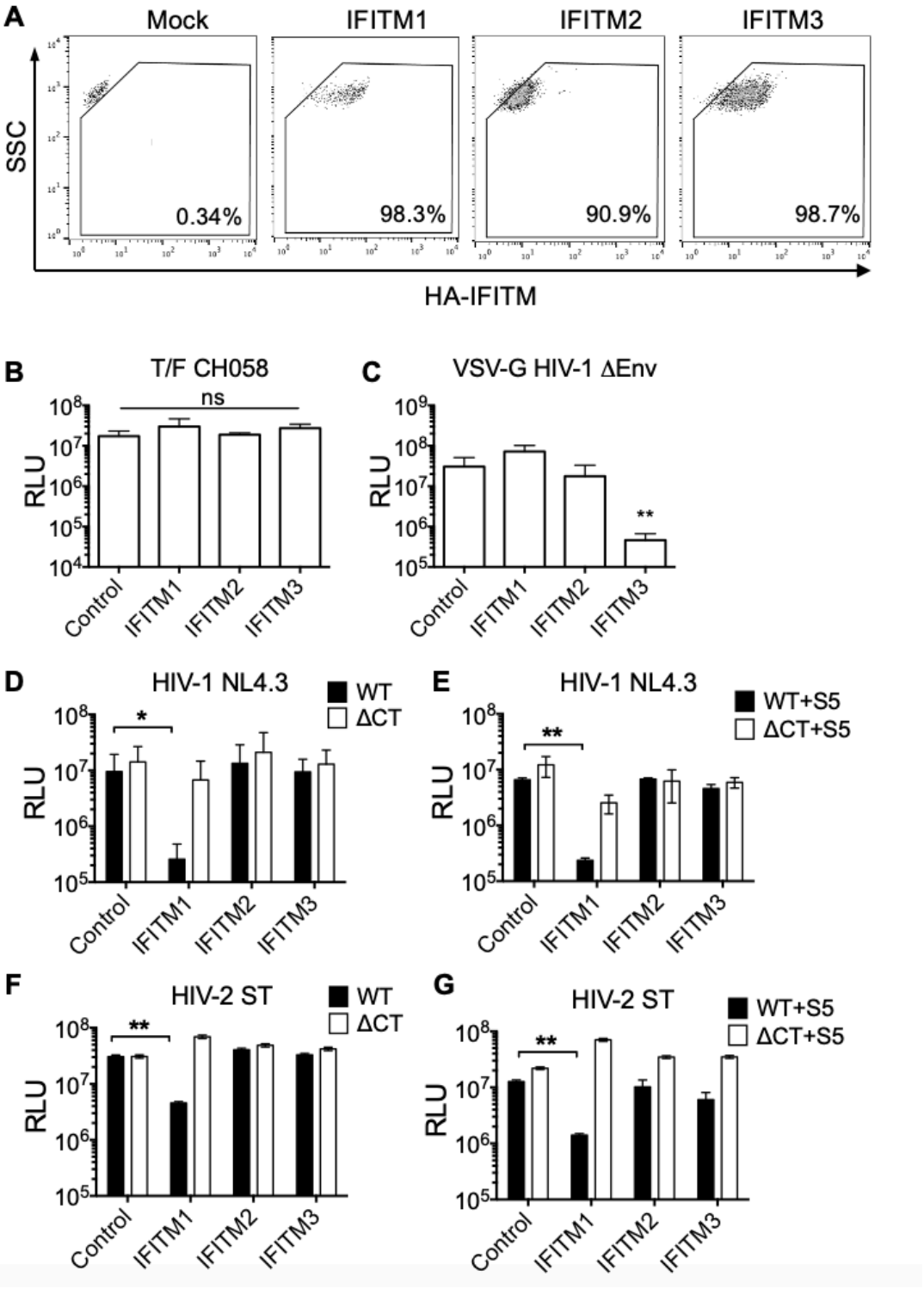

Figure 4.12 HIV EnvCT truncation confers resistance to IFITM1 in HeLa TZM-bl cells. TZM-bl cells were transduced with pSIN vectors expressing IFITM1, IFITM2 or IFITM3 and selected using puromycin. **(A)** Flow cytometry plots confirm expression of HA-tagged IFITM proteins in TZM-bl cells after selection. **(B-G)** Control TZM-bl cells (no IFITM overexpression) and IFITM overexpressing TZM-bl cells were infected with equal RT units of virus for 24 h. Infectivity was measured using the luciferase assay. Bars show mean and error bars represent mean +/- SEM from three independent experiments. Infectivity inhibition was compared using 2-way ANOVA test (*, $p<0.05$; **, $p<0.01$).

4.2.10 EnvCT truncation does not alter sensitivity of HIV-2 viruses to Tetherin.

The results presented in this Chapter so far suggest that truncation of the EnvCT leads to global conformational changes in Env. HIV-2 viruses have evolved to use Env to antagonise the restriction factor Tetherin (Le Tortorec and Neil, 2009), which potently inhibits lentiviral infection by tethering budding virions to the surface of virus producer cells (Neil et al., 2008; Van Damme et al., 2008). Coimmunoprecipitation assays show that HIV-2 Env interacts with Tetherin, resulting in its downmodulation from the cell surface. This interaction is dependent on the conserved YxxL endocytic motif, however a specificity determinant is also required which is present in the extracellular domain of Env (Le Tortorec and Neil, 2009). Therefore, I next tested whether the conformational changes induced by EnvCT truncation resulted in altered HIV-2 sensitivity to Tetherin. 293T cells were cotransfected with full length infectious molecular clones and increasing doses of HA-tagged Tetherin for 48h. After 48h, the virus containing supernatant was purified and the amount of virus budding from the cells was quantified using the SG-PERT assay. As expected, Figure 4.13A and 4.13B show that HIV-1 ΔVpu virus is potently restricted up to 100-fold by only 50ng of Tetherin overexpression. This is because the HIV-1 Tetherin antagonist, Vpu, is not expressed by this mutant virus. By contrast, virus release was rescued in the presence of Vpu (HIV-1 FL), although higher doses of Tetherin overexpression overwhelm Vpu activity, leading to a dose-dependent reduction in virus release by up to 6-fold (Fig. 4.13A,B). Truncation of the HIV-1 EnvCT had no effect on viral budding (Fig. 4.13A,B). Further, Figure 4.13B-D show that HIV-2 viruses with a full length and truncated EnvCT are comparably sensitive to Tetherin, with a maximum of 3-fold inhibition of HIV-2 ST and 5-fold inhibition of HIV-2 7312A. This data confirms that HIV-2 Env is a potent antagonist of Tetherin and truncation of the EnvCT does not significantly alter the potency of this function.

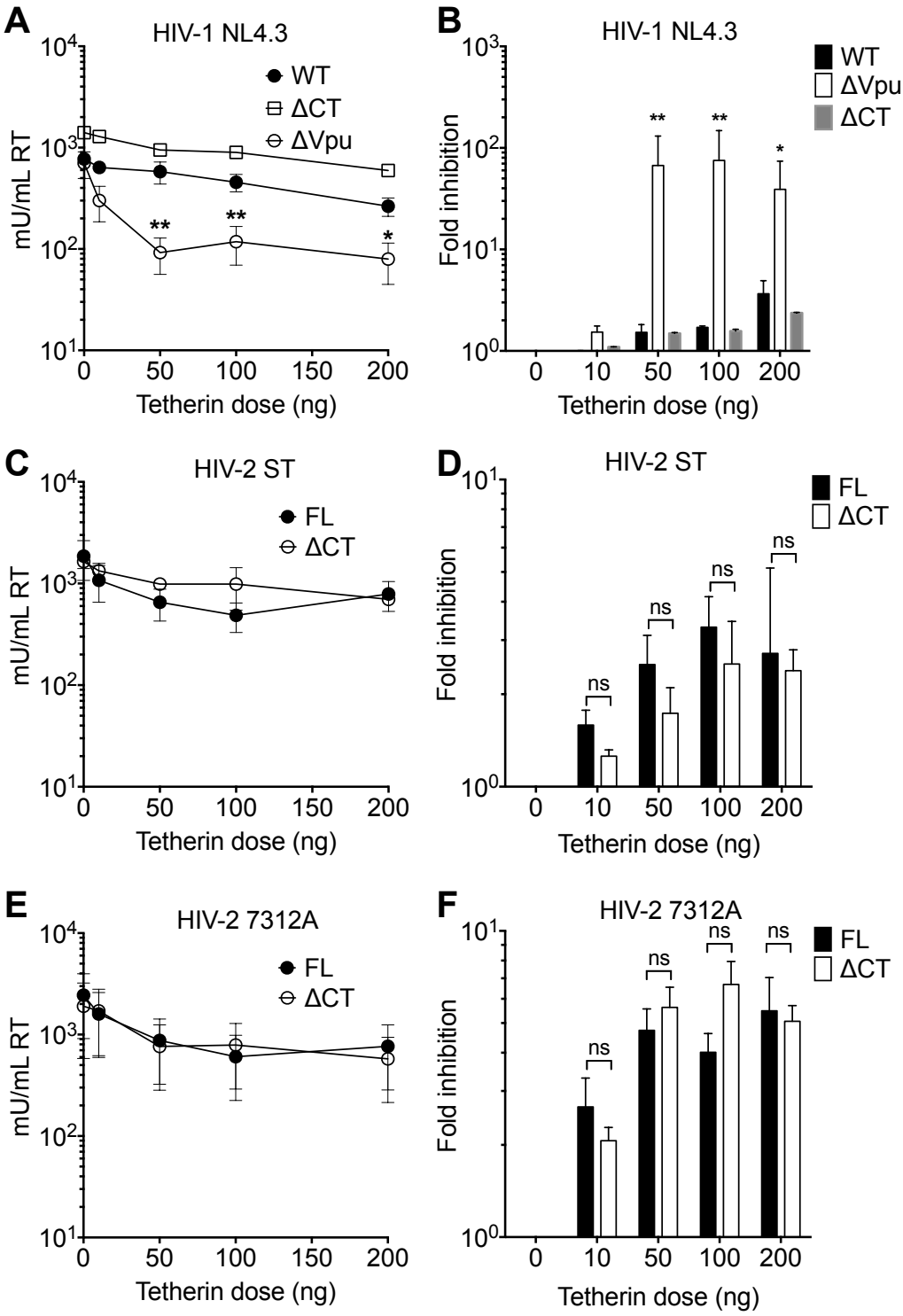

Figure 4.13 Sensitivity of HIV-2 ΔCT viruses to Tetherin. 293T cells were cotransfected with increasing doses of plasmid encoding Tetherin and full length infectious molecular clones of **(A-B)** HIV-1 NL4.3, **(C-D)** HIV-2 ST and **(E-F)** HIV-2 7312A. Virus containing supernatant was collected after 48h and purified for SG-PERT analysis. Fold inhibition was calculated by normalising the amount of virus released at each dose Tetherin overexpression to no Tetherin overexpression (0ng) from three independent experiments. Bars represent mean and error bars represent mean ± SEM. Groups were compared using two-tailed unpaired *t*-test (ns, $p>0.05$; *, $p<0.05$).

4.3 Discussion

In this chapter I have uncovered a mechanism by which HIV-1 and HIV-2 can evade restriction by two potent entry targeting restriction factors, SERINC3/5 and the IFITM proteins. Both families of restriction factors inhibit viral entry at the step of viral fusion and display an Env-dependent phenotype (reviewed by (Foster et al., 2017)). The results in this chapter suggest a commonality in the mechanism of HIV evasion, in which truncation of the EnvCT allows both HIV-1 and HIV-2 to escape inhibition.

SERINC5 restricts viral entry by inhibiting fusion of HIV-1 virions with target cell membranes (Rosa et al., 2015; Sood et al., 2017; Usami et al., 2015). Currently, three broad, but not mutually exclusive, mechanisms for how SERINC5 operates to restrict HIV-1 entry have been proposed, including: **(1)** inhibition of fusion pore formation during viral entry into target cells (Rosa et al., 2015; Sood et al., 2017; Usami et al., 2015); **(2)** spontaneous inactivation of Env trimers (Sood et al., 2017; Zhang et al., 2019a) and **(3)** disruption of Env clustering on membranes (Chen et al., 2020b). Given that viral fusion and entry requires a series of well-orchestrated, sequential Env-dependent events, it is likely that SERINC5 may target any or all of these processes to inhibit the final step in Env-mediated entry, viral fusion. In this chapter, I have shown that truncation of the EnvCT bypasses the SERINC5-mediated block to viral fusion and entry. Importantly, evasion from restriction is not due to complete exclusion of SERINC5 from ∆CT viral particles, consistent with the notion that SERINC5 incorporation is necessary but not sufficient for restriction of HIV-1 infection. This is supported by the identification of SERINC5 mutants which cannot restrict HIV-1 despite being efficiently packaged into virions (Pye et al., 2020). The effect of mutations in extracellular loops (ECL) 3 and 5 of SERINC5, on HIV-1 infectivity, was tested in a single round replication assay, similar to that which was used in this chapter. Mutations in ECL3/5 result in a 10-fold decrease in restrictive activity, relative to wildtype SERINC5 (Pye et al., 2020). Further, virus produced in the presence of these SERINC5 mutants also resulted in loss of sensitisation to antibody neutralisation (Pye et al., 2020). The involvement of SERINC5 ECLs in mediating HIV-1 restriction suggests that the extracellular conformation of SERINC5 might be important in determining restrictive activity and in increasing viral sensitivity to antibody neutralisation. Therefore, the external surface of the virion, where SERINC5 ECLs, Env MPER and the Env gp120 surface subunit are found, must be important in SERINC5 restriction mechanism. Indeed, data in this chapter supports this notion and suggests that removing the EnvCT alters the ectodomain conformation and functionality of Env, which disarms SERINC5's restrictive ability.

Whether SERINC5 directly or indirectly interacts with HIV-1 Env to exert its negative effects on fusion and infectivity remains controversial. Coimmunoprecipitation assays in this study and by others (Zhang et al., 2019a) would suggest that there is an interaction occurring between the two proteins, although it is unclear where and when this interaction would occur. My results suggest that potential interactions between SERINC5 and Env is upstream of residue 722 in HIV-1, as the remainder of the EnvCT is absent in this mutant. In line with this, Env MPER has been suggested to be a potential binding partner of SERINC5 extracellular loops (ECL) 3 and 5 (Pye et al., 2020), although this is not based on any direct evidence but rather on modelling Env and SERINC5 structures within the plasma membrane. An alternative interpretation of the coimmunoprecipitation data is that the interaction between Env-SERINC5 may not be one that allows for SERINC5 restriction. In other words, the nature of the interaction between SERINC5 and ΔCT Env may be different to that which is formed between SERINC5 and FL Env (due to conformational differences between FL and ΔCT Env), such that SERINC5 is unable to induce sufficient conformational changes to the MPER, which would usually induce further changes to gp120 via allostery. Also, coimmunoprecipitation assays are carried out on cell lysates rather than virus particles, which means it is possible that SERINC5-Env interactions occur in producer cells during Env and SERINC5 trafficking to sites of viral assembly, which can either be direct or indirect using host proteins that act as bridging factors between SERINC5 and Env. If this scenario were to be true, premature SERINC5-Env interactions during trafficking would not enable SERINC5 to physically block fusion, as Env is not in the correct location (i.e., not at the plasma membrane, at sites of virus assembly and budding). These interactions may be transient and therefore lost upon virus budding and maturation, possibly due to the removal of a yet to be identified host bridging factor which facilitates SERINC5-Env interactions. Taken together, I propose that any direct interaction occurring between SERINC5 and ΔCT Env is probably non-functional, explained by the differences in Env ectodomain conformation that are indirectly induced by SERINC5.

A key finding in this chapter is that the ΔCT Env has a dysregulated conformation, which impacts on its sensitivity to SERINC5 and IFITM proteins. One of the primary functions of Env, and the target of SERINC5 and IFITM, is the ability to mediate fusion of the viral and target cell membranes. Therefore, I studied the effect of altered conformation on Env functionality, to gain a better understanding of how and why the ΔCT Env is able to evade restriction. Adopting a more closed conformation would impact the ability of ΔCT Env to carry out the process of fusion and entry efficiently, as conformation can have a direct impact on all the steps of viral entry, starting with CD4 receptor binding. In line with this, I have shown that (1) HIV-1 ΔCT is less sensitive to sCD4, suggesting that it may

bind poorly to the primary CD4 receptor on target cells; (2) it is less sensitive to 17b, suggesting that it may bind poorly to coreceptor or is perhaps entering cells in a co-receptor independent manner; (3) HIV-1 ΔCT has slower initial entry kinetics up to 6h post infection and (4) HIV-1 ΔCT infection is more sensitive to T-20 fusion inhibitor. An increased sensitivity to T-20 inhibition and VRC01/PGT151 neutralisation might be explained by the observation that HIV-1 ΔCT viruses enter target cells at a slower rate, by comparison with HIV-1 FL viruses. Thus, ΔCT Env trimers are possibly exposed to the extracellular environment for a longer period of time and are therefore more vulnerable to the blocking effects of bnAbs and T-20. Intriguingly, SERINC5 and IFITMs are also naturally occurring fusion inhibitors expressed by cells, which ΔCT viruses are not sensitive to (by comparison with T-20), thereby suggesting that perhaps the mechanism of fusion inhibition between T-20 and SERINC5/IFITMs differs. For example, SERINC5 might recognise and block a fusion intermediate conformation that ΔCT Env is less likely to adopt due to conformational and fusion dysregulation, thereby bypassing restriction. Alternatively, this data could indicate that SERINC5 indirectly inhibits fusion, rather than physically interacting and blocking the conformational changes that occur in Env during fusion. Some previous studies have shown that truncation of the EnvCT leads to decreased sensitivity to fusion inhibitors such as T-20 and C34 (Abrahamyan et al., 2005; Wyss et al., 2005). However, these studies investigated fusogenicity of HIV-1 ΔCT mutants in a cell-cell fusion assay rather than in the context of a full-length replication competent virus infection. Also, Abrahamyan *et al* (2005) truncated a larger portion of the EnvCT, including the YxxL endocytic motif, compared with the ΔCT mutant used in this study. Therefore, it is possible that the length of the EnvCT determines the extent of conformational change taking place in the Env ectodomain, ultimately determining sensitivity to different fusion inhibitors.

Further, truncating the HIV-1 EnvCT leads to dysregulated fusion, as suggested by slower HIV-1 entry kinetics, despite a consistent trend towards increased fusogenicity in the BlaM-Vpr assay by comparison with FL Env. This suggests that although HIV-1 ΔCT is able to fuse with target cells, the initial stages of fusion and entry (up to 6h post infection) are slower. It is currently difficult to examine exactly which stage of entry is the rate limiting step for HIV-1 ΔCT, but neutralisation data suggest that the ΔCT Env is less efficient at binding CD4 receptor and coreceptor. Alternatively, it is possible that the HIV-1 EnvCT acts as a safety catch to prevent premature activation of Env fusogenicity. It has been postulated that the EnvCT interacts with Gag prior to viral release and this interaction may prevent premature Env trimer 'opening' (Wyma et al., 2000). Once Gag is cleaved during maturation, the EnvCT would be released from this block in order to fuse efficiently with target cell membranes. In the case of ΔCT viruses, the lack of this

safety catch could lead to significantly more ΔCT Env trimers undergoing spontaneous inactivation, due to which viral entry takes a longer period of time, as more functional ΔCT Env trimers are required to complete the process. Regulation of Env-mediated fusion by the cytoplasmic tail is not limited to the lentiviral family. Gamma retroviruses such as Murine Leukaemia virus (MLV) have a short 16 amino acid EnvCT called the R peptide, which is cleaved to activate the fusogenic potential of Env. Therefore, it is possible that the long lentiviral EnvCT plays a similar role in regulating fusion. The R peptide is cleaved by the viral protease enzyme after virions are released from cells, and it is thought that this is a mechanism by which premature Env activation is prevented (Green et al., 1981; Henderson et al., 1984; Schultz and Rein, 1985). Comparisons between virus with and without the R peptide reveal that the presence of R peptide or mutants that are defective for R-peptide cleavage, have significantly reduced ability to form syncytia (Januszeski et al., 1997; Kim et al., 2000; Kubo et al., 2007; Melikyan et al., 2000; Ragheb and Anderson, 1994; Rein et al., 1994; Taylor and Sanders, 2003; Yang and Compans, 1996, 1997). Therefore, the R peptide is a negative regulator of fusion and acts as a safety catch to prevent activation of Env prior to virus budding and maturation. Release of R peptide from the transmembrane domain of MLV Env activates the fusogenic potential of Env, thereby allowing fusion of viral and cellular membranes (Kubo et al., 2012). Whether HIV-1 and HIV-2 EnvCT truncation increases fusogenicity of lentiviral Env glycoproteins is unclear, as there is much discordance in the current literature. This is likely explained by differences in experimental set up (cell-cell fusion vs fusion in the context of viral infection) and also differences in the truncation mutants used, as the length of EnvCT removed probably determines how much change occurs in conformation and therefore Env functionality.

The presence of SERINC5 in HIV-1 FL particles induces spontaneous inactivation of HIV-1 Env trimers, leading to premature gp120 shedding, although exactly how this would happen remains to be elucidated (Sood et al., 2017). Therefore, SERINC5 is able to disrupt the intrinsic stability of Env trimers in order to induce spontaneous inactivation. Here I show that the SERINC5 resistant HIV-1 ΔCT Env has increased thermostability compared with FL Env, as incubation at 37°C for up to 6h has no significant impact on viral infectivity. Therefore, truncation of the EnvCT increases Env stability which prevents SERINC5 from inducing spontaneous inactivation. Increased ΔCT Env stability can further explain the findings that HIV-1 ΔCT infection levels eventually become equivalent to HIV-1 FL infection at 24 hours post infection, and that the BLAM-Vpr assay, in which readouts are taken at 16h post infection, revealed comparable fusogenicity of FL and ΔCT Env, despite slower entry kinetics. Collectively, these data suggest that the ΔCT Env is conformationally dysregulated, probably fixed in an intrinsically hyper-stable

conformation, in turn impacting in its ability to fuse with target cells, leading to evasion of SERINC5 and IFITM inhibition of fusion. This data might also suggest that SERINC5 potentially recognises a late fusion intermediate or post fusion conformation of FL Env, which ΔCT Env is less frequently/efficiently adopting and is thereby evading restriction.

Another explanation for dysregulated fusion could be that conformational differences in ΔCT Env enables it to undergo a different set of sequential conformational changes in order to complete fusion, including differences in fusion stoichiometry. This is a plausible explanation given that comparison of receptor stoichiometry, that is the number of Env glycoproteins required for fusion initiation, differs between X4- and R5-tropic viruses (Iliopoulou et al., 2018). Whilst the X4-tropic HxB2 isolate requires two Env spikes to complete fusion, R5-tropic JRFL requires only one Env spike (Iliopoulou et al., 2018). Therefore, it is possible that truncation of the EnvCT alters the receptor stoichiometry required for fusion initiation, which ultimately impacts the series of conformational changes that Env trimers undergo during fusion. Alternatively, the Env thermostability data in this study shows that ΔCT Env is more stable and neutralisation data suggest that it is in a more closed conformation compared with FL Env. Therefore, ΔCT Env adopts a stable, closed conformation which might prevent SERINC5 and IFITMs from inducing further conformational changes in Env, which is necessary for fusion inhibition and entry. Unliganded HIV-1 Env are intrinsically dynamic and transition between 3 distinct prefusion conformations, as measured by insertion of fluorophores in gp120 variable loops for single molecule FRET studies (Munro et al., 2014). The SERINC5-resistant JRFL Env exhibits reduced intrinsic dynamics compared with HxB2 Env, which can have implications for receptor stoichiometry. Therefore, ΔCT Env might have restricted intrinsic behaviour, similar to JRFL Env, perhaps leading to restricted movement of the Env ectodomain following CD4 and coreceptor binding, resulting in slower, inefficient initiation of fusion. Of course, after approximately 6h ΔCT Env overcomes this barrier and is able to fuse, perhaps by forming a sufficient number of Env clusters to overcome the fusion stoichiometry. Further evidence to suggest that the cytoplasmic tail can regulate Env stability comes from observations made using SIV viral particles with a truncated LLP-1 region, found at the C-terminus of the EnvCT. Truncation of LLP-1 by insertion of stop codons in the EnvCT sequence results in the production of poorly infectious virus as tested in a single-round infectivity assay (Affranchino and Gonzalez, 2006). Immunoblot analysis reveal that significantly less gp120 is incorporated into LLP-1 truncated viruses by comparison with FL Env, despite comparable incorporation of gp41 (Affranchino and Gonzalez, 2006). This cannot be explained by defective gp120 production in transfected cell lysates, which suggests that LLP-1 truncation results in enhanced gp120 shedding on virions, hence reduced stability

and consequent spontaneous inactivation of mutant Env trimers (Affranchino and Gonzalez, 2006). Taken together, these data suggest that the lentiviral EnvCT is indeed a regulator of two important parameters, conformation and stability, both of which determine Env functionality and evasion of entry-targeting restriction factors.

SERINC5 sensitivity has been mapped to the gp120 variable loops, especially the V3 loop (Beitari et al., 2017; Usami et al., 2015; Zhang et al., 2019a). The conformation of Env is dictated by the positioning and accessibility of the V3 loop for coreceptor binding and initiation of fusion. When Env is in a closed, prefusion state, the V3 loop is occluded by V1/2 and therefore the coreceptor binding site is largely inaccessible (Bartesaghi et al., 2013; Lyumkis et al., 2013; Ozorowski et al., 2017; Pancera et al., 2014). Here I show that both HIV-1 (X4-tropic) and HIV-2 (R5-tropic) full length, replication competent viruses are sensitive to SERINC5 overexpression. Thus, the coreceptor usage function of the V3 loop does not explain how V3 determines sensitivity to SERINC5. Rather, Env conformation and functionality, which are regulated by the long EnvCT, determine sensitivity to SERINC5. SERINC5-resistant HIV-1 ΔCT infection is insensitive to neutralisation by 17b, which binds to the coreceptor binding site in the V3 loop. This suggests that truncation of the EnvCT may enable Env to adopt a more closed conformation, compared with HIV-1 FL Env trimers. This is also supported by the observation that ΔCT infection is resistant to neutralisation by bnAbs targeting the MPER of gp41. These bnAbs have previously been described to bind 'cryptic' epitopes in MPER (Chen et al., 2020b; Sood et al., 2017), which are transiently exposed when Env trimers adopt a fusion-intermediate conformation (Frey et al., 2008). Therefore, reduced sensitivity to 2F5 and 10E8 may suggest that ΔCT Env trimers have restricted exposure of MPER epitopes, possibly due to reduced efficiency at adopting fusion-intermediate conformations, in line with the idea that ΔCT Env trimers primarily adopt a closed, prefusion conformation. Results from this study and others (Beitari et al., 2017; Chen et al., 2020b; Sood et al., 2017) have shown that SERINC5 incorporation into HIV-1 FL virions increases sensitivity to MPER targeting bnAbs, but not gp120 targeting bnAbs, possibly by inducing specific conformational changes to the MPER region. However, I did not consistently observe this increased sensitivity of HIV-1 ΔCT infection to 10E8. HIV-1 ΔCT with SERINC5 packaged into virions became more sensitive to 2F5 but not 10E8, which is intriguing given that both bnAbs bind overlapping epitopes on MPER. However, this could be reflective of the different neutralising potencies of 10E8 and 2F5. Taken together, reduced sensitivity of HIV-1 ΔCT to 2F5 and 10E8 (in the absence of SERINC5) suggests that their epitopes are less accessible on ΔCT Env trimers, due to conformational differences induced by truncation of the long EnvCT, and this perhaps prevents SERINC5 from either recognising and directly binding a specific fusion

intermediate conformation which is less frequently adopted by ΔCT Env, or prevents SERINC5 from indirectly inducing further conformational changes which are required to perturb fusion. Indeed, SERINC5 incorporation does not perturb fusion of HIV-1 ΔCT Env with target cell membranes, suggesting a mechanism for evasion of SERINC5 restriction.

As further evidence for altered Env conformation of ΔCT viruses, differences were also observed between the neutralisation profiles of HIV-1 FL and ΔCT infection in the presence of bnAbs targeting gp120. HIV-1 ΔCT infection was significantly more sensitive to neutralisation by VRC01 and PGT151, compared with HIV-1 FL infection, suggesting that EnvCT truncation induces conformational changes in the ectodomain of Env trimers as well as the gp41 MPER. Alternatively, these results may indicate that there are more ΔCT Env trimers present on the surface of virions, hence increasing the probability of VRC01 and PGT151 binding, thus less antibody is required to neutralise infection. However, if the latter explanation is true, it is difficult to reconcile why the same trend is not observed with MPER bnAbs. Increased virion surface exposure of trimers would expose more gp120 and MPER epitopes to be targeted by bnAbs, but instead ΔCT infection is less sensitive to neutralisation by MPER bnAbs. As future work, super resolution single particle imaging of ΔCT viruses would aid our understanding of the number of Env trimers present on the surface of virions. There is much discordance in the literature regarding the effect of EnvCT truncation on antibody neutralisation sensitivity of HIV-1 and SIV infectious molecular clones (Durham et al., 2012; Edwards et al., 2001; Kuwata et al., 2013; Puffer et al., 2002; Vzorov et al., 2005; White et al., 2018; Yuste et al., 2005). Progressive truncation of the HIV-1 EnvCT leads to incremental increases in sensitivity to neutralisation by HIV-1 positive serum (Edwards et al., 2001), whereas the Δ144 mutation did not result in increased sensitivity to MPER antibodies, 4E10 and 2F5 (Durham et al., 2012). This suggests that the Δ144 mutation and the P722* mutation used in this study, have different effects on the Env ectodomain conformation, resulting in differences in sensitivity to neutralisation by the same antibodies. Since HIV-1 Δ144 viruses have a larger portion of the EnvCT removed, this probably results in opening of the Env trimer, thus allowing access to epitopes targeted by bnAbs. Truncation of the SIV EnvCT at Env position 733, which is analogous to the position at which stop codons were inserted in my viruses, showed decreased sensitivity to neutralisation by macaque sera and SIV-targeting monoclonal antibodies (Kuwata et al., 2013; White et al., 2018; Yuste et al., 2004), which is in line with my data. Collectively, these data suggest that EnvCT truncation can induce global changes in the Env ectodomain which alters sensitivity to the adaptive immune system.

To extend the results presented in this chapter, flow cytometry analysis should be used to determine the effect of truncating the cytoplasmic tail on Env antigenicity, by measuring antibody binding capacity of ΔCT Env and HIV-2 Envs. Truncating or deleting the HIV-1 EnvCT leads to altered Env binding to bnAbs targeting the trimer apex, such as PG9 and PGT145, suggesting that the EnvCT regulates Env antigenicity by influencing the conformation of the ectodomain (Chen et al., 2015; Julien et al., 2013; Lee et al., 2017; Pancera et al., 2013). Further, recent NMR studies provide structural evidence that the EnvCT is physically coupled to the Env ectodomain, thus influencing Env conformation and antigenicity, particularly of the gp41 MPER (Piai et al., 2020). The LLP2 region in the EnvCT adopts a unique structural arrangement in which two amphipathic alpha helices form and wrap around the gp41 transmembrane domain (TMD) to form a baseplate which stabilises Env conformation, particularly the MPER and the ectodomain (Piai et al., 2020). NMR dynamics measurements reveal that there is dynamic coupling across the TMD (Piai et al., 2020) and the authors suggest a model in which the TMD undergoes scissor-like motions which are regulated by the CT baseplate and this in turn influences movement of MPER. Therefore, the physical interaction between different gp41 domains explains why changes in the EnvCT can lead to allosteric changes in MPER and gp120 via the TMD. Antibody neutralisation data suggest the EnvCT-TMD interaction preferentially affects the antigenic structure of the trimer apex, because mutations in the interface between TMD and CT result in increased sensitivity to neutralising and non-neutralising antibodies (Piai et al., 2020). This suggests that gp120 adopts an open conformation, which allows these antibodies to more readily access their binding epitopes. In line with this, I have shown that HIV-1 ΔCT infection is more susceptible to neutralisation by VRC01 and PGT151, by comparison with HIV-1 FL infection. To conclude, the effect of EnvCT truncation on Env conformation, hence sensitivity to antibody neutralisation, can be explained by the physical interaction that exists between the EnvCT and the Env ectodomains, including gp120 and the gp41 MPER. The importance of the CT baseplate in viral infectivity is questioned by Piai and colleagues (2020) because no direct infectivity measurements were made in the context of full-length replication competent virus. Data presented in this chapter suggests that the CT baseplate is probably important in viral infectivity, given that deletion of the baseplate in my ΔCT viruses results in increased sensitivity to bnAbs targeting gp120 and the T20 fusion inhibitor, as well as dysregulated entry kinetics. A recent study further emphasises the potential importance of the EnvCT baseplate in regulating viral entry and infectivity (Snetkov et al, unpublished data). Mutating a conserved tryptophan residue at HIV-1 Env position 757 in the LLP2 region of the HIV-1 EnvCT (W757A), results in dramatic loss of viral infectivity. BlaM-Vpr measurements reveal that the W757A mutant is significantly less fusogenic by comparison with HIV-1

FL Env and this cannot be explained by impaired Env incorporation (Snetkov et al, unpublished data). Together, these data suggest that manipulation of the EnvCT, either by mutation of single residues (W757A mutant) or truncation of the EnvCT (ΔCT mutants), leads to global conformational changes in Env ectodomain which impacts Env functionality. As a result, the HIV EnvCT, particularly the EnvCT baseplate structure, plays a crucial role in regulating viral entry and susceptibility to antibodies.

I hypothesised that the conformational changes induced by truncation of the HIV-2 EnvCT, might result in an altered ability of HIV-2 Env to antagonise tetherin. To test this, HIV-2 FL and ΔCT viruses were produced in 293T cells in the presence of tetherin. HIV-2 ΔCT viruses were able to antagonise tetherin as efficiently as their FL counterparts, since viral release was unaffected. This can be explained by the fact that the conserved YxxΦ endocytic motif in the HIV-2 EnvCT is required for antagonism of tetherin (Le Tortorec and Neil, 2009), which is retained in the HIV-2 ΔCT mutants used within this study. This suggests that the conformation of gp120 is probably not important in Tetherin antagonism, as long as the proteins can directly interact with each other.

Resistance of EnvCT truncated viruses to SERINC5 was observed in the presence of a functional Nef protein in FL and ΔCT viruses, which suggests that the effect of EnvCT truncation is dominant over Nef's ability to antagonise SERINC5. However, it is worth noting that this is an overexpression assay and Nef is usually sufficient to antagonise endogenous SERINC5 levels. To test whether EnvCT truncation can rescue HIV-1 ΔNef infectivity, a HIV-1 ΔCT ΔNef double mutant was produced. However, characterisation of this mutant revealed that deletion of both EnvCT and Nef is detrimental to virus production and infectivity. Therefore, it was not possible to determine whether HIV-1 Env truncation rescues infectivity of HIV-1 ΔNef virus in the presence of SERINC5. This is likely attributed to the multiple functions of Nef that determine efficient viral replication, as discussed in Chapter 1 section 1.2.5 (reviewed by (Buffalo et al., 2019)). A recent paper postulated that Nef possibly antagonises an unidentified restriction factor in MOLT3 cells and primary unstimulated PBMCs, which is independent of SERINC5 and SERINC3 restriction (Wu et al., 2019). Replication of SERINC5-sensitive and -resistant viruses (such as NL4.3 and JRFL, respectively) were equally dependent on the presence of a functional Nef protein in SERINC5/3 knockout MOLT3 cells, suggesting that this cell type expresses a novel and as yet unidentified Nef-sensitive antiviral protein (Wu et al., 2019) that EnvCT truncation does not overcome. Further, HIV-1 viruses expressing Nef mutants which are unable to bind the AP2 adaptor protein, have defective replication in MOLT3 cells, suggesting that Nef needs to downmodulate this unidentified antiviral factor from the cell surface to allow efficient replication (Wu et al., 2019).

Like SERINCs, IFITM-mediated restriction of HIV-1 infectivity occurs at the step of fusion and prevents viral entry into target cells (Compton et al., 2014; Foster et al., 2016; Lu et al., 2011a; OhAinle et al., 2018; Qian et al., 2015; Tartour et al., 2014; Yu et al., 2015), however the exact mechanism also remains unclear. The IFITM proteins target a wide range of enveloped viruses including Influenza A virus, Dengue virus, Ebola virus, Hepatitis C virus and HIV-1 (Brass et al., 2009; Huang et al., 2011; Lu et al., 2011a). In the context of HIV-1, sensitivity to IFITM1-3 has also been mapped to the gp120 V3 loop (Foster et al., 2016; Tartour et al., 2014; Wang et al., 2017; Wu et al., 2017) and coreceptor usage is reported to determine sensitivity to different IFITM proteins (Foster et al., 2016). Given the similarities between SERINC5 and IFITM restriction observations, I tested my panel of HIV-1 and HIV-2 viruses with the aim of determining whether truncation of the EnvCT also overcomes IFITM restriction in target cells, and whether SERINC5 incorporation alters sensitivity to IFITMs in target cells.

The first experimental set up used to investigate viral sensitivity to IFITM restriction involved infecting IFITM overexpressing U87 cells with FL and ΔCT viruses and then measuring the percentage of infected cells by flow cytometry, as well as measuring viral output by SG-PERT analysis. HIV-1 FL infection was restricted 5-fold by IFITM1 and as a result, there was approximately 100-fold fewer budding particles. Conversely, no HIV-1 ΔCT infection was detected in U87 control and IFITM1 overexpressing cells by flow cytometry and SG-PERT analysis, suggesting that there is a block to ΔCT viral entry. This might be explained by low surface expression levels of CD4 and CXCR4 receptors on U87 cells, although I would expect HIV-1 FL virus, which infected up to 50% cells in the single round assay, to also be affected by this. However, it is possible that ΔCT Env binds poorly to CD4 and/or coreceptor and therefore requires higher expression to increase the likelihood of binding and facilitating entry. This is in line with my previous discussion regarding the sCD4 neutralisation data, which shows that ΔCT virus has a higher IC50 value compared with FL virus, suggesting that ΔCT might bind to CD4 poorly. Intriguingly, this block to viral entry was not observed in U87 IFITM2 and IFITM3 overexpressing cells, as HIV-1 ΔCT infection reached 13% in both cell types. IFITMs can enhance infection in some settings, for example human coronaviruses (Shi et al., 2021; Zhao et al., 2014; Zhao et al., 2018), although an explanation and mechanism remains to be elucidated. Despite initial infection of U87 IFITM2/3 cells, SG-PERT analysis could not detect any RT activity in the supernatant of infected cells, suggesting that no HIV-1 ΔCT particles were released. This is indicative of a post entry block. Taken together, these data suggest that there are multiple blocks to HIV-1 ΔCT infection in U87 cells and they are non-permissive to EnvCT truncation. Therefore, the U87 model is not ideal for

investigating the effect of restriction factors on EnvCT truncated viruses. Further, HIV-2 viruses were also restricted in U87 cells, irrespective of EnvCT length, providing further precedence for using an alternative model system to investigate IFITM restriction.

To determine the effect of IFITM proteins on HIV-1 ΔCT viral entry, a second model system was used in which HeLa TZM-bl cells were transduced with IFITM expression vectors. Notably, truncation of the EnvCT rendered both HIV-1 and HIV-2 ΔCT viruses resistant to IFITM-mediated restriction, specifically IFITM1. Moreover, the presence of SERINC5 in virions did not alter sensitivity to inhibition by IFITMs in that the restriction effect and hierarchy was unaltered whether virus was produced in the presence or absence of over-expressed SERINC5. Using a panel of HIV-1 T/F and chronic viruses, Foster and colleagues showed that the localisation of IFITM proteins and the Env glycoprotein both determine sensitivity and specificity to IFITMs (Foster et al., 2016). Viruses that require the CCR5 co-receptor were more susceptible to inhibition by IFITM1 at the plasma membrane, whilst CXCR4-using viruses were more sensitive to IFITM2/3 that are predominantly localised within endosomal compartments. Despite HIV-2 ST being an R5-tropic virus, I found that it was restricted by IFITM1 but not IFITM2/3, similar to X4-tropic HIV-1 NL4.3. Further, IFITM-resistant viruses have been reported to be less susceptible to sCD4 and 17b neutralisation by comparison with IFITM-sensitive viruses (Wang et al., 2017), in keeping with my observation that ΔCT viruses (which evade SERINC5 and IFITMs) are less sensitive to sCD4 and 17b neutralisation. Inconsistency exists about the hierarchy of IFITM1-3 inhibition of HIV-1, the magnitude of inhibition and how co-receptor usage dictates differential sensitivity to IFITM1, 2 or 3 (Ding et al., 2014; Foster et al., 2016; Lu et al., 2011a; OhAinle et al., 2018; Qian et al., 2015; Wang et al., 2017; Yu et al., 2015; Yu and Liu, 2018). This likely reflects a combination of differences in the cell types used (i.e., whether viral entry favours plasma membrane or endosomal fusion and the endocytic capacity of certain cell types), how infection is measured (GFP reporter virus, viral protein synthesis or virion infectivity) and the use of pseudotyped viruses compared with replication competent virus (the latter incorporating native levels of Env into virions and also expressing viral accessory proteins, whereas pseudotyped viruses are made using highly overexpressed Env, resulting in high surface Env levels (Piai et al., 2020), which may overcome IFITM1 inhibition). Here, replication-competent infectious molecular clones were used and a direct measure of viral infection by expressing IFITM1-3 in HeLa TZM-bl reporter cells that express HIV-1 Tat-driven luciferase. Having validated this assay using T/F virus CH058 and VSV-G Env, I found that HIV-1 and HIV-2 infection was restricted by IFITM1 but not IFITM2 or 3, consistent with the notion that productive HIV infection is mediated by viral fusion at the plasma membrane. Notably, this data reporting sensitivity of HIV-1 to IFITM1 is supported by

previous studies that also observed IFITM1 inhibition of infection/fusion using replication competent CXCR4-tropic HIV-1 (Foster et al., 2016; OhAinle et al., 2018; Qian et al., 2015; Yu et al., 2015).

Previously, I discussed the idea that any direct interactions between SERINC5 and ΔCT Env are probably non-functional, given that ΔCT viruses are able to evade restriction. This suggests that the primary mode of SERINC5 restriction may be via an indirect mechanism. A recent study investigating Env and SERINC5 clustering on single virus particles, shows a lack of Env and SERINC5 co-clustering (Chen et al., 2020b). Chen and colleagues (2020) suggest that SERINC5 rigidifies the viral and target cell membrane, by sequestering cholesterol from viral assembly points, which prevents efficient Env clustering; a crucial step in initiating HIV-1 fusion. IFITM3 has also been reported to restrict viral fusion and entry via mechanisms involving modulation of the lipid bilayer, although whether this is true for HIV-1 restriction remains to be elucidated (Amini-Bavil-Olyaee et al., 2013; Desai et al., 2014; Li et al., 2013; Lin et al., 2013). Lipids such as cholesterol and sphingomyelin are enriched in viral membranes compared with cell membranes (Brugger et al., 2006; Lorizate et al., 2013), although the functional significance of this enrichment in HIV-1 infectivity remains to be elucidated. The presence of cholesterol in membrane microdomains known as lipid rafts is thought to be important in HIV-1 infectivity, given that depletion of cholesterol using the drug Methyl-β-cyclodextrin (MβCD) leads to inhibition of viral infectivity (Campbell et al., 2002; Graham et al., 2003). Campbell and colleagues (2002) found that preincubation of replication competent HIV-1 viruses with MβCD resulted in up to 90-fold inhibition of infectivity, which could be restored upon cholesterol reconstitution (Campbell et al., 2002). Similarly, Graham and colleagues (2003) report a correlation between the amount of cholesterol depletion in viral particles using MβCD, with loss of SIV and HIV-1 viral infectivity (Graham et al., 2003). This suggests that alterations in the level of lipid-raft associated cholesterol can directly impact viral infectivity, and so drugs or intracellular proteins (such as SERINC5 and IFITMs) that alter the level of cholesterol in viral membranes will have an impact on infectivity. Super resolution nanoscopy (STED) studies show that the EnvCT and cholesterol govern Env clustering (Nieto-Garai et al.2020). HIV-1 virus particles were treated with an enzyme COase, which converts up to 50% of membrane cholesterol to cholestenone thereby removing the hydrophobic group which is required for interaction with proteins. Untreated FL virus particles showed Env clustering, which was lost upon EnvCT truncation (Nieto-Garai et al. 2020). Env clustering directly impacts the ability of viruses to fuse with target membranes (Brandenberg et al., 2015a). BlaM-Vpr analysis revealed that treatment with COase significantly reduced the ability of FL virus to fuse with target cells, as did truncation of

the EnvCT at position 751 (Nieto-Garai et al.2020). These data suggest that SERINC5 and IFITM proteins might indirectly prevent Env mediated fusion by sequestering cholesterol from sites of viral assembly and budding, thereby preventing formation of Env clusters at fusion hot spots. In line with this hypothesis, super resolution microscopy showed that HIV-1 Δ144 is highly mobile in the lipid bilayer, thus cannot cluster efficiently due to loss of interaction with the underlying matrix lattice (Muranyi et al., 2013; Pezeshkian et al., 2019). Therefore, it is possible that a similar phenotype would be observed with the ΔCT Envs used in this study. Increased Env mobility in membranes can have a direct impact on fusogenicity, by impacting the ability to reach the required fusion stoichiometry for initiation of fusion. Fusion stoichiometry is an important concept as it determines the efficacy of viral fusion, entry and ultimately infectivity (Brandenberg et al., 2015a; Brandenberg et al., 2015b). Certain HIV-1 strains are capable of forming functional fusion complexes with fewer Env trimers, such as the SERINC5-resistant HIV-1 JRFL strain, which suggests that low-stoichiometry Envs can evade SERINC5 restriction as they are less reliant on forming large Env clusters for efficient fusion (Brandenberg et al., 2015b). Given that ΔCT viruses in this study are able to fuse with target cell membranes by 16-24h post infection, despite EnvCT truncation possibly increasing mobility in membranes, it is possible that ΔCT viruses have lower stoichiometry compared with their FL counterpart and form a greater quantity of smaller clusters that are ultimately able to overcome the required fusion stoichiometry. Future super resolution single particle tracking microscopy of infected cells would help to better understand this. Taken together, increased mobility and the inability to efficiently cluster at fusion hot spots, whilst having low fusion stoichiometry, may enable my ΔCT mutants to overcome SERINC5 and IFITM's restrictive effects that coalesce on a common mechanism related to altered membrane fluidity (possibly through their effects on cholesterol). In this study I have investigated the effects of SERINC5 in virus producer cells, but given the potential indirect nature of restriction, it is possible that SERINC5 on target cell membranes might also efficiently restrict infection by impacting CD4 and coreceptor clustering which is also important in fusion. Future work looking at SERINC5 in producer cells, using experiments similar to the IFITM experiments in this study, will help aid our understanding of this hypothesis.

To conclude, in this chapter I have shown that EnvCT truncation renders HIV-1 and HIV-2 viruses insensitive to SERINC5 and IFITM restriction. At the beginning of this discussion, I mentioned that ΔCT Env evades three potential mechanisms of SERINC5 restriction: **(1)** inhibition of fusion, which is evaded as a result of conformational changes in the Env ectodomain of gp41 and gp120; **(2)** spontaneous inactivation of Env, which is evaded due to the increased stability of ΔCT Env trimers and **(3)** disruption of Env

clustering, which is evaded possibly due to the ability of ΔCT trimers to have low fusion stoichiometry. Another conclusion from this work is that the main mechanism of SERINC5 and IFITM-mediated HIV restriction is probably not due a direct interaction with Env, rather an indirect consequence of altering the lipid membrane.

5 Role of the EnvCT in activating signalling pathways

5.1 Introduction

In chapter 4 I described and discussed the role of HIV EnvCT in determining sensitivity to various Env-dependent restriction factors. Some HIV restriction factors can act as pattern recognition receptors (PRR) and play an integral role in the cell intrinsic innate immune response to infection. Early stages of the innate immune response involve recognition of HIV-specific pathogen associated molecular patterns (PAMPs) and activation of signalling pathways, which leads to nuclear translocation of transcription factors such as NFκB and IRF3. Once in the nucleus, these transcription factors drive expression of innate immune response genes. As a result, soluble type I Interferon (IFN-I) is produced and binds to the IFN receptor found on the surface of immune cells. this initiates a number of signalling cascades which lead to upregulation of interferon stimulated genes (ISGs) and an antiviral state is induced. Well-studied examples of this include the detection of HIV-1 capsid protein by TRIM5a (Pertel et al., 2011b) and Tetherin's ability to activate NFkB signalling during viral egress (Galao et al., 2012; Hotter et al., 2013b).

The first evidence to suggest that the Env cytoplasmic tail can modulate signalling pathways came from a study investigating the ability of HIV-1 and SIV EnvCTs to activate NFkB signalling (Postler and Desrosiers, 2012). NFkB activation takes place in a TGF-β-activated kinase 1 (TAK1)-dependent manner and this is proposed to increase cell activation and promote viral replication (Postler and Desrosiers, 2012). However, given that NFκB signalling can also activate inflammatory responses and innate immune responses, I sought to further investigate potential activation of NFkB by a panel of lentiviral EnvCTs, and to measure activation of innate immune pathways.

5.2 Results

5.2.1 HIV-1 EnvCT activates NFκB and AP-1 signalling.

To investigate the ability of lentiviral EnvCTs to activate signalling pathways, a dual luciferase reporter gene assay was designed. 293T cells were co-transfected with increasing doses of plasmid encoding lentiviral EnvCTs, various reporter plasmids and a control thymidine kinase (TK) Renilla plasmid which is constitutively expressed. Finally, pcDNA empty vector was used to equalise the total amount of plasmid transfected in each well. The TK renilla control is therefore an indicator of cell viability and transfection efficiency. Each reporter plasmid encodes firefly luciferase; expression of which is driven by activation of promoters upon binding of transcription factors such as NFκB and AP-1, or binding of effector molecules such as ISRE, ISG56 or IFNβ. The EnvCT of different lentiviruses were cloned into a vector with the CD8 ectodomain and transmembrane domain attached to the N-terminus of the EnvCT, as previously described (Groppelli et al., 2014) (Fig. 5.1A). These Env constructs have previously been validated to follow the same intracellular trafficking pathway as full length Env (Groppelli et al., 2014) and were also used in a previous study investigating NFkB activation by the HIV-1 EnvCT (Postler and Desrosiers, 2012). As a control, a CD8-STOP construct was used, which has a stop codon located at the end of the CD8 transmembrane domain so that the CD8 ecto- and transmembrane domain are expressed but not the EnvCT (Fig. 5.1A). Figure 5.1B shows sequences of the different lentiviral EnvCTs that were fused to the CD8 ecto-and transmembrane domains. 48 hours post transfection, firefly luciferase activity was measured using a Dual-Luciferase reporter system (Promega).

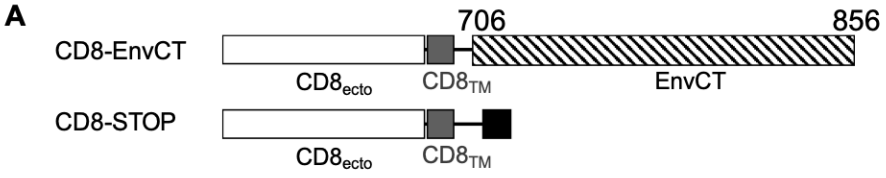

B

Lentivirus	EnvCT sequence
HIV-$1_{NL4.3}$	NRVRQGYSPLSFQTHLPTPRGPDRPEGIEEEGGERDRDRSIRLVNGSLALIWDDLRSLCL FSYHRLRDLLLIVTRIVELLGRRGWEALKYWWNLLQYWSQELKNSAVSLLNATAIAVAEG TDRVIEVVQGACRAIRHIPRRIRQGLERILL*
HIV-1_{Rbf}	VRRIRQGYSPVSLQTLGLNGDPAGIAPGTNEEGGEAGNGRSIRLLDGFLPLVWDDLKNLV VQIYQILVGCILGIKDLLTILWIHLGQLLTRGLNCLRDCFAACGYWTQELKQSATSLLDT VAISVAGWTDQVIIVGQQIGRGFLNIPRRIRQGIERSLL*
HIV-2_{ROD10}	SRLRKGYRPVFSSPPGYIQQIHIHKDRGQPANEETEEDGGSNGGDRYWPWPIAYIHFLIR QLIRLLTRLYSICRDLLSRSFLTLQLIYQNLRDWLRLRTAFLQYGCEWIQEAFQAAARAT RETLAGACRGLWRVLERIGRGILAVPRRIRQGAEIALL*
SIV_{mac239}	AKLRQGYRPVFSSPPSYFQQTHIQQDPALPTREGKERDGGEGGGNSSWPWQIEYIHFLIR QLIRLLTWLFSNCRTLLSRVYQILQPILQRLSATLQRIREVLRTELTYLQYGWSYFHEAV QAVWRSATETLAGAWGDLWETLRRGGRWILAIPRRIRQGLELTLL*
SIV_{smm543}	ARLRQGYRPVFSSPPAYVQQIPIHKGQEPPTKEGEEGDGGDRGGSRSWPWQIEYIHFLIR QLIRLLTWLFSSCRDWLLRSYQILQPVLQSLSTTLQRVREVIRIEIAYLQYGWRYFQEAV QAWWKLARETLASAWGDIWETLGRVGRGILAIPRRIRQGLELTLL*
SIV_{PBi}	ARLRQGYRPVFSSPPAYVQQIPIQTGQELPTKEGEEGDGGGRGGNRSWPWQIEYIHFLIR QLIRLLTWLFSSCRDWLLRNCQTLQPVLQSLSRTLQRAREVIRVQIAYLQYGWRYLQEAA QAWWKFVRETLASAWRDLWETLGRVGRGILAIPRRIRQGLELTLL*
SIV_{tan}	ARVRQGYFPLSPQINIRLGREQPDNAGGEDKDSSSSRDKSPPSVKESLLPNRGGIQAEER AWRQHLTNWCLTISSWLLRLYQILRRSLTTLL

Figure 5.1 Overview of CD8 fusion constructs (A) Schematic showing the EnvCT protein fused to CD8 ectodomain and transmembrane domain. **(B)** EnvCT sequences of lentiviruses tested.

A reporter plasmid under the control of the natural promoter of the immunoglobulin kappa light chain (IgK) gene, was used to measure NFκB activation, as it is sensitive to NFκB subunits p50 and p65 and contains three repeat kB sequences (referred to as the IgK NFκB reporter) (Saksela and Baltimore, 1993). Figure 5.2 shows activation of the IgK NFκB reporter by HIV-1 NL4.3 EnvCT, and this figure will be used to exemplify how data was normalised throughout this chapter. The first step of data normalisation was to divide the raw firefly luciferase (Fig. 5.2A) readings by the TK renilla luciferase readings (Fig. 5.2B) in order to account for differences in transfection efficiency between different reactions, and this is termed FF/TK readings (Fig. 5.2C). Next, the FF/TK readings obtained upon CD8-STOP and CD8-EnvCT expression were normalised to the FF/TK readings of the pcDNA empty vector control to account for the background activity of this assay (Fig. 5.2D). Figure 5.2D shows that the CD8-STOP construct is able to marginally activate IgK NFkB reporter activity up to 2-fold above the background pcDNA only control. Therefore, I introduced another normalisation calculation in which I divided the CD8-EnvCT values by CD8-STOP to account for this and obtain a measurement which reflects how much activation of the reporter was due to expression of the EnvCT only, not the CD8 ectodomain and transmembrane domain (Fig. 5.2E). HIV-1 NL4.3 CD8-EnvCT activates the IgK NFκB promoter in a dose dependent manner, up to 10-fold above CD8-STOP (Fig. 5.2E), in agreement with Postler and colleagues (Postler and Desrosiers, 2012).

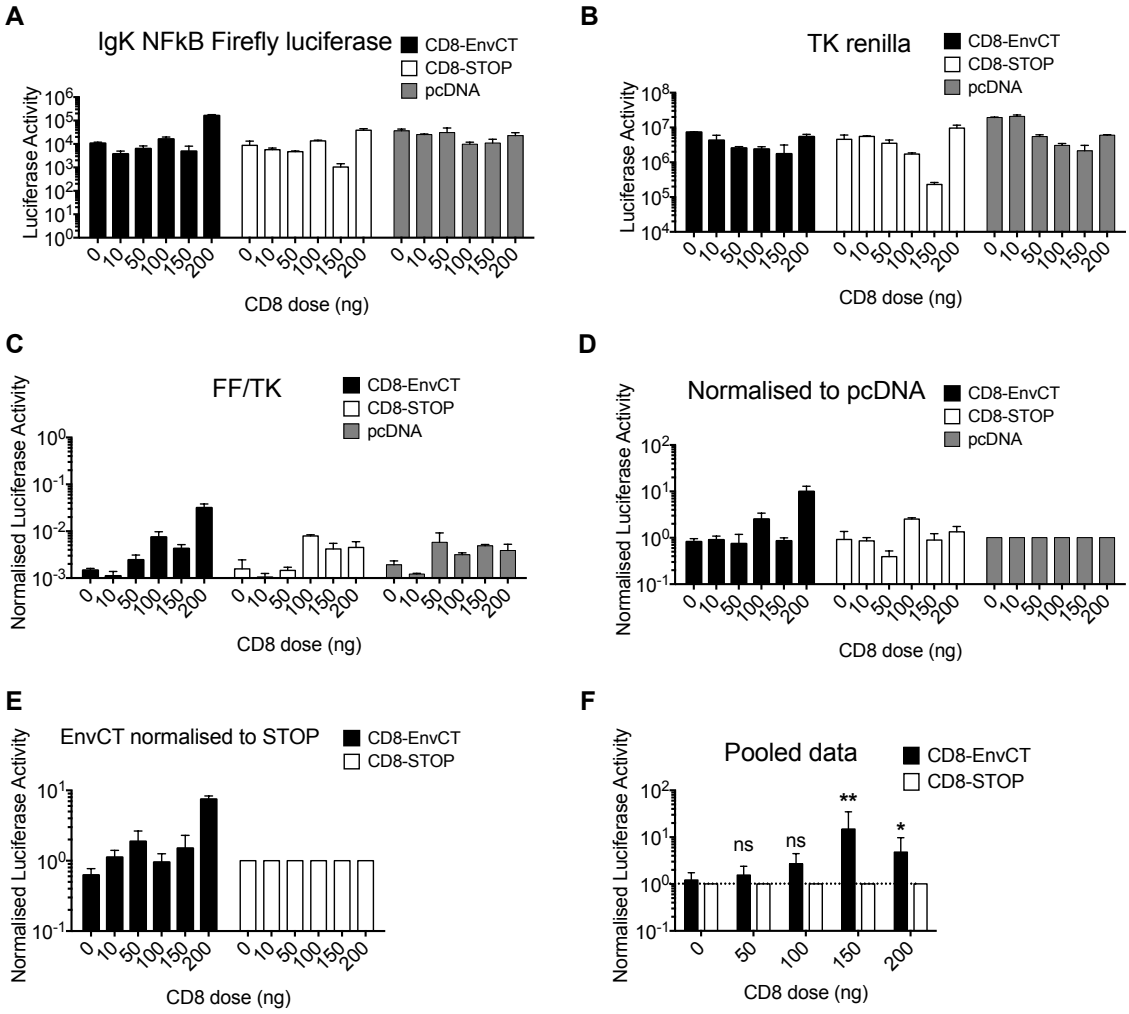

Figure 5.2 HIV-1 EnvCT activates NFκB signalling. 293T cells were transfected with increasing doses of CD8 constructs (EnvCT of HIV-1 NL4.3 and CD8-STOP), 5ng IgK NFkB reporter plasmid, 2.5ng TK renilla control plasmid and pcDNA to equalise total DNA amount. 48h later luciferase activity was measured using the Dual Reporter Gene Assay kit (Promega) **(A)** Firefly (FF) luciferase activity. **(B)** TK renilla luciferase activity, which is constitutively expressed and acts as a transfection efficiency control. **(C)** Normalisation of FF activity to TK renilla (FF/TK) to normalise for differences in transfection efficiency. **(D)** CD8-EnvCT and CD8-STOP FF/TK values divided by pcDNA FF/TK values to account for background luciferase activity of 293T cells. **(E)** EnvCT mediated reporter activation divided by CD8-STOP mediated activation to account for CD8 ecto- and transmembrane domain mediated activation of reporter. A-E show graphs from a representative experiment. **(F)** Pooled data from at 3 experiments. Bars show mean and error bars represent mean +/- SEM from three independent experiments. Fold activation at each dose of CD8-EnvCT was compared with no EnvCT expression (0ng) using two-tailed paired t-tests and 2-way ANOVA (ns, $p>0.05$; *, $p<0.05$; **, $p<0.01$).

Next, I repeated the 293T co-transfection assay and tested whether HIV-1 NL4.3 EnvCT could activate a panel of reporter genes that represent activation of an inflammatory and innate immune response. Figure 5.3 shows that the EnvCT can activate NFkB and AP-1 signalling up to 10-fold, compared with CD8-STOP (Fig. 5.3). By contrast, ISG56, ISRE and IFNβ reporter plasmids are not activated even at high doses of CD8-EnvCT overexpression (Fig. 5.3), which suggests that a typical Type I IFN response is not activated by the HIV-1 EnvCT in 293T cells.

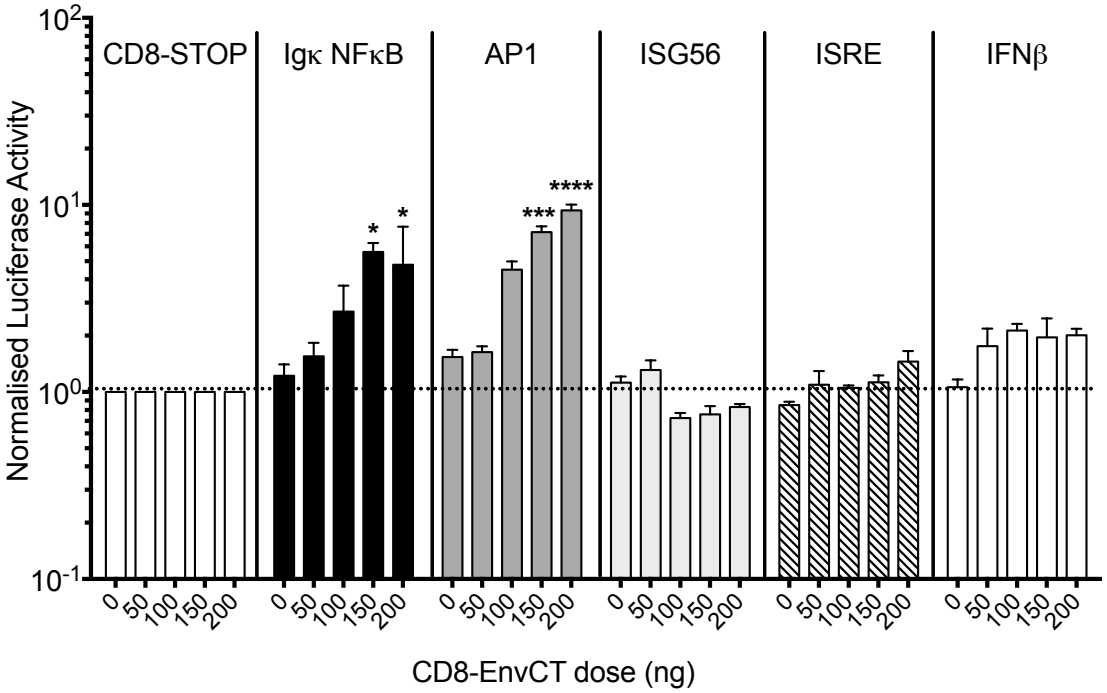

Figure 5.3 HIV-1 EnvCT activates AP-1 signalling. Activation of various reporters was tested by co-transfecting 293T cells with indicated doses of CD8 constructs, 5ng of IgK NFkB, AP-1, ISG56, ISRE and IFNβ reporter plasmids and 2.5ng TK renilla control plasmid. After 48h transfected cells were lysed and luciferase activity was measured using the Dual Reporter Gene Assay kit (Promega). Normalised luciferase values were obtained as describe in Figure 5.2. Bars show mean and error bars represent mean +/- SEM from three independent experiments. Fold activation at each dose of CD8-EnvCT was compared with no EnvCT expression (0ng) using two-tailed paired t-tests and 2-way ANOVA (*, $p<0.05$; ***, $p<0.001$, ****, $p<0.0001$).

5.2.2 Induction of NFκB but not AP-1 promoter activity by lentiviral EnvCTs.

Next, I investigated whether activation of NFκB and AP-1 signalling is specific to HIV-1 EnvCT or whether other lentiviral EnvCTs can also activate these signalling pathways. To test this, the reporter gene assay was repeated as described above, using CD8 fusion constructs encoding the EnvCT of HIV-1 RBF168 (referred to as RBF) which belongs to Group O, HIV-2 ROD10 and several SIV viruses including SIVmac239, SIVsmm543, SIVsmm PBj (referred to as SIV PBj) and SIVtan. Figure 5.4A shows that all the lentiviral EnvCTs included in the panel were able to activate the NFκB pathway to varying degrees, although due to high variability in this assay, some results did not reach statistical significance. Unlike HIV-1 NL4.3 which shows a dose dependent reporter activation, HIV-1 RBF strongly activated NFkB signalling even at low doses, starting from 25ng. Likewise, SIVtan and SIVsmm543 significantly activated NFkB signalling up to 10-fold at the highest dose of expression. HIV-2 ROD10, SIVmac239 and SIV PBj activate the NFkB pathway up to 3-fold over CD8-STOP, however these results were not statistically supported. Turning to AP-1 reporter activation, only Group M HIV-1 NL4.3 CD8-EnvCT activated AP-1 signalling in a dose-dependent manner, up to 10-fold at the highest dose (Fig. 5.4B). Western blot analysis of cell lysates from these experiments confirmed EnvCT expression of all lentiviruses, however the expression levels varied (Fig. 5.4C). Importantly, the level of EnvCT expression does not correlate with the ability to activate NFkB signalling. For example, HIV-1 RBF EnvCT was poorly expressed but was able to activate NFkB signally. By contrast, SIV PBj was highly expressed but was unable to activate NFkB and AP-1 signalling. Taken together, these data suggest that lentiviruses have different abilities to activate NFkB signalling and only HIV-1 NL4.3, belonging to HIV-1 Group M, activates AP-1 signalling.

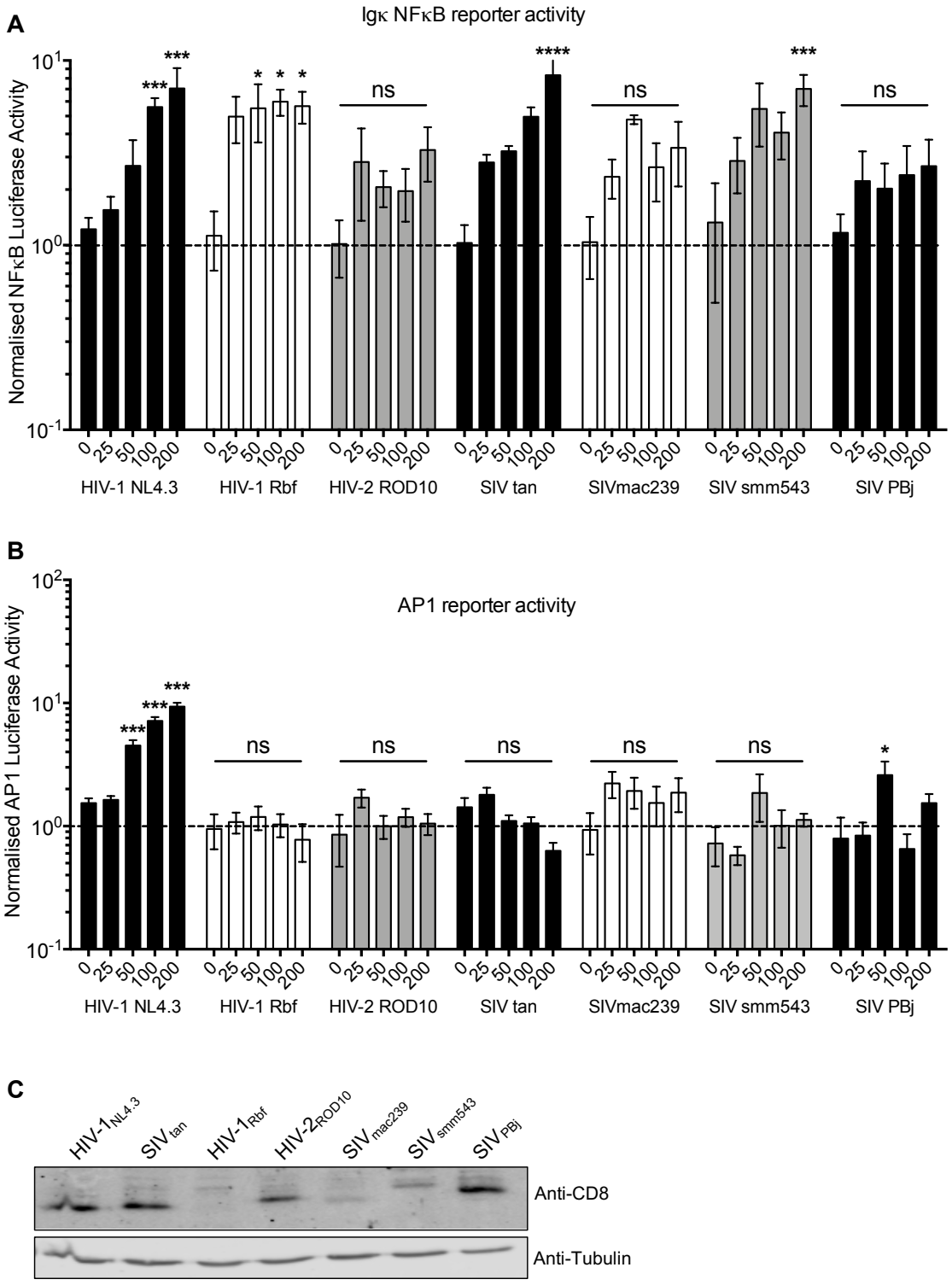

Figure 5.4 Activation of NFκB and AP-1 pathways by lentiviral EnvCTs. Activation of **(A)** NFκB and **(B)** AP-1 reporters were tested by co-transfecting 293T cells with increasing doses of CD8 constructs, 5ng reporter plasmid and 2.5ng TK renilla control plasmid. After 48h cells transfected cells were lysed and luciferase activity was measured using the Dual Reporter Gene Assay kit (Promega). **(C)** Immunoblot showing expression of CD8-EnvCT proteins in transfected cell lysates. Bars show mean and error bars represent mean +/- SEM from three independent experiments. Fold activation at each dose of CD8-EnvCT was compared with no EnvCT expression (0ng) using 2-way ANOVA (*, p<0.05 ***, p<0.001, ****, p<0.0001).

5.2.3 Mapping EnvCT domains responsible for NFκB and AP-1 signalling.

Next, I investigated which domains in the HIV-1 NL4.3 EnvCT are responsible for NFkB and AP-1 activation. To do this, the 293T dual luciferase assay was repeated with CD8 fused EnvCT truncation mutants (Fig. 5.5). Stop codons were inserted in the EnvCT sequence at 10-amino acid intervals.

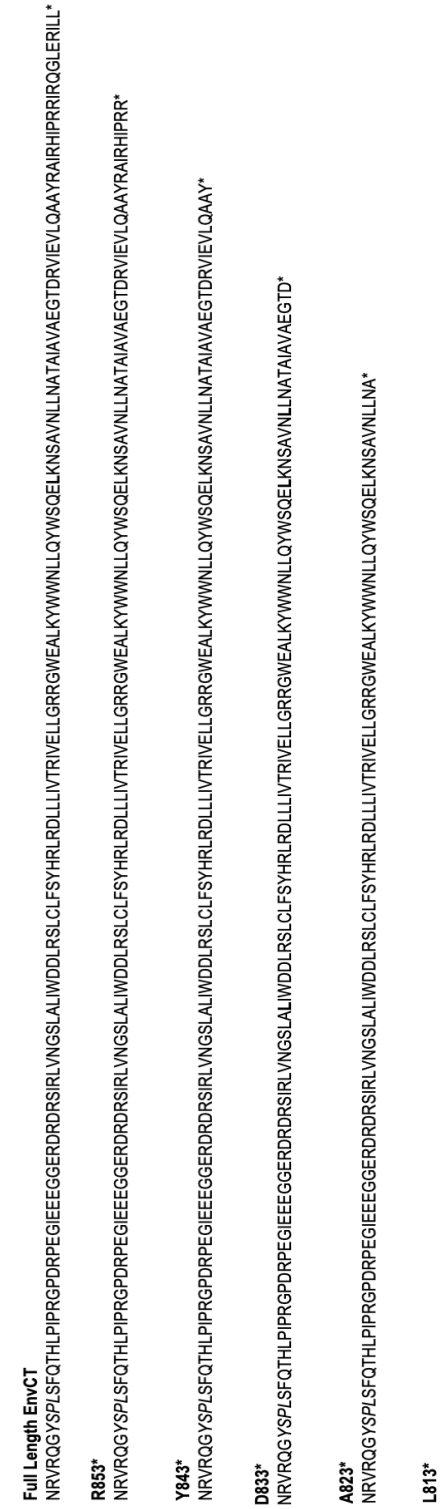

Figure 5.5 EnvCT truncation mutants. Mutants were generated by insertion of a stop codon at 10 amino acid intervals in the CD8-EnvCT constructs as described previously (Groppelli et al., 2014).

Figure 5.6A shows that all the truncation mutants activate NFκB reporter expression, except the shortest L753* mutant. This suggests that the determinant for NFκB activation is between L753 and R786, which is in accordance with previous findings (Postler and Desrosiers, 2012) as will be discussed in detail in **section 5.3**. With regards to AP-1 activation, there is significantly reduced activation upon expression of Y843* and D833* mutants and complete loss of activation when mutant L753* is overexpressed (Fig. 5.6B). This suggests that there may be multiple determinants of AP-1 activation in the EnvCT.

As NFκB and AP-1 luciferase activity is completely abrogated when the shortest mutant of the EnvCT is expressed, it is possible that the activation phenotype is linked to the length of the tail, i.e., the size of the protein being expressed. To investigate this and to determine whether the length of the CD8-fusion protein is causing activation of the reporter plasmids, indicative of a non-specific response, the dual luciferase assay was repeated with a plasmid expressing an unrelated protein of similar size. This plasmid encodes the CD8 endo- and ectodomain fused to the mannose phosphate receptor (CD8-CIMPR), which is 185 amino acids long and traffics in a retromer-dependent manner, similar to HIV-1 EnvCT (Groppelli et al., 2014). Figure 5.6C shows that CD8-CIMPR failed to activate NFκB and AP-1 reporter activity, suggesting that the size of the protein being expressed is not responsible for activation, rather, it is a specific response to EnvCT overexpression.

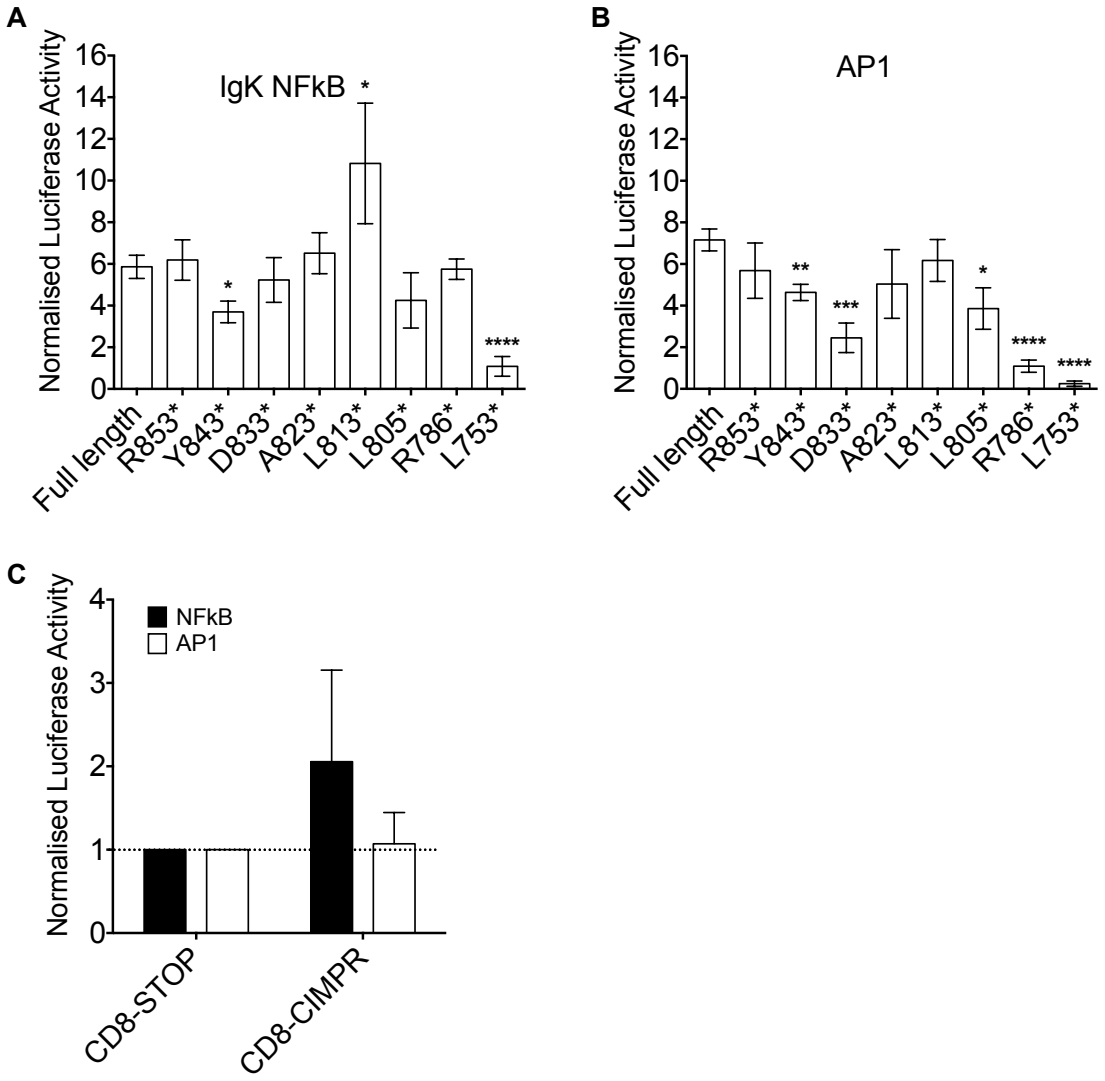

Figure 5.6 EnvCT truncation mapping to find determinants of NFκB and AP-1 activation. Activation of **(A)** NFκB and **(B)** AP-1 reporters were tested by co-transfecting 293T cells with 100ng CD8 constructs, 5ng reporter plasmid and 2.5ng TK renilla control plasmid. After 48h cells transfected cells were lysed and luciferase activity was measured using the Dual Reporter Gene Assay kit (Promega). **(C)** Activation of NFkB and AP-1 reporters was tested by transfecting 293T cells as described using 100ng CD8-CIMPR. Bars show mean and error bars represent mean +/- SEM from three independent experiments. Fold activation of CD8-EnvCT truncation mutants was compared with full length EnvCT using unpaired two-tailed *t*-tests (*, $p<0.05$; **, $p<0.01$; ***, $p<0.001$, ****, $p<0.0001$).

5.2.4 Dissecting the activation of canonical and non-canonical NFkB signalling pathways.

Having established that the NFκB pathway is activated by multiple lentiviral EnvCTs, I next investigated whether the canonical or non-canonical pathway is being activated. The NFκB family of transcription factors is activated by canonical and non-canonical signalling pathways which differ in both signalling components and biological functions (reviewed in (Sun, 2017)). The canonical NFκB pathway involves activation of IκB kinase (IKK), IKK-mediated IκBα phosphorylation, and subsequent IκBα degradation and nuclear translocation of canonical NFκB members, including p50, RELA and c-REL (Sun, 2017) (Fig. 5.7). By contrast, the non-canonical NFκB pathway selectively responds to signals from a subset of tumour necrosis factor receptor superfamily members and involves activation of NFκB-inducing kinase (NIK), NIK-mediated p100 phosphorylation, and subsequent p100 processing and nuclear translocation of non-canonical NFκB members, including p52 and RELB (Sun, 2017) (Fig. 5.7).

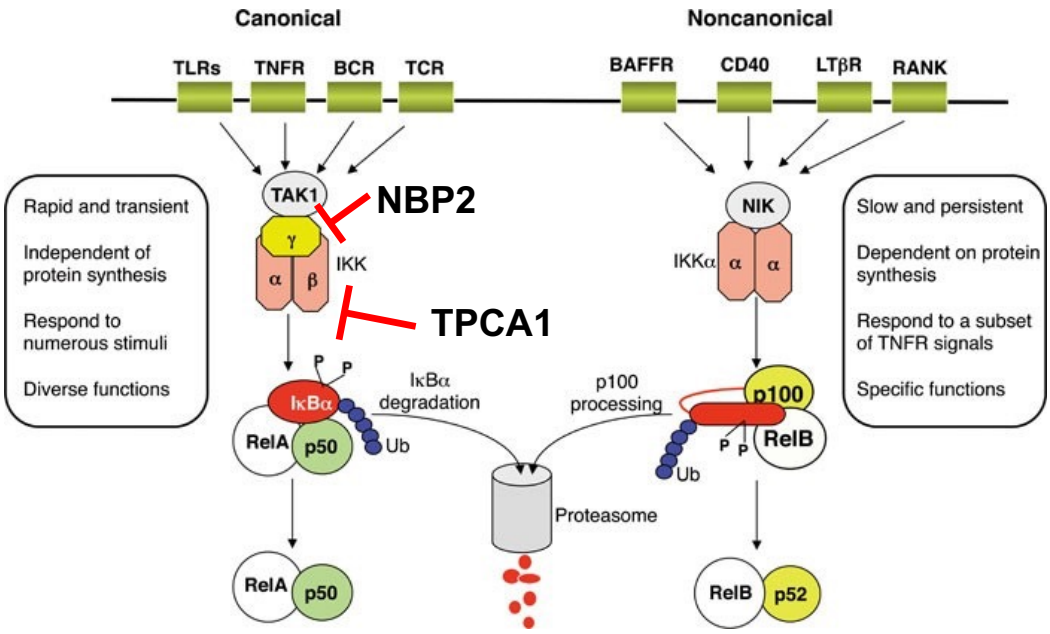

Figure 5.7 Canonical and non-canonical NFκB signalling pathways. Canonical pathway is triggered by numerous signals, including those mediated by innate and adaptive immune receptors. It involves activation of IKK complex by TAK1, IKK-mediated IκBα phosphorylation, and subsequent degradation, resulting in rapid and transient nuclear translocation of the prototypical NFκB heterodimer RelA/p50. Non-canonical NFκB pathway relies on phosphorylation-induced p100 processing, which is triggered by signalling from a subset of TNFR members. This pathway is dependent on NIK and IKKα, but not on the trimeric IKK complex, and mediates the persistent activation of RelB/p52 complex. Targets of NFkB inhibitors, NBP2 and TPCA1, are annotated using red arrows. Adapted from (Sun, 2011).

To determine whether the canonical or non-canonical NFκB pathway is activated, I first repeated the dual luciferase reporter gene assay with a commercially available reporter plasmid (Promega) that specifically drives firefly luciferase expression when the canonical NFκB pathway is activated. Figure 5.8A shows that this NFκB promoter is not activated by EnvCT overexpression. This suggests that the results obtained using the IgK NFκB reporter may not be reflective of canonical NFκB activation.

To further probe this, I tested the effect of two inhibitors targeting the canonical NFκB pathway on IgK promoter activity. The first inhibitor is NBP2 (Novus Biotech), which targets IKKγ and the second inhibitor is TPCA1 (Sigma), which selectively targets the IKK-β protein. 293T cells were pre-treated with increasing doses of inhibitor for 30 mins prior to transfection. Then, cells were transfected with 5ng IgK NFkB reporter plasmid and 150ng HIV-1 CD8-EnvCT. Figures 5.8B shows that there is a dose dependent reduction in reporter activation when cells are treated with TPCA1. By contrast, NBP2 treatment has no effect on reporter activity (Fig. 5.8C). Since both drugs target the same complex in the NFkB signalling pathway (Fig. 5.7), it is unclear why they do not show the same effect. This data does not indicate which of the two NFkB pathways are activated upon CD8-EnvCT expression.

Finally, the viral accessory protein Vpu has been shown to antagonise canonical NFκB activation by stabilising the IκB complex and preventing nuclear translocation of p65 (Sauter et al., 2015). It is also interesting that Env and Vpu are expressed from the same bicistronic mRNA (Anderson et al., 2007; Schwartz et al., 1990), suggesting a potential requirement for coordinated expression of Vpu and Env. Therefore, it would be interesting to investigate whether there is any relationship between Vpu expression and EnvCT mediated activation of NFkB. Also, use of Vpu might shed light on which of the two NFkB pathways is being activated by the EnvCT. To investigate whether Vpu blocks EnvCT-mediated NFκB activation, I repeated the dual luciferase assay by co-transfecting increasing doses of Vpu, 150ng HIV-1 CD8-EnvCT, 5ng IgK NFκB reporter plasmid and 2.5ng TK renilla control plasmid. As a positive control, 293T cells were treated with TNF-α to stimulate a potent NFκB response, which was suppressed by Vpu in a dose-dependent manner (Fig. 5.8D). By contrast, Figure 5.8E shows that overexpression of Vpu does not suppress IgK promoter activation by CD8-EnvCT.

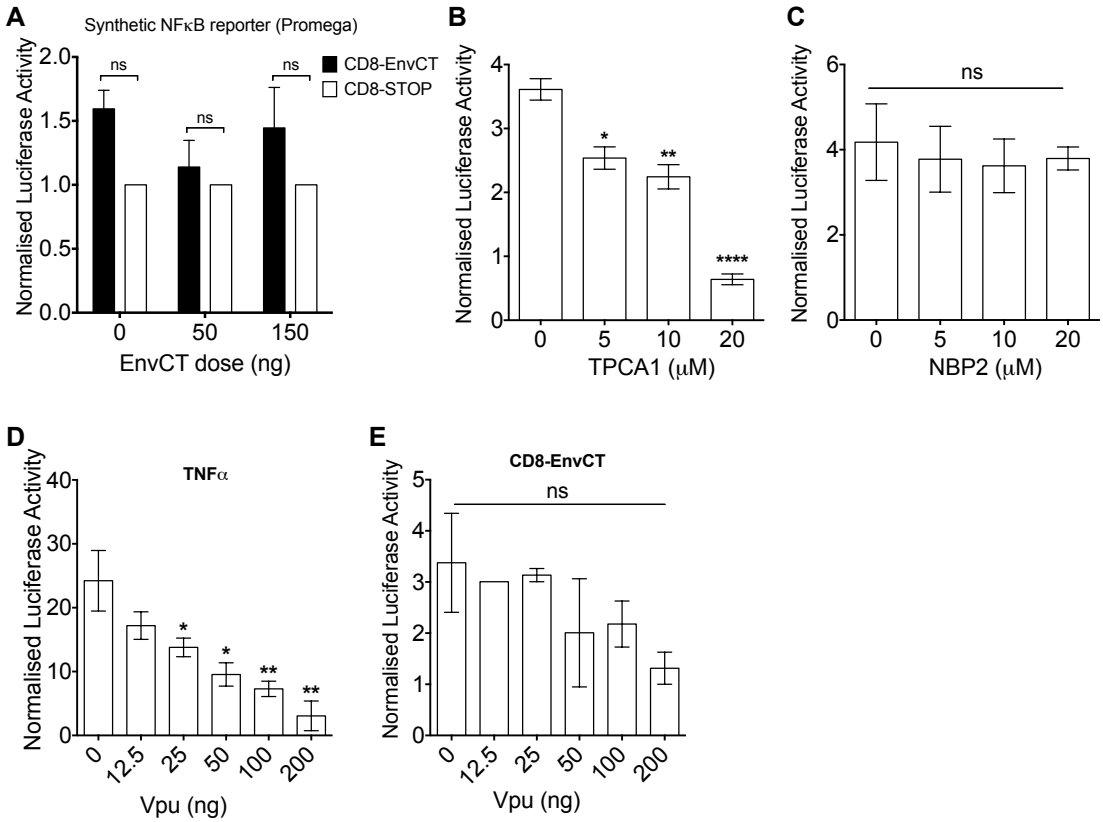

Figure 5.8 Canonical and non-canonical activation of NFκB pathways. Activation of the **(A)** synthetic NFκB reporter (Promega) and **(B-E)** IgK reporter were tested using the Dual Reporter Gene Assay kit (Promega). Luciferase obtained from CD8-EnvCT expression were first normalised to pcDNA empty vector control and then to CD8-STOP, which is also normalised to pcDNA. Fold activation at each dose of CD8-EnvCT was compared with no EnvCT expression (0ng). 293T cells were pretreated with indicated doses of **(B)** TPCA1 and **(C)** NBP2 canonical NFkB pathway inhibitors for 30 mins prior to transfection. Fold activation at each dose of drug was compared with no drug control (0μM) **(D)** 293T cells were cotransfected with indicated doses of Vpu plasmid, 5ng IgK reporter and 2.5ng TK renilla. Cells were treated with TNFα for 6 h prior to cell lysis. **(E)** IgK reporter activation was tested in the presence of indicated doses of Vpu. Fold activation at each dose of CD8-EnvCT was compared with no Vpu expression (0ng). Bars show mean and error bars represent mean +/- SEM from three independent experiments. Fold activation was compared using 2-way ANOVA (*, $p<0.05$; **, $p<0.01$; ***, $p<0.001$, ****, $p<0.0001$).

5.2.5 Env overexpression is toxic in 293T cells.

The results in this chapter demonstrate that the HIV-1 NL4.3 EnvCT activates NFκB and AP-1 signalling. These transcription factors regulate cell activation state, which is important in the context of infection, because activated CD4 T cells are more permissive to HIV-1 infection compared with resting CD4 T cells (Cameron et al., 2010; Swiggard et al., 2005; Yoder et al., 2008). Further, Deng and colleagues (2017) have shown that the Env glycoprotein of HIV-1 plays a role in boosting T cell activation state during cell-cell spread, as Env accumulation at the immunological synapse enhanced T cell receptor-induced CD69 upregulation, IL-2 secretion and cell proliferation (Deng et al., 2016). Further, Postler *et al* (2018) infected T cell lines in the presence and absence of PHA stimulation to show that in activated cells the HIV-1 FL and ΔCT viruses have comparable replication, whereas in sub optimally activated cells (no PHA) the ΔCT virus is unable to spread (Postler and Desrosiers, 2012). This suggests that the EnvCT overcomes a block in sub optimally activated cells by inducing NFκB signalling, indicating a precedent for full length Env protein to activate the NFκB and AP-1 reporter plasmids in our experimental model. To test reporter activation in the presence of full-length HIV-1 NL4.3 Env expression, I repeated the dual luciferase assay using plasmid encoding full length gp160 protein in a pcDNA background. Figure 5.5 shows that there is a 100-fold decrease in TK renilla readings, compared with the pcDNA empty vector control, suggesting that gp160 protein overexpression is cytotoxic. Cytotoxicity can modulate the expression of NFkB and AP-1 signalling components, due to altered cell biology, which masks the effect of Env and therefore these results are not shown.

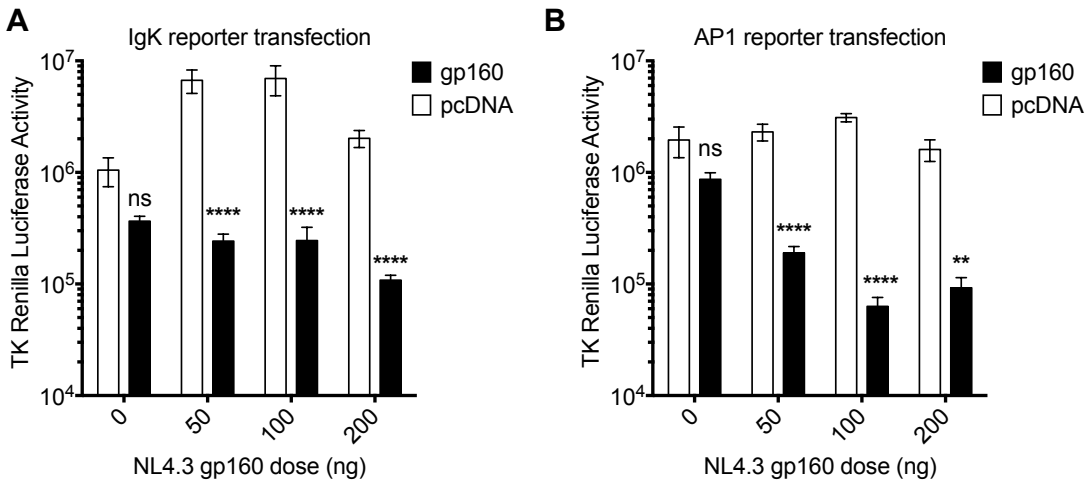

Figure 5.9 HIV-1 gp160 protein expression is cytotoxic. 293T cells were cotransfected with increasing doses of NL4.3 gp160 protein expressed in a pcDNA backbone, 5ng reporter plasmid and 2.5ng TK renilla plasmid. **(A-B)** TK renilla luciferase readings compared with background luciferase upon pcDNA empty vector control expression. Bars show mean and error bars represent mean +/- SEM from three independent experiments. Groups were compared using 2-way ANOVA (ns, $p>0.05$, **, $p<0.01$; ****, $p<0.0001$).

5.3 Discussion

In Chapter 5, I have tested the ability of lentiviral EnvCTs to activate inflammatory and/or antiviral signalling pathways using a dual luciferase reporter gene assay. I have shown that HIV-1 and some SIVs (SIVtan and SIVsmm543), but not HIV-2, activate a reporter plasmid under the control of the natural promoter of the immunoglobulin kappa light chain (IgK) gene, which is also sensitive to NFκB subunits p50 and p65 and contains three repeat kB sequences (referred to as the IgK NFκB reporter). These EnvCTs activate the reporter up to fold compared with the CD8-STOP control. In line with this, a previous study used a similar reporter gene assay and showed that SIVmac239, HIV-1 NL4.3 and two HIV-1 primary isolate EnvCTs, fused to the CD8 ecto- and transmembrane domain, activate NFκB signalling up to 10-fold (Postler and Desrosiers, 2012).

To map the region of the HIV-1 EnvCT responsible for NFκB activation, I used truncation mutants in the CD8-fusion construct to assess reporter gene activation. This showed that the shortest L753* mutant completely abrogated NFκB activation, thus the determinant is within the sequence IWDDLRSLCLFSYHRLRDLLLIVTRIVELLGRR, given that removal of this sequence results in loss of reporter activation. Postler and Desrosiers (2012) used a similar approach to find that the CLFSYHRLRDLL motif (underlined above) is important for NFκB activation (Postler and Desrosiers, 2012). In their study, expression of the CD8-EnvCT truncation mutants resulted in up to 80-fold increased activation of the NFκB reporter by comparison with full length EnvCT which activated the reporter up to 10-fold (Postler and Desrosiers, 2012). This is thought to be as a result of reduced cytotoxicity upon expression of a smaller EnvCT protein, due to EnvCT truncation. Data from this thesis suggests this is probably not true. The TK renilla reporter is constitutively expressed and was therefore used as an internal control for transfection efficiency and cytotoxicity in my experiments, whereby low TK renilla expression is indicative of cellular cytotoxicity. No significant differences were observed in the TK renilla luciferase readings of full length EnvCT expression compared with the EnvCT truncation mutants in this study. This is in contrast to the Postler study which used β-galactosidase as an internal control and suggested that expression of the EnvCT is toxic to 293T cells (Postler and Desrosiers, 2012).

The NFκB family of transcription factors is activated by canonical and non-canonical signalling pathways, which differ in both signalling components and biological functions (Fig. 5.7). Activation of the canonical NFκB pathway leads to activation of IκB kinase (IKK), IKK-mediated IκBα phosphorylation, and subsequent IκBα degradation and nuclear translocation of canonical NFκB members, including p50, RELA and c-REL

(Sun, 2017). By contrast, activation of the non-canonical NFκB pathway is a result of NFκB-inducing kinase (NIK) activation, NIK-mediated p100 phosphorylation, and subsequent p100 processing and nuclear translocation of non-canonical NFκB members, including p52 and RELB (Sun, 2017). Although I have shown that HIV-1 EnvCT can activate NFκB signalling using the IgK NFκB promoter, the commercially available NFκB reporter plasmid containing a synthetic NFκB-sensitive promoter (Promega) was not activated. This suggests that non-canonical NFκB signalling is responsible for luciferase expression in my system. By contrast, Postler *et al* (2012) characterised NFκB activation in their system using an siRNA screen and found that components of the canonical pathway, such as TAK1 and RELA, were required for reporter activation, not RELB which is a component of the non-canonical pathway (Postler and Desrosiers, 2012). Further, coimmunoprecipitation assays and confocal microscopy showed that the EnvCT specifically binds to TAK-1 and the proteins colocalise in transfected cells (Postler and Desrosiers, 2012). It is unclear why these discrepancies exist in our results, although one explanation might be that different NFκB reporter plasmids were used in the two studies, and they both have different sensitivities to stimulation by EnvCTs. To further investigate whether the canonical or canonical pathway is activated, I added NFκB inhibitors that specifically target the canonical pathway to the reporter assay to block pathway activation. TPCA1, which targets the IKKβ subunit, showed a dose dependent reduction in IgK NFκB reporter activity, whereas NBP2, which targets the IKKγ subunit, did not inhibit IgK NFκB activation (Fig. 5.7). Discrepancy between the two drugs might be indicative of different inhibitor potencies. Alternatively, this could be explained by off target effects of TPCA1 on IKKα, which is also part of the non-canonical NFκB pathway (Sun, 2017). Further evidence to suggest that canonical NFκB signalling is not activated in my reporter system, is that the viral accessory protein Vpu was unable to antagonise IgK NFκB reporter activity. The ability of Vpu to exert immunosuppressive activity has been mapped to its ability to suppress NFκB signalling using 293T transfection and reporter gene assays (Hotter et al., 2013a; Manganaro et al., 2015; Sauter et al., 2015). Co-transfection of Vpu, Tetherin (which activates canonical NFκB signalling) and a canonical NFκB reporter plasmid showed that Vpu potently suppresses the canonical NFκB pathway (Hotter et al., 2013a; Manganaro et al., 2015). Further, replication competent HIV-1 ΔVpu mutants induce higher levels of NFκB activity and IFNβ and ISG expression in infected T cells compared with WT virus, suggesting that Vpu is important in antagonising NFκB activity during infection (Sauter et al., 2015). Finally, a recent RNA-seq analysis of HIV-1 infected CD4 T cells also showed that Vpu preferentially suppresses the expression of NFκB target genes that are involved in antiviral responses (Langer et al., 2019).

In this Chapter I show that the Group M HIV-1 NL4.3 EnvCT activates AP-1 signalling up to 10-fold, but not Group O HIV-1 RBF, HIV-2 or SIV EnvCTs. HIV-1 EnvCT truncation mapping revealed that there was a significant loss of AP-1 signalling when mutant Y843*, D833*, R786* and L753* were expressed in the reporter assay. This suggests that there might be multiple determinants in the EnvCT responsible for AP-1 activation. Interestingly, the C-terminal sequence, IWDDLRSLCLFSYHRLRDLLLIVTRIVELLGRR, overlaps with the sequence required for NFκB activation (underlined). This suggests that a common domain in the EnvCT may activate both transcription factors. This sequence is absent in all other lentiviral EnvCTs tested within this study, which might explain why the different HIV and SIV groups do not activate AP-1 reporter activity.

Sequencing of the IgK promoter revealed that the plasmid is a parent or derivative of the IgK CONA Luc plasmid (Genbank LT727454) but does not contain 3 NFκB binding sites from the IgK promoter. Rather, it contains a sequence of unknown origin, which contains a single NFκB binding site that is identical to the site in the HIV-1 LTR, as well as several other predicted NFκB binding sites. Therefore, it is likely that the construct is sensitive to NFκB activation, like the IgK CONA Luc plasmid. The sequencing results also revealed that this region contains 2 identical (in opposite directions) potential AP-1 binding sites (Fig. 5.11), suggesting that IgK promoter activation could be reflective of AP-1 signalling, as well as non-canonical NFκB signalling, in line with the observation that the synthetic NFκB promoter is not activated. However, this does not explain why other viruses, such as HIV-1 RBF and SIVsmm, activate IgK but not the AP-1 reporter. Since these lentiviruses originate from different lineages, it is plausible that they do not behave in a similar manner. The mechanism of NFκB activation may differ between the lentiviruses and perhaps HIV-1 NL4.3 uses a mechanism which results in activation of both AP-1 and the non-canonical NFκB pathway. TAK-1 activation can lead to phosphorylation of MAPK and IKK proteins, resulting in activation of the NFκB and AP-1 signalling pathways (Fig. 5.10) (Dey et al., 2011; Lee et al., 2002b; Ninomiya-Tsuji et al., 1999; Zhou et al., 2003), suggesting that there is crosstalk between these pathways. Also, synergy between NFκB and AP-1 signalling has been suggested previously (Fujioka et al., 2004; Lee et al., 1997; Lee et al., 2002b; Yang et al., 2001). For example, IKK-1 and IKK-2 knock out mice show inhibited *fos* expression due to the fact that NFκB regulates *elk-1* expression. The Elk-1 protein regulates c-Fos, which is a component of the AP-1 complex, and therefore reduced expression of Elk-1 leads to inhibition of AP-1 signalling (Fujioka et al., 2004). This suggests that there is crosstalk between AP-1 and NFκB signalling, which might be manipulated by HIV-1 Group M to enhance viral replication.

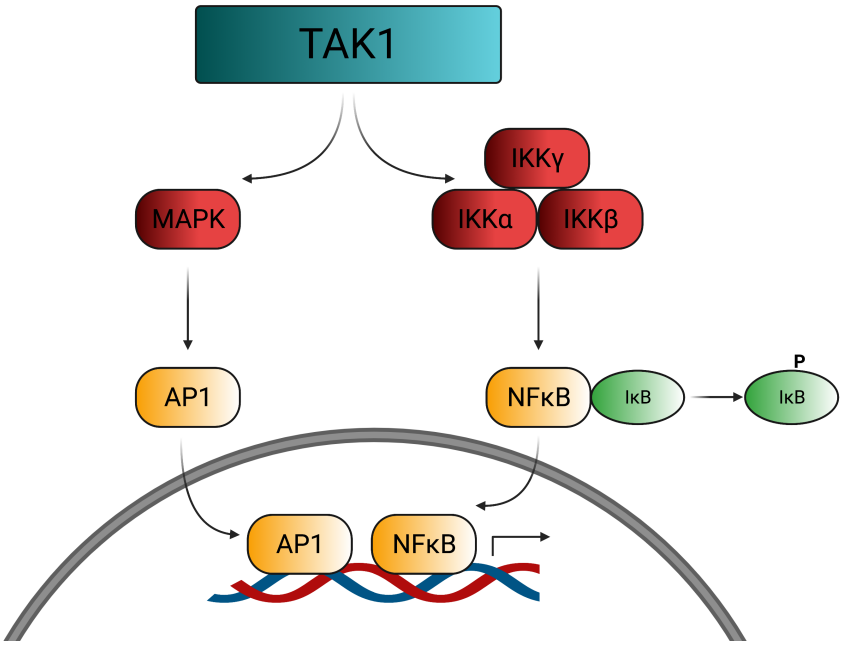

Figure 5.10 TAK1 modulates NFκB and AP-1 signalling. Activation of TAK1 occurs upstream of various stimuli and leads to the phosphorylation of MAPK and IKK proteins. Consequently, IkB is phosphorylated and degraded. The AP-1 and NFκB transcription factors translocate into the nucleus and upregulate inflammatory gene expression.

GCTTCGTACCCCGGGGGATCCTCTTGAGTTGAAGGCTCTCCCCTATTGAGATCCCTG
CATATGAAAGAAGCCCACCCAGTATGTTGAGGCGTTGAGCACCCCCCGCCCCCCAGG
AAATGATGCATGCAAGGAGATGGGGCCCACCAGTTCCCCCGGCCCCGGGGCGTGCCC
CCCTACTCCACGCCGAAAAAGAGGTCTATAGCCCGAAGTGGCGAGCCCGATCTTTCC
CCCTCGGTGATGTTGGCGATATAGGCGCCAGCAACCGCACCTGTGGCGCCGGTGATG
CCGGCCACGATGCGTCCGGCGTAGAGGATATCCCTCTCGGAAAGTACCCTCTGTCTT
CCTCTCTGAAAATCCCCTCTGTCTCCCTCTCGGAAAGTCCCCTCCGTCGATCCTCCC
CTTGAAACAAGGAAGGACAAACAGCGTTTGGTCATTGTTTTTGCAAACACAGCCAGG
GGTGGTCCTTTATAAAAGGGGAAGAAAGAGGCTCCGCAGCCATCACAGACCCAGAGG
GGACGGTCTGTGACCAACACCGCTGCTCCCCCTCCTCAACACCCAGGATCGATCCTA
TTCCAGAAGTAGTGAAGAGGCTTTTTTGGAGGCCTAGGCTTTTGCAAAAAGCTTGGA
ATTCCTTTGTGTTACATTCTTGAACGTCGCTTGCAGTGCCATTAGCATTCCGGTACT
GTGGTAAA

Figure 5.11 IgK promoter sequence. Annotated sequence of the IgK promoter showing a single NFκB site identical to the HIV-1 NL4.3 LTR NFκB site in reverse (highlighted blue), other potential NFκB binding sites (highlighted in yellow) and two potential AP-1 binding sites (highlighted in red).

Similar to the HIV-1 EnvCT, HIV-1 virion-associated Vpr also activates NFκB and AP-1 signalling via enhanced phosphorylation of TAK-1 (Liu et al., 2014). This suggests that both incoming Env gp41 protein and Vpr act early in the viral life cycle, to activate NFκB and AP-1 signalling, which possibly enhances CD4 T cell activation and facilitates viral replication. While the effects of Env gp41 on activating NFkB and AP1 signalling in macrophages has not been evaluated in this thesis, or by Poster et al., it is possible that when infecting macrophages, which are usually quiescent in nature, an early activation event by the EnvCT may also prove be beneficial in initiating viral replication. This could be explored in future work. A direct comparison of HIV-1 replication between viruses that can and cannot activate NFκB signalling, via the EnvCT, in human PBMCs showed that they replicate comparably (Postler and Desrosiers, 2012). However, replication in cells that were cultured in low concentrations of IL-2, revealed that the mutant which does not activate NFκB signalling, replicates less well compared with the wild type counterpart, implying that NFκB activation is required to overcome restrictions that are posed to viral replication by sub-optimally activated cells (Postler and Desrosiers, 2012). Also, during the early stages of viral replication, the restriction factor TRIM5a recognises HIV-1 capsid and activates NFκB and AP-1 signalling in a TAK1-dependent manner, although whether this contributes to innate immune activation remains uncertain (Pertel et al., 2011b). Taken together, these observations show that lentiviruses fine tune the level of NFκB and AP-1 activation upon entry into target cells in order to gain a replicative advantage: Env gp41 and Vpr activate the pathways and concomitantly prevent TRIM5α-induced activation of the same pathways to avoid over stimulation and activation of an antiviral state. During the late stages of the viral life cycle, Tetherin has been shown to activate NFκB signalling, and this is counteracted by HIV-1 Vpu, HIV-2 Env and SIV Nef proteins. Similarly, it is possible that EnvCT-mediated and Vpr-mediated NFκB and AP-1 activation is counteracted by other accessory proteins during late stages of the viral life cycle in order to allow for efficient replication and spread. Finally, I found that reporters that are indicative of a typical type I IFN response, such as IFNβ, ISRE and ISG56 reporters, were not activated by the CD8-EnvCT fusion constructs, arguing against the possibility that an antiviral IFN response is activated by the lentiviral EnvCT. This is further evidence to suggest that NFκB and AP-1 activation by the lentiviral EnvCT is advantageous, possibly by increasing the activation status of infected cells to enhance viral replication, in line with previous studies (Postler and Desrosiers, 2012).

6 Conclusion and Future work

In this thesis, I have uncovered a previously undescribed regulatory role for the enigmatic lentiviral EnvCT: modulation of viral sensitivity to restriction factors that target HIV entry into target cells. Truncation of the EnvCT, downstream of the conserved YxxL endocytic motif, allows HIV-1 and HIV-2 to evade restriction by SERINC and IFITM proteins. To understand how and/or why truncation of the HIV EnvCT allows viral evasion of SERINC5 and IFITMs, I explored the effect of this mutation on Env conformation and functionality. A series of antibody neutralisation assays suggested that the Env ectodomain, including gp120 and gp41 MPER, have dysregulated conformations, since they have altered sensitivity to bnAbs compared with viruses with a full length EnvCT. This in turn had a direct impact on Env's ability to complete fusion, since there was a delay in viral entry into target cells up to 6 hours post infection. However, the ΔCT Envs were more stable compared with FL Envs, thus possibly allowing the ΔCT viruses to eventually complete fusion and reach infectivity levels comparable to the FL virus. This data implies that ΔCT viruses evade SERINC5 and possibly IFITMs, due to the dysregulated nature of the Env ectodomain conformation. The SERINC and IFITM families of restriction factors target Env-mediated fusion of viral and target cell membranes by currently less well understood mechanisms. Data in this thesis suggest that their restriction mechanism is complex and multifaceted. First, SERINC5 and IFITMs might recognise and bind a late fusion intermediate conformation of the Env ectodomain, which then blocks further conformational changes from occurring, that are necessary for the completion of fusion. Alternatively, or perhaps not mutually exclusively, it is possible that the restriction factors modulate the lipid bilayer which indirectly prevents fusion by altering Env conformation as a by-product of lipid modulation. This leads to an unexplored hypothesis that SERINC5 on target cell membranes might also be important in restriction of HIV, like IFITMs. To explore this hypothesis, SERINC5 can be overexpressed in HeLa TZM-bl target cells and infected with virus produced in 293T or T cells, similar to the IFITM experiments described in Chapter 4. It would also be interesting to express IFITM proteins in virus producer cells to determine the effect of EnvCT truncation in this context, given that IFITMs are also postulated to restrict HIV-1 in producer cells (Compton et al., 2014; Tartour et al., 2014; Yu et al., 2015).

A comparative analysis of HIV-1 and HIV-2 replication in T cells revealed that the two human immunodeficiency viruses have differential requirements for the long EnvCT (Chapter 3). HIV-2 can replicate efficiently in the absence of a long EnvCT and could thereby potentially overcome SERINC and IFITM restriction in T cells, whilst HIV-1 cannot. Truncation of the HIV-1 EnvCT leads to a severe defect in viral replication in T cells, which can in part be explained by an Env incorporation defect. An aim of this study

was to understand *why* HIV-1 and HIV-2 have a differential requirement for a long EnvCT, however this still remains elusive. Future studies should compare HIV-1 and HIV-2 assembly, to better understand why there is an Env incorporation defect when HIV-1 EnvCT is truncated but not when HIV-2 EnvCT is truncated. For example, it is possible that the viruses use different mechanisms of Env incorporation, involving different host proteins as cofactors. Nevertheless, this newly described mechanism of restriction factor evasion is not feasible for HIV-1 viruses to utilise *in vivo* or *in vitro* in T cells. Importantly, these data reveal a plasticity of HIV-2 Env towards mechanisms of escape.

Regulation of the Env ectodomain by the EnvCT might have important implications *in vivo*. Indeed, myself and others (Durham et al., 2012; Edwards et al., 2001; Edwards et al., 2002) have shown that truncation of the EnvCT leads to increased sensitivity of HIV-1 to antibodies targeting the gp120 subunit. Perhaps this explains why very few reports on HIV-1 patient isolates describe variants with a truncated EnvCT, as the adaptive immune system clears these variants. Alternatively, this might partly be explained by the fact T cells are not permissive to EnvCT truncation, however it is possible that macrophages may or may not be permissive. Currently, little is known about infection and replication of lentiviruses with ΔCT Env in macrophages, and EnvCT truncation of SIV and HIV-2 has only been reported in T cells. To investigate this, experiments presented in Chapter 3 can be repeated in differentiated THP-1 cells, which have a macrophage-like phenotype, as well as primary macrophages.

In Chapter 3, I discussed data which suggests that HIV-1 ΔCT variants might exist as minority variants *in vivo*, as part of the viral quasispecies (Saha et al., 2005; Zerhouni et al., 2004) and neutralisation assays using gp120 targeting bnAbs in Chapter 4 suggest that these ΔCT variants might remain as minority variants *in vivo* (if they do exist at all) due to the selective pressure exerted by the adaptive immune system. Further, one of the most important functions of the Env glycoprotein is to mediate efficient fusion of viral and target cell membranes. Data in this thesis suggest that the EnvCT regulates this critical function of Env. In Chapter 4, my results show a trend towards increased fusogenicity when the EnvCT is truncated. Previous studies in the SIV model suggest that this increased fusogenicity results in a replicative advantage for the virus, although spreading replication data for my HIV viruses in Chapter 3 do not support the idea of enhanced replication of HIV-2. HIV-2 with a long and short EnvCT replicated comparably in H9 T cells, suggesting that increased fusogenicity may not always correlate with enhanced replication. Future studies using the HIV-2 ST and HIV-2 7312A ΔCT mutants might allow spreading infection to proceed for longer than 9 days in order to ascertain

whether the ΔCT mutants eventually gain a replicative advantage or not. A possible mechanism by which EnvCT truncation might enhance viral replication is by enhancing the ability to perform cell-cell spread, rather than cell-free infection as the former mode of transmission is thought to be at least a magnitude more efficient (Chen et al., 2007; Dimitrov et al., 1993; Martin et al., 2010; Mazurov et al., 2010; Sourisseau et al., 2007). Therefore, an important question which remains to be answered is: does EnvCT truncation allow HIV to perform more efficient cell-cell spread? It is also currently unknown how well HIV-2 performs cell-cell spread compared with HIV-1. These questions can be answered in future studies using well established protocols which quantify viral spread by cell-cell transmission using coculture conditions in which infected donor and target cells are stained to measure viral transfer into target cells. A direct comparison can be made to cell-free infection using a trans-well set up to separate the donor and targets and prevent cell-cell contact.

The cytoplasmic tails of many enveloped viruses have been described as a 'safety catch', which prevents premature activation of Env fusogenicity, as a mechanism of regulating viral fusion and entry. The HIV-1 EnvCT is postulated to interact with Gag in the immature virion, which might prevent premature activation of fusogenicity, before Env trimers are incorporated into virions and HIV buds into the extracellular space. This spontaneous inactivation of Env has been suggested to be induced by SERINC5 present in HIV-1 virions (Sood et al., 2017). Since the ΔCT Env glycoproteins are more stable, it is possible that this is a mechanism by which altered Env conformation allows the virus to evade SERINC5-mediated restriction. Other than HIV-1 EnvCT, cleavage of the cytoplasmic R-peptide of MLV also regulates fusion (Kubo and Amanuma, 2003; Loving et al., 2012) as discussed in previous chapters. Further, recent studies in HCV show that the C-terminal hypervariable region 1 (HVR-1) of the E2 glycoprotein regulates HCV entry efficiency and sensitivity to neutralising antibodies (Stejskal et al., 2020). The HVR-1 region is a highly mobile structure which is constrained at the cell membrane when E2 binds the cell surface receptor SR-B1, thus HRV-1 acts as an entropic safety catch (Stejskal et al., 2020). Long term cell culture of HCV results in mutations which result in preconstrained HVR-1 to allow more efficient E2-SRB1 interactions and viral entry into target cells. However, this results in increased sensitivity to neutralising antibodies which selects against this mutant (Stejskal et al., 2020). This is similar to what I observe with truncation of HIV EnvCTs. Together these data suggest that viruses use their EnvCTs to regulate key viral processes, however this plasticity is not always advantageous *in vivo* due to the selective pressure exerted by the adaptive immune system.

Another interesting observation made in Chapter 4 of this thesis is that HIV-1 ΔCT and HIV-2 viruses with a full length and truncated EnvCT are restricted in U87 cells. Whether this restriction occurs at a pre- or post-entry step remains to be elucidated. This suggests that U87 cells are non-permissive for HIV-1 EnvCT truncation. Also, there might be differences in the utilisation of host cofactors between HIV-1 and HIV-2, such that the cofactors required for HIV-2 are absent in U87 cells, thus there is an infectivity defect. Little data is available of HIV-2 cofactors, therefore this requires further investigation. Future mass spectrometry analysis of HIV-1 FL, HIV-1 ΔCT and HIV-2 viruses might aid our understanding of differences in HIV cofactor usage, which might explain the infectivity defect in U87 cells. Given that HIV-1 and HIV-2 belong to two different lineages, it is plausible that their EnvCT proteins might also behave differently.

SIVs are restricted in human cells and this is possibly due to the presence of a species-specific restriction factor, which SIV evades by truncating the EnvCT. This suggests that this restriction factor may target the EnvCT, which is plausible given that several antiviral proteins, such as MARCH family of proteins (Tada et al., 2015; Zhang et al., 2018; Zhang et al., 2019b) and 90K (Lodermeyer et al., 2018; Lodermeyer et al., 2013), have been described to reduce viral infectivity by targeting Env. A comparative study investigating the sensitivity of HIV-1, HIV-2 and SIV viruses with a long and short EnvCT, to MARCH and 90K might reveal that these proteins are responsible for the EnvCT truncation phenotype. Alternatively, there might be a currently unknown restriction factor which is responsible for SIV truncation and perhaps, HIV-2 is also sensitive to the same restriction factor, explaining why HIV-2 has also been reported to truncate its EnvCT as an adaptation to cell culture (Albert et al., 1987; Evans et al., 1988; Hoxie et al., 1991; Kong et al., 1988; Kumar et al., 1990). This is a plausible hypothesis given that HIV-2 is thought to be less-well adapted to the human host by contrast to the pandemic HIV-1 Group M viruses. In line with this, HIV-2 Nef is a less potent antagonist of SERINC5 compared with its ancestor SIVsmm Nef and HIV-1 Nef (Heigele et al., 2016). Using a heterokaryon system in which permissive infected cells are fused with non-permissive cells could aid in identification of the dominant-acting factor that targets the lentiviral EnvCT and prevents SIV and some HIV-2 viruses with a long EnvCT from replicating in T cells.

Comparative retrovirology has been an important tool to aid our understanding of other lentiviral proteins such as Gag and all the lentiviral accessory proteins. For example, studies focussing on the ability of certain SIV, but not the SIVcpz/HIV-1 lineage, Nef proteins to downmodulate CD3 from the cell surface, revealed that HIV-1 has evolved to retain CD3 in order to enhance viral replication and cell-cell spread (Mesner et al., 2020). Also, there is great plasticity in mechanisms of lentiviral evasion of the restriction factor

Tetherin, whereby HIV-1 uses Vpu (Neil et al., 2008), HIV-2 uses Env (Le Tortorec and Neil, 2009) and most SIVs use Nef (Zhang et al., 2009). This reveals that Tetherin antagonism is a conserved feature of lentiviral biology and that Tetherin exerts a selective pressure which viruses must overcome to replicate successfully. Therefore, such comparative approaches are likely to reveal important and novel insights into the biology of the EnvCT.

To conclude, lentiviruses encode a long, enigmatic EnvCT which is involved in various steps of the viral life cycle including fusion, Env trafficking, Env incorporation and viral assembly (Checkley et al., 2011), as well as regulating Env ectodomain conformation and functionality. This thesis explores the effect of EnvCT truncation on HIV's ability to evade restriction factors, sensitivity to antibody neutralisation and entry efficiency into target cells. I have uncovered a previously unknown mechanism by which HIV-1 and HIV-2 can evade two potent entry targeting restriction factors, SERINC5 and IFITM, however due to differential requirements of the long EnvCT between the two human immunodeficiency viruses, this mechanism of evasion cannot be utilised by HIV-1. This study provides further precedent for the idea that lentiviruses continuously adapt to alterations in selection pressures when introduced into different niches, in order to be able to successfully replicate and transmit.

7 References

Abada, P., Noble, B., and Cannon, P.M. (2005). Functional domains within the human immunodeficiency virus type 2 envelope protein required to enhance virus production. J Virol *79*, 3627-3638.

Abbas, W., Tariq, M., Iqbal, M., Kumar, A., and Herbein, G. (2015). Eradication of HIV-1 from the macrophage reservoir: an uncertain goal? Viruses *7*, 1578-1598.

Abela, I.A., Berlinger, L., Schanz, M., Reynell, L., Gunthard, H.F., Rusert, P., and Trkola, A. (2012). Cell-cell transmission enables HIV-1 to evade inhibition by potent CD4bs directed antibodies. PLoS Pathog *8*, e1002634.

Abrahams, M.R., Anderson, J.A., Giorgi, E.E., Seoighe, C., Mlisana, K., Ping, L.H., Athreya, G.S., Treurnicht, F.K., Keele, B.F., Wood, N.*, et al.* (2009). Quantitating the multiplicity of infection with human immunodeficiency virus type 1 subtype C reveals a non-poisson distribution of transmitted variants. J Virol *83*, 3556-3567.

Abrahamyan, L.G., Mkrtchyan, S.R., Binley, J., Lu, M., Melikyan, G.B., and Cohen, F.S. (2005). The cytoplasmic tail slows the folding of human immunodeficiency virus type 1 Env from a late prebundle configuration into the six-helix bundle. J Virol *79*, 106-115.

Achuthan, V., Perreira, J.M., Sowd, G.A., Puray-Chavez, M., McDougall, W.M., Paulucci-Holthauzen, A., Wu, X., Fadel, H.J., Poeschla, E.M., Multani, A.S.*, et al.* (2018). Capsid-CPSF6 Interaction Licenses Nuclear HIV-1 Trafficking to Sites of Viral DNA Integration. Cell Host Microbe *24*, 392-404 e398.

Affranchino, J.L., and Gonzalez, S.A. (2006). Mutations at the C-terminus of the simian immunodeficiency virus envelope glycoprotein affect gp120-gp41 stability on virions. Virology *347*, 217-225.

Aggarwal, A., Iemma, T.L., Shih, I., Newsome, T.P., McAllery, S., Cunningham, A.L., and Turville, S.G. (2012). Mobilization of HIV spread by diaphanous 2 dependent filopodia in infected dendritic cells. PLoS Pathog *8*, e1002762.

Agosto, L.M., Zhong, P., Munro, J., and Mothes, W. (2014). Highly active antiretroviral therapies are effective against HIV-1 cell-to-cell transmission. PLoS Pathog *10*, e1003982.

Aguilar, H.C., Anderson, W.F., and Cannon, P.M. (2003). Cytoplasmic tail of Moloney murine leukemia virus envelope protein influences the conformation of the extracellular domain: implications for mechanism of action of the R Peptide. J Virol *77*, 1281-1291.

Ahi, Y.S., Zhang, S., Thappeta, Y., Denman, A., Feizpour, A., Gummuluru, S., Reinhard, B., Muriaux, D., Fivash, M.J., and Rein, A. (2016). Functional Interplay Between Murine Leukemia Virus Glycogag, Serinc5, and Surface Glycoprotein Governs Virus Entry, with Opposite Effects on Gammaretroviral and Ebolavirus Glycoproteins. mBio *7*.

Aiken, C., Konner, J., Landau, N.R., Lenburg, M.E., and Trono, D. (1994). Nef induces CD4 endocytosis: requirement for a critical dileucine motif in the membrane-proximal CD4 cytoplasmic domain. Cell *76*, 853-864.

Akari, H., Fukumori, T., and Adachi, A. (2000). Cell-dependent requirement of human immunodeficiency virus type 1 gp41 cytoplasmic tail for Env incorporation into virions. J Virol *74*, 4891-4893.

Albert, J., Bredberg, U., Chiodi, F., Bottiger, B., Fenyo, E.M., Norrby, E., and Biberfeld, G. (1987). A new human retrovirus isolate of West African origin (SBL-6669) and its relationship to HTLV-IV, LAV-II, and HTLV-IIIB. AIDS Res Hum Retroviruses *3*, 3-10.

Alfadhli, A., Barklis, R.L., and Barklis, E. (2009). HIV-1 matrix organizes as a hexamer of trimers on membranes containing phosphatidylinositol-(4,5)-bisphosphate. Virology *387*, 466-472.

Alfadhli, A., Mack, A., Ritchie, C., Cylinder, I., Harper, L., Tedbury, P.R., Freed, E.O., and Barklis, E. (2016). Trimer Enhancement Mutation Effects on HIV-1 Matrix Protein Binding Activities. J Virol *90*, 5657-5664.

Alfadhli, A., Staubus, A.O., Tedbury, P.R., Novikova, M., Freed, E.O., and Barklis, E. (2019). Analysis of HIV-1 Matrix-Envelope Cytoplasmic Tail Interactions. J Virol *93*.

Alkhatib, G., Combadiere, C., Broder, C.C., Feng, Y., Kennedy, P.E., Murphy, P.M., and Berger, E.A. (1996). CC CKR5: a RANTES, MIP-1alpha, MIP-1beta receptor as a fusion cofactor for macrophage-tropic HIV-1. Science *272*, 1955-1958.

Allan, J.S., Coligan, J.E., Barin, F., McLane, M.F., Sodroski, J.G., Rosen, C.A., Haseltine, W.A., Lee, T.H., and Essex, M. (1985). Major glycoprotein antigens that induce antibodies in AIDS patients are encoded by HTLV-III. Science *228*, 1091-1094.

Alvarez, F.J.D., He, S., Perilla, J.R., Jang, S., Schulten, K., Engelman, A.N., Scheres, S.H.W., and Zhang, P. (2017). CryoEM structure of MxB reveals a novel oligomerization interface critical for HIV restriction. Sci Adv *3*, e1701264.

Alvarez, R.A., Barria, M.I., and Chen, B.K. (2014a). Unique features of HIV-1 spread through T cell virological synapses. PLoS Pathog *10*, e1004513.

Alvarez, R.A., Hamlin, R.E., Monroe, A., Moldt, B., Hotta, M.T., Rodriguez Caprio, G., Fierer, D.S., Simon, V., and Chen, B.K. (2014b). HIV-1 Vpu antagonism of tetherin inhibits antibody-dependent cellular cytotoxic responses by natural killer cells. J Virol *88*, 6031-6046.

Amini-Bavil-Olyaee, S., Choi, Y.J., Lee, J.H., Shi, M., Huang, I.C., Farzan, M., and Jung, J.U. (2013). The antiviral effector IFITM3 disrupts intracellular cholesterol homeostasis to block viral entry. Cell Host Microbe *13*, 452-464.

Anderson, J.L., Johnson, A.T., Howard, J.L., and Purcell, D.F. (2007). Both linear and discontinuous ribosome scanning are used for translation initiation from bicistronic human immunodeficiency virus type 1 env mRNAs. J Virol *81*, 4664-4676.

Archin, N.M., Sung, J.M., Garrido, C., Soriano-Sarabia, N., and Margolis, D.M. (2014). Eradicating HIV-1 infection: seeking to clear a persistent pathogen. Nat Rev Microbiol *12*, 750-764.

Arhel, N., Lehmann, M., Clauss, K., Nienhaus, G.U., Piguet, V., and Kirchhoff, F. (2009). The inability to disrupt the immunological synapse between infected human T cells and APCs distinguishes HIV-1 from most other primate lentiviruses. J Clin Invest *119*, 2965-2975.

Arias, J.F., Heyer, L.N., von Bredow, B., Weisgrau, K.L., Moldt, B., Burton, D.R., Rakasz, E.G., and Evans, D.T. (2014). Tetherin antagonism by Vpu protects HIV-infected cells from antibody-dependent cell-mediated cytotoxicity. Proc Natl Acad Sci U S A *111*, 6425-6430.

Arighi, C.N., Hartnell, L.M., Aguilar, R.C., Haft, C.R., and Bonifacino, J.S. (2004). Role of the mammalian retromer in sorting of the cation-independent mannose 6-phosphate receptor. J Cell Biol *165*, 123-133.

Arnold, L.H., Groom, H.C., Kunzelmann, S., Schwefel, D., Caswell, S.J., Ordonez, P., Mann, M.C., Rueschenbaum, S., Goldstone, D.C., Pennell, S.*, et al.* (2015). Phospho-dependent Regulation of SAMHD1 Oligomerisation Couples Catalysis and Restriction. PLoS Pathog *11*, e1005194.

Arrighi, J.F., Pion, M., Garcia, E., Escola, J.M., van Kooyk, Y., Geijtenbeek, T.B., and Piguet, V. (2004). DC-SIGN-mediated infectious synapse formation enhances X4 HIV-1 transmission from dendritic cells to T cells. J Exp Med *200*, 1279-1288.

Arthur, L.O., Bess, J.W., Jr., Sowder, R.C., 2nd, Benveniste, R.E., Mann, D.L., Chermann, J.C., and Henderson, L.E. (1992). Cellular proteins bound to immunodeficiency viruses: implications for pathogenesis and vaccines. Science *258*, 1935-1938.

Autran, B., Carcelain, G., Li, T.S., Blanc, C., Mathez, D., Tubiana, R., Katlama, C., Debre, P., and Leibowitch, J. (1997). Positive effects of combined antiretroviral therapy on CD4+ T cell homeostasis and function in advanced HIV disease. Science *277*, 112-116.

Ayouba, A., Akoua-Koffi, C., Calvignac-Spencer, S., Esteban, A., Locatelli, S., Li, H., Li, Y., Hahn, B.H., Delaporte, E., Leendertz, F.H.*, et al.* (2013). Evidence for continuing cross-species transmission of SIVsmm to humans: characterization of a new HIV-2 lineage in rural Cote d'Ivoire. AIDS *27*, 2488-2491.

Ayyavoo, V., Mahboubi, A., Mahalingam, S., Ramalingam, R., Kudchodkar, S., Williams, W.V., Green, D.R., and Weiner, D.B. (1997). HIV-1 Vpr suppresses immune activation and apoptosis through regulation of nuclear factor kappa B. Nat Med *3*, 1117-1123.

Bailes, E., Gao, F., Bibollet-Ruche, F., Courgnaud, V., Peeters, M., Marx, P.A., Hahn, B.H., and Sharp, P.M. (2003). Hybrid origin of SIV in chimpanzees. Science *300*, 1713.

Bailey, C.C., Kondur, H.R., Huang, I.C., and Farzan, M. (2013). Interferon-induced transmembrane protein 3 is a type II transmembrane protein. J Biol Chem *288*, 32184-32193.

Bailey, C.C., Zhong, G., Huang, I.C., and Farzan, M. (2014). IFITM-Family Proteins: The Cell's First Line of Antiviral Defense. Annu Rev Virol *1*, 261-283.

Bakouche, N., Vandenbroucke, A.T., Goubau, P., and Ruelle, J. (2013). Study of the HIV-2 Env cytoplasmic tail variability and its impact on Tat, Rev and Nef. PLoS One *8*, e79129.

Baldauf, H.M., Pan, X., Erikson, E., Schmidt, S., Daddacha, W., Burggraf, M., Schenkova, K., Ambiel, I., Wabnitz, G., Gramberg, T.*, et al.* (2012). SAMHD1 restricts HIV-1 infection in resting CD4(+) T cells. Nat Med *18*, 1682-1687.

Baldauf, H.M., Stegmann, L., Schwarz, S.M., Ambiel, I., Trotard, M., Martin, M., Burggraf, M., Lenzi, G.M., Lejk, H., Pan, X.*, et al.* (2017). Vpx overcomes a SAMHD1-independent block to HIV reverse transcription that is specific to resting CD4 T cells. Proc Natl Acad Sci U S A *114*, 2729-2734.

Baltimore, D. (1970). RNA-dependent DNA polymerase in virions of RNA tumour viruses. Nature *226*, 1209-1211.

Barnett, S.W., Quiroga, M., Werner, A., Dina, D., and Levy, J.A. (1993). Distinguishing features of an infectious molecular clone of the highly divergent and noncytopathic human immunodeficiency virus type 2 UC1 strain. J Virol *67*, 1006-1014.

Barr, S.D., Ciuffi, A., Leipzig, J., Shinn, P., Ecker, J.R., and Bushman, F.D. (2006). HIV integration site selection: targeting in macrophages and the effects of different routes of viral entry. Mol Ther *14*, 218-225.

Barre-Sinoussi, F., Chermann, J.C., Rey, F., Nugeyre, M.T., Chamaret, S., Gruest, J., Dauguet, C., Axler-Blin, C., Vezinet-Brun, F., Rouzioux, C.*, et al.* (1983). Isolation of a T-lymphotropic retrovirus from a patient at risk for acquired immune deficiency syndrome (AIDS). Science *220*, 868-871.

Bartesaghi, A., Merk, A., Borgnia, M.J., Milne, J.L., and Subramaniam, S. (2013). Prefusion structure of trimeric HIV-1 envelope glycoprotein determined by cryo-electron microscopy. Nat Struct Mol Biol *20*, 1352-1357.

Batorsky, R., Kearney, M.F., Palmer, S.E., Maldarelli, F., Rouzine, I.M., and Coffin, J.M. (2011). Estimate of effective recombination rate and average selection coefficient for HIV in chronic infection. Proc Natl Acad Sci U S A *108*, 5661-5666.

Baxter, A.E., Russell, R.A., Duncan, C.J., Moore, M.D., Willberg, C.B., Pablos, J.L., Finzi, A., Kaufmann, D.E., Ochsenbauer, C., Kappes, J.C.*, et al.* (2014). Macrophage infection via selective capture of HIV-1-infected CD4+ T cells. Cell Host Microbe *16*, 711-721.

Beitari, S., Ding, S., Pan, Q., Finzi, A., and Liang, C. (2017). Effect of HIV-1 Env on SERINC5 Antagonism. J Virol *91*.

Bejarano, D.A., Peng, K., Laketa, V., Borner, K., Jost, K.L., Lucic, B., Glass, B., Lusic, M., Muller, B., and Krausslich, H.G. (2019). HIV-1 nuclear import in macrophages is regulated by CPSF6-capsid interactions at the nuclear pore complex. Elife *8*.

Bennett, A.E., Narayan, K., Shi, D., Hartnell, L.M., Gousset, K., He, H., Lowekamp, B.C., Yoo, T.S., Bliss, D., Freed, E.O.*, et al.* (2009). Ion-abrasion scanning electron microscopy reveals surface-connected tubular conduits in HIV-infected macrophages. PLoS Pathog *5*, e1000591.

Berger, G., Lawrence, M., Hue, S., and Neil, S.J. (2015). G2/M cell cycle arrest correlates with primate lentiviral Vpr interaction with the SLX4 complex. J Virol *89*, 230-240.

Bergeron, J.R., Huthoff, H., Veselkov, D.A., Beavil, R.L., Simpson, P.J., Matthews, S.J., Malim, M.H., and Sanderson, M.R. (2010). The SOCS-box of HIV-1 Vif interacts with ElonginBC by induced-folding to recruit its Cul5-containing ubiquitin ligase complex. PLoS Pathog *6*, e1000925.

Berkhout, B., Silverman, R.H., and Jeang, K.T. (1989). Tat trans-activates the human immunodeficiency virus through a nascent RNA target. Cell *59*, 273-282.

Berlioz-Torrent, C., Shacklett, B.L., Erdtmann, L., Delamarre, L., Bouchaert, I., Sonigo, P., Dokhelar, M.C., and Benarous, R. (1999). Interactions of the cytoplasmic domains of human and simian retroviral transmembrane proteins with components of the clathrin adaptor complexes modulate intracellular and cell surface expression of envelope glycoproteins. J Virol *73*, 1350-1361.

Berman, P.W., Groopman, J.E., Gregory, T., Clapham, P.R., Weiss, R.A., Ferriani, R., Riddle, L., Shimasaki, C., Lucas, C., Lasky, L.A.*, et al.* (1988). Human immunodeficiency virus type 1 challenge of chimpanzees immunized with recombinant envelope glycoprotein gp120. Proc Natl Acad Sci U S A *85*, 5200-5204.

Berndsen, Z.T., Chakraborty, S., Wang, X., Cottrell, C.A., Torres, J.L., Diedrich, J.K., Lopez, C.A., Yates, J.R., 3rd, van Gils, M.J., Paulson, J.C.*, et al.* (2020). Visualization of the HIV-1 Env glycan shield across scales. Proc Natl Acad Sci U S A *117*, 28014-28025.

Bernstein, H.B., Tucker, S.P., Hunter, E., Schutzbach, J.S., and Compans, R.W. (1994). Human immunodeficiency virus type 1 envelope glycoprotein is modified by O-linked oligosaccharides. J Virol *68*, 463-468.

Berry, N., Jaffar, S., Schim van der Loeff, M., Ariyoshi, K., Harding, E., N'Gom, P.T., Dias, F., Wilkins, A., Ricard, D., Aaby, P.*, et al.* (2002). Low level viremia and high CD4% predict normal survival in a cohort of HIV type-2-infected villagers. AIDS Res Hum Retroviruses *18*, 1167-1173.

Bhattacharya, J., Peters, P.J., and Clapham, P.R. (2003). CD4-independent infection of HIV and SIV: implications for envelope conformation and cell tropism in vivo. AIDS *17 Suppl 4*, S35-43.

Bhattacharya, J., Repik, A., and Clapham, P.R. (2006). Gag regulates association of human immunodeficiency virus type 1 envelope with detergent-resistant membranes. J Virol *80*, 5292-5300.

Bichel, K., Price, A.J., Schaller, T., Towers, G.J., Freund, S.M., and James, L.C. (2013). HIV-1 capsid undergoes coupled binding and isomerization by the nuclear pore protein NUP358. Retrovirology *10*, 81.

Bishop, K.N., Holmes, R.K., Sheehy, A.M., Davidson, N.O., Cho, S.J., and Malim, M.H. (2004). Cytidine deamination of retroviral DNA by diverse APOBEC proteins. Curr Biol *14*, 1392-1396.

Bishop, K.N., Verma, M., Kim, E.Y., Wolinsky, S.M., and Malim, M.H. (2008). APOBEC3G inhibits elongation of HIV-1 reverse transcripts. PLoS Pathog *4*, e1000231.

Bleck, M., Itano, M.S., Johnson, D.S., Thomas, V.K., North, A.J., Bieniasz, P.D., and Simon, S.M. (2014). Temporal and spatial organization of ESCRT protein recruitment during HIV-1 budding. Proc Natl Acad Sci U S A *111*, 12211-12216.

Blot, G., Janvier, K., Le Panse, S., Benarous, R., and Berlioz-Torrent, C. (2003). Targeting of the human immunodeficiency virus type 1 envelope to the trans-Golgi network through binding to TIP47 is required for env incorporation into virions and infectivity. J Virol *77*, 6931-6945.

Bobkova, M., Stitz, J., Engelstadter, M., Cichutek, K., and Buchholz, C.J. (2002). Identification of R-peptides in envelope proteins of C-type retroviruses. J Gen Virol *83*, 2241-2246.

Boge, M., Wyss, S., Bonifacino, J.S., and Thali, M. (1998). A membrane-proximal tyrosine-based signal mediates internalization of the HIV-1 envelope glycoprotein via interaction with the AP-2 clathrin adaptor. J Biol Chem *273*, 15773-15778.

Bogerd, H.P., and Cullen, B.R. (2008). Single-stranded RNA facilitates nucleocapsid: APOBEC3G complex formation. RNA *14*, 1228-1236.

Bonavia, A., Bullock, B.T., Gisselman, K.M., Margulies, B.J., and Clements, J.E. (2005). A single amino acid change and truncated TM are sufficient for simian immunodeficiency virus to enter cells using CCR5 in a CD4-independent pathway. Virology *341*, 12-23.

Bonomelli, C., Doores, K.J., Dunlop, D.C., Thaney, V., Dwek, R.A., Burton, D.R., Crispin, M., and Scanlan, C.N. (2011). The glycan shield of HIV is predominantly oligomannose independently of production system or viral clade. PLoS One *6*, e23521.

Bosinger, S.E., Li, Q., Gordon, S.N., Klatt, N.R., Duan, L., Xu, L., Francella, N., Sidahmed, A., Smith, A.J., Cramer, E.M.*, et al.* (2009). Global genomic analysis reveals rapid control of a robust innate response in SIV-infected sooty mangabeys. J Clin Invest *119*, 3556-3572.

Bour, S., Geleziunas, R., and Wainberg, M.A. (1995). The human immunodeficiency virus type 1 (HIV-1) CD4 receptor and its central role in promotion of HIV-1 infection. Microbiol Rev *59*, 63-93.

Bour, S., Perrin, C., Akari, H., and Strebel, K. (2001). The human immunodeficiency virus type 1 Vpu protein inhibits NF-kappa B activation by interfering with beta TrCP-mediated degradation of Ikappa B. J Biol Chem *276*, 15920-15928.

Bowers, K., Pelchen-Matthews, A., Honing, S., Vance, P.J., Creary, L., Haggarty, B.S., Romano, J., Ballensiefen, W., Hoxie, J.A., and Marsh, M. (2000). The simian immunodeficiency virus envelope glycoprotein contains multiple signals that regulate its cell surface expression and endocytosis. Traffic *1*, 661-674.

Brandenberg, O.F., Magnus, C., Regoes, R.R., and Trkola, A. (2015a). The HIV-1 Entry Process: A Stoichiometric View. Trends Microbiol *23*, 763-774.

Brandenberg, O.F., Magnus, C., Rusert, P., Regoes, R.R., and Trkola, A. (2015b). Different infectivity of HIV-1 strains is linked to number of envelope trimers required for entry. PLoS Pathog *11*, e1004595.

Brass, A.L., Dykxhoorn, D.M., Benita, Y., Yan, N., Engelman, A., Xavier, R.J., Lieberman, J., and Elledge, S.J. (2008). Identification of host proteins required for HIV infection through a functional genomic screen. Science *319*, 921-926.

Brass, A.L., Huang, I.C., Benita, Y., John, S.P., Krishnan, M.N., Feeley, E.M., Ryan, B.J., Weyer, J.L., van der Weyden, L., Fikrig, E.*, et al.* (2009). The IFITM proteins mediate cellular resistance to influenza A H1N1 virus, West Nile virus, and dengue virus. Cell *139*, 1243-1254.

Braun, E., Hotter, D., Koepke, L., Zech, F., Gross, R., Sparrer, K.M.J., Muller, J.A., Pfaller, C.K., Heusinger, E., Wombacher, R.*, et al.* (2019). Guanylate-Binding Proteins 2 and 5 Exert Broad Antiviral Activity by Inhibiting Furin-Mediated Processing of Viral Envelope Proteins. Cell Rep *27*, 2092-2104 e2010.

Brenchley, J.M., Paiardini, M., Knox, K.S., Asher, A.I., Cervasi, B., Asher, T.E., Scheinberg, P., Price, D.A., Hage, C.A., Kholi, L.M.*, et al.* (2008). Differential Th17 CD4 T-cell depletion in pathogenic and nonpathogenic lentiviral infections. Blood *112*, 2826-2835.

Brenchley, J.M., Price, D.A., Schacker, T.W., Asher, T.E., Silvestri, G., Rao, S., Kazzaz, Z., Bornstein, E., Lambotte, O., Altmann, D.*, et al.* (2006). Microbial translocation is a cause of systemic immune activation in chronic HIV infection. Nat Med *12*, 1365-1371.

Briggs, J.A., Wilk, T., Welker, R., Krausslich, H.G., and Fuller, S.D. (2003). Structural organization of authentic, mature HIV-1 virions and cores. EMBO J *22*, 1707-1715.

Brown, P.O., Bowerman, B., Varmus, H.E., and Bishop, J.M. (1989). Retroviral integration: structure of the initial covalent product and its precursor, and a role for the viral IN protein. Proc Natl Acad Sci U S A *86*, 2525-2529.

Bruel, T., Guivel-Benhassine, F., Amraoui, S., Malbec, M., Richard, L., Bourdic, K., Donahue, D.A., Lorin, V., Casartelli, N., Noel, N.*, et al.* (2016). Elimination of HIV-1-infected cells by broadly neutralizing antibodies. Nat Commun *7*, 10844.

Brugger, B., Glass, B., Haberkant, P., Leibrecht, I., Wieland, F.T., and Krausslich, H.G. (2006). The HIV lipidome: a raft with an unusual composition. Proc Natl Acad Sci U S A *103*, 2641-2646.

Bruner, K.M., Murray, A.J., Pollack, R.A., Soliman, M.G., Laskey, S.B., Capoferri, A.A., Lai, J., Strain, M.C., Lada, S.M., Hoh, R.*, et al.* (2016). Defective proviruses rapidly accumulate during acute HIV-1 infection. Nat Med *22*, 1043-1049.

Bruner, K.M., Wang, Z., Simonetti, F.R., Bender, A.M., Kwon, K.J., Sengupta, S., Fray, E.J., Beg, S.A., Antar, A.A.R., Jenike, K.M.*, et al.* (2019). A quantitative approach for measuring the reservoir of latent HIV-1 proviruses. Nature *566*, 120-125.

Buffalo, C.Z., Iwamoto, Y., Hurley, J.H., and Ren, X. (2019). How HIV Nef Proteins Hijack Membrane Traffic To Promote Infection. J Virol *93*.

Buffone, C., Schulte, B., Opp, S., and Diaz-Griffero, F. (2015). Contribution of MxB oligomerization to HIV-1 capsid binding and restriction. J Virol *89*, 3285-3294.

Bultmann, A., Muranyi, W., Seed, B., and Haas, J. (2001). Identification of two sequences in the cytoplasmic tail of the human immunodeficiency virus type 1 envelope glycoprotein that inhibit cell surface expression. J Virol *75*, 5263-5276.

Buratti, E., McLain, L., Tisminetzky, S., Cleveland, S.M., Dimmock, N.J., and Baralle, F.E. (1998). The neutralizing antibody response against a conserved region of human immunodeficiency virus type 1 gp41 (amino acid residues 731-752) is uniquely directed against a conformational epitope. J Gen Virol *79 (Pt 11)*, 2709-2716.

Burdick, R.C., Li, C., Munshi, M., Rawson, J.M.O., Nagashima, K., Hu, W.S., and Pathak, V.K. (2020). HIV-1 uncoats in the nucleus near sites of integration. Proc Natl Acad Sci U S A *117*, 5486-5493.

Burnett, J.C., Miller-Jensen, K., Shah, P.S., Arkin, A.P., and Schaffer, D.V. (2009). Control of stochastic gene expression by host factors at the HIV promoter. PLoS Pathog *5*, e1000260.

Burton, D.R., and Hangartner, L. (2016). Broadly Neutralizing Antibodies to HIV and Their Role in Vaccine Design. Annu Rev Immunol *34*, 635-659.

Busnadiego, I., Kane, M., Rihn, S.J., Preugschas, H.F., Hughes, J., Blanco-Melo, D., Strouvelle, V.P., Zang, T.M., Willett, B.J., Boutell, C.*, et al.* (2014). Host and viral determinants of Mx2 antiretroviral activity. J Virol *88*, 7738-7752.

Buttler, C.A., Pezeshkian, N., Fernandez, M.V., Aaron, J., Norman, S., Freed, E.O., and van Engelenburg, S.B. (2018). Single molecule fate of HIV-1 envelope reveals late-stage viral lattice incorporation. Nat Commun *9*, 1861.

Byland, R., Vance, P.J., Hoxie, J.A., and Marsh, M. (2007). A conserved dileucine motif mediates clathrin and AP-2-dependent endocytosis of the HIV-1 envelope protein. Mol Biol Cell *18*, 414-425.

Calantone, N., Wu, F., Klase, Z., Deleage, C., Perkins, M., Matsuda, K., Thompson, E.A., Ortiz, A.M., Vinton, C.L., Ourmanov, I.*, et al.* (2014). Tissue myeloid cells in SIV-infected primates acquire viral DNA through phagocytosis of infected T cells. Immunity *41*, 493-502.

Cameron, P.U., Forsum, U., Teppler, H., Granelli-Piperno, A., and Steinman, R.M. (1992). During HIV-1 infection most blood dendritic cells are not productively infected and can induce allogeneic CD4+ T cells clonal expansion. Clin Exp Immunol *88*, 226-236.

Cameron, P.U., Saleh, S., Sallmann, G., Solomon, A., Wightman, F., Evans, V.A., Boucher, G., Haddad, E.K., Sekaly, R.P., Harman, A.N.*, et al.* (2010). Establishment of HIV-1 latency in resting CD4+ T cells depends on chemokine-induced changes in the actin cytoskeleton. Proc Natl Acad Sci U S A *107*, 16934-16939.

Campbell, S.M., Crowe, S.M., and Mak, J. (2002). Virion-associated cholesterol is critical for the maintenance of HIV-1 structure and infectivity. AIDS *16*, 2253-2261.

Cao, L., Diedrich, J.K., Kulp, D.W., Pauthner, M., He, L., Park, S.R., Sok, D., Su, C.Y., Delahunty, C.M., Menis, S.*, et al.* (2017). Global site-specific N-glycosylation analysis of HIV envelope glycoprotein. Nat Commun *8*, 14954.

Carr, J. M., Hocking, H., Li, P., & Burrell, C. J. (1999). Rapid and efficient cell-to-cell transmission of human immunodeficiency virus infection from monocyte-derived macrophages to peripheral blood lymphocytes. *Virology*, *265*(2), 319–329.

Casartelli, N., Guivel-Benhassine, F., Bouziat, R., Brandler, S., Schwartz, O., and Moris, A. (2010a). The antiviral factor APOBEC3G improves CTL recognition of cultured HIV-infected T cells. J Exp Med *207*, 39-49.

Casartelli, N., Sourisseau, M., Feldmann, J., Guivel-Benhassine, F., Mallet, A., Marcelin, A.G., Guatelli, J., and Schwartz, O. (2010b). Tetherin restricts productive HIV-1 cell-to-cell transmission. PLoS Pathog *6*, e1000955.

Cavrois, M., De Noronha, C., and Greene, W.C. (2002). A sensitive and specific enzyme-based assay detecting HIV-1 virion fusion in primary T lymphocytes. Nat Biotechnol *20*, 1151-1154.

Chahroudi, A., Bosinger, S.E., Vanderford, T.H., Paiardini, M., and Silvestri, G. (2012). Natural SIV hosts: showing AIDS the door. Science *335*, 1188-1193.

Chaipan, C., Smith, J.L., Hu, W.S., and Pathak, V.K. (2013). APOBEC3G restricts HIV-1 to a greater extent than APOBEC3F and APOBEC3DE in human primary CD4+ T cells and macrophages. J Virol *87*, 444-453.

Chakrabarti, L., Guyader, M., Alizon, M., Daniel, M.D., Desrosiers, R.C., Tiollais, P., and Sonigo, P. (1987). Sequence of simian immunodeficiency virus from macaque and its relationship to other human and simian retroviruses. Nature *328*, 543-547.

Chan, D.C., Fass, D., Berger, J.M., and Kim, P.S. (1997). Core structure of gp41 from the HIV envelope glycoprotein. Cell *89*, 263-273.

Chande, A., Cuccurullo, E.C., Rosa, A., Ziglio, S., Carpenter, S., and Pizzato, M. (2016). S2 from equine infectious anemia virus is an infectivity factor which counteracts the retroviral inhibitors SERINC5 and SERINC3. Proc Natl Acad Sci U S A *113*, 13197-13202.

Chaudhuri, R., Mattera, R., Lindwasser, O.W., Robinson, M.S., and Bonifacino, J.S. (2009). A basic patch on alpha-adaptin is required for binding of human immunodeficiency virus type 1 Nef and cooperative assembly of a CD4-Nef-AP-2 complex. J Virol *83*, 2518-2530.

Checkley, M.A., Luttge, B.G., and Freed, E.O. (2011). HIV-1 envelope glycoprotein biosynthesis, trafficking, and incorporation. J Mol Biol *410*, 582-608.

Checkley, M.A., Luttge, B.G., Mercredi, P.Y., Kyere, S.K., Donlan, J., Murakami, T., Summers, M.F., Cocklin, S., and Freed, E.O. (2013). Reevaluation of the requirement for TIP47 in human immunodeficiency virus type 1 envelope glycoprotein incorporation. J Virol *87*, 3561-3570.

Chen, B. (2019). Molecular Mechanism of HIV-1 Entry. Trends Microbiol *27*, 878-891.

Chen, B., and Chou, J.J. (2017). Structure of the transmembrane domain of HIV-1 envelope glycoprotein. FEBS J *284*, 1171-1177.

Chen, J., Kovacs, J.M., Peng, H., Rits-Volloch, S., Lu, J., Park, D., Zablowsky, E., Seaman, M.S., and Chen, B. (2015). HIV-1 ENVELOPE. Effect of the cytoplasmic domain on antigenic characteristics of HIV-1 envelope glycoprotein. Science *349*, 191-195.

Chen, J., Nikolaitchik, O., Singh, J., Wright, A., Bencsics, C.E., Coffin, J.M., Ni, N., Lockett, S., Pathak, V.K., and Hu, W.S. (2009). High efficiency of HIV-1 genomic RNA packaging and heterozygote formation revealed by single virion analysis. Proc Natl Acad Sci U S A *106*, 13535-13540.

Chen, P., Hubner, W., Spinelli, M.A., and Chen, B.K. (2007). Predominant mode of human immunodeficiency virus transfer between T cells is mediated by sustained Env-dependent neutralization-resistant virological synapses. J Virol *81*, 12582-12595.

Chen, S.S., Lee, S.F., and Wang, C.T. (2001). Cellular membrane-binding ability of the C-terminal cytoplasmic domain of human immunodeficiency virus type 1 envelope transmembrane protein gp41. J Virol *75*, 9925-9938.

Chen, Y.C., Sood, C., Marin, M., Aaron, J., Gratton, E., Salaita, K., and Melikyan, G.B. (2020). Super-Resolution Fluorescence Imaging Reveals That Serine Incorporator

Protein 5 Inhibits Human Immunodeficiency Virus Fusion by Disrupting Envelope Glycoprotein Clusters. ACS Nano *14*, 10929-10943.

Cherepanov, P., Maertens, G., Proost, P., Devreese, B., Van Beeumen, J., Engelborghs, Y., De Clercq, E., and Debyser, Z. (2003). HIV-1 integrase forms stable tetramers and associates with LEDGF/p75 protein in human cells. J Biol Chem *278*, 372-381.

Chernomordik, L., Chanturiya, A.N., Suss-Toby, E., Nora, E., and Zimmerberg, J. (1994). An amphipathic peptide from the C-terminal region of the human immunodeficiency virus envelope glycoprotein causes pore formation in membranes. J Virol *68*, 7115-7123.

Cheung, L., McLain, L., Hollier, M.J., Reading, S.A., and Dimmock, N.J. (2005). Part of the C-terminal tail of the envelope gp41 transmembrane glycoprotein of human immunodeficiency virus type 1 is exposed on the surface of infected cells and is involved in virus-mediated cell fusion. J Gen Virol *86*, 131-138.

Chin, C.R., Perreira, J.M., Savidis, G., Portmann, J.M., Aker, A.M., Feeley, E.M., Smith, M.C., and Brass, A.L. (2015). Direct Visualization of HIV-1 Replication Intermediates Shows that Capsid and CPSF6 Modulate HIV-1 Intra-nuclear Invasion and Integration. Cell Rep *13*, 1717-1731.

Chohan, B., Lavreys, L., Rainwater, S.M., and Overbaugh, J. (2005). Evidence for frequent reinfection with human immunodeficiency virus type 1 of a different subtype. J Virol *79*, 10701-10708.

Chojnacki, J., Staudt, T., Glass, B., Bingen, P., Engelhardt, J., Anders, M., Schneider, J., Muller, B., Hell, S.W., and Krausslich, H.G. (2012). Maturation-dependent HIV-1 surface protein redistribution revealed by fluorescence nanoscopy. Science *338*, 524-528.

Chougui, G., Munir-Matloob, S., Matkovic, R., Martin, M.M., Morel, M., Lahouassa, H., Leduc, M., Ramirez, B.C., Etienne, L., and Margottin-Goguet, F. (2018). HIV-2/SIV viral protein X counteracts HUSH repressor complex. Nat Microbiol *3*, 891-897.

Chowers, M.Y., Spina, C.A., Kwoh, T.J., Fitch, N.J., Richman, D.D., and Guatelli, J.C. (1994). Optimal infectivity in vitro of human immunodeficiency virus type 1 requires an intact nef gene. J Virol *68*, 2906-2914.

Chun, T.W., Engel, D., Berrey, M.M., Shea, T., Corey, L., and Fauci, A.S. (1998). Early establishment of a pool of latently infected, resting CD4(+) T cells during primary HIV-1 infection. Proc Natl Acad Sci U S A *95*, 8869-8873.

Chun, T.W., Stuyver, L., Mizell, S.B., Ehler, L.A., Mican, J.A., Baseler, M., Lloyd, A.L., Nowak, M.A., and Fauci, A.S. (1997). Presence of an inducible HIV-1 latent reservoir during highly active antiretroviral therapy. Proc Natl Acad Sci U S A *94*, 13193-13197.

Cihlar, T., and Fordyce, M. (2016). Current status and prospects of HIV treatment. Curr Opin Virol *18*, 50-56.

Clavel, F., Guetard, D., Brun-Vezinet, F., Chamaret, S., Rey, M.A., Santos-Ferreira, M.O., Laurent, A.G., Dauguet, C., Katlama, C., Rouzioux, C.*, et al.* (1986). Isolation of a new human retrovirus from West African patients with AIDS. Science *233*, 343-346.

Cocchi, F., DeVico, A.L., Garzino-Demo, A., Cara, A., Gallo, R.C., and Lusso, P. (1996). The V3 domain of the HIV-1 gp120 envelope glycoprotein is critical for chemokine-mediated blockade of infection. Nat Med *2*, 1244-1247.

Cocka, L.J., and Bates, P. (2012). Identification of alternatively translated Tetherin isoforms with differing antiviral and signaling activities. PLoS Pathog *8*, e1002931.

Coiras, M., Bermejo, M., Descours, B., Mateos, E., Garcia-Perez, J., Lopez-Huertas, M.R., Lederman, M.M., Benkirane, M., and Alcami, J. (2016). IL-7 Induces SAMHD1 Phosphorylation in CD4+ T Lymphocytes, Improving Early Steps of HIV-1 Life Cycle. Cell Rep *14*, 2100-2107.

Cole, G., Simonetti, K., Ademi, I., and Sharpe, S. (2012). Dimerization of the transmembrane domain of human tetherin in membrane mimetic environments. Biochemistry *51*, 5033-5040.

Compton, A.A., Bruel, T., Porrot, F., Mallet, A., Sachse, M., Euvrard, M., Liang, C., Casartelli, N., and Schwartz, O. (2014). IFITM proteins incorporated into HIV-1 virions impair viral fusion and spread. Cell Host Microbe *16*, 736-747.

Cosson, P. (1996). Direct interaction between the envelope and matrix proteins of HIV-1. EMBO J *15*, 5783-5788.

Cribier, A., Descours, B., Valadao, A.L., Laguette, N., and Benkirane, M. (2013). Phosphorylation of SAMHD1 by cyclin A2/CDK1 regulates its restriction activity toward HIV-1. Cell Rep *3*, 1036-1043.

Cronin, J., Zhang, X.Y., and Reiser, J. (2005). Altering the tropism of lentiviral vectors through pseudotyping. Curr Gene Ther *5*, 387-398.

Curlin, M.E., Zioni, R., Hawes, S.E., Liu, Y., Deng, W., Gottlieb, G.S., Zhu, T., and Mullins, J.I. (2010). HIV-1 envelope subregion length variation during disease progression. PLoS Pathog *6*, e1001228.

Dahabieh, M.S., Battivelli, E., and Verdin, E. (2015). Understanding HIV latency: the road to an HIV cure. Annu Rev Med *66*, 407-421.

Dai, W., Usami, Y., Wu, Y., and Gottlinger, H. (2018). A Long Cytoplasmic Loop Governs the Sensitivity of the Anti-viral Host Protein SERINC5 to HIV-1 Nef. Cell Rep *22*, 869-875.

Dalgleish, A.G., Beverley, P.C., Clapham, P.R., Crawford, D.H., Greaves, M.F., and Weiss, R.A. (1984). The CD4 (T4) antigen is an essential component of the receptor for the AIDS retrovirus. Nature *312*, 763-767.

daSilva, L.L., Sougrat, R., Burgos, P.V., Janvier, K., Mattera, R., and Bonifacino, J.S. (2009). Human immunodeficiency virus type 1 Nef protein targets CD4 to the multivesicular body pathway. J Virol *83*, 6578-6590.

Davenport, Y.W., West, A.P., Jr., and Bjorkman, P.J. (2016). Structure of an HIV-2 gp120 in Complex with CD4. J Virol *90*, 2112-2118.

Davis, L.E., Hjelle, B.L., Miller, V.E., Palmer, D.L., Llewellyn, A.L., Merlin, T.L., Young, S.A., Mills, R.G., Wachsman, W., and Wiley, C.A. (1992). Early viral brain invasion in iatrogenic human immunodeficiency virus infection. Neurology *42*, 1736-1739.

Day, J.R., Munk, C., and Guatelli, J.C. (2004). The membrane-proximal tyrosine-based sorting signal of human immunodeficiency virus type 1 gp41 is required for optimal viral infectivity. J Virol *78*, 1069-1079.

De Leys, R., Vanderborght, B., Vanden Haesevelde, M., Heyndrickx, L., van Geel, A., Wauters, C., Bernaerts, R., Saman, E., Nijs, P., Willems, B.*, et al.* (1990). Isolation and partial characterization of an unusual human immunodeficiency retrovirus from two persons of west-central African origin. J Virol *64*, 1207-1216.

de Silva, T.I., Cotten, M., and Rowland-Jones, S.L. (2008). HIV-2: the forgotten AIDS virus. Trends Microbiol *16*, 588-595.

Deacon, N.J., Tsykin, A., Solomon, A., Smith, K., Ludford-Menting, M., Hooker, D.J., McPhee, D.A., Greenway, A.L., Ellett, A., Chatfield, C.*, et al.* (1995). Genomic structure of an attenuated quasi species of HIV-1 from a blood transfusion donor and recipients. Science *270*, 988-991.

Deeks, S.G. (2012). HIV: Shock and kill. Nature *487*, 439-440.

Del Portillo, A., Tripodi, J., Najfeld, V., Wodarz, D., Levy, D.N., and Chen, B.K. (2011). Multiploid inheritance of HIV-1 during cell-to-cell infection. J Virol *85*, 7169-7176.

Demeulemeester, J., De Rijck, J., Gijsbers, R., and Debyser, Z. (2015). Retroviral integration: Site matters: Mechanisms and consequences of retroviral integration site selection. Bioessays *37*, 1202-1214.

Demirov, D.G., Ono, A., Orenstein, J.M., and Freed, E.O. (2002). Overexpression of the N-terminal domain of TSG101 inhibits HIV-1 budding by blocking late domain function. Proc Natl Acad Sci U S A *99*, 955-960.

Denault, J., Bissonnette, L., Longpre, J., Charest, G., Lavigne, P., and Leduc, R. (2002). Ectodomain shedding of furin: kinetics and role of the cysteine-rich region. FEBS Lett *527*, 309-314.

Deneka, M., Pelchen-Matthews, A., Byland, R., Ruiz-Mateos, E., and Marsh, M. (2007). In macrophages, HIV-1 assembles into an intracellular plasma membrane domain containing the tetraspanins CD81, CD9, and CD53. J Cell Biol *177*, 329-341.

Deng, J., Mitsuki, Y.Y., Shen, G., Ray, J.C., Cicala, C., Arthos, J., Dustin, M.L., and Hioe, C.E. (2016). HIV Envelope gp120 Alters T Cell Receptor Mobilization in the

Immunological Synapse of Uninfected CD4 T Cells and Augments T Cell Activation. J Virol *90*, 10513-10526.

Derdeyn, C.A., Decker, J.M., Bibollet-Ruche, F., Mokili, J.L., Muldoon, M., Denham, S.A., Heil, M.L., Kasolo, F., Musonda, R., Hahn, B.H.*, et al.* (2004). Envelope-constrained neutralization-sensitive HIV-1 after heterosexual transmission. Science *303*, 2019-2022.

Desai, T.M., Marin, M., Chin, C.R., Savidis, G., Brass, A.L., and Melikyan, G.B. (2014). IFITM3 restricts influenza A virus entry by blocking the formation of fusion pores following virus-endosome hemifusion. PLoS Pathog *10*, e1004048.

Descours, B., Cribier, A., Chable-Bessia, C., Ayinde, D., Rice, G., Crow, Y., Yatim, A., Schwartz, O., Laguette, N., and Benkirane, M. (2012). SAMHD1 restricts HIV-1 reverse transcription in quiescent CD4(+) T-cells. Retrovirology *9*, 87.

Dev, J., Park, D., Fu, Q., Chen, J., Ha, H.J., Ghantous, F., Herrmann, T., Chang, W., Liu, Z., Frey, G.*, et al.* (2016). Structural basis for membrane anchoring of HIV-1 envelope spike. Science *353*, 172-175.

Dey, N., Liu, T., Garofalo, R.P., and Casola, A. (2011). TAK1 regulates NF-KappaB and AP-1 activation in airway epithelial cells following RSV infection. Virology *418*, 93-101.

Dharan, A., Bachmann, N., Talley, S., Zwikelmaier, V., and Campbell, E.M. (2020). Nuclear pore blockade reveals that HIV-1 completes reverse transcription and uncoating in the nucleus. Nat Microbiol *5*, 1088-1095.

Diaz-Griffero, F., Kar, A., Perron, M., Xiang, S.H., Javanbakht, H., Li, X., and Sodroski, J. (2007). Modulation of retroviral restriction and proteasome inhibitor-resistant turnover by changes in the TRIM5alpha B-box 2 domain. J Virol *81*, 10362-10378.

Dicks, M.D.J., Betancor, G., Jimenez-Guardeno, J.M., Pessel-Vivares, L., Apolonia, L., Goujon, C., and Malim, M.H. (2018). Multiple components of the nuclear pore complex interact with the amino-terminus of MX2 to facilitate HIV-1 restriction. PLoS Pathog *14*, e1007408.

Dimitrov, D.S., Willey, R.L., Sato, H., Chang, L.J., Blumenthal, R., and Martin, M.A. (1993). Quantitation of human immunodeficiency virus type 1 infection kinetics. J Virol *67*, 2182-2190.

DiNapoli, S.R., Ortiz, A.M., Wu, F., Matsuda, K., Twigg, H.L., 3rd, Hirsch, V.M., Knox, K., and Brenchley, J.M. (2017). Tissue-resident macrophages can contain replication-competent virus in antiretroviral-naive, SIV-infected Asian macaques. JCI Insight *2*, e91214.

Ding, S., Pan, Q., Liu, S.L., and Liang, C. (2014). HIV-1 mutates to evade IFITM1 restriction. Virology *454-455*, 11-24.

Dismuke, D.J., and Aiken, C. (2006). Evidence for a functional link between uncoating of the human immunodeficiency virus type 1 core and nuclear import of the viral preintegration complex. J Virol *80*, 3712-3720.

Do, T., Murphy, G., Earl, L.A., Del Prete, G.Q., Grandinetti, G., Li, G.H., Estes, J.D., Rao, P., Trubey, C.M., Thomas, J.*, et al.* (2014). Three-dimensional imaging of HIV-1 virological synapses reveals membrane architectures involved in virus transmission. J Virol *88*, 10327-10339.

Doitsh, G., Galloway, N.L., Geng, X., Yang, Z., Monroe, K.M., Zepeda, O., Hunt, P.W., Hatano, H., Sowinski, S., Munoz-Arias, I.*, et al.* (2014). Cell death by pyroptosis drives CD4 T-cell depletion in HIV-1 infection. Nature *505*, 509-514.

Doitsh, G., and Greene, W.C. (2016). Dissecting How CD4 T Cells Are Lost During HIV Infection. Cell Host Microbe *19*, 280-291.

Doms, R.W., and Moore, J.P. (2000). HIV-1 membrane fusion: targets of opportunity. J Cell Biol *151*, F9-14.

Doores, K.J., Bonomelli, C., Harvey, D.J., Vasiljevic, S., Dwek, R.A., Burton, D.R., Crispin, M., and Scanlan, C.N. (2010). Envelope glycans of immunodeficiency virions are almost entirely oligomannose antigens. Proc Natl Acad Sci U S A *107*, 13800-13805.

Douglas, J.L., Viswanathan, K., McCarroll, M.N., Gustin, J.K., Fruh, K., and Moses, A.V. (2009). Vpu directs the degradation of the human immunodeficiency virus restriction factor BST-2/Tetherin via a {beta}TrCP-dependent mechanism. J Virol *83*, 7931-7947.

Drylewicz, J., Matheron, S., Lazaro, E., Damond, F., Bonnet, F., Simon, F., Dabis, F., Brun-Vezinet, F., Chene, G., and Thiebaut, R. (2008). Comparison of viro-immunological marker changes between HIV-1 and HIV-2-infected patients in France. AIDS *22*, 457-468.

Dubay, J.W., Dubay, S.R., Shin, H.J., and Hunter, E. (1995). Analysis of the cleavage site of the human immunodeficiency virus type 1 glycoprotein: requirement of precursor cleavage for glycoprotein incorporation. J Virol *69*, 4675-4682.

Dubay, J.W., Roberts, S.J., Hahn, B.H., and Hunter, E. (1992). Truncation of the human immunodeficiency virus type 1 transmembrane glycoprotein cytoplasmic domain blocks virus infectivity. J Virol *66*, 6616-6625.

Dube, M., Paquay, C., Roy, B.B., Bego, M.G., Mercier, J., and Cohen, E.A. (2011). HIV-1 Vpu antagonizes BST-2 by interfering mainly with the trafficking of newly synthesized BST-2 to the cell surface. Traffic *12*, 1714-1729.

Dube, M., Roy, B.B., Guiot-Guillain, P., Mercier, J., Binette, J., Leung, G., and Cohen, E.A. (2009). Suppression of Tetherin-restricting activity upon human immunodeficiency virus type 1 particle release correlates with localization of Vpu in the trans-Golgi network. J Virol *83*, 4574-4590.

Duncan, C.J., Russell, R.A., and Sattentau, Q.J. (2013). High multiplicity HIV-1 cell-to-cell transmission from macrophages to CD4+ T cells limits antiretroviral efficacy. AIDS *27*, 2201-2206.

Duncan, C.J., Williams, J.P., Schiffner, T., Gartner, K., Ochsenbauer, C., Kappes, J., Russell, R.A., Frater, J., and Sattentau, Q.J. (2014). High-multiplicity HIV-1 infection and neutralizing antibody evasion mediated by the macrophage-T cell virological synapse. J Virol *88*, 2025-2034.

Durham, N.D., Yewdall, A.W., Chen, P., Lee, R., Zony, C., Robinson, J.E., and Chen, B.K. (2012). Neutralization resistance of virological synapse-mediated HIV-1 Infection is regulated by the gp41 cytoplasmic tail. J Virol *86*, 7484-7495.

Duvall, M.G., Lore, K., Blaak, H., Ambrozak, D.A., Adams, W.C., Santos, K., Geldmacher, C., Mascola, J.R., McMichael, A.J., Jaye, A.*, et al.* (2007). Dendritic cells are less susceptible to human immunodeficiency virus type 2 (HIV-2) infection than to HIV-1 infection. J Virol *81*, 13486-13498.

Duvall, M.G., Precopio, M.L., Ambrozak, D.A., Jaye, A., McMichael, A.J., Whittle, H.C., Roederer, M., Rowland-Jones, S.L., and Koup, R.A. (2008). Polyfunctional T cell responses are a hallmark of HIV-2 infection. Eur J Immunol *38*, 350-363.

Earl, P.L., Doms, R.W., and Moss, B. (1990). Oligomeric structure of the human immunodeficiency virus type 1 envelope glycoprotein. Proc Natl Acad Sci U S A *87*, 648-652.

Eaton, S. (2008). Retromer retrieves wntless. Dev Cell *14*, 4-6.

Edmonson, P., Murphey-Corb, M., Martin, L.N., Delahunty, C., Heeney, J., Kornfeld, H., Donahue, P.R., Learn, G.H., Hood, L., and Mullins, J.I. (1998). Evolution of a simian immunodeficiency virus pathogen. J Virol *72*, 405-414.

Edwards, T.G., Hoffman, T.L., Baribaud, F., Wyss, S., LaBranche, C.C., Romano, J., Adkinson, J., Sharron, M., Hoxie, J.A., and Doms, R.W. (2001). Relationships between CD4 independence, neutralization sensitivity, and exposure of a CD4-induced epitope in a human immunodeficiency virus type 1 envelope protein. J Virol *75*, 5230-5239.

Edwards, T.G., Wyss, S., Reeves, J.D., Zolla-Pazner, S., Hoxie, J.A., Doms, R.W., and Baribaud, F. (2002). Truncation of the cytoplasmic domain induces exposure of conserved regions in the ectodomain of human immunodeficiency virus type 1 envelope protein. J Virol *76*, 2683-2691.

Egan, M.A., Carruth, L.M., Rowell, J.F., Yu, X., and Siliciano, R.F. (1996). Human immunodeficiency virus type 1 envelope protein endocytosis mediated by a highly conserved intrinsic internalization signal in the cytoplasmic domain of gp41 is suppressed in the presence of the Pr55gag precursor protein. J Virol *70*, 6547-6556.

Emerson, V., Holtkotte, D., Pfeiffer, T., Wang, I.H., Schnolzer, M., Kempf, T., and Bosch, V. (2010). Identification of the cellular prohibitin 1/prohibitin 2 heterodimer as an interaction partner of the C-terminal cytoplasmic domain of the HIV-1 glycoprotein. J Virol *84*, 1355-1365.

Espeseth, A.S., Felock, P., Wolfe, A., Witmer, M., Grobler, J., Anthony, N., Egbertson, M., Melamed, J.Y., Young, S., Hamill, T.*, et al.* (2000). HIV-1 integrase inhibitors that compete with the target DNA substrate define a unique strand transfer conformation for integrase. Proc Natl Acad Sci U S A *97*, 11244-11249.

Etienne, L., Hahn, B.H., Sharp, P.M., Matsen, F.A., and Emerman, M. (2013). Gene loss and adaptation to hominids underlie the ancient origin of HIV-1. Cell Host Microbe *14*, 85-92.

Eugenin, E.A., Gaskill, P.J., and Berman, J.W. (2009). Tunneling nanotubes (TNT) are induced by HIV-infection of macrophages: a potential mechanism for intercellular HIV trafficking. Cell Immunol *254*, 142-148.

Evans, L.A., Moreau, J., Odehouri, K., Legg, H., Barboza, A., Cheng-Mayer, C., and Levy, J.A. (1988). Characterization of a noncytopathic HIV-2 strain with unusual effects on CD4 expression. Science *240*, 1522-1525.

Fackler, O.T., Kienzle, N., Kremmer, E., Boese, A., Schramm, B., Klimkait, T., Kucherer, C., and Mueller-Lantzsch, N. (1997). Association of human immunodeficiency virus Nef protein with actin is myristoylation dependent and influences its subcellular localization. Eur J Biochem *247*, 843-851.

Falkowska, E., Le, K.M., Ramos, A., Doores, K.J., Lee, J.H., Blattner, C., Ramirez, A., Derking, R., van Gils, M.J., Liang, C.H.*, et al.* (2014). Broadly neutralizing HIV antibodies define a glycan-dependent epitope on the prefusion conformation of gp41 on cleaved envelope trimers. Immunity *40*, 657-668.

Farber, C.R., Reich, A., Barnes, A.M., Becerra, P., Rauch, F., Cabral, W.A., Bae, A., Quinlan, A., Glorieux, F.H., Clemens, T.L.*, et al.* (2014). A novel IFITM5 mutation in severe atypical osteogenesis imperfecta type VI impairs osteoblast production of pigment epithelium-derived factor. J Bone Miner Res *29*, 1402-1411.

Farnet, C.M., and Haseltine, W.A. (1991). Determination of viral proteins present in the human immunodeficiency virus type 1 preintegration complex. J Virol *65*, 1910-1915.

Fassati, A., and Goff, S.P. (2001). Characterization of intracellular reverse transcription complexes of human immunodeficiency virus type 1. J Virol *75*, 3626-3635.

Fauci, A.S. (1996). Host factors and the pathogenesis of HIV-induced disease. Nature *384*, 529-534.

Favre, D., Lederer, S., Kanwar, B., Ma, Z.M., Proll, S., Kasakow, Z., Mold, J., Swainson, L., Barbour, J.D., Baskin, C.R.*, et al.* (2009). Critical loss of the balance between Th17 and T regulatory cell populations in pathogenic SIV infection. PLoS Pathog *5*, e1000295.

Feeley, E.M., Sims, J.S., John, S.P., Chin, C.R., Pertel, T., Chen, L.M., Gaiha, G.D., Ryan, B.J., Donis, R.O., Elledge, S.J.*, et al.* (2011). IFITM3 inhibits influenza A virus infection by preventing cytosolic entry. PLoS Pathog *7*, e1002337.

Felts, R.L., Narayan, K., Estes, J.D., Shi, D., Trubey, C.M., Fu, J., Hartnell, L.M., Ruthel, G.T., Schneider, D.K., Nagashima, K.*, et al.* (2010). 3D visualization of HIV transfer at the virological synapse between dendritic cells and T cells. Proc Natl Acad Sci U S A *107*, 13336-13341.

Felzien, L.K., Woffendin, C., Hottiger, M.O., Subbramanian, R.A., Cohen, E.A., and Nabel, G.J. (1998). HIV transcriptional activation by the accessory protein, VPR, is mediated by the p300 co-activator. Proc Natl Acad Sci U S A *95*, 5281-5286.

Feng, Y., Love, R.P., and Chelico, L. (2013). HIV-1 viral infectivity factor (Vif) alters processive single-stranded DNA scanning of the retroviral restriction factor APOBEC3G. J Biol Chem *288*, 6083-6094.

Fenton-May, A.E., Dibben, O., Emmerich, T., Ding, H., Pfafferott, K., Aasa-Chapman, M.M., Pellegrino, P., Williams, I., Cohen, M.S., Gao, F.*, et al.* (2013). Relative resistance of HIV-1 founder viruses to control by interferon-alpha. Retrovirology *10*, 146.

Finzi, D., Hermankova, M., Pierson, T., Carruth, L.M., Buck, C., Chaisson, R.E., Quinn, T.C., Chadwick, K., Margolick, J., Brookmeyer, R.*, et al.* (1997). Identification of a reservoir for HIV-1 in patients on highly active antiretroviral therapy. Science *278*, 1295-1300.

Fjorback, A.W., Seaman, M., Gustafsen, C., Mehmedbasic, A., Gokool, S., Wu, C., Militz, D., Schmidt, V., Madsen, P., Nyengaard, J.R.*, et al.* (2012). Retromer binds the FANSHY sorting motif in SorLA to regulate amyloid precursor protein sorting and processing. J Neurosci *32*, 1467-1480.

Fletcher, A.J., and Towers, G.J. (2013). Inhibition of retroviral replication by members of the TRIM protein family. Curr Top Microbiol Immunol *371*, 29-66.

Forshey, B.M., Shi, J., and Aiken, C. (2005). Structural requirements for recognition of the human immunodeficiency virus type 1 core during host restriction in owl monkey cells. J Virol *79*, 869-875.

Forster, F., Medalia, O., Zauberman, N., Baumeister, W., and Fass, D. (2005). Retrovirus envelope protein complex structure in situ studied by cryo-electron tomography. Proc Natl Acad Sci U S A *102*, 4729-4734.

Foster, T.L., Pickering, S., and Neil, S.J.D. (2017). Inhibiting the Ins and Outs of HIV Replication: Cell-Intrinsic Antiretroviral Restrictions at the Plasma Membrane. Front Immunol *8*, 1853.

Foster, T.L., Wilson, H., Iyer, S.S., Coss, K., Doores, K., Smith, S., Kellam, P., Finzi, A., Borrow, P., Hahn, B.H.*, et al.* (2016). Resistance of Transmitted Founder HIV-1 to IFITM-Mediated Restriction. Cell Host Microbe *20*, 429-442.

Franchini, G., Fargnoli, K.A., Giombini, F., Jagodzinski, L., De Rossi, A., Bosch, M., Biberfeld, G., Fenyo, E.M., Albert, J., Gallo, R.C.*, et al.* (1989). Molecular and biological

characterization of a replication competent human immunodeficiency type 2 (HIV-2) proviral clone. Proc Natl Acad Sci U S A *86*, 2433-2437.

Francis, A.C., and Melikyan, G.B. (2018). Single HIV-1 Imaging Reveals Progression of Infection through CA-Dependent Steps of Docking at the Nuclear Pore, Uncoating, and Nuclear Transport. Cell Host Microbe *23*, 536-548 e536.

Frank, G.A., Narayan, K., Bess, J.W., Jr., Del Prete, G.Q., Wu, X., Moran, A., Hartnell, L.M., Earl, L.A., Lifson, J.D., and Subramaniam, S. (2015). Maturation of the HIV-1 core by a non-diffusional phase transition. Nat Commun *6*, 5854.

Freed, E.O. (2015). HIV-1 assembly, release and maturation. Nat Rev Microbiol *13*, 484-496.

Freed, E.O., and Martin, M.A. (1995). Virion incorporation of envelope glycoproteins with long but not short cytoplasmic tails is blocked by specific, single amino acid substitutions in the human immunodeficiency virus type 1 matrix. J Virol *69*, 1984-1989.

Frey, G., Peng, H., Rits-Volloch, S., Morelli, M., Cheng, Y., and Chen, B. (2008). A fusion-intermediate state of HIV-1 gp41 targeted by broadly neutralizing antibodies. Proc Natl Acad Sci U S A *105*, 3739-3744.

Fribourgh, J.L., Nguyen, H.C., Matreyek, K.A., Alvarez, F.J.D., Summers, B.J., Dewdney, T.G., Aiken, C., Zhang, P., Engelman, A., and Xiong, Y. (2014). Structural insight into HIV-1 restriction by MxB. Cell Host Microbe *16*, 627-638.

Fricke, T., Brandariz-Nunez, A., Wang, X., Smith, A.B., 3rd, and Diaz-Griffero, F. (2013). Human cytosolic extracts stabilize the HIV-1 core. J Virol *87*, 10587-10597.

Fricke, T., White, T.E., Schulte, B., de Souza Aranha Vieira, D.A., Dharan, A., Campbell, E.M., Brandariz-Nunez, A., and Diaz-Griffero, F. (2014). MxB binds to the HIV-1 core and prevents the uncoating process of HIV-1. Retrovirology *11*, 68.

Friedman-Kien, A.E. (1981). Disseminated Kaposi's sarcoma syndrome in young homosexual men. J Am Acad Dermatol *5*, 468-471.

Fujii, K., Munshi, U.M., Ablan, S.D., Demirov, D.G., Soheilian, F., Nagashima, K., Stephen, A.G., Fisher, R.J., and Freed, E.O. (2009). Functional role of Alix in HIV-1 replication. Virology *391*, 284-292.

Fujioka, S., Niu, J., Schmidt, C., Sclabas, G.M., Peng, B., Uwagawa, T., Li, Z., Evans, D.B., Abbruzzese, J.L., and Chiao, P.J. (2004). NF-kappaB and AP-1 connection: mechanism of NF-kappaB-dependent regulation of AP-1 activity. Mol Cell Biol *24*, 7806-7819.

Fujita, K., Omura, S., and Silver, J. (1997). Rapid degradation of CD4 in cells expressing human immunodeficiency virus type 1 Env and Vpu is blocked by proteasome inhibitors. J Gen Virol *78 (Pt 3)*, 619-625.

Fujiwara, T., and Mizuuchi, K. (1988). Retroviral DNA integration: structure of an integration intermediate. Cell *54*, 497-504.

Fultz, P.N., Vance, P.J., Endres, M.J., Tao, B., Dvorin, J.D., Davis, I.C., Lifson, J.D., Montefiori, D.C., Marsh, M., Malim, M.H*., et al.* (2001). In vivo attenuation of simian immunodeficiency virus by disruption of a tyrosine-dependent sorting signal in the envelope glycoprotein cytoplasmic tail. J Virol *75*, 278-291.

Furman, P.A., Fyfe, J.A., St Clair, M.H., Weinhold, K., Rideout, J.L., Freeman, G.A., Lehrman, S.N., Bolognesi, D.P., Broder, S., Mitsuya, H*., et al.* (1986). Phosphorylation of 3'-azido-3'-deoxythymidine and selective interaction of the 5'-triphosphate with human immunodeficiency virus reverse transcriptase. Proc Natl Acad Sci U S A *83*, 8333-8337.

Gabuzda, D.H., Lawrence, K., Langhoff, E., Terwilliger, E., Dorfman, T., Haseltine, W.A., and Sodroski, J. (1992). Role of vif in replication of human immunodeficiency virus type 1 in CD4+ T lymphocytes. J Virol *66*, 6489-6495.

Galao, R.P., Le Tortorec, A., Pickering, S., Kueck, T., and Neil, S.J. (2012). Innate sensing of HIV-1 assembly by Tetherin induces NFkappaB-dependent proinflammatory responses. Cell Host Microbe *12*, 633-644.

Galao, R.P., Pickering, S., Curnock, R., and Neil, S.J. (2014). Retroviral retention activates a Syk-dependent HemITAM in human tetherin. Cell Host Microbe *16*, 291-303.

Gallo, R.C., Salahuddin, S.Z., Popovic, M., Shearer, G.M., Kaplan, M., Haynes, B.F., Palker, T.J., Redfield, R., Oleske, J., Safai, B*., et al.* (1984). Frequent detection and isolation of cytopathic retroviruses (HTLV-III) from patients with AIDS and at risk for AIDS. Science *224*, 500-503.

Gallo, S.A., Puri, A., and Blumenthal, R. (2001). HIV-1 gp41 six-helix bundle formation occurs rapidly after the engagement of gp120 by CXCR4 in the HIV-1 Env-mediated fusion process. Biochemistry *40*, 12231-12236.

Galloway, N.L., Doitsh, G., Monroe, K.M., Yang, Z., Munoz-Arias, I., Levy, D.N., and Greene, W.C. (2015). Cell-to-Cell Transmission of HIV-1 Is Required to Trigger Pyroptotic Death of Lymphoid-Tissue-Derived CD4 T Cells. Cell Rep *12*, 1555-1563.

Gamble, T.R., Vajdos, F.F., Yoo, S., Worthylake, D.K., Houseweart, M., Sundquist, W.I., and Hill, C.P. (1996). Crystal structure of human cyclophilin A bound to the amino-terminal domain of HIV-1 capsid. Cell *87*, 1285-1294.

Ganser, B.K., Li, S., Klishko, V.Y., Finch, J.T., and Sundquist, W.I. (1999). Assembly and analysis of conical models for the HIV-1 core. Science *283*, 80-83.

Garcia, J.V., and Miller, A.D. (1991). Serine phosphorylation-independent downregulation of cell-surface CD4 by nef. Nature *350*, 508-511.

Garrus, J.E., von Schwedler, U.K., Pornillos, O.W., Morham, S.G., Zavitz, K.H., Wang, H.E., Wettstein, D.A., Stray, K.M., Cote, M., Rich, R.L*., et al.* (2001). Tsg101 and the vacuolar protein sorting pathway are essential for HIV-1 budding. Cell *107*, 55-65.

Gawrisch, K., Han, K.H., Yang, J.S., Bergelson, L.D., and Ferretti, J.A. (1993). Interaction of peptide fragment 828-848 of the envelope glycoprotein of human immunodeficiency virus type I with lipid bilayers. Biochemistry *32*, 3112-3118.

Geijtenbeek, T.B., Kwon, D.S., Torensma, R., van Vliet, S.J., van Duijnhoven, G.C., Middel, J., Cornelissen, I.L., Nottet, H.S., KewalRamani, V.N., Littman, D.R.*, et al.* (2000). DC-SIGN, a dendritic cell-specific HIV-1-binding protein that enhances trans-infection of T cells. Cell *100*, 587-597.

Geyer, M., Fackler, O.T., and Peterlin, B.M. (2001). Structure--function relationships in HIV-1 Nef. EMBO Rep *2*, 580-585.

Geyer, M., Munte, C.E., Schorr, J., Kellner, R., and Kalbitzer, H.R. (1999). Structure of the anchor-domain of myristoylated and non-myristoylated HIV-1 Nef protein. J Mol Biol *289*, 123-138.

Geyer, M., and Peterlin, B.M. (2001). Domain assembly, surface accessibility and sequence conservation in full length HIV-1 Nef. FEBS Lett *496*, 91-95.

Gheysen, D., Jacobs, E., de Foresta, F., Thiriart, C., Francotte, M., Thines, D., and De Wilde, M. (1989). Assembly and release of HIV-1 precursor Pr55gag virus-like particles from recombinant baculovirus-infected insect cells. Cell *59*, 103-112.

Giese, S., & Marsh, M. (2014). Tetherin can restrict cell-free and cell-cell transmission of HIV from primary macrophages to T cells. *PLoS pathogens*, *10*(7), e1004189.

Gillick, K., Pollpeter, D., Phalora, P., Kim, E.Y., Wolinsky, S.M., and Malim, M.H. (2013). Suppression of HIV-1 infection by APOBEC3 proteins in primary human CD4(+) T cells is associated with inhibition of processive reverse transcription as well as excessive cytidine deamination. J Virol *87*, 1508-1517.

Gnanakaran, S., Bhattacharya, T., Daniels, M., Keele, B.F., Hraber, P.T., Lapedes, A.S., Shen, T., Gaschen, B., Krishnamoorthy, M., Li, H.*, et al.* (2011). Recurrent signature patterns in HIV-1 B clade envelope glycoproteins associated with either early or chronic infections. PLoS Pathog *7*, e1002209.

Go, E.P., Cupo, A., Ringe, R., Pugach, P., Moore, J.P., and Desaire, H. (2015). Native Conformation and Canonical Disulfide Bond Formation Are Interlinked Properties of HIV-1 Env Glycoproteins. J Virol *90*, 2884-2894.

Goffinet, C., Allespach, I., Homann, S., Tervo, H.M., Habermann, A., Rupp, D., Oberbremer, L., Kern, C., Tibroni, N., Welsch, S.*, et al.* (2009). HIV-1 antagonism of CD317 is species specific and involves Vpu-mediated proteasomal degradation of the restriction factor. Cell Host Microbe *5*, 285-297.

Goila-Gaur, R., Khan, M.A., Miyagi, E., Kao, S., Opi, S., Takeuchi, H., and Strebel, K. (2008). HIV-1 Vif promotes the formation of high molecular mass APOBEC3G complexes. Virology *372*, 136-146.

Goldstone, D.C., Ennis-Adeniran, V., Hedden, J.J., Groom, H.C., Rice, G.I., Christodoulou, E., Walker, P.A., Kelly, G., Haire, L.F., Yap, M.W.*, et al.* (2011). HIV-1 restriction factor SAMHD1 is a deoxynucleoside triphosphate triphosphohydrolase. Nature *480*, 379-382.

Gorry, P.R., McPhee, D.A., Verity, E., Dyer, W.B., Wesselingh, S.L., Learmont, J., Sullivan, J.S., Roche, M., Zaunders, J.J., Gabuzda, D.*, et al.* (2007). Pathogenicity and immunogenicity of attenuated, nef-deleted HIV-1 strains in vivo. Retrovirology *4*, 66.

Gottlieb, G.S., Hawes, S.E., Agne, H.D., Stern, J.E., Critchlow, C.W., Kiviat, N.B., and Sow, P.S. (2006). Lower levels of HIV RNA in semen in HIV-2 compared with HIV-1 infection: implications for differences in transmission. AIDS *20*, 895-900.

Gottlinger, H.G., Dorfman, T., Sodroski, J.G., and Haseltine, W.A. (1991). Effect of mutations affecting the p6 gag protein on human immunodeficiency virus particle release. Proc Natl Acad Sci U S A *88*, 3195-3199.

Gottlinger, H.G., Sodroski, J.G., and Haseltine, W.A. (1989). Role of capsid precursor processing and myristoylation in morphogenesis and infectivity of human immunodeficiency virus type 1. Proc Natl Acad Sci U S A *86*, 5781-5785.

Goujon, C., Moncorge, O., Bauby, H., Doyle, T., Barclay, W.S., and Malim, M.H. (2014). Transfer of the amino-terminal nuclear envelope targeting domain of human MX2 converts MX1 into an HIV-1 resistance factor. J Virol *88*, 9017-9026.

Goujon, C., Moncorge, O., Bauby, H., Doyle, T., Ward, C.C., Schaller, T., Hue, S., Barclay, W.S., Schulz, R., and Malim, M.H. (2013). Human MX2 is an interferon-induced post-entry inhibitor of HIV-1 infection. Nature *502*, 559-562.

Gousset, K., Ablan, S.D., Coren, L.V., Ono, A., Soheilian, F., Nagashima, K., Ott, D.E., and Freed, E.O. (2008). Real-time visualization of HIV-1 GAG trafficking in infected macrophages. PLoS Pathog *4*, e1000015.

Graham, D.R., Chertova, E., Hilburn, J.M., Arthur, L.O., and Hildreth, J.E. (2003). Cholesterol depletion of human immunodeficiency virus type 1 and simian immunodeficiency virus with beta-cyclodextrin inactivates and permeabilizes the virions: evidence for virion-associated lipid rafts. J Virol *77*, 8237-8248.

Green, N., Shinnick, T.M., Witte, O., Ponticelli, A., Sutcliffe, J.G., and Lerner, R.A. (1981). Sequence-specific antibodies show that maturation of Moloney leukemia virus envelope polyprotein involves removal of a COOH-terminal peptide. Proc Natl Acad Sci U S A *78*, 6023-6027.

Greenwood, E.J., Matheson, N.J., Wals, K., van den Boomen, D.J., Antrobus, R., Williamson, J.C., and Lehner, P.J. (2016). Temporal proteomic analysis of HIV infection reveals remodelling of the host phosphoproteome by lentiviral Vif variants. Elife *5*.

Greenwood, E.J.D., Williamson, J.C., Sienkiewicz, A., Naamati, A., Matheson, N.J., and Lehner, P.J. (2019). Promiscuous Targeting of Cellular Proteins by Vpr Drives Systems-Level Proteomic Remodeling in HIV-1 Infection. Cell Rep *27*, 1579-1596 e1577.

Groot, F., Welsch, S., and Sattentau, Q.J. (2008). Efficient HIV-1 transmission from macrophages to T cells across transient virological synapses. Blood *111*, 4660-4663.

Groppelli, E., Len, A.C., Granger, L.A., and Jolly, C. (2014). Retromer regulates HIV-1 envelope glycoprotein trafficking and incorporation into virions. PLoS Pathog *10*, e1004518.

Groppelli, E., Starling, S., and Jolly, C. (2015). Contact-induced mitochondrial polarization supports HIV-1 virological synapse formation. J Virol *89*, 14-24.

Grossman, T.R., Luque, J.M., and Nelson, N. (2000). Identification of a ubiquitous family of membrane proteins and their expression in mouse brain. J Exp Biol *203*, 447-457.

Grutter, M.G., and Luban, J. (2012). TRIM5 structure, HIV-1 capsid recognition, and innate immune signaling. Curr Opin Virol *2*, 142-150.

Grzesiek, S., Stahl, S.J., Wingfield, P.T., and Bax, A. (1996). The CD4 determinant for downregulation by HIV-1 Nef directly binds to Nef. Mapping of the Nef binding surface by NMR. Biochemistry *35*, 10256-10261.

Guo, F., Cen, S., Niu, M., Yang, Y., Gorelick, R.J., and Kleiman, L. (2007). The interaction of APOBEC3G with human immunodeficiency virus type 1 nucleocapsid inhibits tRNA3Lys annealing to viral RNA. J Virol *81*, 11322-11331.

Guo, Y., Dong, L., Qiu, X., Wang, Y., Zhang, B., Liu, H., Yu, Y., Zang, Y., Yang, M., and Huang, Z. (2014). Structural basis for hijacking CBF-beta and CUL5 E3 ligase complex by HIV-1 Vif. Nature *505*, 229-233.

Gupta, P., Balachandran, R., Ho, M., Enrico, A., and Rinaldo, C. (1989). Cell-to-cell transmission of human immunodeficiency virus type 1 in the presence of azidothymidine and neutralizing antibody. J Virol *63*, 2361-2365.

Gupta, R.K., Mlcochova, P., Pelchen-Matthews, A., Petit, S.J., Mattiuzzo, G., Pillay, D., Takeuchi, Y., Marsh, M., and Towers, G.J. (2009). Simian immunodeficiency virus envelope glycoprotein counteracts tetherin/BST-2/CD317 by intracellular sequestration. Proc Natl Acad Sci U S A *106*, 20889-20894.

Haaland, R.E., Hawkins, P.A., Salazar-Gonzalez, J., Johnson, A., Tichacek, A., Karita, E., Manigart, O., Mulenga, J., Keele, B.F., Shaw, G.M.*, et al.* (2009). Inflammatory genital infections mitigate a severe genetic bottleneck in heterosexual transmission of subtype A and C HIV-1. PLoS Pathog *5*, e1000274.

Haffar, O.K., Dowbenko, D.J., and Berman, P.W. (1988). Topogenic analysis of the human immunodeficiency virus type 1 envelope glycoprotein, gp160, in microsomal membranes. J Cell Biol *107*, 1677-1687.

Hahn, B.H., Kong, L.I., Lee, S.W., Kumar, P., Taylor, M.E., Arya, S.K., and Shaw, G.M. (1987). Relation of HTLV-4 to simian and human immunodeficiency-associated viruses. Nature *330*, 184-186.

Hahn, B.H., Shaw, G.M., De Cock, K.M., and Sharp, P.M. (2000). AIDS as a zoonosis: scientific and public health implications. Science *287*, 607-614.

Haim, H., Si, Z., Madani, N., Wang, L., Courter, J.R., Princiotto, A., Kassa, A., DeGrace, M., McGee-Estrada, K., Mefford, M.*, et al.* (2009). Soluble CD4 and CD4-mimetic compounds inhibit HIV-1 infection by induction of a short-lived activated state. PLoS Pathog *5*, e1000360.

Hallenberger, S., Bosch, V., Angliker, H., Shaw, E., Klenk, H.D., and Garten, W. (1992). Inhibition of furin-mediated cleavage activation of HIV-1 glycoprotein gp160. Nature *360*, 358-361.

Haller, C., Tibroni, N., Rudolph, J.M., Grosse, R., and Fackler, O.T. (2011). Nef does not inhibit F-actin remodelling and HIV-1 cell-cell transmission at the T lymphocyte virological synapse. Eur J Cell Biol *90*, 913-921.

Haller, O., and Kochs, G. (2011). Human MxA protein: an interferon-induced dynamin-like GTPase with broad antiviral activity. J Interferon Cytokine Res *31*, 79-87.

Halper-Stromberg, A., Lu, C.L., Klein, F., Horwitz, J.A., Bournazos, S., Nogueira, L., Eisenreich, T.R., Liu, C., Gazumyan, A., Schaefer, U.*, et al.* (2014). Broadly neutralizing antibodies and viral inducers decrease rebound from HIV-1 latent reservoirs in humanized mice. Cell *158*, 989-999.

Halwani, R., Khorchid, A., Cen, S., and Kleiman, L. (2003). Rapid localization of Gag/GagPol complexes to detergent-resistant membrane during the assembly of human immunodeficiency virus type 1. J Virol *77*, 3973-3984.

Hammonds, J., Wang, J.J., Yi, H., and Spearman, P. (2010). Immunoelectron microscopic evidence for Tetherin/BST2 as the physical bridge between HIV-1 virions and the plasma membrane. PLoS Pathog *6*, e1000749.

Hammonds, J. E., Beeman, N., Ding, L., Takushi, S., Francis, A. C., Wang, J. J., Melikyan, G. B., & Spearman, P. (2017). Siglec-1 initiates formation of the virus-containing compartment and enhances macrophage-to-T cell transmission of HIV-1. *PLoS pathogens*, *13*(1), e1006181.

Han, Y., Lassen, K., Monie, D., Sedaghat, A.R., Shimoji, S., Liu, X., Pierson, T.C., Margolick, J.B., Siliciano, R.F., and Siliciano, J.D. (2004). Resting CD4+ T cells from human immunodeficiency virus type 1 (HIV-1)-infected individuals carry integrated HIV-1 genomes within actively transcribed host genes. J Virol *78*, 6122-6133.

Hanson, A., Sarr, A.D., Shea, A., Jones, N., Mboup, S., Kanki, P., and Cao, H. (2005). Distinct profile of T cell activation in HIV type 2 compared to HIV type 1 infection: differential mechanism for immunoprotection. AIDS Res Hum Retroviruses *21*, 791-798.

Hanson, P.I., Shim, S., and Merrill, S.A. (2009). Cell biology of the ESCRT machinery. Curr Opin Cell Biol *21*, 568-574.

Hanson, P.J., Zhang, H.M., Hemida, M.G., Ye, X., Qiu, Y., and Yang, D. (2012). IRES-Dependent Translational Control during Virus-Induced Endoplasmic Reticulum Stress and Apoptosis. Front Microbiol *3*, 92.

Hare, S., Gupta, S.S., Valkov, E., Engelman, A., and Cherepanov, P. (2010). Retroviral intasome assembly and inhibition of DNA strand transfer. Nature *464*, 232-236.

Harris, R.S., Bishop, K.N., Sheehy, A.M., Craig, H.M., Petersen-Mahrt, S.K., Watt, I.N., Neuberger, M.S., and Malim, M.H. (2003). DNA deamination mediates innate immunity to retroviral infection. Cell *113*, 803-809.

Hase, K., Kimura, S., Takatsu, H., Ohmae, M., Kawano, S., Kitamura, H., Ito, M., Watarai, H., Hazelett, C.C., Yeaman, C.*, et al.* (2009). M-Sec promotes membrane nanotube formation by interacting with Ral and the exocyst complex. Nat Cell Biol *11*, 1427-1432.

Hashimoto, M., Bhuyan, F., Hiyoshi, M., Noyori, O., Nasser, H., Miyazaki, M., Saito, T., Kondoh, Y., Osada, H., Kimura, S.*, et al.* (2016). Potential Role of the Formation of Tunneling Nanotubes in HIV-1 Spread in Macrophages. J Immunol *196*, 1832-1841.

Hatziioannou, T., Perez-Caballero, D., Cowan, S., and Bieniasz, P.D. (2005). Cyclophilin interactions with incoming human immunodeficiency virus type 1 capsids with opposing effects on infectivity in human cells. J Virol *79*, 176-183.

Heap, C.J., Reading, S.A., and Dimmock, N.J. (2005). An antibody specific for the C-terminal tail of the gp41 transmembrane protein of human immunodeficiency virus type 1 mediates post-attachment neutralization, probably through inhibition of virus-cell fusion. J Gen Virol *86*, 1499-1507.

Heigele, A., Kmiec, D., Regensburger, K., Langer, S., Peiffer, L., Sturzel, C.M., Sauter, D., Peeters, M., Pizzato, M., Learn, G.H.*, et al.* (2016). The Potency of Nef-Mediated SERINC5 Antagonism Correlates with the Prevalence of Primate Lentiviruses in the Wild. Cell Host Microbe *20*, 381-391.

Henderson, L.E., Sowder, R., Copeland, T.D., Smythers, G., and Oroszlan, S. (1984). Quantitative separation of murine leukemia virus proteins by reversed-phase high-pressure liquid chromatography reveals newly described gag and env cleavage products. J Virol *52*, 492-500.

Hessell, A.J., Rakasz, E.G., Poignard, P., Hangartner, L., Landucci, G., Forthal, D.N., Koff, W.C., Watkins, D.I., and Burton, D.R. (2009). Broadly neutralizing human anti-HIV antibody 2G12 is effective in protection against mucosal SHIV challenge even at low serum neutralizing titers. PLoS Pathog *5*, e1000433.

Hessell, A.J., Rakasz, E.G., Tehrani, D.M., Huber, M., Weisgrau, K.L., Landucci, G., Forthal, D.N., Koff, W.C., Poignard, P., Watkins, D.I.*, et al.* (2010). Broadly neutralizing

monoclonal antibodies 2F5 and 4E10 directed against the human immunodeficiency virus type 1 gp41 membrane-proximal external region protect against mucosal challenge by simian-human immunodeficiency virus SHIVBa-L. J Virol *84*, 1302-1313.

Hill, C.P., Worthylake, D., Bancroft, D.P., Christensen, A.M., and Sundquist, W.I. (1996). Crystal structures of the trimeric human immunodeficiency virus type 1 matrix protein: implications for membrane association and assembly. Proc Natl Acad Sci U S A *93*, 3099-3104.

Hinz, A., Miguet, N., Natrajan, G., Usami, Y., Yamanaka, H., Renesto, P., Hartlieb, B., McCarthy, A.A., Simorre, J.P., Gottlinger, H.*, et al.* (2010). Structural basis of HIV-1 tethering to membranes by the BST-2/tetherin ectodomain. Cell Host Microbe *7*, 314-323.

Hirsch, V., Riedel, N., and Mullins, J.I. (1987). The genome organization of STLV-3 is similar to that of the AIDS virus except for a truncated transmembrane protein. Cell *49*, 307-319.

Hirsch, V.M., Edmondson, P., Murphey-Corb, M., Arbeille, B., Johnson, P.R., and Mullins, J.I. (1989a). SIV adaptation to human cells. Nature *341*, 573-574.

Hirsch, V.M., Olmsted, R.A., Murphey-Corb, M., Purcell, R.H., and Johnson, P.R. (1989b). An African primate lentivirus (SIVsm) closely related to HIV-2. Nature *339*, 389-392.

Hogue, I.B., Grover, J.R., Soheilian, F., Nagashima, K., and Ono, A. (2011). Gag induces the coalescence of clustered lipid rafts and tetraspanin-enriched microdomains at HIV-1 assembly sites on the plasma membrane. J Virol *85*, 9749-9766.

Hotter, D., Kirchhoff, F., and Sauter, D. (2013a). HIV-1 Vpu does not degrade interferon regulatory factor 3. J Virol *87*, 7160-7165.

Hotter, D., Sauter, D., and Kirchhoff, F. (2013b). Emerging role of the host restriction factor tetherin in viral immune sensing. J Mol Biol *425*, 4956-4964.

Hourioux, C., Brand, D., Sizaret, P.Y., Lemiale, F., Lebigot, S., Barin, F., and Roingeard, P. (2000). Identification of the glycoprotein 41(TM) cytoplasmic tail domains of human immunodeficiency virus type 1 that interact with Pr55Gag particles. AIDS Res Hum Retroviruses *16*, 1141-1147.

Hoxie, J.A., Brass, L.F., Pletcher, C.H., Haggarty, B.S., and Hahn, B.H. (1991). Cytopathic variants of an attenuated isolate of human immunodeficiency virus type 2 exhibit increased affinity for CD4. J Virol *65*, 5096-5101.

Hrecka, K., Hao, C., Gierszewska, M., Swanson, S.K., Kesik-Brodacka, M., Srivastava, S., Florens, L., Washburn, M.P., and Skowronski, J. (2011). Vpx relieves inhibition of HIV-1 infection of macrophages mediated by the SAMHD1 protein. Nature *474*, 658-661.

Hu, W.S., and Hughes, S.H. (2012). HIV-1 reverse transcription. Cold Spring Harb Perspect Med *2*.

Huang, C.C., Lam, S.N., Acharya, P., Tang, M., Xiang, S.H., Hussan, S.S., Stanfield, R.L., Robinson, J., Sodroski, J., Wilson, I.A*., et al.* (2007). Structures of the CCR5 N terminus and of a tyrosine-sulfated antibody with HIV-1 gp120 and CD4. Science *317*, 1930-1934.

Huang, I.C., Bailey, C.C., Weyer, J.L., Radoshitzky, S.R., Becker, M.M., Chiang, J.J., Brass, A.L., Ahmed, A.A., Chi, X., Dong, L*., et al.* (2011). Distinct patterns of IFITM-mediated restriction of filoviruses, SARS coronavirus, and influenza A virus. PLoS Pathog *7*, e1001258.

Huang, M., Orenstein, J.M., Martin, M.A., and Freed, E.O. (1995). p6Gag is required for particle production from full-length human immunodeficiency virus type 1 molecular clones expressing protease. J Virol *69*, 6810-6818.

Hubner, W., McNerney, G.P., Chen, P., Dale, B.M., Gordon, R.E., Chuang, F.Y., Li, X.D., Asmuth, D.M., Huser, T., and Chen, B.K. (2009). Quantitative 3D video microscopy of HIV transfer across T cell virological synapses. Science *323*, 1743-1747.

Hungnes, O., Tjotta, E., and Grinde, B. (1992). Mutations in the central polypurine tract of HIV-1 result in delayed replication. Virology *190*, 440-442.

Huthoff, H., Autore, F., Gallois-Montbrun, S., Fraternali, F., and Malim, M.H. (2009). RNA-dependent oligomerization of APOBEC3G is required for restriction of HIV-1. PLoS Pathog *5*, e1000330.

Igakura T, Stinchcombe JC, Goon PK, Taylor GP, Weber JN, Griffiths GM, Tanaka Y, Osame M, Bangham CR. (2003) Spread of HTLV-I between lymphocytes by virus-induced polarization of the cytoskeleton. Science. 299(5613):1713-6.

Iliopoulou, M., Nolan, R., Alvarez, L., Watanabe, Y., Coomer, C.A., Jakobsdottir, G.M., Bowden, T.A., and Padilla-Parra, S. (2018). A dynamic three-step mechanism drives the HIV-1 pre-fusion reaction. Nat Struct Mol Biol *25*, 814-822.

Iliopoulou, M., Nolan, R., Alvarez, L., Watanabe, Y., Coomer, C.A., Jakobsdottir, G.M., Bowden, T.A., and Padilla-Parra, S. (2019). Author Correction: A dynamic three-step mechanism drives the HIV-1 pre-fusion reaction. Nat Struct Mol Biol *26*, 526.

Isel, C., Ehresmann, C., Ehresmann, B., and Marquet, R. (1996). Determining the conformation of RNAs in solution. Application to a retroviral system: structure of the HIV-1 primer binding site region and effect of tRNA(3Lys) binding. Pharm Acta Helv *71*, 11-19.

Iwatani, Y., Chan, D.S., Wang, F., Stewart-Maynard, K., Sugiura, W., Gronenborn, A.M., Rouzina, I., Williams, M.C., Musier-Forsyth, K., and Levin, J.G. (2007). Deaminase-independent inhibition of HIV-1 reverse transcription by APOBEC3G. Nucleic Acids Res *35*, 7096-7108.

Iyer, S.S., Bibollet-Ruche, F., Sherrill-Mix, S., Learn, G.H., Plenderleith, L., Smith, A.G., Barbian, H.J., Russell, R.M., Gondim, M.V., Bahari, C.Y*., et al.* (2017). Resistance to

type 1 interferons is a major determinant of HIV-1 transmission fitness. Proc Natl Acad Sci U S A *114*, E590-E599.

Jacks, T., Power, M.D., Masiarz, F.R., Luciw, P.A., Barr, P.J., and Varmus, H.E. (1988). Characterization of ribosomal frameshifting in HIV-1 gag-pol expression. Nature *331*, 280-283.

Jacquelin, B., Mayau, V., Targat, B., Liovat, A.S., Kunkel, D., Petitjean, G., Dillies, M.A., Roques, P., Butor, C., Silvestri, G.*, et al.* (2009). Nonpathogenic SIV infection of African green monkeys induces a strong but rapidly controlled type I IFN response. J Clin Invest *119*, 3544-3555.

Jacques, D.A., McEwan, W.A., Hilditch, L., Price, A.J., Towers, G.J., and James, L.C. (2016). HIV-1 uses dynamic capsid pores to import nucleotides and fuel encapsidated DNA synthesis. Nature *536*, 349-353.

Jaenisch, R., and Bird, A. (2003). Epigenetic regulation of gene expression: how the genome integrates intrinsic and environmental signals. Nat Genet *33 Suppl*, 245-254.

Jaffar, S., Wilkins, A., Ngom, P.T., Sabally, S., Corrah, T., Bangali, J.E., Rolfe, M., and Whittle, H.C. (1997). Rate of decline of percentage CD4+ cells is faster in HIV-1 than in HIV-2 infection. J Acquir Immune Defic Syndr Hum Retrovirol *16*, 327-332.

Jager, S., Kim, D.Y., Hultquist, J.F., Shindo, K., LaRue, R.S., Kwon, E., Li, M., Anderson, B.D., Yen, L., Stanley, D.*, et al.* (2011). Vif hijacks CBF-beta to degrade APOBEC3G and promote HIV-1 infection. Nature *481*, 371-375.

Januszeski, M.M., Cannon, P.M., Chen, D., Rozenberg, Y., and Anderson, W.F. (1997). Functional analysis of the cytoplasmic tail of Moloney murine leukemia virus envelope protein. J Virol *71*, 3613-3619.

Javanbakht, H., Diaz-Griffero, F., Stremlau, M., Si, Z., and Sodroski, J. (2005). The contribution of RING and B-box 2 domains to retroviral restriction mediated by monkey TRIM5alpha. J Biol Chem *280*, 26933-26940.

Ji, X., Wu, Y., Yan, J., Mehrens, J., Yang, H., DeLucia, M., Hao, C., Gronenborn, A.M., Skowronski, J., Ahn, J.*, et al.* (2013). Mechanism of allosteric activation of SAMHD1 by dGTP. Nat Struct Mol Biol *20*, 1304-1309.

Jia, B., Serra-Moreno, R., Neidermyer, W., Rahmberg, A., Mackey, J., Fofana, I.B., Johnson, W.E., Westmoreland, S., and Evans, D.T. (2009). Species-specific activity of SIV Nef and HIV-1 Vpu in overcoming restriction by tetherin/BST2. PLoS Pathog *5*, e1000429.

Jia, R., Pan, Q., Ding, S., Rong, L., Liu, S.L., Geng, Y., Qiao, W., and Liang, C. (2012). The N-terminal region of IFITM3 modulates its antiviral activity by regulating IFITM3 cellular localization. J Virol *86*, 13697-13707.

Jia, R., Xu, F., Qian, J., Yao, Y., Miao, C., Zheng, Y.M., Liu, S.L., Guo, F., Geng, Y., Qiao, W.*, et al.* (2014). Identification of an endocytic signal essential for the antiviral action of IFITM3. Cell Microbiol *16*, 1080-1093.

Jiang, J., and Aiken, C. (2007). Maturation-dependent human immunodeficiency virus type 1 particle fusion requires a carboxyl-terminal region of the gp41 cytoplasmic tail. J Virol *81*, 9999-10008.

Jin, M., and Goldenring, J.R. (2006). The Rab11-FIP1/RCP gene codes for multiple protein transcripts related to the plasma membrane recycling system. Biochim Biophys Acta *1759*, 281-295.

Jin, M.J., Rogers, J., Phillips-Conroy, J.E., Allan, J.S., Desrosiers, R.C., Shaw, G.M., Sharp, P.M., and Hahn, B.H. (1994). Infection of a yellow baboon with simian immunodeficiency virus from African green monkeys: evidence for cross-species transmission in the wild. J Virol *68*, 8454-8460.

Jin, S.W., Alsahafi, N., Kuang, X.T., Swann, S.A., Toyoda, M., Gottlinger, H., Walker, B.D., Ueno, T., Finzi, A., Brumme, Z.L.*, et al.* (2019). Natural HIV-1 Nef Polymorphisms Impair SERINC5 Downregulation Activity. Cell Rep *29*, 1449-1457 e1445.

John, S.P., Chin, C.R., Perreira, J.M., Feeley, E.M., Aker, A.M., Savidis, G., Smith, S.E., Elia, A.E., Everitt, A.R., Vora, M.*, et al.* (2013). The CD225 domain of IFITM3 is required for both IFITM protein association and inhibition of influenza A virus and dengue virus replication. J Virol *87*, 7837-7852.

Johnston, P.B., Dubay, J.W., and Hunter, E. (1993). Truncations of the simian immunodeficiency virus transmembrane protein confer expanded virus host range by removing a block to virus entry into cells. J Virol *67*, 3077-3086.

Johnston, S.H., Lobritz, M.A., Nguyen, S., Lassen, K., Delair, S., Posta, F., Bryson, Y.J., Arts, E.J., Chou, T., and Lee, B. (2009). A quantitative affinity-profiling system that reveals distinct CD4/CCR5 usage patterns among human immunodeficiency virus type 1 and simian immunodeficiency virus strains. J Virol *83*, 11016-11026.

Jolly, C., Booth, N.J., and Neil, S.J. (2010). Cell-cell spread of human immunodeficiency virus type 1 overcomes tetherin/BST-2-mediated restriction in T cells. J Virol *84*, 12185-12199.

Jolly, C., Kashefi, K., Hollinshead, M., and Sattentau, Q.J. (2004). HIV-1 cell to cell transfer across an Env-induced, actin-dependent synapse. J Exp Med *199*, 283-293.

Jolly, C., Mitar, I., and Sattentau, Q.J. (2007a). Adhesion molecule interactions facilitate human immunodeficiency virus type 1-induced virological synapse formation between T cells. J Virol *81*, 13916-13921.

Jolly, C., Mitar, I., and Sattentau, Q.J. (2007b). Requirement for an intact T-cell actin and tubulin cytoskeleton for efficient assembly and spread of human immunodeficiency virus type 1. J Virol *81*, 5547-5560.

Jolly, C., and Sattentau, Q.J. (2004). Retroviral spread by induction of virological synapses. Traffic *5*, 643-650.

Jolly, C., and Sattentau, Q.J. (2005). Human immunodeficiency virus type 1 virological synapse formation in T cells requires lipid raft integrity. J Virol *79*, 12088-12094.

Jolly, C., and Sattentau, Q.J. (2007). Human immunodeficiency virus type 1 assembly, budding, and cell-cell spread in T cells take place in tetraspanin-enriched plasma membrane domains. J Virol *81*, 7873-7884.

Jolly, C., Welsch, S., Michor, S., and Sattentau, Q.J. (2011). The regulated secretory pathway in CD4(+) T cells contributes to human immunodeficiency virus type-1 cell-to-cell spread at the virological synapse. PLoS Pathog *7*, e1002226.

Jones, D.R., Suzuki, K., and Piller, S.C. (2002). A 100-amino acid truncation in the cytoplasmic tail of glycoprotein 41 in the reference HIV type 1 strain RF. AIDS Res Hum Retroviruses *18*, 513-517.

Jordan, A., Bisgrove, D., and Verdin, E. (2003). HIV reproducibly establishes a latent infection after acute infection of T cells in vitro. EMBO J *22*, 1868-1877.

Josefsson, L., King, M.S., Makitalo, B., Brannstrom, J., Shao, W., Maldarelli, F., Kearney, M.F., Hu, W.S., Chen, J., Gaines, H.*, et al.* (2011). Majority of CD4+ T cells from peripheral blood of HIV-1-infected individuals contain only one HIV DNA molecule. Proc Natl Acad Sci U S A *108*, 11199-11204.

Josefsson, L., Palmer, S., Faria, N.R., Lemey, P., Casazza, J., Ambrozak, D., Kearney, M., Shao, W., Kottilil, S., Sneller, M.*, et al.* (2013). Single cell analysis of lymph node tissue from HIV-1 infected patients reveals that the majority of CD4+ T-cells contain one HIV-1 DNA molecule. PLoS Pathog *9*, e1003432.

Joseph, S.B., Swanstrom, R., Kashuba, A.D., and Cohen, M.S. (2015). Bottlenecks in HIV-1 transmission: insights from the study of founder viruses. Nat Rev Microbiol *13*, 414-425.

Jouve, M., Sol-Foulon, N., Watson, S., Schwartz, O., and Benaroch, P. (2007). HIV-1 buds and accumulates in "nonacidic" endosomes of macrophages. Cell Host Microbe *2*, 85-95.

Jouvenet, N., Bieniasz, P.D., and Simon, S.M. (2008). Imaging the biogenesis of individual HIV-1 virions in live cells. Nature *454*, 236-240.

Jowett, J.B., Planelles, V., Poon, B., Shah, N.P., Chen, M.L., and Chen, I.S. (1995). The human immunodeficiency virus type 1 vpr gene arrests infected T cells in the G2 + M phase of the cell cycle. J Virol *69*, 6304-6313.

Julien, J.P., Lee, J.H., Cupo, A., Murin, C.D., Derking, R., Hoffenberg, S., Caulfield, M.J., King, C.R., Marozsan, A.J., Klasse, P.J.*, et al.* (2013). Asymmetric recognition of the HIV-1 trimer by broadly neutralizing antibody PG9. Proc Natl Acad Sci U S A *110*, 4351-4356.

Jung, A., Maier, R., Vartanian, J.P., Bocharov, G., Jung, V., Fischer, U., Meese, E., Wain-Hobson, S., and Meyerhans, A. (2002). Recombination: Multiply infected spleen cells in HIV patients. Nature *418*, 144.

Kadiu, I., and Gendelman, H.E. (2011a). Human immunodeficiency virus type 1 endocytic trafficking through macrophage bridging conduits facilitates spread of infection. J Neuroimmune Pharmacol *6*, 658-675.

Kadiu, I., and Gendelman, H.E. (2011b). Macrophage bridging conduit trafficking of HIV-1 through the endoplasmic reticulum and Golgi network. J Proteome Res *10*, 3225-3238.

Kalia, V., Sarkar, S., Gupta, P., and Montelaro, R.C. (2003). Rational site-directed mutations of the LLP-1 and LLP-2 lentivirus lytic peptide domains in the intracytoplasmic tail of human immunodeficiency virus type 1 gp41 indicate common functions in cell-cell fusion but distinct roles in virion envelope incorporation. J Virol *77*, 3634-3646.

Kane, M., Rebensburg, S.V., Takata, M.A., Zang, T.M., Yamashita, M., Kvaratskhelia, M., and Bieniasz, P.D. (2018). Nuclear pore heterogeneity influences HIV-1 infection and the antiviral activity of MX2. Elife *7*.

Kane, M., Yadav, S.S., Bitzegeio, J., Kutluay, S.B., Zang, T., Wilson, S.J., Schoggins, J.W., Rice, C.M., Yamashita, M., Hatziioannou, T.*, et al.* (2013). MX2 is an interferon-induced inhibitor of HIV-1 infection. Nature *502*, 563-566.

Kanki, P.J., Barin, F., M'Boup, S., Allan, J.S., Romet-Lemonne, J.L., Marlink, R., McLane, M.F., Lee, T.H., Arbeille, B., Denis, F.*, et al.* (1986). New human T-lymphotropic retrovirus related to simian T-lymphotropic virus type III (STLV-IIIAGM). Science *232*, 238-243.

Kaplan, A.H., Zack, J.A., Knigge, M., Paul, D.A., Kempf, D.J., Norbeck, D.W., and Swanstrom, R. (1993). Partial inhibition of the human immunodeficiency virus type 1 protease results in aberrant virus assembly and the formation of noninfectious particles. J Virol *67*, 4050-4055.

Kariuki, S.M., Selhorst, P., Arien, K.K., and Dorfman, J.R. (2017). The HIV-1 transmission bottleneck. Retrovirology *14*, 22.

Kaur, A., Grant, R.M., Means, R.E., McClure, H., Feinberg, M., and Johnson, R.P. (1998). Diverse host responses and outcomes following simian immunodeficiency virus SIVmac239 infection in sooty mangabeys and rhesus macaques. J Virol *72*, 9597-9611.

Keckesova, Z., Ylinen, L.M., and Towers, G.J. (2006). Cyclophilin A renders human immunodeficiency virus type 1 sensitive to Old World monkey but not human TRIM5 alpha antiviral activity. J Virol *80*, 4683-4690.

Keele, B.F., and Derdeyn, C.A. (2009). Genetic and antigenic features of the transmitted virus. Curr Opin HIV AIDS *4*, 352-357.

Keele, B.F., Giorgi, E.E., Salazar-Gonzalez, J.F., Decker, J.M., Pham, K.T., Salazar, M.G., Sun, C., Grayson, T., Wang, S., Li, H.*, et al.* (2008). Identification and

characterization of transmitted and early founder virus envelopes in primary HIV-1 infection. Proc Natl Acad Sci U S A *105*, 7552-7557.

Kempf, D.J., Marsh, K.C., Denissen, J.F., McDonald, E., Vasavanonda, S., Flentge, C.A., Green, B.E., Fino, L., Park, C.H., Kong, X.P.*, et al.* (1995). ABT-538 is a potent inhibitor of human immunodeficiency virus protease and has high oral bioavailability in humans. Proc Natl Acad Sci U S A *92*, 2484-2488.

Kiernan, R.E., and Freed, E.O. (1998). Cleavage of the murine leukemia virus transmembrane env protein by human immunodeficiency virus type 1 protease: transdominant inhibition by matrix mutations. J Virol *72*, 9621-9627.

Kilzer, J.M., Stracker, T., Beitzel, B., Meek, K., Weitzman, M., and Bushman, F.D. (2003). Roles of host cell factors in circularization of retroviral dna. Virology *314*, 460-467.

Kim, E.M., Lee, K.H., and Kim, J.W. (1999). The cytoplasmic domain of HIV-1 gp41 interacts with the carboxyl-terminal region of alpha-catenin. Mol Cells *9*, 281-285.

Kim, E.Y., Bhattacharya, T., Kunstman, K., Swantek, P., Koning, F.A., Malim, M.H., and Wolinsky, S.M. (2010). Human APOBEC3G-mediated editing can promote HIV-1 sequence diversification and accelerate adaptation to selective pressure. J Virol *84*, 10402-10405.

Kim, F.J., Seiliez, I., Denesvre, C., Lavillette, D., Cosset, F.L., and Sitbon, M. (2000). Definition of an amino-terminal domain of the human T-cell leukemia virus type 1 envelope surface unit that extends the fusogenic range of an ecotropic murine leukemia virus. J Biol Chem *275*, 23417-23420.

Kim, K., Dauphin, A., Komurlu, S., McCauley, S.M., Yurkovetskiy, L., Carbone, C., Diehl, W.E., Strambio-De-Castillia, C., Campbell, E.M., and Luban, J. (2019). Cyclophilin A protects HIV-1 from restriction by human TRIM5alpha. Nat Microbiol *4*, 2044-2051.

King, M.C., Raposo, G., and Lemmon, M.A. (2004). Inhibition of nuclear import and cell-cycle progression by mutated forms of the dynamin-like GTPase MxB. Proc Natl Acad Sci U S A *101*, 8957-8962.

Kirchhoff, F. (2010). Immune evasion and counteraction of restriction factors by HIV-1 and other primate lentiviruses. Cell Host Microbe *8*, 55-67.

Kirchhoff, F., Greenough, T.C., Brettler, D.B., Sullivan, J.L., and Desrosiers, R.C. (1995). Brief report: absence of intact nef sequences in a long-term survivor with nonprogressive HIV-1 infection. N Engl J Med *332*, 228-232.

Kirschman, J., Qi, M., Ding, L., Hammonds, J., Dienger-Stambaugh, K., Wang, J.J., Lapierre, L.A., Goldenring, J.R., and Spearman, P. (2018). HIV-1 Envelope Glycoprotein Trafficking through the Endosomal Recycling Compartment Is Required for Particle Incorporation. J Virol *92*.

Klatt, N.R., Villinger, F., Bostik, P., Gordon, S.N., Pereira, L., Engram, J.C., Mayne, A., Dunham, R.M., Lawson, B., Ratcliffe, S.J.*, et al.* (2008). Availability of activated CD4+ T

cells dictates the level of viremia in naturally SIV-infected sooty mangabeys. J Clin Invest *118*, 2039-2049.

Klatzmann, D., Champagne, E., Chamaret, S., Gruest, J., Guetard, D., Hercend, T., Gluckman, J.C., and Montagnier, L. (1984). T-lymphocyte T4 molecule behaves as the receptor for human retrovirus LAV. Nature *312*, 767-768.

Klaver, B., and Berkhout, B. (1994). Comparison of 5' and 3' long terminal repeat promoter function in human immunodeficiency virus. J Virol *68*, 3830-3840.

Klimkait, T., Strebel, K., Hoggan, M.D., Martin, M.A., and Orenstein, J.M. (1990). The human immunodeficiency virus type 1-specific protein vpu is required for efficient virus maturation and release. J Virol *64*, 621-629.

Kluge, S.F., Mack, K., Iyer, S.S., Pujol, F.M., Heigele, A., Learn, G.H., Usmani, S.M., Sauter, D., Joas, S., Hotter, D.*, et al.* (2014). Nef proteins of epidemic HIV-1 group O strains antagonize human tetherin. Cell Host Microbe *16*, 639-650.

Kodama, T., Wooley, D.P., Naidu, Y.M., Kestler, H.W., 3rd, Daniel, M.D., Li, Y., and Desrosiers, R.C. (1989). Significance of premature stop codons in env of simian immunodeficiency virus. J Virol *63*, 4709-4714.

Koh, Y., Wu, X., Ferris, A.L., Matreyek, K.A., Smith, S.J., Lee, K., KewalRamani, V.N., Hughes, S.H., and Engelman, A. (2013). Differential effects of human immunodeficiency virus type 1 capsid and cellular factors nucleoporin 153 and LEDGF/p75 on the efficiency and specificity of viral DNA integration. J Virol *87*, 648-658.

Kohl, N.E., Emini, E.A., Schleif, W.A., Davis, L.J., Heimbach, J.C., Dixon, R.A., Scolnick, E.M., and Sigal, I.S. (1988). Active human immunodeficiency virus protease is required for viral infectivity. Proc Natl Acad Sci U S A *85*, 4686-4690.

Kohlstaedt, L.A., Wang, J., Friedman, J.M., Rice, P.A., and Steitz, T.A. (1992). Crystal structure at 3.5 A resolution of HIV-1 reverse transcriptase complexed with an inhibitor. Science *256*, 1783-1790.

Kong, L.I., Lee, S.W., Kappes, J.C., Parkin, J.S., Decker, D., Hoxie, J.A., Hahn, B.H., and Shaw, G.M. (1988). West African HIV-2-related human retrovirus with attenuated cytopathicity. Science *240*, 1525-1529.

Kong, R., Li, H., Bibollet-Ruche, F., Decker, J.M., Zheng, N.N., Gottlieb, G.S., Kiviat, N.B., Sow, P.S., Georgiev, I., Hahn, B.H.*, et al.* (2012a). Broad and potent neutralizing antibody responses elicited in natural HIV-2 infection. J Virol *86*, 947-960.

Kong, R., Li, H., Georgiev, I., Changela, A., Bibollet-Ruche, F., Decker, J.M., Rowland-Jones, S.L., Jaye, A., Guan, Y., Lewis, G.K.*, et al.* (2012b). Epitope mapping of broadly neutralizing HIV-2 human monoclonal antibodies. J Virol *86*, 12115-12128.

Koning, F.A., Goujon, C., Bauby, H., and Malim, M.H. (2011). Target cell-mediated editing of HIV-1 cDNA by APOBEC3 proteins in human macrophages. J Virol *85*, 13448-13452.

Koning, F.A., Newman, E.N., Kim, E.Y., Kunstman, K.J., Wolinsky, S.M., and Malim, M.H. (2009). Defining APOBEC3 expression patterns in human tissues and hematopoietic cell subsets. J Virol *83*, 9474-9485.

Kramski, M., Parsons, M.S., Stratov, I., and Kent, S.J. (2013). HIV-specific antibody immunity mediated through NK cells and monocytes. Curr HIV Res *11*, 388-406.

Krapp, C., Hotter, D., Gawanbacht, A., McLaren, P.J., Kluge, S.F., Sturzel, C.M., Mack, K., Reith, E., Engelhart, S., Ciuffi, A.*, et al.* (2016). Guanylate Binding Protein (GBP) 5 Is an Interferon-Inducible Inhibitor of HIV-1 Infectivity. Cell Host Microbe *19*, 504-514.

Krishnan, L., Matreyek, K.A., Oztop, I., Lee, K., Tipper, C.H., Li, X., Dar, M.J., Kewalramani, V.N., and Engelman, A. (2010). The requirement for cellular transportin 3 (TNPO3 or TRN-SR2) during infection maps to human immunodeficiency virus type 1 capsid and not integrase. J Virol *84*, 397-406.

Krummheuer, J., Johnson, A.T., Hauber, I., Kammler, S., Anderson, J.L., Hauber, J., Purcell, D.F., and Schaal, H. (2007). A minimal uORF within the HIV-1 vpu leader allows efficient translation initiation at the downstream env AUG. Virology *363*, 261-271.

Kubo, Y., and Amanuma, H. (2003). Mutational analysis of the R peptide cleavage site of Moloney murine leukaemia virus envelope protein. J Gen Virol *84*, 2253-2257.

Kubo, Y., Hayashi, H., Matsuyama, T., Sato, H., and Yamamoto, N. (2012). Retrovirus entry by endocytosis and cathepsin proteases. Adv Virol *2012*, 640894.

Kubo, Y., Tominaga, C., Yoshii, H., Kamiyama, H., Mitani, C., Amanuma, H., and Yamamoto, N. (2007). Characterization of R peptide of murine leukemia virus envelope glycoproteins in syncytium formation and entry. Arch Virol *152*, 2169-2182.

Kueck, T., Foster, T.L., Weinelt, J., Sumner, J.C., Pickering, S., and Neil, S.J. (2015). Serine Phosphorylation of HIV-1 Vpu and Its Binding to Tetherin Regulates Interaction with Clathrin Adaptors. PLoS Pathog *11*, e1005141.

Kumar, P., Hui, H.X., Kappes, J.C., Haggarty, B.S., Hoxie, J.A., Arya, S.K., Shaw, G.M., and Hahn, B.H. (1990). Molecular characterization of an attenuated human immunodeficiency virus type 2 isolate. J Virol *64*, 890-901.

Kupzig, S., Korolchuk, V., Rollason, R., Sugden, A., Wilde, A., and Banting, G. (2003). Bst-2/HM1.24 is a raft-associated apical membrane protein with an unusual topology. Traffic *4*, 694-709.

Kutluay, S.B., Perez-Caballero, D., and Bieniasz, P.D. (2013). Fates of retroviral core components during unrestricted and TRIM5-restricted infection. PLoS Pathog *9*, e1003214.

Kuwata, T., Kaori, T., Enomoto, I., Yoshimura, K., and Matsushita, S. (2013). Increased infectivity in human cells and resistance to antibody-mediated neutralization by truncation of the SIV gp41 cytoplasmic tail. Front Microbiol *4*, 117.

Kwon, Y.D., Finzi, A., Wu, X., Dogo-Isonagie, C., Lee, L.K., Moore, L.R., Schmidt, S.D., Stuckey, J., Yang, Y., Zhou, T.*, et al.* (2012). Unliganded HIV-1 gp120 core structures assume the CD4-bound conformation with regulation by quaternary interactions and variable loops. Proc Natl Acad Sci U S A *109*, 5663-5668.

Kwong, P.D., Wyatt, R., Robinson, J., Sweet, R.W., Sodroski, J., and Hendrickson, W.A. (1998). Structure of an HIV gp120 envelope glycoprotein in complex with the CD4 receptor and a neutralizing human antibody. Nature *393*, 648-659.

LaBranche, C.C., Hoffman, T.L., Romano, J., Haggarty, B.S., Edwards, T.G., Matthews, T.J., Doms, R.W., and Hoxie, J.A. (1999). Determinants of CD4 independence for a human immunodeficiency virus type 1 variant map outside regions required for coreceptor specificity. J Virol *73*, 10310-10319.

Ladinsky, M.S., Kieffer, C., Olson, G., Deruaz, M., Vrbanac, V., Tager, A.M., Kwon, D.S., and Bjorkman, P.J. (2014). Electron tomography of HIV-1 infection in gut-associated lymphoid tissue. PLoS Pathog *10*, e1003899.

Laguette, N., Bregnard, C., Hue, P., Basbous, J., Yatim, A., Larroque, M., Kirchhoff, F., Constantinou, A., Sobhian, B., and Benkirane, M. (2014). Premature activation of the SLX4 complex by Vpr promotes G2/M arrest and escape from innate immune sensing. Cell *156*, 134-145.

Laguette, N., Sobhian, B., Casartelli, N., Ringeard, M., Chable-Bessia, C., Segeral, E., Yatim, A., Emiliani, S., Schwartz, O., and Benkirane, M. (2011). SAMHD1 is the dendritic- and myeloid-cell-specific HIV-1 restriction factor counteracted by Vpx. Nature *474*, 654-657.

Lahaye, X., Satoh, T., Gentili, M., Cerboni, S., Conrad, C., Hurbain, I., El Marjou, A., Lacabaratz, C., Lelievre, J.D., and Manel, N. (2013). The capsids of HIV-1 and HIV-2 determine immune detection of the viral cDNA by the innate sensor cGAS in dendritic cells. Immunity *39*, 1132-1142.

Lahouassa, H., Blondot, M.L., Chauveau, L., Chougui, G., Morel, M., Leduc, M., Guillonneau, F., Ramirez, B.C., Schwartz, O., and Margottin-Goguet, F. (2016). HIV-1 Vpr degrades the HLTF DNA translocase in T cells and macrophages. Proc Natl Acad Sci U S A *113*, 5311-5316.

Lahti, A.L., Manninen, A., and Saksela, K. (2003). Regulation of T cell activation by HIV-1 accessory proteins: Vpr acts via distinct mechanisms to cooperate with Nef in NFAT-directed gene expression and to promote transactivation by CREB. Virology *310*, 190-196.

Langer, S., Hammer, C., Hopfensperger, K., Klein, L., Hotter, D., De Jesus, P.D., Herbert, K.M., Pache, L., Smith, N., van der Merwe, J.A.*, et al.* (2019). HIV-1 Vpu is a potent transcriptional suppressor of NF-kappaB-elicited antiviral immune responses. Elife *8*.

Langlois, M.A., and Neuberger, M.S. (2008). Human APOBEC3G can restrict retroviral infection in avian cells and acts independently of both UNG and SMUG1. J Virol *82*, 4660-4664.

Larder, B.A., Kemp, S.D., and Harrigan, P.R. (1995). Potential mechanism for sustained antiretroviral efficacy of AZT-3TC combination therapy. Science *269*, 696-699.

Lascano, J., Uchil, P.D., Mothes, W., and Luban, J. (2016). TRIM5 Retroviral Restriction Activity Correlates with the Ability To Induce Innate Immune Signaling. J Virol *90*, 308-316.

Lasky, L.A., Groopman, J.E., Fennie, C.W., Benz, P.M., Capon, D.J., Dowbenko, D.J., Nakamura, G.R., Nunes, W.M., Renz, M.E., and Berman, P.W. (1986). Neutralization of the AIDS retrovirus by antibodies to a recombinant envelope glycoprotein. Science *233*, 209-212.

Lazzarino, D.A., Diego, M., Musi, E., Hirschman, S.Z., and Alexander, R.J. (2000). CXCR4 and CCR5 expression by H9 T-cells is downregulated by a peptide-nucleic acid immunomodulator. Immunol Lett *74*, 189-195.

Le Rouzic, E., Belaidouni, N., Estrabaud, E., Morel, M., Rain, J.C., Transy, C., and Margottin-Goguet, F. (2007). HIV1 Vpr arrests the cell cycle by recruiting DCAF1/VprBP, a receptor of the Cul4-DDB1 ubiquitin ligase. Cell Cycle *6*, 182-188.

Le Tortorec, A., and Neil, S.J. (2009). Antagonism to and intracellular sequestration of human tetherin by the human immunodeficiency virus type 2 envelope glycoprotein. J Virol *83*, 11966-11978.

Lederer, S., Favre, D., Walters, K.A., Proll, S., Kanwar, B., Kasakow, Z., Baskin, C.R., Palermo, R., McCune, J.M., and Katze, M.G. (2009). Transcriptional profiling in pathogenic and non-pathogenic SIV infections reveals significant distinctions in kinetics and tissue compartmentalization. PLoS Pathog *5*, e1000296.

Lee, F.S., Hagler, J., Chen, Z.J., and Maniatis, T. (1997). Activation of the IkappaB alpha kinase complex by MEKK1, a kinase of the JNK pathway. Cell *88*, 213-222.

Lee, J.H., Andrabi, R., Su, C.Y., Yasmeen, A., Julien, J.P., Kong, L., Wu, N.C., McBride, R., Sok, D., Pauthner, M.*, et al.* (2017). A Broadly Neutralizing Antibody Targets the Dynamic HIV Envelope Trimer Apex via a Long, Rigidified, and Anionic beta-Hairpin Structure. Immunity *46*, 690-702.

Lee, J.H., Ozorowski, G., and Ward, A.B. (2016). Cryo-EM structure of a native, fully glycosylated, cleaved HIV-1 envelope trimer. Science *351*, 1043-1048.

Lee, K., Ambrose, Z., Martin, T.D., Oztop, I., Mulky, A., Julias, J.G., Vandegraaff, N., Baumann, J.G., Wang, R., Yuen, W.*, et al.* (2010). Flexible use of nuclear import pathways by HIV-1. Cell Host Microbe *7*, 221-233.

Lee, S.F., Ko, C.Y., Wang, C.T., and Chen, S.S. (2002a). Effect of point mutations in the N terminus of the lentivirus lytic peptide-1 sequence of human immunodeficiency virus type 1 transmembrane protein gp41 on Env stability. J Biol Chem *277*, 15363-15375.

Lee, S.W., Han, S.I., Kim, H.H., and Lee, Z.H. (2002b). TAK1-dependent activation of AP-1 and c-Jun N-terminal kinase by receptor activator of NF-kappaB. J Biochem Mol Biol *35*, 371-376.

Lee, W.S., and Kent, S.J. (2018). Anti-HIV-1 antibody-dependent cellular cytotoxicity: is there more to antibodies than neutralization? Curr Opin HIV AIDS *13*, 160-166.

Len, A.C.L., Starling, S., Shivkumar, M., and Jolly, C. (2017). HIV-1 Activates T Cell Signaling Independently of Antigen to Drive Viral Spread. Cell Rep *18*, 1062-1074.

Leonard, C.K., Spellman, M.W., Riddle, L., Harris, R.J., Thomas, J.N., and Gregory, T.J. (1990). Assignment of intrachain disulfide bonds and characterization of potential glycosylation sites of the type 1 recombinant human immunodeficiency virus envelope glycoprotein (gp120) expressed in Chinese hamster ovary cells. J Biol Chem *265*, 10373-10382.

Letko, M., Silvestri, G., Hahn, B.H., Bibollet-Ruche, F., Gokcumen, O., Simon, V., and Ooms, M. (2013). Vif proteins from diverse primate lentiviral lineages use the same binding site in APOBEC3G. J Virol *87*, 11861-11871.

Leung, K., Kim, J.O., Ganesh, L., Kabat, J., Schwartz, O., and Nabel, G.J. (2008). HIV-1 assembly: viral glycoproteins segregate quantally to lipid rafts that associate individually with HIV-1 capsids and virions. Cell Host Microbe *3*, 285-292.

Levy, J.A., Hoffman, A.D., Kramer, S.M., Landis, J.A., Shimabukuro, J.M., and Oshiro, L.S. (1984). Isolation of lymphocytopathic retroviruses from San Francisco patients with AIDS. Science *225*, 840-842.

Lewinski, M.K., Yamashita, M., Emerman, M., Ciuffi, A., Marshall, H., Crawford, G., Collins, F., Shinn, P., Leipzig, J., Hannenhalli, S*., et al.* (2006). Retroviral DNA integration: viral and cellular determinants of target-site selection. PLoS Pathog *2*, e60.

Li, K., Markosyan, R.M., Zheng, Y.M., Golfetto, O., Bungart, B., Li, M., Ding, S., He, Y., Liang, C., Lee, J.C*., et al.* (2013). IFITM proteins restrict viral membrane hemifusion. PLoS Pathog *9*, e1003124.

Li, L., Olvera, J.M., Yoder, K.E., Mitchell, R.S., Butler, S.L., Lieber, M., Martin, S.L., and Bushman, F.D. (2001). Role of the non-homologous DNA end joining pathway in the early steps of retroviral infection. EMBO J *20*, 3272-3281.

Li, X., and Sodroski, J. (2008). The TRIM5alpha B-box 2 domain promotes cooperative binding to the retroviral capsid by mediating higher-order self-association. J Virol *82*, 11495-11502.

Li, X.Y., Guo, F., Zhang, L., Kleiman, L., and Cen, S. (2007). APOBEC3G inhibits DNA strand transfer during HIV-1 reverse transcription. J Biol Chem *282*, 32065-32074.

Li, Y.L., Chandrasekaran, V., Carter, S.D., Woodward, C.L., Christensen, D.E., Dryden, K.A., Pornillos, O., Yeager, M., Ganser-Pornillos, B.K., Jensen, G.J.*, et al.* (2016). Primate TRIM5 proteins form hexagonal nets on HIV-1 capsids. Elife *5*.

Liao, H.X., Bonsignori, M., Alam, S.M., McLellan, J.S., Tomaras, G.D., Moody, M.A., Kozink, D.M., Hwang, K.K., Chen, X., Tsao, C.Y.*, et al.* (2013). Vaccine induction of antibodies against a structurally heterogeneous site of immune pressure within HIV-1 envelope protein variable regions 1 and 2. Immunity *38*, 176-186.

Lightfoote, M.M., Coligan, J.E., Folks, T.M., Fauci, A.S., Martin, M.A., and Venkatesan, S. (1986). Structural characterization of reverse transcriptase and endonuclease polypeptides of the acquired immunodeficiency syndrome retrovirus. J Virol *60*, 771-775.

Lim, E.S., Fregoso, O.I., McCoy, C.O., Matsen, F.A., Malik, H.S., and Emerman, M. (2012). The ability of primate lentiviruses to degrade the monocyte restriction factor SAMHD1 preceded the birth of the viral accessory protein Vpx. Cell Host Microbe *11*, 194-204.

Lin, T.Y., Chin, C.R., Everitt, A.R., Clare, S., Perreira, J.M., Savidis, G., Aker, A.M., John, S.P., Sarlah, D., Carreira, E.M.*, et al.* (2013). Amphotericin B increases influenza A virus infection by preventing IFITM3-mediated restriction. Cell Rep *5*, 895-908.

Linde, M.E., Colquhoun, D.R., Ubaida Mohien, C., Kole, T., Aquino, V., Cotter, R., Edwards, N., Hildreth, J.E., and Graham, D.R. (2013). The conserved set of host proteins incorporated into HIV-1 virions suggests a common egress pathway in multiple cell types. J Proteome Res *12*, 2045-2054.

Ling, S., Zhang, C., Wang, W., Cai, X., Yu, L., Wu, F., Zhang, L., and Tian, C. (2016). Combined approaches of EPR and NMR illustrate only one transmembrane helix in the human IFITM3. Sci Rep *6*, 24029.

Liu, C., Perilla, J.R., Ning, J., Lu, M., Hou, G., Ramalho, R., Himes, B.A., Zhao, G., Bedwell, G.J., Byeon, I.J.*, et al.* (2016). Cyclophilin A stabilizes the HIV-1 capsid through a novel non-canonical binding site. Nat Commun *7*, 10714.

Liu, N., Lee, C.H., Swigut, T., Grow, E., Gu, B., Bassik, M.C., and Wysocka, J. (2018). Selective silencing of euchromatic L1s revealed by genome-wide screens for L1 regulators. Nature *553*, 228-232.

Liu, R., Lin, Y., Jia, R., Geng, Y., Liang, C., Tan, J., and Qiao, W. (2014). HIV-1 Vpr stimulates NF-kappaB and AP-1 signaling by activating TAK1. Retrovirology *11*, 45.

Liu, Z., Pan, Q., Ding, S., Qian, J., Xu, F., Zhou, J., Cen, S., Guo, F., and Liang, C. (2013). The interferon-inducible MxB protein inhibits HIV-1 infection. Cell Host Microbe *14*, 398-410.

Liu, Z., Pan, Q., Liang, Z., Qiao, W., Cen, S., and Liang, C. (2015). The highly polymorphic cyclophilin A-binding loop in HIV-1 capsid modulates viral resistance to MxB. Retrovirology *12*, 1.

Llewellyn, G.N., Hogue, I.B., Grover, J.R., and Ono, A. (2010). Nucleocapsid promotes localization of HIV-1 gag to uropods that participate in virological synapses between T cells. PLoS Pathog *6*, e1001167.

Lodermeyer, V., Ssebyatika, G., Passos, V., Ponnurangam, A., Malassa, A., Ewald, E., Sturzel, C.M., Kirchhoff, F., Rotger, M., Falk, C.S.*, et al.* (2018). The Antiviral Activity of the Cellular Glycoprotein LGALS3BP/90K Is Species Specific. J Virol *92*.

Lodermeyer, V., Suhr, K., Schrott, N., Kolbe, C., Sturzel, C.M., Krnavek, D., Munch, J., Dietz, C., Waldmann, T., Kirchhoff, F.*, et al.* (2013). 90K, an interferon-stimulated gene product, reduces the infectivity of HIV-1. Retrovirology *10*, 111.

Lopez-Verges, S., Camus, G., Blot, G., Beauvoir, R., Benarous, R., and Berlioz-Torrent, C. (2006). Tail-interacting protein TIP47 is a connector between Gag and Env and is required for Env incorporation into HIV-1 virions. Proc Natl Acad Sci U S A *103*, 14947-14952.

Lorizate, M., Sachsenheimer, T., Glass, B., Habermann, A., Gerl, M.J., Krausslich, H.G., and Brugger, B. (2013). Comparative lipidomics analysis of HIV-1 particles and their producer cell membrane in different cell lines. Cell Microbiol *15*, 292-304.

Loving, R., Wu, S.R., Sjoberg, M., Lindqvist, B., and Garoff, H. (2012). Maturation cleavage of the murine leukemia virus Env precursor separates the transmembrane subunits to prime it for receptor triggering. Proc Natl Acad Sci U S A *109*, 7735-7740.

Lu, J., Pan, Q., Rong, L., He, W., Liu, S.L., and Liang, C. (2011a). The IFITM proteins inhibit HIV-1 infection. J Virol *85*, 2126-2137.

Lu, K., Heng, X., Garyu, L., Monti, S., Garcia, E.L., Kharytonchyk, S., Dorjsuren, B., Kulandaivel, G., Jones, S., Hiremath, A.*, et al.* (2011b). NMR detection of structures in the HIV-1 5'-leader RNA that regulate genome packaging. Science *334*, 242-245.

Lu, K., Heng, X., and Summers, M.F. (2011c). Structural determinants and mechanism of HIV-1 genome packaging. J Mol Biol *410*, 609-633.

Lu, L., Zhu, Y., Huang, J., Chen, X., Yang, H., Jiang, S., and Chen, Y.H. (2008). Surface exposure of the HIV-1 env cytoplasmic tail LLP2 domain during the membrane fusion process: interaction with gp41 fusion core. J Biol Chem *283*, 16723-16731.

Luciw, P.A., Shaw, K.E., Shacklett, B.L., and Marthas, M.L. (1998). Importance of the intracytoplasmic domain of the simian immunodeficiency virus (SIV) envelope glycoprotein for pathogenesis. Virology *252*, 9-16.

Luo, K., Xiao, Z., Ehrlich, E., Yu, Y., Liu, B., Zheng, S., and Yu, X.F. (2005). Primate lentiviral virion infectivity factors are substrate receptors that assemble with cullin 5-E3 ligase through a HCCH motif to suppress APOBEC3G. Proc Natl Acad Sci U S A *102*, 11444-11449.

Lusic, M., and Siliciano, R.F. (2017). Nuclear landscape of HIV-1 infection and integration. Nat Rev Microbiol *15*, 69-82.

Lusso, P., di Marzo Veronese, F., Ensoli, B., Franchini, G., Jemma, C., DeRocco, S.E., Kalyanaraman, V.S., and Gallo, R.C. (1990). Expanded HIV-1 cellular tropism by phenotypic mixing with murine endogenous retroviruses. Science *247*, 848-852.

Lyumkis, D., Julien, J.P., de Val, N., Cupo, A., Potter, C.S., Klasse, P.J., Burton, D.R., Sanders, R.W., Moore, J.P., Carragher, B.*, et al.* (2013). Cryo-EM structure of a fully glycosylated soluble cleaved HIV-1 envelope trimer. Science *342*, 1484-1490.

MacKenzie, K.R., Prestegard, J.H., and Engelman, D.M. (1997). A transmembrane helix dimer: structure and implications. Science *276*, 131-133.

Maddon, P.J., Dalgleish, A.G., McDougal, J.S., Clapham, P.R., Weiss, R.A., and Axel, R. (1986). The T4 gene encodes the AIDS virus receptor and is expressed in the immune system and the brain. Cell *47*, 333-348.

Maertens, G., Cherepanov, P., Pluymers, W., Busschots, K., De Clercq, E., Debyser, Z., and Engelborghs, Y. (2003). LEDGF/p75 is essential for nuclear and chromosomal targeting of HIV-1 integrase in human cells. J Biol Chem *278*, 33528-33539.

Maertens, G.N., Hare, S., and Cherepanov, P. (2010). The mechanism of retroviral integration from X-ray structures of its key intermediates. Nature *468*, 326-329.

Magadan, J.G., Perez-Victoria, F.J., Sougrat, R., Ye, Y., Strebel, K., and Bonifacino, J.S. (2010). Multilayered mechanism of CD4 downregulation by HIV-1 Vpu involving distinct ER retention and ERAD targeting steps. PLoS Pathog *6*, e1000869.

Malbec, M., Porrot, F., Rua, R., Horwitz, J., Klein, F., Halper-Stromberg, A., Scheid, J.F., Eden, C., Mouquet, H., Nussenzweig, M.C.*, et al.* (2013). Broadly neutralizing antibodies that inhibit HIV-1 cell to cell transmission. J Exp Med *210*, 2813-2821.

Malim, M.H., and Bieniasz, P.D. (2012). HIV Restriction Factors and Mechanisms of Evasion. Cold Spring Harb Perspect Med *2*, a006940.

Mamede, J.I., Cianci, G.C., Anderson, M.R., and Hope, T.J. (2017). Early cytoplasmic uncoating is associated with infectivity of HIV-1. Proc Natl Acad Sci U S A *114*, E7169-E7178.

Mammano, F., Kondo, E., Sodroski, J., Bukovsky, A., and Gottlinger, H.G. (1995). Rescue of human immunodeficiency virus type 1 matrix protein mutants by envelope glycoproteins with short cytoplasmic domains. J Virol *69*, 3824-3830.

Manches, O., Frleta, D., and Bhardwaj, N. (2014). Dendritic cells in progression and pathology of HIV infection. Trends Immunol *35*, 114-122.

Manganaro, L., de Castro, E., Maestre, A.M., Olivieri, K., Garcia-Sastre, A., Fernandez-Sesma, A., and Simon, V. (2015). HIV Vpu Interferes with NF-kappaB Activity but Not with Interferon Regulatory Factor 3. J Virol *89*, 9781-9790.

Manganaro, L., Hong, P., Hernandez, M.M., Argyle, D., Mulder, L.C.F., Potla, U., Diaz-Griffero, F., Lee, B., Fernandez-Sesma, A., and Simon, V. (2018). IL-15 regulates

susceptibility of CD4(+) T cells to HIV infection. Proc Natl Acad Sci U S A *115*, E9659-E9667.

Mangeat, B., Gers-Huber, G., Lehmann, M., Zufferey, M., Luban, J., and Piguet, V. (2009). HIV-1 Vpu neutralizes the antiviral factor Tetherin/BST-2 by binding it and directing its beta-TrCP2-dependent degradation. PLoS Pathog *5*, e1000574.

Mangeat, B., Turelli, P., Caron, G., Friedli, M., Perrin, L., and Trono, D. (2003). Broad antiretroviral defence by human APOBEC3G through lethal editing of nascent reverse transcripts. Nature *424*, 99-103.

Manrique, J.M., Celma, C.C., Affranchino, J.L., Hunter, E., and Gonzalez, S.A. (2001). Small variations in the length of the cytoplasmic domain of the simian immunodeficiency virus transmembrane protein drastically affect envelope incorporation and virus entry. AIDS Res Hum Retroviruses *17*, 1615-1624.

Margottin, F., Bour, S.P., Durand, H., Selig, L., Benichou, S., Richard, V., Thomas, D., Strebel, K., and Benarous, R. (1998). A novel human WD protein, h-beta TrCp, that interacts with HIV-1 Vpu connects CD4 to the ER degradation pathway through an F-box motif. Mol Cell *1*, 565-574.

Marini, B., Kertesz-Farkas, A., Ali, H., Lucic, B., Lisek, K., Manganaro, L., Pongor, S., Luzzati, R., Recchia, A., Mavilio, F.*, et al.* (2015). Nuclear architecture dictates HIV-1 integration site selection. Nature *521*, 227-231.

Markosyan, R.M., Cohen, F.S., and Melikyan, G.B. (2003). HIV-1 envelope proteins complete their folding into six-helix bundles immediately after fusion pore formation. Mol Biol Cell *14*, 926-938.

Markosyan, R.M., Leung, M.Y., and Cohen, F.S. (2009). The six-helix bundle of human immunodeficiency virus Env controls pore formation and enlargement and is initiated at residues proximal to the hairpin turn. J Virol *83*, 10048-10057.

Marlink, R., Kanki, P., Thior, I., Travers, K., Eisen, G., Siby, T., Traore, I., Hsieh, C.C., Dia, M.C., Gueye, E.H.*, et al.* (1994). Reduced rate of disease development after HIV-2 infection as compared to HIV-1. Science *265*, 1587-1590.

Martin, N., Welsch, S., Jolly, C., Briggs, J.A., Vaux, D., and Sattentau, Q.J. (2010). Virological synapse-mediated spread of human immunodeficiency virus type 1 between T cells is sensitive to entry inhibition. J Virol *84*, 3516-3527.

Martin-Serrano, J., Zang, T., and Bieniasz, P.D. (2001). HIV-1 and Ebola virus encode small peptide motifs that recruit Tsg101 to sites of particle assembly to facilitate egress. Nat Med *7*, 1313-1319.

Mascola, J.R., Stiegler, G., VanCott, T.C., Katinger, H., Carpenter, C.B., Hanson, C.E., Beary, H., Hayes, D., Frankel, S.S., Birx, D.L.*, et al.* (2000). Protection of macaques against vaginal transmission of a pathogenic HIV-1/SIV chimeric virus by passive infusion of neutralizing antibodies. Nat Med *6*, 207-210.

Mashiba, M., Collins, D.R., Terry, V.H., and Collins, K.L. (2014). Vpr overcomes macrophage-specific restriction of HIV-1 Env expression and virion production. Cell Host Microbe *16*, 722-735.

Mathez, D., Schinazi, R.F., Liotta, D.C., and Leibowitch, J. (1993). Infectious amplification of wild-type human immunodeficiency virus from patients' lymphocytes and modulation by reverse transcriptase inhibitors in vitro. Antimicrob Agents Chemother *37*, 2206-2211.

Mathys, L., Francois, K.O., Quandte, M., Braakman, I., and Balzarini, J. (2014). Deletion of the highly conserved N-glycan at Asn260 of HIV-1 gp120 affects folding and lysosomal degradation of gp120, and results in loss of viral infectivity. PLoS One *9*, e101181.

Matreyek, K.A., Yucel, S.S., Li, X., and Engelman, A. (2013). Nucleoporin NUP153 phenylalanine-glycine motifs engage a common binding pocket within the HIV-1 capsid protein to mediate lentiviral infectivity. PLoS Pathog *9*, e1003693.

Mattila, P.K., and Lappalainen, P. (2008). Filopodia: molecular architecture and cellular functions. Nat Rev Mol Cell Biol *9*, 446-454.

Maudet, C., Sourisce, A., Dragin, L., Lahouassa, H., Rain, J.C., Bouaziz, S., Ramirez, B.C., and Margottin-Goguet, F. (2013). HIV-1 Vpr induces the degradation of ZIP and sZIP, adaptors of the NuRD chromatin remodeling complex, by hijacking DCAF1/VprBP. PLoS One *8*, e77320.

Mazurov, D., Ilinskaya, A., Heidecker, G., Lloyd, P., and Derse, D. (2010). Quantitative comparison of HTLV-1 and HIV-1 cell-to-cell infection with new replication dependent vectors. PLoS Pathog *6*, e1000788.

McBrien, J.B., Mavigner, M., Franchitti, L., Smith, S.A., White, E., Tharp, G.K., Walum, H., Busman-Sahay, K., Aguilera-Sandoval, C.R., Thayer, W.O.*, et al.* (2020). Robust and persistent reactivation of SIV and HIV by N-803 and depletion of CD8(+) cells. Nature *578*, 154-159.

McCoy, L.E., and Burton, D.R. (2017). Identification and specificity of broadly neutralizing antibodies against HIV. Immunol Rev *275*, 11-20.

McCoy, L.E., Groppelli, E., Blanchetot, C., de Haard, H., Verrips, T., Rutten, L., Weiss, R.A., and Jolly, C. (2014). Neutralisation of HIV-1 cell-cell spread by human and llama antibodies. Retrovirology *11*, 83.

McCune, J.M., Rabin, L.B., Feinberg, M.B., Lieberman, M., Kosek, J.C., Reyes, G.R., and Weissman, I.L. (1988). Endoproteolytic cleavage of gp160 is required for the activation of human immunodeficiency virus. Cell *53*, 55-67.

McDonald, D., Wu, L., Bohks, S.M., KewalRamani, V.N., Unutmaz, D., and Hope, T.J. (2003). Recruitment of HIV and its receptors to dendritic cell-T cell junctions. Science *300*, 1295-1297.

Melikyan, G.B. (2008). Common principles and intermediates of viral protein-mediated fusion: the HIV-1 paradigm. Retrovirology *5*, 111.

Melikyan, G.B. (2014). HIV entry: a game of hide-and-fuse? Curr Opin Virol *4*, 1-7.

Melikyan, G.B., Markosyan, R.M., Brener, S.A., Rozenberg, Y., and Cohen, F.S. (2000). Role of the cytoplasmic tail of ecotropic moloney murine leukemia virus Env protein in fusion pore formation. J Virol *74*, 447-455.

Mercenne, G., Bernacchi, S., Richer, D., Bec, G., Henriet, S., Paillart, J.C., and Marquet, R. (2010). HIV-1 Vif binds to APOBEC3G mRNA and inhibits its translation. Nucleic Acids Res *38*, 633-646.

Mercredi, P.Y., Bucca, N., Loeliger, B., Gaines, C.R., Mehta, M., Bhargava, P., Tedbury, P.R., Charlier, L., Floquet, N., Muriaux, D*., et al.* (2016). Structural and Molecular Determinants of Membrane Binding by the HIV-1 Matrix Protein. J Mol Biol *428*, 1637-1655.

Meroni, G., and Diez-Roux, G. (2005). TRIM/RBCC, a novel class of 'single protein RING finger' E3 ubiquitin ligases. Bioessays *27*, 1147-1157.

Mesner, D., Hotter, D., Kirchhoff, F., and Jolly, C. (2020). Loss of Nef-mediated CD3 down-regulation in the HIV-1 lineage increases viral infectivity and spread. Proc Natl Acad Sci U S A *117*, 7382-7391.

Meusser, B., Hirsch, C., Jarosch, E., and Sommer, T. (2005). ERAD: the long road to destruction. Nat Cell Biol *7*, 766-772.

Mielke, D., Bandawe, G., Pollara, J., Abrahams, M.R., Nyanhete, T., Moore, P.L., Thebus, R., Yates, N.L., Kappes, J.C., Ochsenbauer, C*., et al.* (2019). Antibody-Dependent Cellular Cytotoxicity (ADCC)-Mediating Antibodies Constrain Neutralizing Antibody Escape Pathway. Front Immunol *10*, 2875.

Miles, R.J., Kerridge, C., Hilditch, L., Monit, C., Jacques, D.A., and Towers, G.J. (2020). MxB sensitivity of HIV-1 is determined by a highly variable and dynamic capsid surface. Elife *9*.

Miller, M.A., Cloyd, M.W., Liebmann, J., Rinaldo, C.R., Jr., Islam, K.R., Wang, S.Z., Mietzner, T.A., and Montelaro, R.C. (1993). Alterations in cell membrane permeability by the lentivirus lytic peptide (LLP-1) of HIV-1 transmembrane protein. Virology *196*, 89-100.

Miller, M.D., Farnet, C.M., and Bushman, F.D. (1997). Human immunodeficiency virus type 1 preintegration complexes: studies of organization and composition. J Virol *71*, 5382-5390.

Mitchell, R.S., Beitzel, B.F., Schroder, A.R., Shinn, P., Chen, H., Berry, C.C., Ecker, J.R., and Bushman, F.D. (2004). Retroviral DNA integration: ASLV, HIV, and MLV show distinct target site preferences. PLoS Biol *2*, E234.

Mitchell, R.S., Katsura, C., Skasko, M.A., Fitzpatrick, K., Lau, D., Ruiz, A., Stephens, E.B., Margottin-Goguet, F., Benarous, R., and Guatelli, J.C. (2009). Vpu antagonizes BST-2-mediated restriction of HIV-1 release via beta-TrCP and endo-lysosomal trafficking. PLoS Pathog *5*, e1000450.

Mizutani, S., Boettiger, D., and Temin, H.M. (1970). A DNA-depenent DNA polymerase and a DNA endonuclease in virions of Rous sarcoma virus. Nature *228*, 424-427.

Mlcochova, P., Pelchen-Matthews, A., and Marsh, M. (2013). Organization and regulation of intracellular plasma membrane-connected HIV-1 assembly compartments in macrophages. BMC Biol *11*, 89.

Mlcochova, P., Sutherland, K.A., Watters, S.A., Bertoli, C., de Bruin, R.A., Rehwinkel, J., Neil, S.J., Lenzi, G.M., Kim, B., Khwaja, A.*, et al.* (2017). A G1-like state allows HIV-1 to bypass SAMHD1 restriction in macrophages. EMBO J *36*, 604-616.

Moldt, B., Rakasz, E.G., Schultz, N., Chan-Hui, P.Y., Swiderek, K., Weisgrau, K.L., Piaskowski, S.M., Bergman, Z., Watkins, D.I., Poignard, P.*, et al.* (2012). Highly potent HIV-specific antibody neutralization in vitro translates into effective protection against mucosal SHIV challenge in vivo. Proc Natl Acad Sci U S A *109*, 18921-18925.

Monroe, K.M., Yang, Z., Johnson, J.R., Geng, X., Doitsh, G., Krogan, N.J., and Greene, W.C. (2014). IFI16 DNA sensor is required for death of lymphoid CD4 T cells abortively infected with HIV. Science *343*, 428-432.

Montefiori, D.C., Roederer, M., Morris, L., and Seaman, M.S. (2018). Neutralization tiers of HIV-1. Curr Opin HIV AIDS *13*, 128-136.

Moore, M.D., Nikolaitchik, O.A., Chen, J., Hammarskjold, M.L., Rekosh, D., and Hu, W.S. (2009). Probing the HIV-1 genomic RNA trafficking pathway and dimerization by genetic recombination and single virion analyses. PLoS Pathog *5*, e1000627.

Mori, K., Ringler, D.J., Kodama, T., and Desrosiers, R.C. (1992). Complex determinants of macrophage tropism in env of simian immunodeficiency virus. J Virol *66*, 2067-2075.

Morita, E., Sandrin, V., McCullough, J., Katsuyama, A., Baci Hamilton, I., and Sundquist, W.I. (2011). ESCRT-III protein requirements for HIV-1 budding. Cell Host Microbe *9*, 235-242.

Moulard, M., and Decroly, E. (2000). Maturation of HIV envelope glycoprotein precursors by cellular endoproteases. Biochim Biophys Acta *1469*, 121-132.

Mucksch, F., Laketa, V., Muller, B., Schultz, C., and Krausslich, H.G. (2017). Synchronized HIV assembly by tunable PIP2 changes reveals PIP2 requirement for stable Gag anchoring. Elife *6*.

Mulligan, M.J., Kumar, P., Hui, H.X., Owens, R.J., Ritter, G.D., Jr., Hahn, B.H., and Compans, R.W. (1990). The env protein of an infectious noncytopathic HIV-2 is deficient in syncytium formation. AIDS Res Hum Retroviruses *6*, 707-720.

Mulligan, M.J., Yamshchikov, G.V., Ritter, G.D., Jr., Gao, F., Jin, M.J., Nail, C.D., Spies, C.P., Hahn, B.H., and Compans, R.W. (1992). Cytoplasmic domain truncation enhances fusion activity by the exterior glycoprotein complex of human immunodeficiency virus type 2 in selected cell types. J Virol *66*, 3971-3975.

Munch, J., Rajan, D., Schindler, M., Specht, A., Rucker, E., Novembre, F.J., Nerrienet, E., Muller-Trutwin, M.C., Peeters, M., Hahn, B.H.*, et al.* (2007). Nef-mediated enhancement of virion infectivity and stimulation of viral replication are fundamental properties of primate lentiviruses. J Virol *81*, 13852-13864.

Munro, J.B., Gorman, J., Ma, X., Zhou, Z., Arthos, J., Burton, D.R., Koff, W.C., Courter, J.R., Smith, A.B., 3rd, Kwong, P.D.*, et al.* (2014). Conformational dynamics of single HIV-1 envelope trimers on the surface of native virions. Science *346*, 759-763.

Murakami, T., Ablan, S., Freed, E.O., and Tanaka, Y. (2004). Regulation of human immunodeficiency virus type 1 Env-mediated membrane fusion by viral protease activity. J Virol *78*, 1026-1031.

Murakami, T., and Freed, E.O. (2000). The long cytoplasmic tail of gp41 is required in a cell type-dependent manner for HIV-1 envelope glycoprotein incorporation into virions. Proc Natl Acad Sci U S A *97*, 343-348.

Muranyi, W., Malkusch, S., Muller, B., Heilemann, M., and Krausslich, H.G. (2013). Super-resolution microscopy reveals specific recruitment of HIV-1 envelope proteins to viral assembly sites dependent on the envelope C-terminal tail. PLoS Pathog *9*, e1003198.

Murooka, T.T., Deruaz, M., Marangoni, F., Vrbanac, V.D., Seung, E., von Andrian, U.H., Tager, A.M., Luster, A.D., and Mempel, T.R. (2012). HIV-infected T cells are migratory vehicles for viral dissemination. Nature *490*, 283-287.

Murphy, R.E., Samal, A.B., Vlach, J., Mas, V., Prevelige, P.E., and Saad, J.S. (2019). Structural and biophysical characterizations of HIV-1 matrix trimer binding to lipid nanodiscs shed light on virus assembly. J Biol Chem *294*, 18600-18612.

Murphy, R.E., Samal, A.B., Vlach, J., and Saad, J.S. (2017). Solution Structure and Membrane Interaction of the Cytoplasmic Tail of HIV-1 gp41 Protein. Structure *25*, 1708-1718 e1705.

Murrell, B., Vollbrecht, T., Guatelli, J., and Wertheim, J.O. (2016). The Evolutionary Histories of Antiretroviral Proteins SERINC3 and SERINC5 Do Not Support an Evolutionary Arms Race in Primates. J Virol *90*, 8085-8089.

Naamati, A., Williamson, J.C., Greenwood, E.J., Marelli, S., Lehner, P.J., and Matheson, N.J. (2019). Functional proteomic atlas of HIV infection in primary human CD4+ T cells. Elife *8*.

Naidu, Y.M., Kestler, H.W., 3rd, Li, Y., Butler, C.V., Silva, D.P., Schmidt, D.K., Troup, C.D., Sehgal, P.K., Sonigo, P., Daniel, M.D.*, et al.* (1988). Characterization of infectious

molecular clones of simian immunodeficiency virus (SIVmac) and human immunodeficiency virus type 2: persistent infection of rhesus monkeys with molecularly cloned SIVmac. J Virol *62*, 4691-4696.

Neher, R.A., and Leitner, T. (2010). Recombination rate and selection strength in HIV intra-patient evolution. PLoS Comput Biol *6*, e1000660.

Neil, S.J. (2013). The antiviral activities of tetherin. Curr Top Microbiol Immunol *371*, 67-104.

Neil, S.J., Zang, T., and Bieniasz, P.D. (2008). Tetherin inhibits retrovirus release and is antagonized by HIV-1 Vpu. Nature *451*, 425-430.

Nermut, M.V., and Fassati, A. (2003). Structural analyses of purified human immunodeficiency virus type 1 intracellular reverse transcription complexes. J Virol *77*, 8196-8206.

Nguyen, D.H., and Hildreth, J.E. (2000). Evidence for budding of human immunodeficiency virus type 1 selectively from glycolipid-enriched membrane lipid rafts. J Virol *74*, 3264-3272.

Nie, J., Zhao, J., Chen, Q., Huang, W., and Wang, Y. (2014). Three amino acid residues in the envelope of human immunodeficiency virus type 1 CRF07_BC regulate viral neutralization susceptibility to the human monoclonal neutralizing antibody IgG1b12. Virol Sin *29*, 299-307.

Nielsen, M.S., Gustafsen, C., Madsen, P., Nyengaard, J.R., Hermey, G., Bakke, O., Mari, M., Schu, P., Pohlmann, R., Dennes, A.*, et al.* (2007). Sorting by the cytoplasmic domain of the amyloid precursor protein binding receptor SorLA. Mol Cell Biol *27*, 6842-6851.

Nieto-Garai, J.A., Arboleya, A., Otaegi, S., Chojnacki, J., Casas, J., Fabriàs, G., Contreras, F.-X., Kräusslich, H.-G., and Lorizate, M. (2020) Cholesterol in the Viral Membrane is a Molecular Switch Governing HIV-1 Env Clustering. Advanced Science *n/a*, 2003468.

Nikolaitchik, O.A., Dilley, K.A., Fu, W., Gorelick, R.J., Tai, S.H., Soheilian, F., Ptak, R.G., Nagashima, K., Pathak, V.K., and Hu, W.S. (2013). Dimeric RNA recognition regulates HIV-1 genome packaging. PLoS Pathog *9*, e1003249.

Nikolic, D.S., Lehmann, M., Felts, R., Garcia, E., Blanchet, F.P., Subramaniam, S., and Piguet, V. (2011). HIV-1 activates Cdc42 and induces membrane extensions in immature dendritic cells to facilitate cell-to-cell virus propagation. Blood *118*, 4841-4852.

Ninomiya-Tsuji, J., Kishimoto, K., Hiyama, A., Inoue, J., Cao, Z., and Matsumoto, K. (1999). The kinase TAK1 can activate the NIK-I kappaB as well as the MAP kinase cascade in the IL-1 signalling pathway. Nature *398*, 252-256.

Nixon, C.C., Mavigner, M., Sampey, G.C., Brooks, A.D., Spagnuolo, R.A., Irlbeck, D.M., Mattingly, C., Ho, P.T., Schoof, N., Cammon, C.G.*, et al.* (2020). Systemic HIV and SIV latency reversal via non-canonical NF-kappaB signalling in vivo. Nature *578*, 160-165.

Norman, J.M., Mashiba, M., McNamara, L.A., Onafuwa-Nuga, A., Chiari-Fort, E., Shen, W., and Collins, K.L. (2011). The antiviral factor APOBEC3G enhances the recognition of HIV-infected primary T cells by natural killer cells. Nat Immunol *12*, 975-983.

Nowarski, R., Prabhu, P., Kenig, E., Smith, Y., Britan-Rosich, E., and Kotler, M. (2014). APOBEC3G inhibits HIV-1 RNA elongation by inactivating the viral trans-activation response element. J Mol Biol *426*, 2840-2853.

Nuvor, S.V., van der Sande, M., Rowland-Jones, S., Whittle, H., and Jaye, A. (2006). Natural killer cell function is well preserved in asymptomatic human immunodeficiency virus type 2 (HIV-2) infection but similar to that of HIV-1 infection when CD4 T-cell counts fall. J Virol *80*, 2529-2538.

Nyamweya, S., Hegedus, A., Jaye, A., Rowland-Jones, S., Flanagan, K.L., and Macallan, D.C. (2013). Comparing HIV-1 and HIV-2 infection: Lessons for viral immunopathogenesis. Rev Med Virol *23*, 221-240.

OhAinle, M., Helms, L., Vermeire, J., Roesch, F., Humes, D., Basom, R., Delrow, J.J., Overbaugh, J., and Emerman, M. (2018). A virus-packageable CRISPR screen identifies host factors mediating interferon inhibition of HIV. Elife *7*.

Ohno, H., Aguilar, R.C., Fournier, M.C., Hennecke, S., Cosson, P., and Bonifacino, J.S. (1997). Interaction of endocytic signals from the HIV-1 envelope glycoprotein complex with members of the adaptor medium chain family. Virology *238*, 305-315.

Ohta, Y., Masuda, T., Tsujimoto, H., Ishikawa, K., Kodama, T., Morikawa, S., Nakai, M., Honjo, S., and Hayami, M. (1988). Isolation of simian immunodeficiency virus from African green monkeys and seroepidemiologic survey of the virus in various non-human primates. Int J Cancer *41*, 115-122.

Olesen, J.S., Jespersen, S., da Silva, Z.J., Rodrigues, A., Erikstrup, C., Aaby, P., Wejse, C., and Honge, B.L. (2018). HIV-2 continues to decrease, whereas HIV-1 is stabilizing in Guinea-Bissau. AIDS *32*, 1193-1198.

Ono, A., Ablan, S.D., Lockett, S.J., Nagashima, K., and Freed, E.O. (2004). Phosphatidylinositol (4,5) bisphosphate regulates HIV-1 Gag targeting to the plasma membrane. Proc Natl Acad Sci U S A *101*, 14889-14894.

Ono, A., and Freed, E.O. (2001). Plasma membrane rafts play a critical role in HIV-1 assembly and release. Proc Natl Acad Sci U S A *98*, 13925-13930.

Ono, A., and Freed, E.O. (2004). Cell-type-dependent targeting of human immunodeficiency virus type 1 assembly to the plasma membrane and the multivesicular body. J Virol *78*, 1552-1563.

Orenstein, J.M., Meltzer, M.S., Phipps, T., and Gendelman, H.E. (1988). Cytoplasmic assembly and accumulation of human immunodeficiency virus types 1 and 2 in recombinant human colony-stimulating factor-1-treated human monocytes: an ultrastructural study. J Virol *62*, 2578-2586.

Osman, N., Lucas, S., and Cantrell, D. (1995). The role of tyrosine phosphorylation in the interaction of cellular tyrosine kinases with the T cell receptor zeta chain tyrosine-based activation motif. Eur J Immunol *25*, 2863-2869.

Ott, D.E. (2008). Cellular proteins detected in HIV-1. Rev Med Virol *18*, 159-175.

Ozorowski, G., Pallesen, J., de Val, N., Lyumkis, D., Cottrell, C.A., Torres, J.L., Copps, J., Stanfield, R.L., Cupo, A., Pugach, P.*, et al.* (2017). Open and closed structures reveal allostery and pliability in the HIV-1 envelope spike. Nature *547*, 360-363.

Page, K.A., Landau, N.R., and Littman, D.R. (1990). Construction and use of a human immunodeficiency virus vector for analysis of virus infectivity. J Virol *64*, 5270-5276.

Paiardini, M., Cervasi, B., Engram, J.C., Gordon, S.N., Klatt, N.R., Muthukumar, A., Else, J., Mittler, R.S., Staprans, S.I., Sodora, D.L.*, et al.* (2009). Bone marrow-based homeostatic proliferation of mature T cells in nonhuman primates: implications for AIDS pathogenesis. Blood *113*, 612-621.

Paiardini, M., Cervasi, B., Reyes-Aviles, E., Micci, L., Ortiz, A.M., Chahroudi, A., Vinton, C., Gordon, S.N., Bosinger, S.E., Francella, N.*, et al.* (2011). Low levels of SIV infection in sooty mangabey central memory CD(4)(+) T cells are associated with limited CCR5 expression. Nat Med *17*, 830-836.

Pancera, M., Shahzad-Ul-Hussan, S., Doria-Rose, N.A., McLellan, J.S., Bailer, R.T., Dai, K., Loesgen, S., Louder, M.K., Staupe, R.P., Yang, Y.*, et al.* (2013). Structural basis for diverse N-glycan recognition by HIV-1-neutralizing V1-V2-directed antibody PG16. Nat Struct Mol Biol *20*, 804-813.

Pancera, M., Zhou, T., Druz, A., Georgiev, I.S., Soto, C., Gorman, J., Huang, J., Acharya, P., Chuang, G.Y., Ofek, G.*, et al.* (2014). Structure and immune recognition of trimeric pre-fusion HIV-1 Env. Nature *514*, 455-461.

Pandrea, I.V., Gautam, R., Ribeiro, R.M., Brenchley, J.M., Butler, I.F., Pattison, M., Rasmussen, T., Marx, P.A., Silvestri, G., Lackner, A.A.*, et al.* (2007). Acute loss of intestinal CD4+ T cells is not predictive of simian immunodeficiency virus virulence. J Immunol *179*, 3035-3046.

Panganiban, A.T., and Fiore, D. (1988). Ordered interstrand and intrastrand DNA transfer during reverse transcription. Science *241*, 1064-1069.

Parren, P.W., Marx, P.A., Hessell, A.J., Luckay, A., Harouse, J., Cheng-Mayer, C., Moore, J.P., and Burton, D.R. (2001). Antibody protects macaques against vaginal challenge with a pathogenic R5 simian/human immunodeficiency virus at serum levels giving complete neutralization in vitro. J Virol *75*, 8340-8347.

Parrish, N.F., Gao, F., Li, H., Giorgi, E.E., Barbian, H.J., Parrish, E.H., Zajic, L., Iyer, S.S., Decker, J.M., Kumar, A.*, et al.* (2013). Phenotypic properties of transmitted founder HIV-1. Proc Natl Acad Sci U S A *110*, 6626-6633.

Passos, V., Zillinger, T., Casartelli, N., Wachs, A.S., Xu, S., Malassa, A., Steppich, K., Schilling, H., Franz, S., Todt, D.*, et al.* (2019). Characterization of Endogenous SERINC5 Protein as Anti-HIV-1 Factor. J Virol *93*.

Pauls, E., Ruiz, A., Badia, R., Permanyer, M., Gubern, A., Riveira-Munoz, E., Torres-Torronteras, J., Alvarez, M., Mothe, B., Brander, C.*, et al.* (2014). Cell cycle control and HIV-1 susceptibility are linked by CDK6-dependent CDK2 phosphorylation of SAMHD1 in myeloid and lymphoid cells. J Immunol *193*, 1988-1997.

Pear, W.S., Nolan, G.P., Scott, M.L., and Baltimore, D. (1993). Production of high-titer helper-free retroviruses by transient transfection. Proc Natl Acad Sci U S A *90*, 8392-8396.

Peeters, M., Gueye, A., Mboup, S., Bibollet-Ruche, F., Ekaza, E., Mulanga, C., Ouedrago, R., Gandji, R., Mpele, P., Dibanga, G.*, et al.* (1997). Geographical distribution of HIV-1 group O viruses in Africa. AIDS *11*, 493-498.

Pegu, A., Yang, Z.Y., Boyington, J.C., Wu, L., Ko, S.Y., Schmidt, S.D., McKee, K., Kong, W.P., Shi, W., Chen, X.*, et al.* (2014). Neutralizing antibodies to HIV-1 envelope protect more effectively in vivo than those to the CD4 receptor. Sci Transl Med *6*, 243ra288.

Pelchen-Matthews, A., Kramer, B., and Marsh, M. (2003). Infectious HIV-1 assembles in late endosomes in primary macrophages. J Cell Biol *162*, 443-455.

Peng, C., Ho, B.K., Chang, T.W., and Chang, N.T. (1989). Role of human immunodeficiency virus type 1-specific protease in core protein maturation and viral infectivity. J Virol *63*, 2550-2556.

Peng, K., Muranyi, W., Glass, B., Laketa, V., Yant, S.R., Tsai, L., Cihlar, T., Muller, B., and Krausslich, H.G. (2014). Quantitative microscopy of functional HIV post-entry complexes reveals association of replication with the viral capsid. Elife *3*, e04114.

Pereira, L.A., Bentley, K., Peeters, A., Churchill, M.J., and Deacon, N.J. (2000). A compilation of cellular transcription factor interactions with the HIV-1 LTR promoter. Nucleic Acids Res *28*, 663-668.

Permanyer, M., Ballana, E., Ruiz, A., Badia, R., Riveira-Munoz, E., Gonzalo, E., Clotet, B., and Este, J.A. (2012). Antiretroviral agents effectively block HIV replication after cell-to-cell transfer. J Virol *86*, 8773-8780.

Pertel, S.S., Gorkunenko, O.A., Kakayan, E.S., and Chirva, V.J. (2011a). Synthesis of 1,2-cis- and 1,2-trans-glycosides of 2-acetamido-4,6-O-benzylidene-2-deoxy-D-glucopyranose by anomeric O-alkylation. Carbohydr Res *346*, 685-688.

Pertel, T., Hausmann, S., Morger, D., Zuger, S., Guerra, J., Lascano, J., Reinhard, C., Santoni, F.A., Uchil, P.D., Chatel, L.*, et al.* (2011b). TRIM5 is an innate immune sensor for the retrovirus capsid lattice. Nature *472*, 361-365.

Perugi, F., Muriaux, D., Ramirez, B.C., Chabani, S., Decroly, E., Darlix, J.L., Blot, V., and Pique, C. (2009). Human Discs Large is a new negative regulator of human immunodeficiency virus-1 infectivity. Mol Biol Cell *20*, 498-508.

Peterson, K., and Rowland-Jones, S. (2012). Novel agents for the treatment of HIV-2 infection. Antivir Ther *17*, 435-438.

Pettit, S.C., Moody, M.D., Wehbie, R.S., Kaplan, A.H., Nantermet, P.V., Klein, C.A., and Swanstrom, R. (1994). The p2 domain of human immunodeficiency virus type 1 Gag regulates sequential proteolytic processing and is required to produce fully infectious virions. J Virol *68*, 8017-8027.

Pezeshkian, N., Groves, N.S., and van Engelenburg, S.B. (2019). Single-molecule imaging of HIV-1 envelope glycoprotein dynamics and Gag lattice association exposes determinants responsible for virus incorporation. Proc Natl Acad Sci U S A *116*, 25269-25277.

Piai, A., Fu, Q., Cai, Y., Ghantous, F., Xiao, T., Shaik, M.M., Peng, H., Rits-Volloch, S., Chen, W., Seaman, M.S.*, et al.* (2020). Structural basis of transmembrane coupling of the HIV-1 envelope glycoprotein. Nat Commun *11*, 2317.

Pickering, S., Hue, S., Kim, E.Y., Reddy, S., Wolinsky, S.M., and Neil, S.J. (2014). Preservation of tetherin and CD4 counter-activities in circulating Vpu alleles despite extensive sequence variation within HIV-1 infected individuals. PLoS Pathog *10*, e1003895.

Piguet, V., and Sattentau, Q. (2004). Dangerous liaisons at the virological synapse. J Clin Invest *114*, 605-610.

Piller, S.C., Dubay, J.W., Derdeyn, C.A., and Hunter, E. (2000). Mutational analysis of conserved domains within the cytoplasmic tail of gp41 from human immunodeficiency virus type 1: effects on glycoprotein incorporation and infectivity. J Virol *74*, 11717-11723.

Ping, L.H., Jabara, C.B., Rodrigo, A.G., Hudelson, S.E., Piwowar-Manning, E., Wang, L., Eshleman, S.H., Cohen, M.S., and Swanstrom, R. (2013). HIV-1 transmission during early antiretroviral therapy: evaluation of two HIV-1 transmission events in the HPTN 052 prevention study. PLoS One *8*, e71557.

Pinter, A., Honnen, W.J., Tilley, S.A., Bona, C., Zaghouani, H., Gorny, M.K., and Zolla-Pazner, S. (1989). Oligomeric structure of gp41, the transmembrane protein of human immunodeficiency virus type 1. J Virol *63*, 2674-2679.

Pitman, M.C., Lau, J.S.Y., McMahon, J.H., and Lewin, S.R. (2018). Barriers and strategies to achieve a cure for HIV. Lancet HIV *5*, e317-e328.

Plaimauer, B., Mohr, G., Wernhart, W., Himmelspach, M., Dorner, F., and Schlokat, U. (2001). 'Shed' furin: mapping of the cleavage determinants and identification of its C-terminus. Biochem J *354*, 689-695.

Plantier, J.C., Leoz, M., Dickerson, J.E., De Oliveira, F., Cordonnier, F., Lemee, V., Damond, F., Robertson, D.L., and Simon, F. (2009). A new human immunodeficiency virus derived from gorillas. Nat Med *15*, 871-872.

Poiesz, B.J., Ruscetti, F.W., Gazdar, A.F., Bunn, P.A., Minna, J.D., and Gallo, R.C. (1980). Detection and isolation of type C retrovirus particles from fresh and cultured lymphocytes of a patient with cutaneous T-cell lymphoma. Proc Natl Acad Sci U S A *77*, 7415-7419.

Pollpeter, D., Parsons, M., Sobala, A.E., Coxhead, S., Lang, R.D., Bruns, A.M., Papaioannou, S., McDonnell, J.M., Apolonia, L., Chowdhury, J.A.*, et al.* (2018). Deep sequencing of HIV-1 reverse transcripts reveals the multifaceted antiviral functions of APOBEC3G. Nat Microbiol *3*, 220-233.

Pope, M., Betjes, M.G., Romani, N., Hirmand, H., Cameron, P.U., Hoffman, L., Gezelter, S., Schuler, G., and Steinman, R.M. (1994). Conjugates of dendritic cells and memory T lymphocytes from skin facilitate productive infection with HIV-1. Cell *78*, 389-398.

Popovic, M., Sarngadharan, M.G., Read, E., and Gallo, R.C. (1984). Detection, isolation, and continuous production of cytopathic retroviruses (HTLV-III) from patients with AIDS and pre-AIDS. Science *224*, 497-500.

Popper, S.J., Sarr, A.D., Gueye-Ndiaye, A., Mboup, S., Essex, M.E., and Kanki, P.J. (2000). Low plasma human immunodeficiency virus type 2 viral load is independent of proviral load: low virus production in vivo. J Virol *74*, 1554-1557.

Pornillos, O., Ganser-Pornillos, B.K., and Yeager, M. (2011). Atomic-level modelling of the HIV capsid. Nature *469*, 424-427.

Postler, T.S., and Desrosiers, R.C. (2012). The cytoplasmic domain of the HIV-1 glycoprotein gp41 induces NF-kappaB activation through TGF-beta-activated kinase 1. Cell Host Microbe *11*, 181-193.

Postler, T.S., and Desrosiers, R.C. (2013). The tale of the long tail: the cytoplasmic domain of HIV-1 gp41. J Virol *87*, 2-15.

Preusser, A., Briese, L., Baur, A.S., and Willbold, D. (2001). Direct in vitro binding of full-length human immunodeficiency virus type 1 Nef protein to CD4 cytoplasmic domain. J Virol *75*, 3960-3964.

Price, A.J., Fletcher, A.J., Schaller, T., Elliott, T., Lee, K., KewalRamani, V.N., Chin, J.W., Towers, G.J., and James, L.C. (2012). CPSF6 defines a conserved capsid interface that modulates HIV-1 replication. PLoS Pathog *8*, e1002896.

Price, A.J., Jacques, D.A., McEwan, W.A., Fletcher, A.J., Essig, S., Chin, J.W., Halambage, U.D., Aiken, C., and James, L.C. (2014). Host cofactors and pharmacologic ligands share an essential interface in HIV-1 capsid that is lost upon disassembly. PLoS Pathog *10*, e1004459.

Pritchard, L.K., Vasiljevic, S., Ozorowski, G., Seabright, G.E., Cupo, A., Ringe, R., Kim, H.J., Sanders, R.W., Doores, K.J., Burton, D.R.*, et al.* (2015). Structural Constraints Determine the Glycosylation of HIV-1 Envelope Trimers. Cell Rep *11*, 1604-1613.

Puffer, B.A., Pohlmann, S., Edinger, A.L., Carlin, D., Sanchez, M.D., Reitter, J., Watry, D.D., Fox, H.S., Desrosiers, R.C., and Doms, R.W. (2002). CD4 independence of simian immunodeficiency virus Envs is associated with macrophage tropism, neutralization sensitivity, and attenuated pathogenicity. J Virol *76*, 2595-2605.

Pullen, K.A., Ishimoto, L.K., and Champoux, J.J. (1992). Incomplete removal of the RNA primer for minus-strand DNA synthesis by human immunodeficiency virus type 1 reverse transcriptase. J Virol *66*, 367-373.

Purcell, D.F., and Martin, M.A. (1993). Alternative splicing of human immunodeficiency virus type 1 mRNA modulates viral protein expression, replication, and infectivity. J Virol *67*, 6365-6378.

Pye, V.E., Rosa, A., Bertelli, C., Struwe, W.B., Maslen, S.L., Corey, R., Liko, I., Hassall, M., Mattiuzzo, G., Ballandras-Colas, A.*, et al.* (2020). A bipartite structural organization defines the SERINC family of HIV-1 restriction factors. Nat Struct Mol Biol *27*, 78-83.

Qi, M., Chu, H., Chen, X., Choi, J., Wen, X., Hammonds, J., Ding, L., Hunter, E., and Spearman, P. (2015). A tyrosine-based motif in the HIV-1 envelope glycoprotein tail mediates cell-type- and Rab11-FIP1C-dependent incorporation into virions. Proc Natl Acad Sci U S A *112*, 7575-7580.

Qi, M., Williams, J.A., Chu, H., Chen, X., Wang, J.J., Ding, L., Akhirome, E., Wen, X., Lapierre, L.A., Goldenring, J.R.*, et al.* (2013). Rab11-FIP1C and Rab14 direct plasma membrane sorting and particle incorporation of the HIV-1 envelope glycoprotein complex. PLoS Pathog *9*, e1003278.

Qian, J., Le Duff, Y., Wang, Y., Pan, Q., Ding, S., Zheng, Y.M., Liu, S.L., and Liang, C. (2015). Primate lentiviruses are differentially inhibited by interferon-induced transmembrane proteins. Virology *474*, 10-18.

Ragheb, J.A., and Anderson, W.F. (1994). pH-independent murine leukemia virus ecotropic envelope-mediated cell fusion: implications for the role of the R peptide and p12E TM in viral entry. J Virol *68*, 3220-3231.

Rankovic, S., Ramalho, R., Aiken, C., and Rousso, I. (2018). PF74 Reinforces the HIV-1 Capsid To Impair Reverse Transcription-Induced Uncoating. J Virol *92*.

Rankovic, S., Varadarajan, J., Ramalho, R., Aiken, C., and Rousso, I. (2017). Reverse Transcription Mechanically Initiates HIV-1 Capsid Disassembly. J Virol *91*.

Rao, Z., Belyaev, A.S., Fry, E., Roy, P., Jones, I.M., and Stuart, D.I. (1995). Crystal structure of SIV matrix antigen and implications for virus assembly. Nature *378*, 743-747.

Rasaiyaah, J., Tan, C.P., Fletcher, A.J., Price, A.J., Blondeau, C., Hilditch, L., Jacques, D.A., Selwood, D.L., James, L.C., Noursadeghi, M.*, et al.* (2013). HIV-1 evades innate immune recognition through specific cofactor recruitment. Nature *503*, 402-405.

Re, F., Braaten, D., Franke, E.K., and Luban, J. (1995). Human immunodeficiency virus type 1 Vpr arrests the cell cycle in G2 by inhibiting the activation of p34cdc2-cyclin B. J Virol *69*, 6859-6864.

Reading, S.A., Heap, C.J., and Dimmock, N.J. (2003). A novel monoclonal antibody specific to the C-terminal tail of the gp41 envelope transmembrane protein of human immunodeficiency virus type 1 that preferentially neutralizes virus after it has attached to the target cell and inhibits the production of infectious progeny. Virology *315*, 362-372.

Rein, A., Mirro, J., Haynes, J.G., Ernst, S.M., and Nagashima, K. (1994). Function of the cytoplasmic domain of a retroviral transmembrane protein: p15E-p2E cleavage activates the membrane fusion capability of the murine leukemia virus Env protein. J Virol *68*, 1773-1781.

Reitter, J., Means, R. & Desrosiers, R. (1998) A role for carbohydrates in immune evasion in AIDS. *Nat Med* **4,** 679–684

Rhee, S.S., and Marsh, J.W. (1994). Human immunodeficiency virus type 1 Nef-induced down-modulation of CD4 is due to rapid internalization and degradation of surface CD4. J Virol *68*, 5156-5163.

Richardson, M.W., Carroll, R.G., Stremlau, M., Korokhov, N., Humeau, L.M., Silvestri, G., Sodroski, J., and Riley, J.L. (2008). Mode of transmission affects the sensitivity of human immunodeficiency virus type 1 to restriction by rhesus TRIM5alpha. J Virol *82*, 11117-11128.

Ritter, G.D., Jr., Mulligan, M.J., Lydy, S.L., and Compans, R.W. (1993). Cell fusion activity of the simian immunodeficiency virus envelope protein is modulated by the intracytoplasmic domain. Virology *197*, 255-264.

Rittner, K., Churcher, M.J., Gait, M.J., and Karn, J. (1995). The human immunodeficiency virus long terminal repeat includes a specialised initiator element which is required for Tat-responsive transcription. J Mol Biol *248*, 562-580.

Roa, A., Hayashi, F., Yang, Y., Lienlaf, M., Zhou, J., Shi, J., Watanabe, S., Kigawa, T., Yokoyama, S., Aiken, C.*, et al.* (2012). RING domain mutations uncouple TRIM5alpha restriction of HIV-1 from inhibition of reverse transcription and acceleration of uncoating. J Virol *86*, 1717-1727.

Robbez-Masson, L., Tie, C.H.C., Conde, L., Tunbak, H., Husovsky, C., Tchasovnikarova, I.A., Timms, R.T., Herrero, J., Lehner, P.J., and Rowe, H.M. (2018). The HUSH complex cooperates with TRIM28 to repress young retrotransposons and new genes. Genome Res *28*, 836-845.

Rodriguez, S.K., Sarr, A.D., MacNeil, A., Thakore-Meloni, S., Gueye-Ndiaye, A., Traore, I., Dia, M.C., Mboup, S., and Kanki, P.J. (2007). Comparison of heterologous neutralizing antibody responses of human immunodeficiency virus type 1 (HIV-1)- and HIV-2-infected Senegalese patients: distinct patterns of breadth and magnitude distinguish HIV-1 and HIV-2 infections. J Virol *81*, 5331-5338.

Rollason, R., Korolchuk, V., Hamilton, C., Schu, P., and Banting, G. (2007). Clathrin-mediated endocytosis of a lipid-raft-associated protein is mediated through a dual tyrosine motif. J Cell Sci *120*, 3850-3858.

Rosa, A., Chande, A., Ziglio, S., De Sanctis, V., Bertorelli, R., Goh, S.L., McCauley, S.M., Nowosielska, A., Antonarakis, S.E., Luban, J.*, et al.* (2015). HIV-1 Nef promotes infection by excluding SERINC5 from virion incorporation. Nature *526*, 212-217.

Rosen, O., Sharon, M., Quadt-Akabayov, S.R., and Anglister, J. (2006). Molecular switch for alternative conformations of the HIV-1 V3 region: implications for phenotype conversion. Proc Natl Acad Sci U S A *103*, 13950-13955.

Rossi, F., Gallina, A., and Milanesi, G. (1996). Nef-CD4 physical interaction sensed with the yeast two-hybrid system. Virology *217*, 397-403.

Rousso, I., Mixon, M.B., Chen, B.K., and Kim, P.S. (2000). Palmitoylation of the HIV-1 envelope glycoprotein is critical for viral infectivity. Proc Natl Acad Sci U S A *97*, 13523-13525.

Roux, P., Alfieri, C., Hrimech, M., Cohen, E.A., and Tanner, J.E. (2000). Activation of transcription factors NF-kappaB and NF-IL-6 by human immunodeficiency virus type 1 protein R (Vpr) induces interleukin-8 expression. J Virol *74*, 4658-4665.

Rowell, J.F., Ruff, A.L., Guarnieri, F.G., Staveley-O'Carroll, K., Lin, X., Tang, J., August, J.T., and Siliciano, R.F. (1995). Lysosome-associated membrane protein-1-mediated targeting of the HIV-1 envelope protein to an endosomal/lysosomal compartment enhances its presentation to MHC class II-restricted T cells. J Immunol *155*, 1818-1828.

Roy, N.H., Chan, J., Lambele, M., and Thali, M. (2013). Clustering and mobility of HIV-1 Env at viral assembly sites predict its propensity to induce cell-cell fusion. J Virol *87*, 7516-7525.

Rudicell, R.S., Kwon, Y.D., Ko, S.Y., Pegu, A., Louder, M.K., Georgiev, I.S., Wu, X., Zhu, J., Boyington, J.C., Chen, X.*, et al.* (2014). Enhanced potency of a broadly neutralizing HIV-1 antibody in vitro improves protection against lentiviral infection in vivo. J Virol *88*, 12669-12682.

Rudnicka, D., Feldmann, J., Porrot, F., Wietgrefe, S., Guadagnini, S., Prevost, M.C., Estaquier, J., Haase, A.T., Sol-Foulon, N., and Schwartz, O. (2009). Simultaneous cell-to-cell transmission of human immunodeficiency virus to multiple targets through polysynapses. J Virol *83*, 6234-6246.

Russell, R.A., Martin, N., Mitar, I., Jones, E., and Sattentau, Q.J. (2013). Multiple proviral integration events after virological synapse-mediated HIV-1 spread. Virology *443*, 143-149.

Saad, J.S., Miller, J., Tai, J., Kim, A., Ghanam, R.H., and Summers, M.F. (2006). Structural basis for targeting HIV-1 Gag proteins to the plasma membrane for virus assembly. Proc Natl Acad Sci U S A *103*, 11364-11369.

Sagar, M., Kirkegaard, E., Lavreys, L., and Overbaugh, J. (2006). Diversity in HIV-1 envelope V1-V3 sequences early in infection reflects sequence diversity throughout the HIV-1 genome but does not predict the extent of sequence diversity during chronic infection. AIDS Res Hum Retroviruses *22*, 430-437.

Saha, K., Yan, H., Nelson, J.A., and Zerhouni-Layachi, B. (2005). Infection of human and non-human cells by a highly fusogenic primary CD4-independent HIV-1 isolate with a truncated envelope cytoplasmic tail. Virology *337*, 30-44.

Saksela, K., and Baltimore, D. (1993). Negative regulation of immunoglobulin kappa light-chain gene transcription by a short sequence homologous to the murine B1 repetitive element. Mol Cell Biol *13*, 3698-3705.

Sallman Almen, M., Bringeland, N., Fredriksson, R., and Schioth, H.B. (2012). The dispanins: a novel gene family of ancient origin that contains 14 human members. PLoS One *7*, e31961.

Sanders, R.W., and Moore, J.P. (2017). Native-like Env trimers as a platform for HIV-1 vaccine design. Immunol Rev *275*, 161-182.

Sanders, R.W., Vesanen, M., Schuelke, N., Master, A., Schiffner, L., Kalyanaraman, R., Paluch, M., Berkhout, B., Maddon, P.J., Olson, W.C*., et al.* (2002). Stabilization of the soluble, cleaved, trimeric form of the envelope glycoprotein complex of human immunodeficiency virus type 1. J Virol *76*, 8875-8889.

Sandgren, K.J., Smed-Sorensen, A., Forsell, M.N., Soldemo, M., Adams, W.C., Liang, F., Perbeck, L., Koup, R.A., Wyatt, R.T., Karlsson Hedestam, G.B*., et al.* (2013). Human plasmacytoid dendritic cells efficiently capture HIV-1 envelope glycoproteins via CD4 for antigen presentation. J Immunol *191*, 60-69.

Santos da Silva, E., Mulinge, M., and Perez Bercoff, D. (2013). The frantic play of the concealed HIV envelope cytoplasmic tail. Retrovirology *10*, 54.

Sato, H., Orenstein, J., Dimitrov, D., and Martin, M. (1992). Cell-to-cell spread of HIV-1 occurs within minutes and may not involve the participation of virus particles. Virology *186*, 712-724.

Sato, K., Takeuchi, J.S., Misawa, N., Izumi, T., Kobayashi, T., Kimura, Y., Iwami, S., Takaori-Kondo, A., Hu, W.S., Aihara, K*., et al.* (2014). APOBEC3D and APOBEC3F potently promote HIV-1 diversification and evolution in humanized mouse model. PLoS Pathog *10*, e1004453.

Sauter, D., Hotter, D., Van Driessche, B., Sturzel, C.M., Kluge, S.F., Wildum, S., Yu, H., Baumann, B., Wirth, T., Plantier, J.C*., et al.* (2015). Differential regulation of NF-kappaB-mediated proviral and antiviral host gene expression by primate lentiviral Nef and Vpu proteins. Cell Rep *10*, 586-599.

Sauter, D., and Kirchhoff, F. (2019). Key Viral Adaptations Preceding the AIDS Pandemic. Cell Host Microbe *25*, 27-38.

Sauter, D., Schindler, M., Specht, A., Landford, W.N., Munch, J., Kim, K.A., Votteler, J., Schubert, U., Bibollet-Ruche, F., Keele, B.F*., et al.* (2009). Tetherin-driven adaptation of Vpu and Nef function and the evolution of pandemic and nonpandemic HIV-1 strains. Cell Host Microbe *6*, 409-421.

Sayah, D.M., Sokolskaja, E., Berthoux, L., and Luban, J. (2004). Cyclophilin A retrotransposition into TRIM5 explains owl monkey resistance to HIV-1. Nature *430*, 569-573.

Schacker, T., Little, S., Connick, E., Gebhard-Mitchell, K., Zhang, Z.Q., Krieger, J., Pryor, J., Havlir, D., Wong, J.K., Richman, D*., et al.* (2000). Rapid accumulation of human immunodeficiency virus (HIV) in lymphatic tissue reservoirs during acute and early HIV infection: implications for timing of antiretroviral therapy. J Infect Dis *181*, 354-357.

Schaefer, T.M., Bell, I., Fallert, B.A., and Reinhart, T.A. (2000). The T-cell receptor zeta chain contains two homologous domains with which simian immunodeficiency virus Nef interacts and mediates down-modulation. J Virol *74*, 3273-3283.

Schaller, T., Ocwieja, K.E., Rasaiyaah, J., Price, A.J., Brady, T.L., Roth, S.L., Hue, S., Fletcher, A.J., Lee, K., KewalRamani, V.N*., et al.* (2011). HIV-1 capsid-cyclophilin interactions determine nuclear import pathway, integration targeting and replication efficiency. PLoS Pathog *7*, e1002439.

Schindler, M., Munch, J., Kutsch, O., Li, H., Santiago, M.L., Bibollet-Ruche, F., Muller-Trutwin, M.C., Novembre, F.J., Peeters, M., Courgnaud, V*., et al.* (2006). Nef-mediated suppression of T cell activation was lost in a lentiviral lineage that gave rise to HIV-1. Cell *125*, 1055-1067.

Schmidt, S., Fritz, J.V., Bitzegeio, J., Fackler, O.T., and Keppler, O.T. (2011). HIV-1 Vpu blocks recycling and biosynthetic transport of the intrinsic immunity factor CD317/tetherin to overcome the virion release restriction. mBio *2*, e00036-00011.

Schroder, A.R., Shinn, P., Chen, H., Berry, C., Ecker, J.R., and Bushman, F. (2002). HIV-1 integration in the human genome favors active genes and local hotspots. Cell *110*, 521-529.

Schrofelbauer, B., Chen, D., and Landau, N.R. (2004). A single amino acid of APOBEC3G controls its species-specific interaction with virion infectivity factor (Vif). Proc Natl Acad Sci U S A *101*, 3927-3932.

Schubert, H.L., Zhai, Q., Sandrin, V., Eckert, D.M., Garcia-Maya, M., Saul, L., Sundquist, W.I., Steiner, R.A., and Hill, C.P. (2010). Structural and functional studies on the extracellular domain of BST2/tetherin in reduced and oxidized conformations. Proc Natl Acad Sci U S A *107*, 17951-17956.

Schubert, U., Anton, L.C., Bacik, I., Cox, J.H., Bour, S., Bennink, J.R., Orlowski, M., Strebel, K., and Yewdell, J.W. (1998). CD4 glycoprotein degradation induced by human immunodeficiency virus type 1 Vpu protein requires the function of proteasomes and the ubiquitin-conjugating pathway. J Virol *72*, 2280-2288.

Schulte, B., Buffone, C., Opp, S., Di Nunzio, F., De Souza Aranha Vieira, D.A., Brandariz-Nunez, A., and Diaz-Griffero, F. (2015). Restriction of HIV-1 Requires the N-Terminal Region of MxB as a Capsid-Binding Motif but Not as a Nuclear Localization Signal. J Virol *89*, 8599-8610.

Schulte, B., Selyutina, A., Opp, S., Herschhorn, A., Sodroski, J.G., Pizzato, M., and Diaz-Griffero, F. (2018). Localization to detergent-resistant membranes and HIV-1 core entry inhibition correlate with HIV-1 restriction by SERINC5. Virology *515*, 52-65.

Schultz, A., and Rein, A. (1985). Maturation of murine leukemia virus env proteins in the absence of other viral proteins. Virology *145*, 335-339.

Schwartz, E.L., Brechbuhl, A.B., Kahl, P., Miller, M.A., Selwyn, P.A., and Friedland, G.H. (1992). Pharmacokinetic interactions of zidovudine and methadone in intravenous drug-using patients with HIV infection. J Acquir Immune Defic Syndr (1988) *5*, 619-626.

Schwartz, S., Felber, B.K., Fenyo, E.M., and Pavlakis, G.N. (1990). Env and Vpu proteins of human immunodeficiency virus type 1 are produced from multiple bicistronic mRNAs. J Virol *64*, 5448-5456.

Schwefel, D., Groom, H.C., Boucherit, V.C., Christodoulou, E., Walker, P.A., Stoye, J.P., Bishop, K.N., and Taylor, I.A. (2014). Structural basis of lentiviral subversion of a cellular protein degradation pathway. Nature *505*, 234-238.

Scourfield, E.J., and Martin-Serrano, J. (2017). Growing functions of the ESCRT machinery in cell biology and viral replication. Biochem Soc Trans *45*, 613-634.

Seaman, M.N. (2004). Cargo-selective endosomal sorting for retrieval to the Golgi requires retromer. J Cell Biol *165*, 111-122.

Seaman, M.N. (2012). The retromer complex - endosomal protein recycling and beyond. J Cell Sci *125*, 4693-4702.

Seaman, M.S., Janes, H., Hawkins, N., Grandpre, L.E., Devoy, C., Giri, A., Coffey, R.T., Harris, L., Wood, B., Daniels, M.G.*, et al.* (2010). Tiered categorization of a diverse panel of HIV-1 Env pseudoviruses for assessment of neutralizing antibodies. J Virol *84*, 1439-1452.

Sebastian, S., and Luban, J. (2005). TRIM5alpha selectively binds a restriction-sensitive retroviral capsid. Retrovirology *2*, 40.

Seligmann, M., Aractingi, S., Oksenhendler, E., Rabian, C., Ferchal, F., and Gonnot, G. (1991). CD4+ lymphocytopenia without HIV in patient with cryptococcal disease. Lancet *337*, 57-58.

Serra-Moreno, R., Zimmermann, K., Stern, L.J., and Evans, D.T. (2013). Tetherin/BST-2 antagonism by Nef depends on a direct physical interaction between Nef and tetherin, and on clathrin-mediated endocytosis. PLoS Pathog *9*, e1003487.

Sewald, X., Gonzalez, D.G., Haberman, A.M., and Mothes, W. (2012). In vivo imaging of virological synapses. Nat Commun *3*, 1320.

Sewald, X., Ladinsky, M.S., Uchil, P.D., Beloor, J., Pi, R., Herrmann, C., Motamedi, N., Murooka, T.T., Brehm, M.A., Greiner, D.L.*, et al.* (2015). Retroviruses use CD169-mediated trans-infection of permissive lymphocytes to establish infection. Science *350*, 563-567.

Shah, V.B., Shi, J., Hout, D.R., Oztop, I., Krishnan, L., Ahn, J., Shotwell, M.S., Engelman, A., and Aiken, C. (2013). The host proteins transportin SR2/TNPO3 and cyclophilin A exert opposing effects on HIV-1 uncoating. J Virol *87*, 422-432.

Shaik, M.M., Peng, H., Lu, J., Rits-Volloch, S., Xu, C., Liao, M., and Chen, B. (2019). Structural basis of coreceptor recognition by HIV-1 envelope spike. Nature *565*, 318-323.

Sharp, P.M., and Hahn, B.H. (2011). Origins of HIV and the AIDS pandemic. Cold Spring Harb Perspect Med *1*, a006841.

Shaw, G.M., and Hunter, E. (2012). HIV transmission. Cold Spring Harb Perspect Med *2*.

Sheehy, A.M., Gaddis, N.C., and Malim, M.H. (2003). The antiretroviral enzyme APOBEC3G is degraded by the proteasome in response to HIV-1 Vif. Nat Med *9*, 1404-1407.

Shen, Q.T., Schuh, A.L., Zheng, Y., Quinney, K., Wang, L., Hanna, M., Mitchell, J.C., Otegui, M.S., Ahlquist, P., Cui, Q.*, et al.* (2014). Structural analysis and modeling reveals new mechanisms governing ESCRT-III spiral filament assembly. J Cell Biol *206*, 763-777.

Sherer, N.M., Lehmann, M.J., Jimenez-Soto, L.F., Horensavitz, C., Pypaert, M., and Mothes, W. (2007). Retroviruses can establish filopodial bridges for efficient cell-to-cell transmission. Nat Cell Biol *9*, 310-315.

Sherrill-Mix, S., Lewinski, M.K., Famiglietti, M., Bosque, A., Malani, N., Ocwieja, K.E., Berry, C.C., Looney, D., Shan, L., Agosto, L.M.*, et al.* (2013). HIV latency and integration site placement in five cell-based models. Retrovirology *10*, 90.

Shi, G., Kenney, A.D., Kudryashova, E., Zani, A., Zhang, L., Lai, K.K., Hall-Stoodley, L., Robinson, R.T., Kudryashov, D.S., Compton, A.A.*, et al.* (2021). Opposing activities of IFITM proteins in SARS-CoV-2 infection. EMBO J *40*, e106501.

Shi, J., and Aiken, C. (2006). Saturation of TRIM5 alpha-mediated restriction of HIV-1 infection depends on the stability of the incoming viral capsid. Virology *350*, 493-500.

Shi, J., Xiong, R., Zhou, T., Su, P., Zhang, X., Qiu, X., Li, H., Li, S., Yu, C., Wang, B.*, et al.* (2018). HIV-1 Nef Antagonizes SERINC5 Restriction by Downregulation of SERINC5 via the Endosome/Lysosome System. J Virol *92*.

Shi, Y., Brandin, E., Vincic, E., Jansson, M., Blaxhult, A., Gyllensten, K., Moberg, L., Brostrom, C., Fenyo, E.M., and Albert, J. (2005). Evolution of human immunodeficiency virus type 2 coreceptor usage, autologous neutralization, envelope sequence and glycosylation. J Gen Virol *86*, 3385-3396.

Shimizu, H., Morikawa, S., Yamaguchi, K., Tsuchie, H., Hachimori, K., Ushijima, H., and Kitamura, T. (1990). Shorter size of transmembrane glycoprotein of an HIV-1 isolate. AIDS *4*, 575-576.

Shu, W., Liu, J., Ji, H., Radigen, L., Jiang, S., and Lu, M. (2000). Helical interactions in the HIV-1 gp41 core reveal structural basis for the inhibitory activity of gp41 peptides. Biochemistry *39*, 1634-1642.

Sigal, A., Kim, J.T., Balazs, A.B., Dekel, E., Mayo, A., Milo, R., and Baltimore, D. (2011). Cell-to-cell spread of HIV permits ongoing replication despite antiretroviral therapy. Nature *477*, 95-98.

Siliciano, J.D., Kajdas, J., Finzi, D., Quinn, T.C., Chadwick, K., Margolick, J.B., Kovacs, C., Gange, S.J., and Siliciano, R.F. (2003). Long-term follow-up studies confirm the stability of the latent reservoir for HIV-1 in resting CD4+ T cells. Nat Med *9*, 727-728.

Siliciano, R.F., and Greene, W.C. (2011). HIV latency. Cold Spring Harb Perspect Med *1*, a007096.

Silvestri, G., Sodora, D.L., Koup, R.A., Paiardini, M., O'Neil, S.P., McClure, H.M., Staprans, S.I., and Feinberg, M.B. (2003). Nonpathogenic SIV infection of sooty mangabeys is characterized by limited bystander immunopathology despite chronic high-level viremia. Immunity *18*, 441-452.

Simon, F., Mauclere, P., Roques, P., Loussert-Ajaka, I., Muller-Trutwin, M.C., Saragosti, S., Georges-Courbot, M.C., Barre-Sinoussi, F., and Brun-Vezinet, F. (1998). Identification of a new human immunodeficiency virus type 1 distinct from group M and group O. Nat Med *4*, 1032-1037.

Skasko, M., Wang, Y., Tian, Y., Tokarev, A., Munguia, J., Ruiz, A., Stephens, E.B., Opella, S.J., and Guatelli, J. (2012). HIV-1 Vpu protein antagonizes innate restriction factor BST-2 via lipid-embedded helix-helix interactions. J Biol Chem *287*, 58-67.

Smalls-Mantey, A., Connors, M., and Sattentau, Q.J. (2013). Comparative efficiency of HIV-1-infected T cell killing by NK cells, monocytes and neutrophils. PLoS One *8*, e74858.

Smed-Sorensen, A., Lore, K., Vasudevan, J., Louder, M.K., Andersson, J., Mascola, J.R., Spetz, A.L., and Koup, R.A. (2005). Differential susceptibility to human immunodeficiency virus type 1 infection of myeloid and plasmacytoid dendritic cells. J Virol *79*, 8861-8869.

Smith, J.S., and Roth, M.J. (1992). Specificity of human immunodeficiency virus-1 reverse transcriptase-associated ribonuclease H in removal of the minus-strand primer, tRNA(Lys3). J Biol Chem *267*, 15071-15079.

Sok, D., Doores, K.J., Briney, B., Le, K.M., Saye-Francisco, K.L., Ramos, A., Kulp, D.W., Julien, J.P., Menis, S., Wickramasinghe, L.*, et al.* (2014). Promiscuous glycan site recognition by antibodies to the high-mannose patch of gp120 broadens neutralization of HIV. Sci Transl Med *6*, 236ra263.

Sol-Foulon, N., Sourisseau, M., Porrot, F., Thoulouze, M.I., Trouillet, C., Nobile, C., Blanchet, F., di Bartolo, V., Noraz, N., Taylor, N.*, et al.* (2007). ZAP-70 kinase regulates HIV cell-to-cell spread and virological synapse formation. EMBO J *26*, 516-526.

Sood, C., Marin, M., Chande, A., Pizzato, M., and Melikyan, G.B. (2017). SERINC5 protein inhibits HIV-1 fusion pore formation by promoting functional inactivation of envelope glycoproteins. J Biol Chem *292*, 6014-6026.

Soriano, V., Gomes, P., Heneine, W., Holguin, A., Doruana, M., Antunes, R., Mansinho, K., Switzer, W.M., Araujo, C., Shanmugam, V.*, et al.* (2000). Human immunodeficiency virus type 2 (HIV-2) in Portugal: clinical spectrum, circulating subtypes, virus isolation, and plasma viral load. J Med Virol *61*, 111-116.

Sourisseau, M., Sol-Foulon, N., Porrot, F., Blanchet, F., and Schwartz, O. (2007). Inefficient human immunodeficiency virus replication in mobile lymphocytes. J Virol *81*, 1000-1012.

Sowinski, S., Jolly, C., Berninghausen, O., Purbhoo, M.A., Chauveau, A., Kohler, K., Oddos, S., Eissmann, P., Brodsky, F.M., Hopkins, C.*, et al.* (2008). Membrane nanotubes physically connect T cells over long distances presenting a novel route for HIV-1 transmission. Nat Cell Biol *10*, 211-219.

Spies, C.P., Ritter, G.D., Jr., Mulligan, M.J., and Compans, R.W. (1994). Truncation of the cytoplasmic domain of the simian immunodeficiency virus envelope glycoprotein alters the conformation of the external domain. J Virol *68*, 585-591.

Srivastava, S., Swanson, S.K., Manel, N., Florens, L., Washburn, M.P., and Skowronski, J. (2008). Lentiviral Vpx accessory factor targets VprBP/DCAF1 substrate adaptor for cullin 4 E3 ubiquitin ligase to enable macrophage infection. PLoS Pathog *4*, e1000059.

St Clair, M.H., Richards, C.A., Spector, T., Weinhold, K.J., Miller, W.H., Langlois, A.J., and Furman, P.A. (1987). 3'-Azido-3'-deoxythymidine triphosphate as an inhibitor and substrate of purified human immunodeficiency virus reverse transcriptase. Antimicrob Agents Chemother *31*, 1972-1977.

Starling, S., and Jolly, C. (2016). LFA-1 Engagement Triggers T Cell Polarization at the HIV-1 Virological Synapse. J Virol *90*, 9841-9854.

Stavrou, S., Blouch, K., Kotla, S., Bass, A., and Ross, S.R. (2015). Nucleic acid recognition orchestrates the anti-viral response to retroviruses. Cell Host Microbe *17*, 478-488.

Stejskal, L., Kalemera, M.D., Palor, M., Walker, L., Daviter, T., Lees, W.D., Moss, D.S., Kremyda-Vlachou, M., Kozlakidis, Z., Rosenberg, W.*, et al.* (2020). An Entropic Safety Catch Controls Hepatitis C Virus Entry and Antibody Resistance. bioRxiv, 2020.2011.2011.377218.

Stevenson, M., Haggerty, S., Lamonica, C.A., Meier, C.M., Welch, S.K., and Wasiak, A.J. (1990). Integration is not necessary for expression of human immunodeficiency virus type 1 protein products. J Virol *64*, 2421-2425.

Stewart-Jones, G.B., Soto, C., Lemmin, T., Chuang, G.Y., Druz, A., Kong, R., Thomas, P.V., Wagh, K., Zhou, T., Behrens, A.J.*, et al.* (2016). Trimeric HIV-1-Env Structures Define Glycan Shields from Clades A, B, and G. Cell *165*, 813-826.

Stoneham, C.A., Singh, R., Jia, X., Xiong, Y., and Guatelli, J. (2017). Endocytic activity of HIV-1 Vpu: Phosphoserine-dependent interactions with clathrin adaptors. Traffic *18*, 545-561.

Stremlau, M., Owens, C.M., Perron, M.J., Kiessling, M., Autissier, P., and Sodroski, J. (2004). The cytoplasmic body component TRIM5alpha restricts HIV-1 infection in Old World monkeys. Nature *427*, 848-853.

Stremlau, M., Perron, M., Lee, M., Li, Y., Song, B., Javanbakht, H., Diaz-Griffero, F., Anderson, D.J., Sundquist, W.I., and Sodroski, J. (2006). Specific recognition and accelerated uncoating of retroviral capsids by the TRIM5alpha restriction factor. Proc Natl Acad Sci U S A *103*, 5514-5519.

Sullivan, N., Sun, Y., Sattentau, Q., Thali, M., Wu, D., Denisova, G., Gershoni, J., Robinson, J., Moore, J., and Sodroski, J. (1998). CD4-Induced conformational changes in the human immunodeficiency virus type 1 gp120 glycoprotein: consequences for virus entry and neutralization. J Virol *72*, 4694-4703.

Sumner, R.P., Thorne, L.G., Fink, D.L., Khan, H., Milne, R.S., and Towers, G.J. (2017). Are Evolution and the Intracellular Innate Immune System Key Determinants in HIV Transmission? Front Immunol *8*, 1246.

Sun, S.C. (2011). Non-canonical NF-kappaB signaling pathway. Cell Res *21*, 71-85.

Sun, S.C. (2017). The non-canonical NF-kappaB pathway in immunity and inflammation. Nat Rev Immunol *17*, 545-558.

Swarbrick, J.D., Shaw, D.J., Chhabra, S., Ghai, R., Valkov, E., Norwood, S.J., Seaman, M.N., and Collins, B.M. (2011). VPS29 is not an active metallo-phosphatase but is a rigid scaffold required for retromer interaction with accessory proteins. PLoS One *6*, e20420.

Swingler, S., Brichacek, B., Jacque, J. M., Ulich, C., Zhou, J., & Stevenson, M. (2003). HIV-1 Nef intersects the macrophage CD40L signalling pathway to promote resting-cell infection. *Nature*, *424*(6945), 213–219.

Swiggard, W.J., Baytop, C., Yu, J.J., Dai, J., Li, C., Schretzenmair, R., Theodosopoulos, T., and O'Doherty, U. (2005). Human immunodeficiency virus type 1 can establish latent infection in resting CD4+ T cells in the absence of activating stimuli. J Virol *79*, 14179-14188.

Swigut, T., Greenberg, M., and Skowronski, J. (2003). Cooperative interactions of simian immunodeficiency virus Nef, AP-2, and CD3-zeta mediate the selective induction of T-cell receptor-CD3 endocytosis. J Virol *77*, 8116-8126.

Tabuchi, M., Yanatori, I., Kawai, Y., and Kishi, F. (2010). Retromer-mediated direct sorting is required for proper endosomal recycling of the mammalian iron transporter DMT1. J Cell Sci *123*, 756-766.

Tada, T., Zhang, Y., Koyama, T., Tobiume, M., Tsunetsugu-Yokota, Y., Yamaoka, S., Fujita, H., and Tokunaga, K. (2015). MARCH8 inhibits HIV-1 infection by reducing virion incorporation of envelope glycoproteins. Nat Med *21*, 1502-1507.

Tartour, K., Appourchaux, R., Gaillard, J., Nguyen, X.N., Durand, S., Turpin, J., Beaumont, E., Roch, E., Berger, G., Mahieux, R*., et al.* (2014). IFITM proteins are incorporated onto HIV-1 virion particles and negatively imprint their infectivity. Retrovirology *11*, 103.

Taylor, G.M., and Sanders, D.A. (2003). Structural criteria for regulation of membrane fusion and virion incorporation by the murine leukemia virus TM cytoplasmic domain. Virology *312*, 295-305.

Tchasovnikarova, I.A., Timms, R.T., Douse, C.H., Roberts, R.C., Dougan, G., Kingston, R.E., Modis, Y., and Lehner, P.J. (2017). Hyperactivation of HUSH complex function by Charcot-Marie-Tooth disease mutation in MORC2. Nat Genet *49*, 1035-1044.

Tchasovnikarova, I.A., Timms, R.T., Matheson, N.J., Wals, K., Antrobus, R., Gottgens, B., Dougan, G., Dawson, M.A., and Lehner, P.J. (2015). GENE SILENCING. Epigenetic silencing by the HUSH complex mediates position-effect variegation in human cells. Science *348*, 1481-1485.

Tedbury, P.R., Ablan, S.D., and Freed, E.O. (2013). Global rescue of defects in HIV-1 envelope glycoprotein incorporation: implications for matrix structure. PLoS Pathog *9*, e1003739.

Tedbury, P.R., Novikova, M., Ablan, S.D., and Freed, E.O. (2016). Biochemical evidence of a role for matrix trimerization in HIV-1 envelope glycoprotein incorporation. Proc Natl Acad Sci U S A *113*, E182-190.

Temkin, P., Lauffer, B., Jager, S., Cimermancic, P., Krogan, N.J., and von Zastrow, M. (2011). SNX27 mediates retromer tubule entry and endosome-to-plasma membrane trafficking of signalling receptors. Nat Cell Biol *13*, 715-721.

Thiebaut, R., Matheron, S., Taieb, A., Brun-Vezinet, F., Chene, G., Autran, B., and immunology group of the, A.C.O.H.I.V.c. (2011). Long-term nonprogressors and elite controllers in the ANRS CO5 HIV-2 cohort. AIDS *25*, 865-867.

Thimon, V., Belghazi, M., Dacheux, J.L., and Gatti, J.L. (2006). Analysis of furin ectodomain shedding in epididymal fluid of mammals: demonstration that shedding of furin occurs in vivo. Reproduction *132*, 899-908.

Titanji, B.K., Aasa-Chapman, M., Pillay, D., and Jolly, C. (2013). Protease inhibitors effectively block cell-to-cell spread of HIV-1 between T cells. Retrovirology *10*, 161.

Titanji, B.K., Pillay, D., and Jolly, C. (2017). Combination antiretroviral therapy and cell-cell spread of wild-type and drug-resistant human immunodeficiency virus-1. J Gen Virol *98*, 821-834.

Tokarev, A., Suarez, M., Kwan, W., Fitzpatrick, K., Singh, R., and Guatelli, J. (2013). Stimulation of NF-kappaB activity by the HIV restriction factor BST2. J Virol *87*, 2046-2057.

Tokarev, A.A., Munguia, J., and Guatelli, J.C. (2011). Serine-threonine ubiquitination mediates downregulation of BST-2/tetherin and relief of restricted virion release by HIV-1 Vpu. J Virol *85*, 51-63.

Tokunaga, K., Kojima, A., Kurata, T., Ikuta, K., Akari, H., Koyama, A.H., Kawamura, M., Inubushi, R., Shimano, R., and Adachi, A. (1998). Enhancement of human immunodeficiency virus type 1 infectivity by Nef is producer cell-dependent. J Gen Virol *79 (Pt 10)*, 2447-2453.

Towers, G.J., Hatziioannou, T., Cowan, S., Goff, S.P., Luban, J., and Bieniasz, P.D. (2003). Cyclophilin A modulates the sensitivity of HIV-1 to host restriction factors. Nat Med *9*, 1138-1143.

Tran, E.E., Borgnia, M.J., Kuybeda, O., Schauder, D.M., Bartesaghi, A., Frank, G.A., Sapiro, G., Milne, J.L., and Subramaniam, S. (2012). Structural mechanism of trimeric HIV-1 envelope glycoprotein activation. PLoS Pathog *8*, e1002797.

Trautz, B., Pierini, V., Wombacher, R., Stolp, B., Chase, A.J., Pizzato, M., and Fackler, O.T. (2016). The Antagonism of HIV-1 Nef to SERINC5 Particle Infectivity Restriction Involves the Counteraction of Virion-Associated Pools of the Restriction Factor. J Virol *90*, 10915-10927.

Trickey, A., May, M.T., and Sterne, J.A. (2017). Methodological and statistical issues related to analysis of survival - Authors' reply. Lancet HIV *4*, e330.

Tristem, M., Hill, F., and Karpas, A. (1991). Nucleotide sequence of a Guinea-Bissau-derived human immunodeficiency virus type 2 proviral clone (HIV-2CAM2). J Gen Virol *72 (Pt 3)*, 721-724.

Tristem, M., Marshall, C., Karpas, A., Petrik, J., and Hill, F. (1990). Origin of vpx in lentiviruses. Nature *347*, 341-342.

Tsujimoto, H., Cooper, R.W., Kodama, T., Fukasawa, M., Miura, T., Ohta, Y., Ishikawa, K., Nakai, M., Frost, E., Roelants, G.E.*, et al.* (1988). Isolation and characterization of simian immunodeficiency virus from mandrills in Africa and its relationship to other human and simian immunodeficiency viruses. J Virol *62*, 4044-4050.

Tully, D.C., Ogilvie, C.B., Batorsky, R.E., Bean, D.J., Power, K.A., Ghebremichael, M., Bedard, H.E., Gladden, A.D., Seese, A.M., Amero, M.A.*, et al.* (2016). Differences in the Selection Bottleneck between Modes of Sexual Transmission Influence the Genetic Composition of the HIV-1 Founder Virus. PLoS Pathog *12*, e1005619.

Tunbak, H., Enriquez-Gasca, R., Tie, C.H.C., Gould, P.A., Mlcochova, P., Gupta, R.K., Fernandes, L., Holt, J., van der Veen, A.G., Giampazolias, E.*, et al.* (2020). The HUSH complex is a gatekeeper of type I interferon through epigenetic regulation of LINE-1s. Nat Commun *11*, 5387.

Turville, S.G., Cameron, P.U., Handley, A., Lin, G., Pohlmann, S., Doms, R.W., and Cunningham, A.L. (2002). Diversity of receptors binding HIV on dendritic cell subsets. Nat Immunol *3*, 975-983.

Turville, S.G., Santos, J.J., Frank, I., Cameron, P.U., Wilkinson, J., Miranda-Saksena, M., Dable, J., Stossel, H., Romani, N., Piatak, M., Jr.*, et al.* (2004). Immunodeficiency virus uptake, turnover, and 2-phase transfer in human dendritic cells. Blood *103*, 2170-2179.

Usami, Y., and Gottlinger, H. (2013). HIV-1 Nef responsiveness is determined by Env variable regions involved in trimer association and correlates with neutralization sensitivity. Cell Rep *5*, 802-812.

Usami, Y., Wu, Y., and Gottlinger, H.G. (2015). SERINC3 and SERINC5 restrict HIV-1 infectivity and are counteracted by Nef. Nature *526*, 218-223.

Vallejos, M., Carvajal, F., Pino, K., Navarrete, C., Ferres, M., Huidobro-Toro, J.P., Sargueil, B., and Lopez-Lastra, M. (2012). Functional and structural analysis of the internal ribosome entry site present in the mRNA of natural variants of the HIV-1. PLoS One *7*, e35031.

Van Damme, N., Goff, D., Katsura, C., Jorgenson, R.L., Mitchell, R., Johnson, M.C., Stephens, E.B., and Guatelli, J. (2008). The interferon-induced protein BST-2 restricts HIV-1 release and is downregulated from the cell surface by the viral Vpu protein. Cell Host Microbe *3*, 245-252.

van der Loeff, M.F., Awasana, A.A., Sarge-Njie, R., van der Sande, M., Jaye, A., Sabally, S., Corrah, T., McConkey, S.J., and Whittle, H.C. (2006). Sixteen years of HIV surveillance in a West African research clinic reveals divergent epidemic trends of HIV-1 and HIV-2. Int J Epidemiol *35*, 1322-1328.

van der Loeff, M.F., Larke, N., Kaye, S., Berry, N., Ariyoshi, K., Alabi, A., van Tienen, C., Leligdowicz, A., Sarge-Njie, R., da Silva, Z.*, et al.* (2010). Undetectable plasma viral load predicts normal survival in HIV-2-infected people in a West African village. Retrovirology *7*, 46.

Van Engelenburg, S.B., Shtengel, G., Sengupta, P., Waki, K., Jarnik, M., Ablan, S.D., Freed, E.O., Hess, H.F., and Lippincott-Schwartz, J. (2014). Distribution of ESCRT machinery at HIV assembly sites reveals virus scaffolding of ESCRT subunits. Science *343*, 653-656.

Veillette, M., Coutu, M., Richard, J., Batraville, L.A., Dagher, O., Bernard, N., Tremblay, C., Kaufmann, D.E., Roger, M., and Finzi, A. (2015). The HIV-1 gp120 CD4-bound conformation is preferentially targeted by antibody-dependent cellular cytotoxicity-mediating antibodies in sera from HIV-1-infected individuals. J Virol *89*, 545-551.

Veillette, M., Desormeaux, A., Medjahed, H., Gharsallah, N.E., Coutu, M., Baalwa, J., Guan, Y., Lewis, G., Ferrari, G., Hahn, B.H.*, et al.* (2014). Interaction with cellular CD4 exposes HIV-1 envelope epitopes targeted by antibody-dependent cell-mediated cytotoxicity. J Virol *88*, 2633-2644.

Venkatesh, S., and Bieniasz, P.D. (2013). Mechanism of HIV-1 virion entrapment by tetherin. PLoS Pathog *9*, e1003483.

VerPlank, L., Bouamr, F., LaGrassa, T.J., Agresta, B., Kikonyogo, A., Leis, J., and Carter, C.A. (2001). Tsg101, a homologue of ubiquitin-conjugating (E2) enzymes, binds the L domain in HIV type 1 Pr55(Gag). Proc Natl Acad Sci U S A *98*, 7724-7729.

Vigan, R., and Neil, S.J. (2010). Determinants of tetherin antagonism in the transmembrane domain of the human immunodeficiency virus type 1 Vpu protein. J Virol *84*, 12958-12970.

Visseaux, B., Damond, F., Matheron, S., Descamps, D., and Charpentier, C. (2016). Hiv-2 molecular epidemiology. Infect Genet Evol *46*, 233-240.

von Appen, A., Kosinski, J., Sparks, L., Ori, A., DiGuilio, A.L., Vollmer, B., Mackmull, M.T., Banterle, N., Parca, L., Kastritis, P.*, et al.* (2015). In situ structural analysis of the human nuclear pore complex. Nature *526*, 140-143.

von Bredow, B., Arias, J.F., Heyer, L.N., Gardner, M.R., Farzan, M., Rakasz, E.G., and Evans, D.T. (2015). Envelope Glycoprotein Internalization Protects Human and Simian Immunodeficiency Virus-Infected Cells from Antibody-Dependent Cell-Mediated Cytotoxicity. J Virol *89*, 10648-10655.

von Bredow, B., Arias, J.F., Heyer, L.N., Moldt, B., Le, K., Robinson, J.E., Zolla-Pazner, S., Burton, D.R., and Evans, D.T. (2016). Comparison of Antibody-Dependent Cell-Mediated Cytotoxicity and Virus Neutralization by HIV-1 Env-Specific Monoclonal Antibodies. J Virol *90*, 6127-6139.

Vzorov, A.N., and Compans, R.W. (1996). Assembly and release of SIV env proteins with full-length or truncated cytoplasmic domains. Virology *221*, 22-33.

Vzorov, A.N., Gernert, K.M., and Compans, R.W. (2005). Multiple domains of the SIV Env protein determine virus replication efficiency and neutralization sensitivity. Virology *332*, 89-101.

Wagner, J.M., Zadrozny, K.K., Chrustowicz, J., Purdy, M.D., Yeager, M., Ganser-Pornillos, B.K., and Pornillos, O. (2016). Crystal structure of an HIV assembly and maturation switch. Elife *5*.

Wang, H., Barnes, C.O., Yang, Z., Nussenzweig, M.C., and Bjorkman, P.J. (2018). Partially Open HIV-1 Envelope Structures Exhibit Conformational Changes Relevant for Coreceptor Binding and Fusion. Cell Host Microbe *24*, 579-592 e574.

Wang, L., Sandmeyer, A., Hübner, W., Li, H., Huser, T., and Chen, B.K. (2020). Recruitment of Env to the HIV-1 T cell virological synapse by targeted and sustained Env recycling. bioRxiv, 2020.2012.2008.417188.

Wang, Y., Pan, Q., Ding, S., Wang, Z., Yu, J., Finzi, A., Liu, S.L., and Liang, C. (2017). The V3 Loop of HIV-1 Env Determines Viral Susceptibility to IFITM3 Impairment of Viral Infectivity. J Virol *91*.

Ward, A.B., and Wilson, I.A. (2017). The HIV-1 envelope glycoprotein structure: nailing down a moving target. Immunol Rev *275*, 21-32.

Wei, P., Garber, M.E., Fang, S.M., Fischer, W.H., and Jones, K.A. (1998). A novel CDK9-associated C-type cyclin interacts directly with HIV-1 Tat and mediates its high-affinity, loop-specific binding to TAR RNA. Cell *92*, 451-462.

Wei, W., Guo, H., Ma, M., Markham, R., and Yu, X.F. (2016). Accumulation of MxB/Mx2-resistant HIV-1 Capsid Variants During Expansion of the HIV-1 Epidemic in Human Populations. EBioMedicine *8*, 230-236.

Wei, X., Decker, J.M., Liu, H., Zhang, Z., Arani, R.B., Kilby, J.M., Saag, M.S., Wu, X., Shaw, G.M., and Kappes, J.C. (2002). Emergence of resistant human immunodeficiency virus type 1 in patients receiving fusion inhibitor (T-20) monotherapy. Antimicrob Agents Chemother *46*, 1896-1905.

Wei, X., Decker, J.M., Wang, S., Hui, H., Kappes, J.C., Wu, X., Salazar-Gonzalez, J.F., Salazar, M.G., Kilby, J.M., Saag, M.S.*, et al.* (2003). Antibody neutralization and escape by HIV-1. Nature *422*, 307-312.

Welsch, S., Keppler, O.T., Habermann, A., Allespach, I., Krijnse-Locker, J., and Krausslich, H.G. (2007). HIV-1 buds predominantly at the plasma membrane of primary human macrophages. PLoS Pathog *3*, e36.

Welsch, S., Groot, F., Kräusslich, H. G., Keppler, O. T., & Sattentau, Q. J. (2011). Architecture and regulation of the HIV-1 assembly and holding compartment in macrophages. *Journal of virology*, *85*(15), 7922–7927.

Weng, J., Krementsov, D.N., Khurana, S., Roy, N.H., and Thali, M. (2009). Formation of syncytia is repressed by tetraspanins in human immunodeficiency virus type 1-producing cells. J Virol *83*, 7467-7474.

Weston, S., Czieso, S., White, I.J., Smith, S.E., Kellam, P., and Marsh, M. (2014). A membrane topology model for human interferon inducible transmembrane protein 1. PLoS One *9*, e104341.

Whitcomb, J.M., Kumar, R., and Hughes, S.H. (1990). Sequence of the circle junction of human immunodeficiency virus type 1: implications for reverse transcription and integration. J Virol *64*, 4903-4906.

White, E., Wu, F., Chertova, E., Bess, J., Roser, J.D., Lifson, J.D., and Hirsch, V.M. (2018). Truncating the gp41 Cytoplasmic Tail of Simian Immunodeficiency Virus Decreases Sensitivity to Neutralizing Antibodies without Increasing the Envelope Content of Virions. J Virol *92*.

Wildum, S., Schindler, M., Munch, J., and Kirchhoff, F. (2006). Contribution of Vpu, Env, and Nef to CD4 down-modulation and resistance of human immunodeficiency virus type 1-infected T cells to superinfection. J Virol *80*, 8047-8059.

Wilk, T., Pfeiffer, T., and Bosch, V. (1992). Retained in vitro infectivity and cytopathogenicity of HIV-1 despite truncation of the C-terminal tail of the env gene product. Virology *189*, 167-177.

Willey, R.L., Maldarelli, F., Martin, M.A., and Strebel, K. (1992). Human immunodeficiency virus type 1 Vpu protein induces rapid degradation of CD4. J Virol *66*, 7193-7200.

Williams, S.A., Kwon, H., Chen, L.F., and Greene, W.C. (2007). Sustained induction of NF-kappa B is required for efficient expression of latent human immunodeficiency virus type 1. J Virol *81*, 6043-6056.

Wlodawer, A., and Erickson, J.W. (1993). Structure-based inhibitors of HIV-1 protease. Annu Rev Biochem *62*, 543-585.

Wu, S.R., Sjoberg, M., Wallin, M., Lindqvist, B., Ekstrom, M., Hebert, H., Koeck, P.J., and Garoff, H. (2008). Turning of the receptor-binding domains opens up the murine leukaemia virus Env for membrane fusion. EMBO J *27*, 2799-2808.

Wu, W.L., Grotefend, C.R., Tsai, M.T., Wang, Y.L., Radic, V., Eoh, H., and Huang, I.C. (2017). Delta20 IFITM2 differentially restricts X4 and R5 HIV-1. Proc Natl Acad Sci U S A *114*, 7112-7117.

Wu, X., Anderson, J.L., Campbell, E.M., Joseph, A.M., and Hope, T.J. (2006). Proteasome inhibitors uncouple rhesus TRIM5alpha restriction of HIV-1 reverse transcription and infection. Proc Natl Acad Sci U S A *103*, 7465-7470.

Wu, Y., Olety, B., Weiss, E.R., Popova, E., Yamanaka, H., and Gottlinger, H. (2019). Potent Enhancement of HIV-1 Replication by Nef in the Absence of SERINC3 and SERINC5. mBio *10*.

Wyma, D.J., Jiang, J., Shi, J., Zhou, J., Lineberger, J.E., Miller, M.D., and Aiken, C. (2004). Coupling of human immunodeficiency virus type 1 fusion to virion maturation: a novel role of the gp41 cytoplasmic tail. J Virol *78*, 3429-3435.

Wyma, D.J., Kotov, A., and Aiken, C. (2000). Evidence for a stable interaction of gp41 with Pr55(Gag) in immature human immunodeficiency virus type 1 particles. J Virol *74*, 9381-9387.

Wyss, S., Berlioz-Torrent, C., Boge, M., Blot, G., Honing, S., Benarous, R., and Thali, M. (2001). The highly conserved C-terminal dileucine motif in the cytosolic domain of the human immunodeficiency virus type 1 envelope glycoprotein is critical for its association with the AP-1 clathrin adaptor [correction of adapter]. J Virol *75*, 2982-2992.

Wyss, S., Dimitrov, A.S., Baribaud, F., Edwards, T.G., Blumenthal, R., and Hoxie, J.A. (2005). Regulation of human immunodeficiency virus type 1 envelope glycoprotein fusion by a membrane-interactive domain in the gp41 cytoplasmic tail. J Virol *79*, 12231-12241.

Yamashita, M., and Emerman, M. (2006). Retroviral infection of non-dividing cells: old and new perspectives. Virology *344*, 88-93.

Yan, J., Kaur, S., DeLucia, M., Hao, C., Mehrens, J., Wang, C., Golczak, M., Palczewski, K., Gronenborn, A.M., Ahn, J.*, et al.* (2013). Tetramerization of SAMHD1 is required for biological activity and inhibition of HIV infection. J Biol Chem *288*, 10406-10417.

Yang, B., Chen, K., Zhang, C., Huang, S., and Zhang, H. (2007). Virion-associated uracil DNA glycosylase-2 and apurinic/apyrimidinic endonuclease are involved in the degradation of APOBEC3G-edited nascent HIV-1 DNA. J Biol Chem *282*, 11667-11675.

Yang, C., and Compans, R.W. (1996). Analysis of the cell fusion activities of chimeric simian immunodeficiency virus-murine leukemia virus envelope proteins: inhibitory effects of the R peptide. J Virol *70*, 248-254.

Yang, C., and Compans, R.W. (1997). Analysis of the murine leukemia virus R peptide: delineation of the molecular determinants which are important for its fusion inhibition activity. J Virol *71*, 8490-8496.

Yang, J., Lin, Y., Guo, Z., Cheng, J., Huang, J., Deng, L., Liao, W., Chen, Z., Liu, Z., and Su, B. (2001). The essential role of MEKK3 in TNF-induced NF-kappaB activation. Nat Immunol *2*, 620-624.

Yang, P., Ai, L.S., Huang, S.C., Li, H.F., Chan, W.E., Chang, C.W., Ko, C.Y., and Chen, S.S. (2010). The cytoplasmic domain of human immunodeficiency virus type 1 transmembrane protein gp41 harbors lipid raft association determinants. J Virol *84*, 59-75.

Yang, X., Kurteva, S., Ren, X., Lee, S., and Sodroski, J. (2005). Stoichiometry of envelope glycoprotein trimers in the entry of human immunodeficiency virus type 1. J Virol *79*, 12132-12147.

Ylinen, L.M., Keckesova, Z., Webb, B.L., Gifford, R.J., Smith, T.P., and Towers, G.J. (2006). Isolation of an active Lv1 gene from cattle indicates that tripartite motif protein-mediated innate immunity to retroviral infection is widespread among mammals. J Virol *80*, 7332-7338.

Yoder, A., Yu, D., Dong, L., Iyer, S.R., Xu, X., Kelly, J., Liu, J., Wang, W., Vorster, P.J., Agulto, L.*, et al.* (2008). HIV envelope-CXCR4 signaling activates cofilin to overcome cortical actin restriction in resting CD4 T cells. Cell *134*, 782-792.

Yu, J., Li, M., Wilkins, J., Ding, S., Swartz, T.H., Esposito, A.M., Zheng, Y.M., Freed, E.O., Liang, C., Chen, B.K.*, et al.* (2015). IFITM Proteins Restrict HIV-1 Infection by Antagonizing the Envelope Glycoprotein. Cell Rep *13*, 145-156.

Yu, J., and Liu, S.L. (2018). The Inhibition of HIV-1 Entry Imposed by Interferon Inducible Transmembrane Proteins Is Independent of Co-Receptor Usage. Viruses *10*.

Yu, X., Yuan, X., McLane, M.F., Lee, T.H., and Essex, M. (1993). Mutations in the cytoplasmic domain of human immunodeficiency virus type 1 transmembrane protein impair the incorporation of Env proteins into mature virions. J Virol *67*, 213-221.

Yurkovetskiy, L., Guney, M.H., Kim, K., Goh, S.L., McCauley, S., Dauphin, A., Diehl, W.E., and Luban, J. (2018). Primate immunodeficiency virus proteins Vpx and Vpr counteract transcriptional repression of proviruses by the HUSH complex. Nat Microbiol *3*, 1354-1361.

Yuste, E., Johnson, W., Pavlakis, G.N., and Desrosiers, R.C. (2005). Virion envelope content, infectivity, and neutralization sensitivity of simian immunodeficiency virus. J Virol *79*, 12455-12463.

Yuste, E., Reeves, J.D., Doms, R.W., and Desrosiers, R.C. (2004). Modulation of Env content in virions of simian immunodeficiency virus: correlation with cell surface expression and virion infectivity. J Virol *78*, 6775-6785.

Zerhouni, B., Nelson, J.A., and Saha, K. (2004). Isolation of CD4-independent primary human immunodeficiency virus type 1 isolates that are syncytium inducing and acutely cytopathic for CD8+ lymphocytes. J Virol *78*, 1243-1255.

Zhang, F., Landford, W.N., Ng, M., McNatt, M.W., Bieniasz, P.D., and Hatziioannou, T. (2011). SIV Nef proteins recruit the AP-2 complex to antagonize Tetherin and facilitate virion release. PLoS Pathog *7*, e1002039.

Zhang, F., Wilson, S.J., Landford, W.C., Virgen, B., Gregory, D., Johnson, M.C., Munch, J., Kirchhoff, F., Bieniasz, P.D., and Hatziioannou, T. (2009). Nef proteins from simian immunodeficiency viruses are tetherin antagonists. Cell Host Microbe *6*, 54-67.

Zhang, X., Shi, J., Qiu, X., Chai, Q., Frabutt, D.A., Schwartz, R.C., and Zheng, Y.H. (2019a). CD4 Expression and Env Conformation Are Critical for HIV-1 Restriction by SERINC5. J Virol *93*.

Zhang, Y., Lu, J., and Liu, X. (2018). MARCH2 is upregulated in HIV-1 infection and inhibits HIV-1 production through envelope protein translocation or degradation. Virology *518*, 293-300.

Zhang, Y., Tada, T., Ozono, S., Yao, W., Tanaka, M., Yamaoka, S., Kishigami, S., Fujita, H., and Tokunaga, K. (2019b). Membrane-associated RING-CH (MARCH) 1 and 2 are MARCH family members that inhibit HIV-1 infection. J Biol Chem *294*, 3397-3405.

Zhang, Z., Gu, Q., de Manuel Montero, M., Bravo, I.G., Marques-Bonet, T., Haussinger, D., and Munk, C. (2017). Stably expressed APOBEC3H forms a barrier for cross-species transmission of simian immunodeficiency virus of chimpanzee to humans. PLoS Pathog *13*, e1006746.

Zhang, Z., Li, S., Gu, Y., and Xia, N. (2016). Antiviral Therapy by HIV-1 Broadly Neutralizing and Inhibitory Antibodies. Int J Mol Sci *17*.

Zhang, Z., Liu, J., Li, M., Yang, H., and Zhang, C. (2012). Evolutionary dynamics of the interferon-induced transmembrane gene family in vertebrates. PLoS One *7*, e49265.

Zhang, F., & Bieniasz, P. D. (2020). HIV-1 Vpr induces cell cycle arrest and enhances viral gene expression by depleting CCDC137. *eLife*, *9*, e55806.

Zhao, G., Perilla, J.R., Yufenyuy, E.L., Meng, X., Chen, B., Ning, J., Ahn, J., Gronenborn, A.M., Schulten, K., Aiken, C.*, et al.* (2013). Mature HIV-1 capsid structure by cryo-electron microscopy and all-atom molecular dynamics. Nature *497*, 643-646.

Zhao, X., Guo, F., Liu, F., Cuconati, A., Chang, J., Block, T.M., and Guo, J.T. (2014). Interferon induction of IFITM proteins promotes infection by human coronavirus OC43. Proc Natl Acad Sci U S A *111*, 6756-6761.

Zhao, X., Sehgal, M., Hou, Z., Cheng, J., Shu, S., Wu, S., Guo, F., Le Marchand, S.J., Lin, H., Chang, J.*, et al.* (2018). Identification of Residues Controlling Restriction versus Enhancing Activities of IFITM Proteins on Entry of Human Coronaviruses. J Virol *92*.

Zhong, P., Agosto, L.M., Ilinskaya, A., Dorjbal, B., Truong, R., Derse, D., Uchil, P.D., Heidecker, G., and Mothes, W. (2013). Cell-to-cell transmission can overcome multiple donor and target cell barriers imposed on cell-free HIV. PLoS One *8*, e53138.

Zhou, L., Sokolskaja, E., Jolly, C., James, W., Cowley, S.A., and Fassati, A. (2011). Transportin 3 promotes a nuclear maturation step required for efficient HIV-1 integration. PLoS Pathog *7*, e1002194.

Zhou, L., Tan, A., Iasvovskaia, S., Li, J., Lin, A., and Hershenson, M.B. (2003). Ras and mitogen-activated protein kinase kinase kinase-1 coregulate activator protein-1- and nuclear factor-kappaB-mediated gene expression in airway epithelial cells. Am J Respir Cell Mol Biol *28*, 762-769.

Zhou, T., Dang, Y., and Zheng, Y.H. (2014). The mitochondrial translocator protein, TSPO, inhibits HIV-1 envelope glycoprotein biosynthesis via the endoplasmic reticulum-associated protein degradation pathway. J Virol *88*, 3474-3484.

Zhou, T., Frabutt, D.A., Moremen, K.W., and Zheng, Y.H. (2015). ERManI (Endoplasmic Reticulum Class I alpha-Mannosidase) Is Required for HIV-1 Envelope Glycoprotein Degradation via Endoplasmic Reticulum-associated Protein Degradation Pathway. J Biol Chem *290*, 22184-22192.

Zhou, T., Georgiev, I., Wu, X., Yang, Z.Y., Dai, K., Finzi, A., Kwon, Y.D., Scheid, J.F., Shi, W., Xu, L.*, et al.* (2010). Structural basis for broad and potent neutralization of HIV-1 by antibody VRC01. Science *329*, 811-817.

Zhou, X., DeLucia, M., and Ahn, J. (2016). SLX4-SLX1 Protein-independent Down-regulation of MUS81-EME1 Protein by HIV-1 Viral Protein R (Vpr). J Biol Chem *291*, 16936-16947.

Zhu, P., Chertova, E., Bess, J., Jr., Lifson, J.D., Arthur, L.O., Liu, J., Taylor, K.A., and Roux, K.H. (2003). Electron tomography analysis of envelope glycoprotein trimers on HIV and simian immunodeficiency virus virions. Proc Natl Acad Sci U S A *100*, 15812-15817.

Zhu, P., Liu, J., Bess, J., Jr., Chertova, E., Lifson, J.D., Grise, H., Ofek, G.A., Taylor, K.A., and Roux, K.H. (2006). Distribution and three-dimensional structure of AIDS virus envelope spikes. Nature *441*, 847-852.

Zhu, Y., Wang, G.Z., Cingoz, O., and Goff, S.P. (2018). NP220 mediates silencing of unintegrated retroviral DNA. Nature *564*, 278-282.

Zila, V., Margiotta, E., Turonova, B., Muller, T.G., Zimmerli, C.E., Mattei, S., Allegretti, M., Borner, K., Rada, J., Muller, B.*, et al.* (2021). Cone-shaped HIV-1 capsids are transported through intact nuclear pores. Cell *184*, 1032-1046 e1018.

Zingler, K., and Littman, D.R. (1993). Truncation of the cytoplasmic domain of the simian immunodeficiency virus envelope glycoprotein increases env incorporation into particles and fusogenicity and infectivity. J Virol *67*, 2824-2831.